Molecular Genetic Studies of Deafness

Jessica Grace Tyson

A thesis submitted in fulfilment of the requirements of the University of London for the degree of Doctor of Philosophy.

March 1999.

Institute of Child Health
30 Guilford Street
London. WC1N 1EH

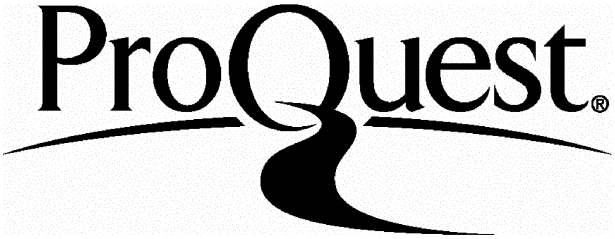

ABSTRACT

The aim of this work on the molecular genetics of deafness was to study the molecular basis of deafness in several families with non-syndromic and syndromic forms of deafness, including X-linked deafness and autosomal recessive Jervell and Lange-Nielsen syndrome (JLNS).

From one of the first studies on mapping of genes for X-linked deafness, it was shown that X-linked deafness, although very rare, is genetically heterogeneous. Linkage analysis of a single large family identified a novel locus for X-linked deafness, DFN2. Several candidate genes, including COL4A5, DDP and Diaphanous X, were screened. A major locus for X-linked deafness, DFN3, has previously been identified at Xq13-q21. Deafness in most of the families mapping to this region is accounted for by mutation in the transcription factor gene, POU3F4. However, the remaining families have microdeletions proximal to, but not encompassing, the POU3F4 coding region, leaving the precise reason for their deafness unexplained. POU3F4 expression was studied in these individuals to determine whether there is a position effect on the POU3F4 gene, or a second gene proximal to it.

Homozygosity mapping in conjunction with screening of candidate loci identified a new locus for the cardioauditory syndrome, JLNS. A positional candidate approach identified IsK as the causative gene. An IsK mutant construct has been created to study the mechanism of action of this mutation. During the course of this work, the potassium channel gene KVLQT1 was implicated in JLNS. Haplotype analysis of 12 additional JLNS families in this study was consistent with mutation in KVLQT1. Exons of the KVLQT1 gene were identified and primers designed for use with genomic DNA. Novel mutations were identified, confirming the role of KVLQT1 in JLNS and demonstrating that KVLQT1 is the major locus for this syndrome.

ACKNOWLEDGEMENTS

I would like to express many thanks to my two supervisors, Dr. Maria Bitner-Glindzicz and Professor Sue Malcolm, for all their help and support with this work. Thank you also to Professor Shomi Bhattacharya at the Institute of Ophthalmology, for his support during the six months I spent in his department.

Many thanks to all the members, past and present, of the Molecular Genetics laboratory for all their help and friendship. Special thanks go to Una, Karen and Sara for their support and encouragement during my writing (and pregnancy) and Maria for her constant support and friendship, making the last 3 years of research enjoyable and exciting. A big thank you to my parents, and finally to Jim, thanks for everything.

LIST OF CONTENTS

CHAPTER 3

RESULTS

LIST OF FIGURES

LIST OF TABLES

LIST OF ABBREVIATIONS

A	Adenine
APS	Ammonium persulphate
BAC	Bacterial artificial chromosome
bp	Base pair
BLAST	Basic local alignment search tool
Brn-4	*Brain-4*, a member of the Class IV POU domain gene family
BSA	Bovine serum albumin
C	Cytosine
°C	Degrees centigrade
cDNA	Complementary deoxyribonucleic acid
CHLC	Co-operative Human Linkage Centre
Ci	Curie
cm	Centimetre
CT	Computerised tomography
dNTP	2'-Deoxynucleotide 5'-triphosphate
dATP	2'-Deoxyadenine 5'-triphosphate
dCTP	2'-Deoxycytosine 5'-triphosphate
dGTP	2'-Deoxyguanine 5'-triphosphate
dTTP	2'-Deoxythymine 5'-triphosphate
dITP	2'-Deoxyinosine 5'-triphosphate
DEPC	Diethylpyrocarbonate
DFN	Deafness
DFNA	Non-syndromic autosomal dominant deafness locus
DFNB	Non-syndromic autosomal recessive deafness locus
dH_2O	Distilled water
DNA	Deoxyribonucleic acid
dpm	Disintegrations per minute
DTT	Dithiothreitol
EDTA	Ethylenediamine tetra-acetic acid
EST	Expressed sequence tag

FAM	6-carboxyfluorescein
g	Gram
g	Gravitational force
G	Guanine
GDB	Genome Database
HCl	Hydrochloric acid
HEX	4,7,2',4',5',7'-hexachloro-6-carboxyrhodamine
HL	Hearing loss
HPRT	Hypoxanthine phosphoribosyltransferase gene
HUGO	Human Genome Organisation
IMAGE	Integrated molecular analysis of Genomes and their expression
JLNS	Jervell and Lange-Nielsen syndrome
Kb	Kilobase
l	litre
LB	Luria-Bertani medium
LOD	Logarithm of odds ratio
Mb	Megabase
MDE	Mutation Detection Enhancement gel system
mg	Milligram
$MgSO_4$	Magnesium sulphate
$MgCl_2$	Magnesium chloride
ml	Millilitre
mM	Millimolar
mmol	Millimole
mol	mole
mRNA	messenger ribonucleic acid
Ms	Milliseconds
mV	Millivolts
NaAc	Sodium acetate
NaCl	Sodium chloride
NaH_2PO_4	Sodium dihydrogen phosphate
Na_2HPO_4	Disodium hydrogen phosphate

NaOH	Sodium hydroxide
NBL	Northumbria Biologicals Limited
ng	Nanogram
NP40	Nonidet P-40
NZY	Enzymatic casein hydrolysate
^{32}P	Phosphorus 32
PBS	Phosphate buffered saline
PCR	Polymerase chain reaction
PEG	Poly-ethylene-glycol
pmol	Picomole
PNK	Polynucleotide kinase
POU	Pit-1, Oct-1, Unc-86
R6G	N,N'-diethyl-2',7'-dimethyl-6-carboxyrhodamine
R110	6-carboxyrhodamine
ROX	6-carboxy-X-rhodamine
RNA	Ribonucleic acid
RNase	Ribonuclease
rpm	Revolutions per minute
RT	Reverse transcriptase
RWS	Romano Ward syndrome
SDS	Sodium dodecyl sulphate
SNHL	Sensorineural hearing loss
STS	Sequence tagged site
SSC	Single strand conformation
T	Thymine
TAE	Tris-acetate-EDTA buffer
TAMRA	N,N,N',N'-tetramethyl-6-carboxyrhodamine
TBE	Tris-borate-EDTA buffer
TE	Tris-EDTA buffer
TEMED	(N,N,N',N')-tetramethylethylenediamine
Tm	Melting temperature
UV	Ultraviolet
μM	Micromolar

μg	Microgram
μl	Microlitre
V	Volt
W	Watt
YAC	Yeast artificial chromosome

Families

CN	Family CN, G file number *G6317
FP	Family FP, G file number *G20775
NB	Individual NB, G file number *G15272
UK1S	Family UK1S, G file number *G14929
UK2T	Family UK2T, G file number *G10165
UK3C	Family UK3C, G file number *G15272

*G files, number of file held in the Clinical Genetics Department, Institute of Child Health, London.

CHAPTER 1: INTRODUCTION

1.1. The Auditory pathway

The human ear is the organ of hearing and balance. It consists of three distinct compartments, the external, the middle, and the inner ear.

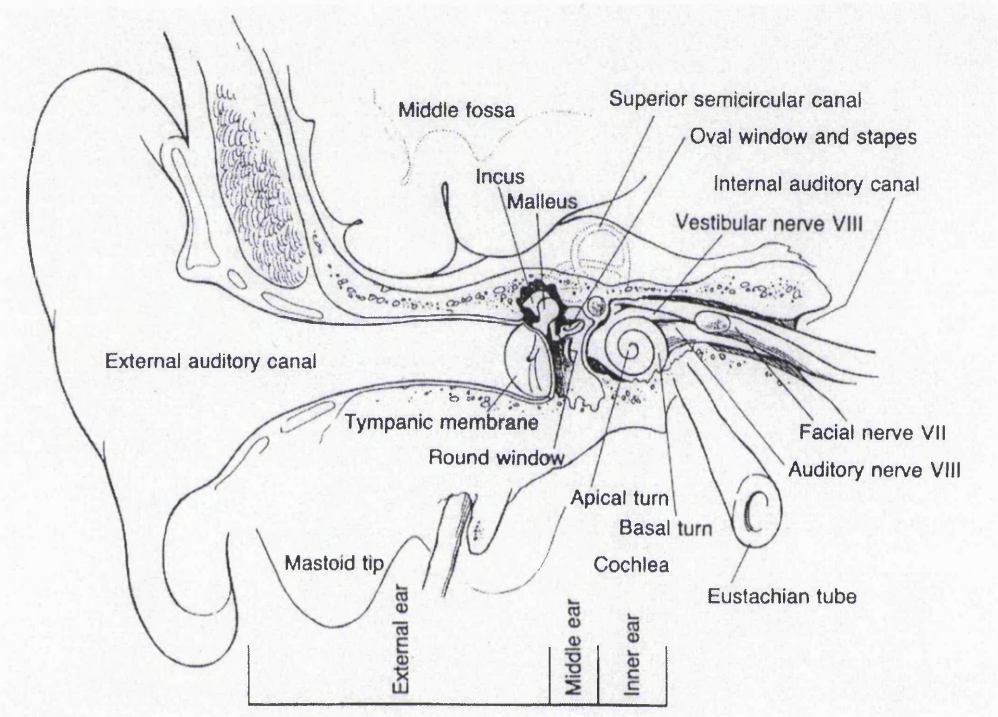

Figure 1.1.
The human outer, middle and inner ear. From "Hearing loss", by J Nadol.

The pinna or auricle and the external acoustic (auditory) meatus, which constitute the external ear, act as a channel for sound to reach the middle ear and also plays a part in sound localisation. The middle ear contains a chain of three small bones: the malleus, connected to the tympanic membrane; the incus; and the stapes, which inserts into the oval window of the inner ear. These ossicles together with the tympanic

membrane, serve to transmit the sound energy to the inner ear. The inner ear can be divided into two parts: the cochlea which contains the auditory receptors and the vestibular apparatus containing the balance and gravity receptors. The hair cells in both auditory and vestibular parts of the inner ear are basically very similar, and all respond to deflections of the stereocilia that extend from their apical surfaces. The cochlea consists of a bony tube spiralling around a central core divided by a central partition along its length. This partition, the basilar membrane, vibrates when sound energy is introduced into the cochlea. The auditory hair cells are arranged in rows along the length of the basilar membrane and their stereocilia are topped by the tectorial membrane. The hair cells and their supporting cells on the basilar membrane together are called the organ of Corti.

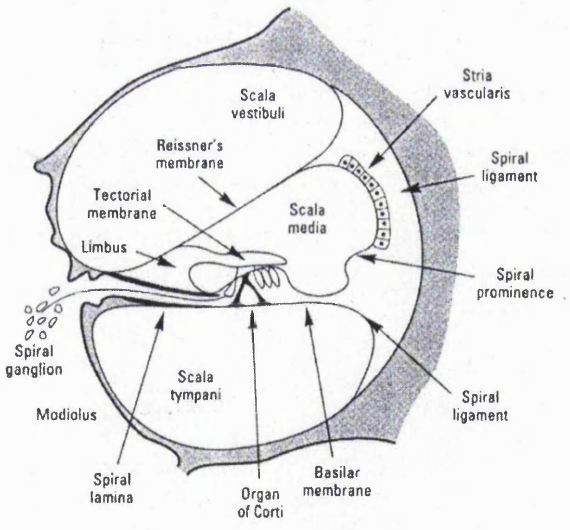

Figure 1.2.

Cross-section of the cochlea, showing the organ of Corti and the three scalae of the cochlea. From "Review of Medical Physiology" by WF Ganong.

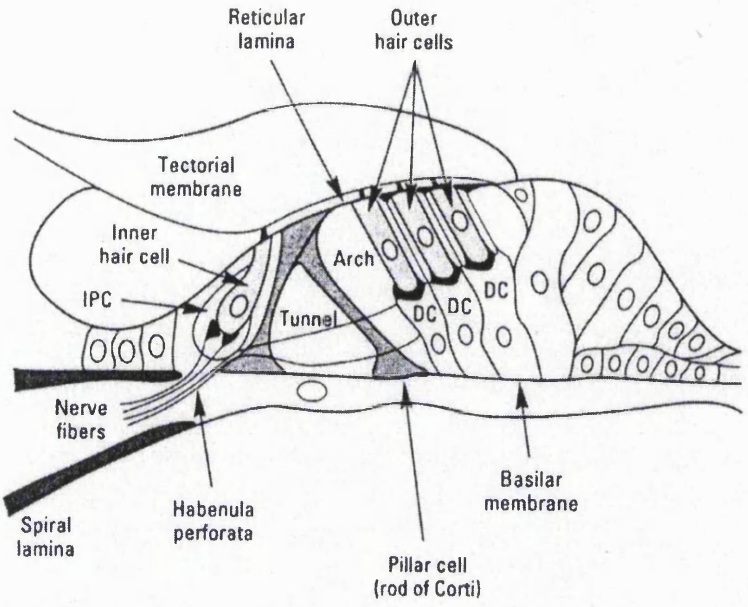

Figure 1.3.

Structure of the organ of Corti, as it appears in the basal turn of the cochlea. From "Review of Medical Physiology" by WF Ganong.

A potassium rich fluid, the endolymph, bathes the upper surface of the organ of Corti. Sound induced vibration of the basilar membrane causes a shearing motion between the tops of the hair cells and the tectorial membrane, which in turn deflects the stereocilia. During the process of hearing, the mechanical force of sound is converted into electrical signals. The sliding of adjacent stereocilia opens transduction channels, allowing an influx of endolymphatic K^+ into the hair cells, which leads to cell membrane depolarisation. Depolarisation activates voltage-sensitive Ca^{2+} channels in the basolateral surface of the hair cell, and subsequent Ca^{2+} inflow triggers neurotransmitter release. On neurotransmitter release, an afferent nerve fibre at the base of the hair cell transmits a

pattern of action potentials to the brain, which in turn interprets the characteristic intensity, frequency and time course of the stimulus.

1.2. The structure and development of the ear

1.2.1. The internal ear

The internal ear comprises a series of fluid filled spaces known as the labyrinth, which is enclosed in the temporal bone. The internal ear develops from the ectoderm, and is the first portion of the ear to begin development. The first stage, in the fourth week of gestation, is the thickening of the ectoderm to form the otic placode (figure 1.4).

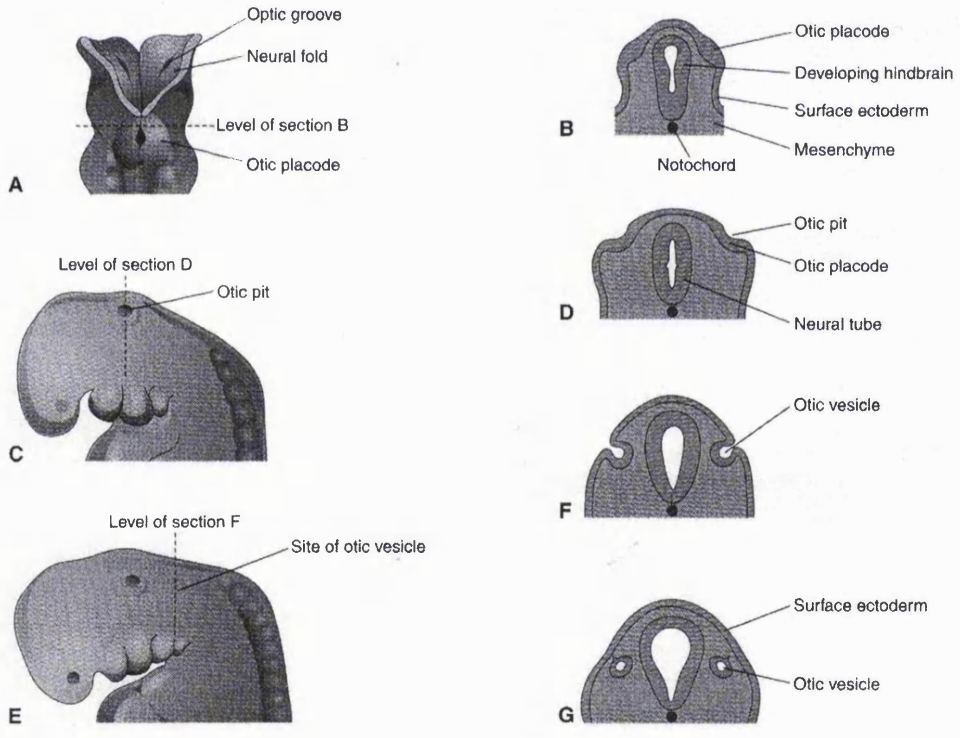

Figure 1.4.

Early development of the internal ear. A, Dorsal view of the otic placodes. B,D,F,G, illustrates the development of the otic vesicles. C and E, lateral views of the cranial region of 24 and 28 day embryos. From "The Developing Human. Clinically orientated embryology" by KL Moore.

The placode then invaginates to give rise to the otic pit, which in turn fuses to form an otic vesicle (otocyst). In the next stage of development, in the fifth week, the otic vesicle elongates (figure 1.5). The dorsal or utricular part of the otic vesicle gives rise to the endolymphatic duct, utricle and the semicircular ducts, and the ventral or saccular part of the otic vesicle gives rise to the saccule and eventually the cochlear duct.

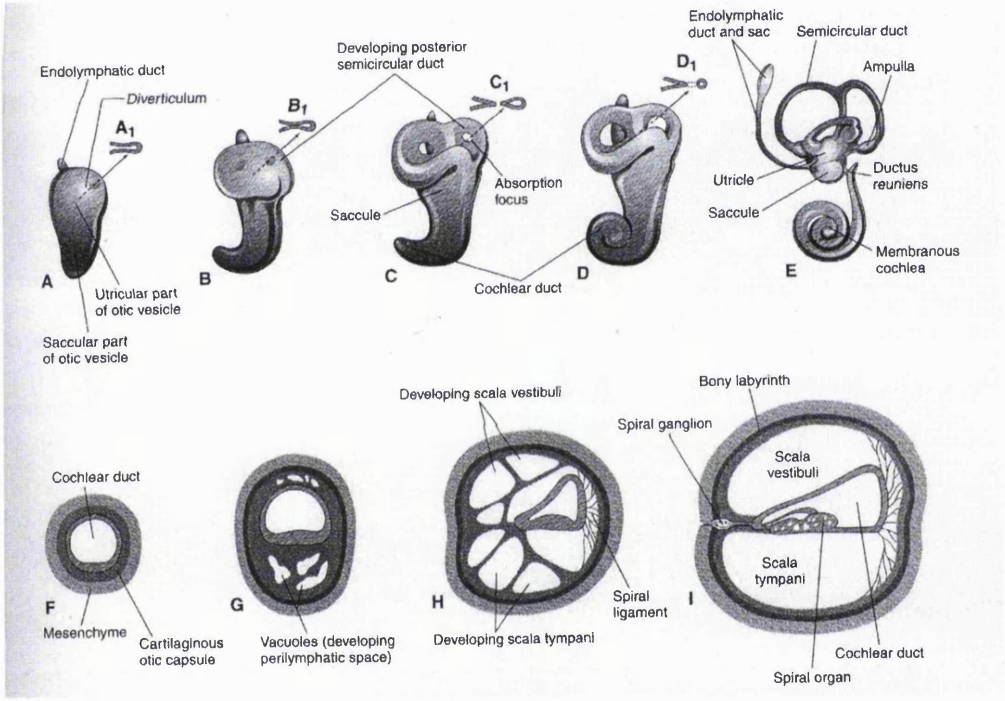

Figure 1.5.

The otic vesicle, showing development of the membranous and bony labyrinths of the internal ear. *A* to *E*, fifth to eighth week of development. *F* to *I*, sections through the cochlear duct, showing successive stages in the development of the organ of Corti and the perilymphatic space From "The Developing Human. Clinically orientated embryology" by KL Moore.

Three elevations resembling plates grow out from the dorsal/utricular part of the otic vesicle, these indicate the sites of the future semicircular ducts. The central parts of these fuse, leaving the peripheral unfused parts to become the semicircular ducts (figure 1.6). These ducts are attached to the utricle and become enclosed in the semicircular canals of the bony labyrinth at a later stage. The semicircular ducts are well-defined structures by the end of the eighth week.

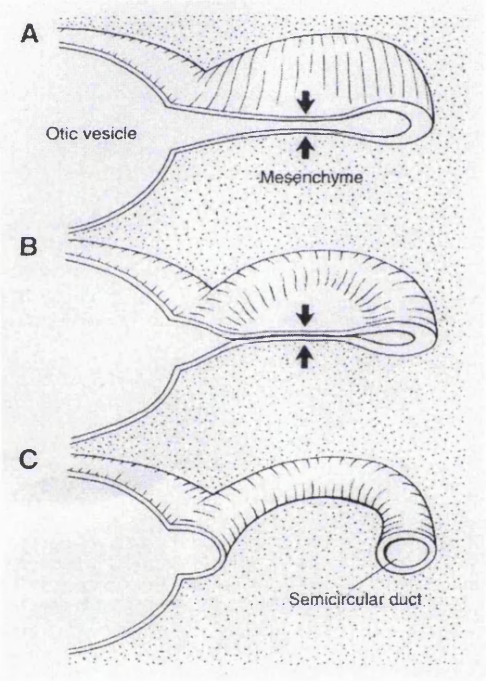

Figure 1.6.
Formation of the semicircular duct. *A*, a plate extends from the otic vesicle; *B*, fusion of the epithelial surfaces; and *C*, the recognisable structure of the semicircular duct. From "Human Embryology and Teratology" by O'Rahilly and Muller.

At the same time, the cochlear duct grows from the ventral or saccular part of the otocyst and begins to coil (figure 1.5). This structure gives rise

to the spiral organ of Corti, with its characteristic 2 1/2 turns. The utricle is connected to the semicircular ducts whilst the saccule becomes separated from the coiled cochlea by a constriction, the ductus reuniens. This complete, differentiated otocyst is called the membranous labyrinth.

Early in the fetal period, the epithelium of the floor of the cochlear duct becomes thickened and acquires a covering termed the tectorial membrane. The thickened epithelium, which rests on the basilar membrane, constitutes the spiral organ, and hair cells develop within it.

The perilymphatic space develops as a consequence of the mesenchyme surrounding the otic vesicle condensing and differentiating into a cartilaginous otic capsule (figure 1.5). Vacuoles appear in the otic capsule and the membranous labyrinth enlarges. These vacuoles eventually fuse to form the perilymphatic space. At this point, the membranous labyrinth is suspended in perilymphatic fluid. The perilymphatic space develops two divisions, the scala tympani and the scala vestibuli, one above and one below the cochlea duct. The Reissner's membrane separates the scala vestibuli from the cavity of the cochlea duct and mesenchyme condenses to form the basilar membrane which separates the cochlear duct from the scala tympani. Functional development of the cochlea occurs during trimesters 2 and 3.

The cartilaginous otic capsule later ossifies to form the bony labyrinth of the internal ear. The internal ear reaches its adult size and shape by week 20 to 22.

1.2.2. The middle ear

The middle ear consists largely of an air space, the tympanic cavity, in the temporal bone. The cavity contains the auditory ossicles.

At about 4 weeks of gestation, the middle ear begins to develop. The cavity of the middle ear develops from the tubotympanic recess, which itself arises from the first pharyngeal pouch. As the endodermal tubotympanic recess and the ectodermal external acoustic meatus approach each other, the ossicles and a branch of the facial nerve develop in the intervening mesenchyme. Near the end of the embryonic period, an area of the external meatus, the tip of the tubotympanic recess and the intervening mesenchyme will form the three layers of the tympanic membrane.

The ossicles develop from mesenchymal cartilage (figure 1.7). The malleus and incus arise from the first pharyngeal arch and the stapes from the second. At first, the ossicles are embedded in mesenchyme. The epithelium of the tympanic cavity gradually envelops them, and the ossicles begin to ossify during the second trimester. As development progresses, the malleus attaches to the tympanic membrane, the stapes

attaches to the oval window of the perilymphatic space and the incus articulates with the malleus and the stapes.

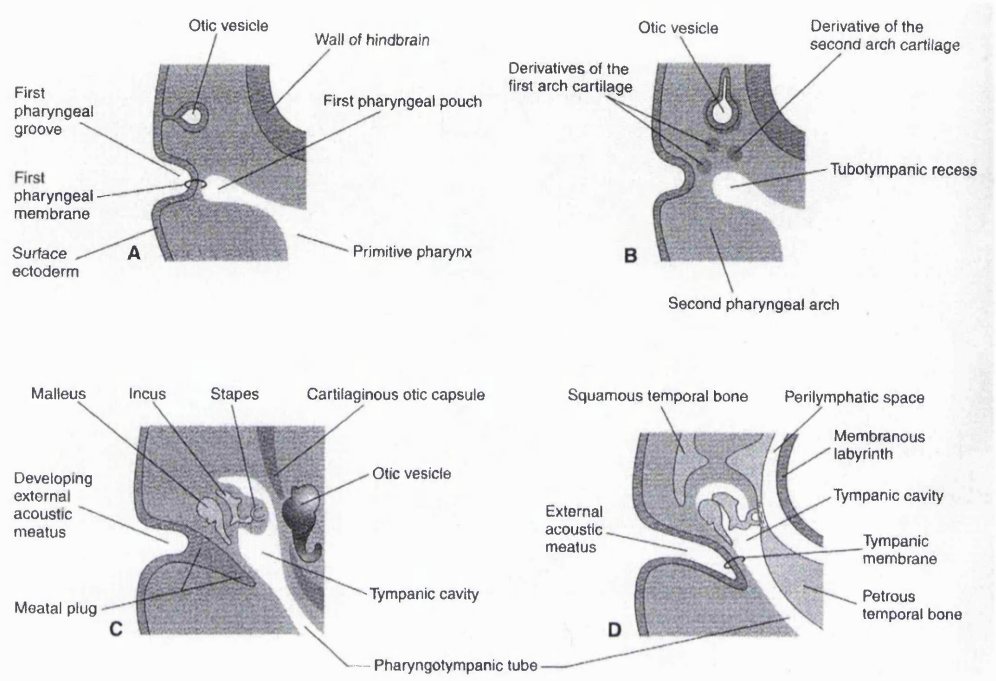

Figure 1.7.

Development of the external and middle ear. A, development at 4 weeks, B, at 5 weeks, C, later stage showing tubotympanic recess beginning to envelop the ossicles and D, final stage of ear development. From "The Developing Human. Clinically orientated embryology" by KL Moore.

1.2.3. The external ear

The external ear consists of the auricle or pinna, and the external acoustic meatus. The external acoustic meatus develops from the first pharyngeal cleft. The auricle arises from a series of elevations, the auricular hillocks, around the first pharyngeal cleft. The hillocks appear in pharyngeal arches 1 and 2, and in arch number 3 by 6 weeks gestation,

when there are the characteristic 6 hillocks. Complex fusion of these hillocks forms the auricles, which initially lie in the neck region but as the mandible develops, they move to the side of the head at the level of the eyes.

1.3. Pathology of the auditory system

Inner ear defects account for the vast majority of severe human genetic hearing impairment. Despite the difficulties in assessing human cochlear pathology using temporal bone specimens, there is similarity between mice and humans in the types of inner ear defects observed. Mouse mutants with hearing impairment are useful for elucidating the pathological processes underlying auditory system defects.

Inner ear defects can be divided into three main classes that reflect different mechanisms of interference in the development and function of the ear: morphogenic, cochleosaccular, and neuroepithelial abnormalities (Steel and Bock, 1983; Reviewed in Steel, 1995).

1.3.1. Morphogenic defects.

These defects occur when there is an early interference in the formation of the labyrinth, leading to a malformed inner ear. The malformation can affect the vestibular part of the inner ear or the cochlea or both. It can range from slight restriction of one of the semicircular canals or a slight widening of the internal acoustic meatus through which the auditory nerve leaves the inner ear, one of the abnormalities seen in X-linked

mixed deafness, DFN3 (Phelps *et al*, 1991), to the formation of a grossly distorted cyst, with little resemblance to the normal inner ear. An interesting feature of morphogenic defects is the occasional association of neural tube and inner ear anomalies. From studies in mice, the neural tube in the developing mammal is known to have an influence on the morphogenesis of the inner ear (Deol, 1966; Reviewed in Steel and Brown, 1994). A gene identified as underlying a morphogenic defect in the mouse, the *kreisler* phenotype, is expressed only in the neural tube and not in the inner ear at the critical time of development (Cordes and Barsh, 1994). Due to the interaction of the neural crest and the inner ear, genes underlying morphogenic defects may not be expressed in the developing inner ear, but only in the hindbrain and the neural crest.

1.3.2. Cochleosaccular defects

In this group of defects, and in the Neuroepithelial group, the gross shape of the labyrinth develops normally, but there are abnormalities in the development and differentiation of different cell types within the inner ear. Figure 1.8 illustrates the key features of cochleosaccular and neuroepithelial defects.

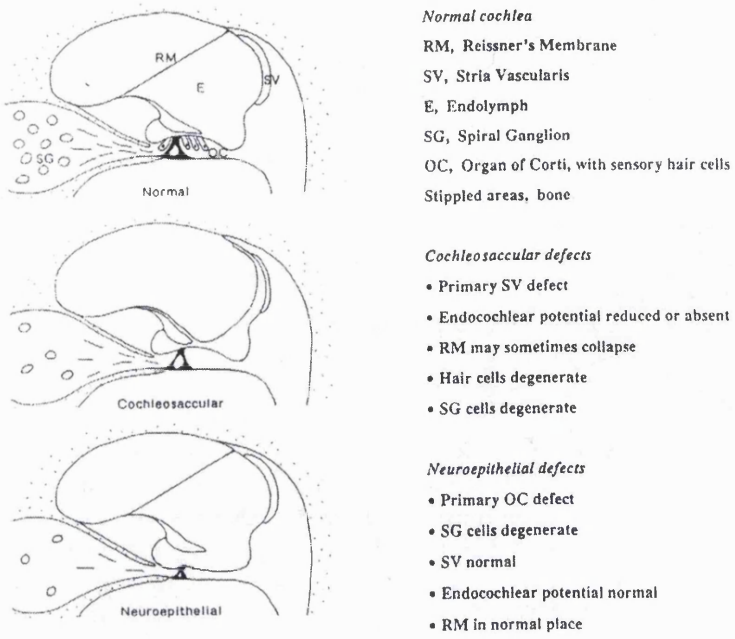

Figure 1.8.

Illustration of the key features of cochleosaccular and neuroepithelial inner ear defects. Top: the normal cochlear duct. Middle: cochleosaccular defect. Bottom: Neuroepithelial defect. From Basic mechanisms of hearing and hearing impairment by Steel and Palmer in "Genetics of Hearing Impairment".

In cochleosaccular defects, there is a primary abnormality of the stria vascularis. The stria vascularis generates the endocochlear potential and the high potassium level in endolymph, both of which are essential for normal hearing. In cochleosaccular defects the stria is abnormally thin and does not function properly and no endocochlear potential is generated. This dysfunction can result in the collapse of the Reissner's membrane, the thin membrane that separates the scala media from the scala vestibuli, leading to destruction of the organ of Corti.

Many mammals with this form of hearing impairment also have associated pigmentary abnormalities, such as white spotting of the hair or skin. Auditory/pigmentary syndromes are caused by the physical absence of melanocytes. There is no requirement for melanin. On examination of the stria of these animals, this also is lacking in melanocytes. Alleles of the *dominant spotting* (*W*) locus, which produce white spotting of the coat have been analysed to investigate the role of melanocytes in cochlear function. In the *W* mutant, melanoblast migration away from the neural crest starts as normal. The precursor cells start to differentiate normally, but there are fewer in number as compared to control mice (Reviewed in Steel and Brown, 1994). The number decreases, suggesting the gene encoding *W*, the c-kit growth factor, may act as a survival factor for melanoblasts. From this it appears that the presence of normal melanocytes, which have migrated from the neural crest, are essential for normal functioning of the stria. Lack of melanocytes in the stria prevents it from generating the normal endocochlear potential, which is fundamental for normal hair cell function. However, the exact role of melanocytes in the generation of the endocochlear potential is not understood. Since melanoblasts migrate to the inner ear from the neural crest, genes underlying cochleosaccular defects may not necessarily be expressed in the inner ear.

1.3.3. Neuroepithelial defects

In this group of defects the primary pathological changes affect the sensory neuroepithelium; the organ of Corti in the cochlea and the

saccular and utricular maculae and cristae in the vestibular system. Some or all of these sensory regions may be affected. The gross morphogenesis of the inner ear occurs normally. The Reissner's membrane is usually in its normal position and the stria vascularis initially functions normally, but may later degenerate.

This group of mutants is of great interest. The neuroepithelial group of defects may be a very common type of inner ear pathology in humans. In mice, this type of cochlear pathology often occurs in autosomal recessive deafness (Steel, 1995). Since, approximately 70% of human non-syndromic deafness is autosomal recessive, the group of mouse mutants with this type of inner ear pathology may serve as models for human deafness. The gene encoding the *shaker-1* mouse mutant, Myosin VIIA (Gibson *et al*, 1995) was the first gene to be identified in which mutations are known to cause this type of inner ear pathology. In contrast to morphogenic defects of the ear, in which the genes involved are not necessarily expressed in the developing labyrinth, the genes causing neuroepithelial-type deafness are more likely to be cochlear specific.

1.4. Hearing impairment

Hearing impairment can be classified according to several criteria. The first is the type of hearing defect, and this can be divided into two main types: conductive, in which the conduction of sound to the inner ear is affected by abnormalities of the outer or middle ear, and sensorineural, which includes any interference with cochlear function or neural

responses. Mixed hearing impairment has both a conductive and a sensorineural element. The second criterion is the degree of hearing loss: mild hearing impairment corresponds to a loss of 21-40 decibels (dB); moderate hearing impairment 41-60dB; moderate severe 61-80dB; severe 81-100dB and profound hearing impairment corresponds to a loss of greater than 100dB (Arslan and Orzan, 1996). The age of onset and the progressiveness of the hearing impairment are the third criterion. Finally, forms of deafness range from simple or non-syndromic deafness, in which the hearing loss is not associated with other clinically recognisable features outside the auditory system, to complex syndromes exhibiting multiple clinical features.

1.4.1. Epidemiology of deafness

The incidence of childhood deafness is ~1/2000 of which approximately half is considered to have a genetic origin (Fraser, 1976; Morton, 1991). Non-syndromic forms of deafness account for approximately 70% of cases of inherited hearing loss, of this ~ 75% has an autosomal recessive form of inheritance, ~10-20% autosomal dominant, ~2-3% X-linked inheritance (Rose, 1977; Fraser, 1976). Maternally inherited hearing loss due to a mitochondrial mutation has also been described (Prezant *et al*, 1993; Reid *et al*, 1994), and this form may be more common than originally thought. Syndromic forms of deafness account for approximately 30% of inherited deafness in children. Over 480 entries have been described in the Oxford Medical database (Dysmorphology

Database) in which the hearing loss is associated with a variety of anomalies (Winter and Baraitser, 1998).

1.5. Non-syndromic deafness

1.5.1. Progress in mapping of deafness genes

The number of genes involved in non-syndromic deafness has been estimated to be between 30 and 100 (Morton, 1991). Genetic heterogeneity of non-syndromic deafness in humans has complicated the chromosomal localisation and isolation of responsible genes. Until early 1994, only one gene responsible for an autosomal dominant form (Leon *et al*, 1992) and one for an X-linked form (Wallis *et al*, 1988; Brunner *et al*, 1988; Reardon *et al*, 1991) had been assigned to human chromosomes. The phenomenon of genetic heterogeneity precludes pooling of families for linkage studies. Other problems encountered in the mapping of genes for deafness include absence of clinical characteristics to distinguish different types of deafness, and the complicating factor of environmental causes of hearing loss. The inability to distinguish different types of deafness is primarily due to the inaccessibility of the ear to clinical examination and the lack of sophisticated tests, since deafness is simply the same end point of many pathological processes. Secondly, deafness can be due to genetic or environmental causes or a combination of both. The main contributing environmental factors are meningitis, perinatal complications, maternal infections such as toxoplasma and pre-natal rubella, acoustic trauma and ototoxic drugs

(Cremers and van Rijn, 1991; Reviewed in Kalatzis and Petit, 1998). Finally, a regular consequence of heterogeneity is the presence of more than one deafness gene within the same affected family. In the USA, 90% of deaf adults marry another deaf person (Reviewed in Reardon, 1992) and marriage between the hearing children of deaf adults is also frequent.

Some of the obstacles to genetic mapping have been circumvented by the study of large families living in geographically isolated regions for several generations (Guilford *et al*, 1994a) and by studying small consanguineous families by homozygosity mapping (Fukushima *et al*, 1995a). The first two loci identified for autosomal dominant forms of non-syndromic deafness were localised using families from isolated populations in Costa Rica (DFNA1; Leon *et al*, 1992) and Java (DFNA2, Coucke *et al*, 1994).

1.5.2. Autosomal loci

To date, 22 autosomal recessive (denoted DFNB) and 21 autosomal dominant (denoted DFNA) non-syndromic deafness gene localisations have been reported (Van Camp and Smith, 1999). Present locations of non-syndromic autosomal recessive and autosomal dominant deafness genes are shown in tables 1.1 and 1.2. This information is available electronically on the Hereditary Hearing loss homepage (URL, http://dnalab-www.uia.ac.be/dnalab/hhh).

Table 1.1. Present locations of non-syndromic autosomal recessive deafness genes

Locus name	Location	Phenotype	Reference
DFNB1	13q12	Profound congenital SNHL	Guilford *et al*, 1994a
DFNB2	11q13.5	Profound SNHL, variable onset	Guilford *et al*, 1994b
DFNB3	17p11.2	Profound congenital SNHL	Friedman *et al*, 1995
DFNB4	7q31	Profound congenital SNHL	Baldwin *et al*, 1995 Li *et al* ,1998
DFNB5	14q12	Profound congenital SNHL	Fukushima *et al*, 1995a
DFNB6	3p14-p21	Profound congenital SNHL	Fukushima *et al*, 1995b
DFNB7	9q13-q21	Profound congenital SNHL	Jain *et al*, 1995
DFNB8	21q22	Profound congenital SNHL	Veske *et al*, 1996
DFNB9	2p22-p23	Profound congenital SNHL	Chaib *et al*, 1996a
DFNB10	21q22.3	Profound congenital SNHL	Bonné-Tamir *et al*, 1996
DFNB11	9q13-q21	Profound congenital SNHL	Scott *et al*, 1996
DFNB12	10q21-q22	Profound congenital SNHL	Chaib *et al*,1996b
DFNB13	7q34-q36	Severe, progressive SNHL	Mustapha *et al*, 1998
DFNB14	7q31	No details available	Unpublished data available on HHH
DFNB15	3q21-q25 19p13	Severe-Profound SNHL	Chen *et al*, 1997
DFNB16	15q21-q22	Profound congenital SNHL	Campbell *et al*, 1997
DFNB17	7q31	Profound congenital SNHL	Greinwald *et al*, 1998
DFNB18	11p14-p15.1	Profound congenital SNHL	Jain *et al*, 1998
DFNB19	18p11	Profound congenital SNHL	Green *et al*, 1998a
DFNB20	11q25	No details available	Unpublished data available on HHH
DFNB21	11q23-25	Prelingual, severe/profound SNHL	Mustapha *et al*, 1999
DFNB22	Pending		

SNHL, Sensorineural hearing loss
HHH, Hereditary Hearing loss homepage
Pending, The localisation has been reported to HUGO Nomenclature Committee but has not yet been published

Table 1.2. Present locations of non-syndromic autosomal dominant deafness genes.

Locus name	Location	Phenotype	Reference
DFNA1	5q31	Low freq. SNHL starting 2nd decade progressing to profound loss, all freq. by 4th decade	Leon *et al*, 1992
DFNA2	1p34	High freq. SNHL	Coucke *et al*, 1994
DFNA3	13q12	Prelingual high frequency HL	Chaib *et al*, 1994
DFNA4	19q13	Progressive SNHL, starting 2nd decade, leading to severe/profound by 4th decade	Chen *et al*, 1995
DFNA5	7p15	High frequency progressive HL	Van Camp *et al*, 1995
DFNA6	4p16.3	Progressive low frequency HL	Lesperance *et al*, 1995
DFNA7	1q21-q23	Progressive SNHL beginning in the high frequencies	Fagerheim *et al*, 1996
DFNA8	11q22-q24	Prelingual, moderate to severe SNHL, involving all frequencies	Kirschhofer *et al*, 1998
DFNA9	14q12-q13	Progressive SNHL beginning in the high frequencies	Manolis *et al*, 1996
DFNA10	6q22-q23	Progressive SNHL starting 2nd to 5th decade, leading to severe/profound HL	O'Neill *et al*, 1996
DFNA11	11q12.3-q21	Bilateral progressive SNHL beginning 1st decade	Tamagawa *et al*, 1996
DFNA12	11q22-q24	Prelingual, moderate to severe SNHL, involving all frequencies	Verhoeven *et al*, 1997
DFNA13	6p21	Progressive hearing loss beginning in the low frequencies	Brown *et al*, 1997
DFNA14	4p16	Bilateral progressive SNHL beginning 1st or 2nd decade	Van Camp *et al*, 1997a
DFNA15	5q31	Progressive SNHL, starting 2nd to 3rd decade, leading to moderate to severe by 5th decade	Vahava *et al*, 1998
DFNA16	2q24	Mild-moderate high freq. progressive HL	Fukushima *et al*, 1998

Table 1.2 continued. Present locations of non-syndromic autosomal dominant deafness genes.

DFNA17	22q	Mild HL in high frequency, progressing to moderate/severe by third decade	Lalwani *et al*, 1999
DFNA18	3q22	Prelingual	Boensch *et al*, 1998
DFNA19	10 peri-centromeric	Mild to moderate congenital SNHL	Green *et al*, 1998b
DFNA20	Pending		
DFNA21	Pending		

SNHL, sensorineural hearing loss
HL, hearing loss
Pending, The localisation has been reported to HUGO Nomenclature Committee but has not yet been published

Due to the high genetic heterogeneity, chromosomal localisations tend to be based on linkage analysis of single large families, but for several of the loci, linkage of more than one family has been demonstrated. Examples of this are the loci DFNB1 on chromosome 13q12 (Maw, 1995; Gasparini *et al*, 1997) and DFNA2 on chromosome 1p34 (Coucke *et al*, 1994; Van Camp *et al*, 1997b).

A number of loci have been mapped to overlapping chromosomal regions, including DFNB8/DFNB10 on chromosome 21q22 (Veske *et al*, 1996; Bonné-Tamir *et al*, 1996), suggesting that the same gene may be responsible for the deafness in the two families. In a few cases, both recessive and dominant loci map to the same chromosomal region, for example DFNB1 and DFNA3 on chromosome 13q12 (Guilford *et al*, 1994a; Chaib *et al*, 1994). This suggested that mutations in the same gene may result in both a recessive and a dominant phenotype, which was recently confirmed for mutations in *GJB2* (connexin 26) (Kelsell *et al*, 1997; Denoyelle *et al*, 1998).

Interestingly, in the mapping of DFNB15, two regions of homozygosity were observed on chromosomes 3q and 19p. Lod scores for both regions were identical (Chen *et al*, 1997). Although only one of these loci may harbour the causative gene, digenic inheritance cannot be ruled out in this family. Digenic inheritance has been reported in a form of retinitis pigmentosa caused by the co-inheritance of both a mutation in the peripherin/RDS gene on chromosome 6 and the ROM1 gene on

chromosome 11 (Kajiwara *et al*, 1994). Digenic inheritance has also been suggested in an extended Swedish pedigree segregating autosomal dominant postlingual progressive deafness. Linkage was established with markers for the loci DFNA2 on chromosome 1p and DFNA12 on chromosome 11q, suggesting that both genes contribute to the basis of the hearing loss in this family (Balciuniene *et al*, 1998). Two phenotypes were observed amongst affected individuals. Individuals with severe hearing impairment shared haplotypes linked to the disease allele on both chromosomes (11q22-24; 1p32), whereas individuals showing milder hearing loss carried only one of the disease haplotypes, on chromosome 1 or chromosome 11. The results suggest that the two independent loci segregate with the more severe form of hearing loss, there is an additive effect of independently segregating loci. It is possible that only one locus causes the hearing loss, whilst the other segregates by chance. The gene underlying DFNA12 has now been identified (Verhoeven *et al*, 1998), therefore, the molecular basis of the hearing loss in at least some individuals of this family can now be investigated.

Some forms of non-syndromic deafness in humans have been assigned to chromosomal intervals that overlap with syndromic forms, as is the case for DFNB4 and Pendred Syndrome (Baldwin *et al*, 1995; Coyle *et al*, 1996; Sheffield *et al*, 1996) and DFNB2 and Usher syndrome type 1B (Guilford *et al*, 1994b; Weil *et al*, 1995; Liu *et al*, 1997a; Weil *et al*, 1997). The suggestion that allelic variants of a gene at the molecular level may result in either a syndromic form or an isolated form of deafness has

recently been demonstrated for the genes *Myosin VIIA* and *PDS*. The gene *Myosin VIIA* had previously been implicated in Usher syndrome type 1B (Weil *et al*, 1995), which is an autosomal recessive disorder characterised by hearing loss and retinitis pigmentosa (RP). Two groups independently described mutations in *myosin VIIA* in families with isolated hearing loss that map to the DFNB2 locus on chromosome 11 (Liu *et al*, 1997a; Weil *et al*, 1997) and the autosomal dominant locus DFNA11 (Liu *et al*, 1997b). Pendred syndrome, an autosomal recessive disorder characterised by congenital sensorineural deafness and thyroid goitre, was first mapped to chromosome 7q31 (Coyle *et al*, 1996; Sheffield *et al*, 1996), overlapping with a locus for autosomal recessive non-syndromic deafness, DFNB4 (Baldwin *et al*, 1995). Affected members of the original DFNB4 family were later found to have goitres and thus Pendred syndrome rather than non-syndromic deafness. However, molecular analysis of a large consanguineous family from India segregating congenital profound non-syndromic autosomal recessive deafness has now confirmed that mutations in the gene *PDS* result in a syndromic and a non-syndromic form of deafness (Everett *et al*, 1997; Li *et al*, 1998).

1.5.3. X-linked loci

X-linked deafness accounts for only a few percent of all non-syndromic deafness but is nevertheless genetically heterogeneous. A summary of X-linked loci is shown in table 1.3.

The locus DFN1 has been assigned to the phenotype of progressive sensorineural hearing loss, MIM 304700 (Mohr and Magerøy, 1960), but recent restudy of the same family has revealed the additional clinical features of blindness, dystonia, spasticity and fractures, which define this clinical entity as a new syndrome, Mohr-Tranebjærg Syndrome (Tranebjærg *et al*, 1995). This syndrome has been mapped to Xq22 (Tranebjærg *et al*, 1995) and is caused by mutation in a novel X-linked gene, Deafness/Dystonia peptide, *DDP* (Jin *et al*, 1996).

The symbol DFN2 has been assigned to profound congenital sensorineural deafness (MIM 304500) and was unmapped until 1996. The mapping of this locus forms the basis of part of this thesis.

The locus DFN3, to which the majority of families with non-syndromic X-linked deafness map, was assigned to a gene causing progressive mixed deafness with perilymphatic gusher at stapes surgery (MIM 304400). This locus was mapped by linkage analysis to Xq13-q21 (Wallis *et al*, 1988; Brunner *et al*, 1988; Reardon *et al*, 1991) and by the molecular characterisation of large and submicroscopic deletions (Bach *et al*, 1992). It has now been shown that both mixed and pure sensorineural deafness may be caused by mutations in the same gene, POU3F4, at this locus (de Kok *et al*, 1995; Bitner-Glindzicz *et al*, 1995), and they share the same distinct radiological phenotype (Phelps *et al*, 1991). The inner ear deformity observed in some males is characterised not only by dilation of the lateral end of the internal auditory canal but also by the

deficiency of bone between the lateral end of the internal acoustic canal and basal turn of the cochlea. Computerised tomography (CT) scanning of the petrous bones show these anomalies. However, not all cases of mixed or sensorineural deafness, which map to Xq13-q21 are accounted for by mutations in POU3F4. Microdeletions that do not encompass the POU3F4 gene were identified in patients with the radiological phenotype and DFN3 (de Kok *et al*, 1996). These deletions overlap in an 8kb segment, 900kb proximal to the POU3F4 gene. Whether another gene is located at this proximal position or whether this region is involved in the regulation of expression of the POU3F4 gene has yet to be determined.

DFN4 has been mapped to Xp21.2 in a region containing the Duchenne Muscular Dystrophy locus and mutation at this locus results in congenital, profound sensorineural deafness in males and mild to moderate high frequency sensorineural hearing loss of adult onset in females (Lalwani *et al*, 1994). Linkage of a second family with non-syndromic hearing loss linked to Xp21.1 refined the DFN4 locus entirely within the DMD locus, thus suggesting either a role for Dystrophin in hearing (Pfister *et al*, 1998) or the presence of an additional transcript within the DMD locus as has been shown in the Neurofibromatosis type I (NFI) gene (Viskochil *et al*, 1991).

DFN6 at Xp22 is phenotypically associated with a progressive, postlingual hearing loss (del Castillo *et al*, 1996).

Table 1.3. Present locations of non-syndromic X-linked deafness genes.

Locus name	Location	Phenotype	Reference
DFN1	Xq22	Postlingual, progressive. All frequencies affected	Tranebjærg *et al*, 1995
DFN2		Prelingual. All frequencies affected	
DFN3	Xq21.1	Prelingual. Stable, mixed hearing loss affecting all frequencies	de Kok *et al*, 1995
DFN4	Xp21.1	Prelingual. All frequencies affected	Lalwani *et al*, 1994; Pfister *et al*, 1998
DFN5	Reserved		
DFN6	Xp22	Progressive, postlingual. High frequencies affected	del Castillo *et al*, 1996

Reserved: The localisation has been reported to HUGO Nomenclature Committee but has not yet been published.

1.6. Identification of genes for deafness

The isolation of genes responsible for deafness, followed by the characterisation of the function of the defective proteins should provide knowledge of the molecular and cellular basis of normal auditory development and function. Additionally, the molecular basis of cochlear function will benefit our understanding of the mechanism of deterioration of hearing and the environmental factors affecting hearing loss.

In the last few years there has been enormous progress in the identification of genes for deafness. The genes implicated in causing deafness identified to date show that not only inner-ear specific genes when mutated cause hearing loss (*TECTA*, *POU4F3*), but genes more widely expressed also result in isolated hearing loss (MYO7, *MYO15*, *GJB2*).

The successful identification of genes for non-syndromic deafness has employed a different range of strategies. The genes identified to date are listed in table 1.4 and encode a diverse range of molecules.

Table 1.4. Genes underlying non-syndromic forms of human deafness.

	Gene	Encoded molecule	Locus	Reference
Extracellular matrix component	*TECTA*	α-tectorin	DFNA8/12	Verhoeven *et al*, 1998
			DFNB21	Mustapha *et al*, 1999
Transcription factors	*POU3F4*	POU3F4	DFN3	de Kok *et al*, 1995
	POU4F3	POU4F3	DFNA15	Vahava *et al*, 1998
Cytoskeletal components	*MYO7A*	Myosin VIIA	DFNB2	Liu *et al*, 1997a; Weil *et al*, 1997.
			DFNA11	Liu *et al*, 1997b
	MYO15	Myosin XV	DFNB3	Wang *et al*, 1998
	diaphanous	Diaphanous	DFNA1	Lynch *et al*, 1997
	GJB2	Connexin 26	DFNB1	Kelsell *et al*, 1997
			DFNA3	Denoyelle *et al*, 1998
	GJB3	Connexin 31	DFNA2	Xia *et al*, 1998
Transporters	*PDS*	Pendrin	DFNB4	Li *et al*, 1998
Ion channels	*KCNQ4*	KCNQ4	DFNA2	Kubisch *et al*, 1999
Mitochondrial genes	12s rRNA	12S rRNA	*	Prezant *et al*, 1993
	$tRNA^{ser(UCN)}$	tRNA ser(UCN)	*	Reid *et al*, 1994

* Maternally inherited non-syndromic deafness

1.6.1. Functional cloning

Functional cloning refers to the identification of the gene causing a human disease based on information about the basic biochemical defect. The gene is isolated using information regarding the protein product (such as amino acid sequence) or its function. cDNA libraries can be screened using a variety of probes including antibodies and degenerate oligonucleotides. This approach was successful in the identification of the gene for phenylketonuria. Phenylketonuria was known to be caused by lack of the enzyme phenylalanine hydroxylase. The enzyme was purified from liver, where it was known to be expressed. Specific antibodies were raised and mRNA purified. The mRNA was then converted to cDNA and a specific cDNA clone was isolated (Robson *et al*, 1982). This approach would not be suited to the identification of genes for deafness since, at the moment, little is known about genes involved in normal auditory development and function.

1.6.2. Positional cloning

Positional cloning describes the strategy used to identify a gene based solely on its chromosomal localisation, without any knowledge of the disease pathology. This approach involves mapping a mutant gene, usually by family linkage studies, followed by the physical mapping of the chromosomal region, and detection of mutations in a candidate gene.

1.6.2.1. Genetic mapping

The first step in the positional cloning of a gene is chromosomal assignment. Assignment of a disease locus to the X-chromosome is evident from the characteristic pattern of inheritance observed in the pedigree. Cytogenetic abnormalities, such as chromosome translocations, may provide crucial clues to the position of the disease gene locus. Cloning of translocation breakpoints were instrumental in the isolation of the gene causing Neurofibromatosis type I (Wallace *et al*, 1990). Chromosomal rearrangements can be starting points for positional cloning strategies, but cannot be used as the sole criteria in evaluating candidate genes as breakpoints do not necessarily disrupt a structural gene. The position of the Sathre-Chotzen gene was previously refined by FISH analysis of patients carrying balance translocations involving 7p21, but it has now been shown that these breakpoints do not disrupt the coding sequence of the TWIST gene (Rose et al, 1997).

In the absence of such clues, family linkage studies are able to localise the gene of interest to a chromosomal region. In order to establish linkage, a large number of polymorphic markers are required, as well as sufficient meioses to confirm or refute linkage at a particular level of significance.

1.6.2.1.1. DNA polymorphisms.

The human genome shows an enormous amount of DNA sequence variation. On average, one nucleotide in 200 is significantly polymorphic.

The most common type of DNA polymorphisms used in linkage analysis are microsatellites.

Microsatellites

Microsatellites are genetic markers consisting of variable length runs of a simple tandemly repeated sequence, typically CA. The length of the repeat varies between chromosomes and therefore between individuals. The power of microsatellites in linkage mapping is their informativeness and that they are amenable to PCR amplification. A sequence including the variable repeat is amplified by PCR, and the products of amplification, varying in length within and between individuals, are resolved on polyacrylamide gels. One of the main achievements of the Human Genome Project has been the generation, characterisation and mapping of over 5000 microsatellite polymorphisms (Dib *et al*, 1996).

1.6.2.2. Linkage analysis

Genetic linkage is the tendency of genes or other DNA sequences at a specific chromosomal location to be inherited together at meiosis more often than would be expected by chance. This is a consequence of their physical proximity on a single chromosome. If a high degree of co-segregation is observed for a disease trait and a polymorphic marker, it implies that they are linked and lie close to each other on the same chromosome. Two regions of DNA, which are distant from each other, may be separated by recombination, depending on their distance apart, and not be inherited together.

Two homologous chromosomes segregate independently; an allele at one locus on one chromosome segregates together with an allele at another locus on another chromosome with 50% probability. Alleles at loci on the same chromosome segregate together at a rate related to the distance between them on the chromosome. This rate is the probability of a recombination event occurring between the two loci, and is denoted as the recombination fraction (θ).

$$\theta = \frac{\text{number of recombinants}}{\text{number of recombinants plus number of non-recombinants}}$$

θ can be taken as an approximate measure of genetic distance. The genetic distance between two loci is defined in centimorgans (cM). Two loci are 1cM apart if they show recombination once in 100 meioses.

Recombination fractions range from $\theta=0$ for loci next to each other, to $\theta=0.5$ if two loci are unlinked i.e. loci far apart or on different chromosomes. Two loci are said to be linked when θ is less than 0.5, and the phenomenon describing this is genetic linkage.

In order to show that linkage has not occurred by chance when loci are not actually close to each other, evidence of linkage between two loci is defined in terms of statistical probabilities. The lod score (**Log**arithm$_{10}$ of the **od**ds ratio, of linkage versus no linkage) is a measure of the

likelihood of genetic linkage between loci. This ratio is computed for several values of θ and the results are expressed as the $\log_{10}$ of the likelihood ratio, Z, the lod score.

$$Z = \log_{10} \frac{\text{Likelihood (data}/\theta)}{\text{Likelihood (data/no linkage)}}$$

A lod score of 3, representing an odds ratio of 1000:1 is taken as evidence that two loci are linked. A lod score of -2 is often taken as evidence against linkage.

Standard lod score analysis is a powerful method for scanning segments of DNA to locate a disease gene, but it has some drawbacks. These include (i) the need to specify a particular genetic model, such as mode of inheritance, (ii) limits on the resolution achievable, resulting in the region showing linkage to a particular disease trait too large for a positional cloning approach, and (iii) problems with locus heterogeneity.

A genome wide search is a systematic search for linkage across the entire genome using a coverage of highly polymorphic microsatellite markers. For recessive diseases a systematic screening of the entire genome is feasible using a variation of conventional linkage analysis, homozygosity mapping.

Homozygosity mapping can be used specifically to map the disease gene of rare recessive disease, in small consanguineous families (Lander and Botstein, 1987). It is the search for homozygous markers at the disease locus. The principle is that a fraction of the genome of offspring of a consanguineous marriage is expected to be homozygous because of identity by descent. These areas of homozygosity would be expected to be random between different offspring, except a common disease locus shared by affected offspring. The affected children have inherited two identical copies of the disease allele from a carrier ancestor. These affected individuals are homozygous-by-descent for the disease bearing gene and almost always for a region of several centimorgans spanning the disease locus. Homozygosity mapping has not only been successful in mapping genes for hearing loss (Fukushima *et al*, 1995) but has been applied successfully to other rare autosomal recessive diseases such as alkaptonuria (Pollack *et al*, 1993) and pseudohypoaldosteronism (Strautnieks *et al*, 1996).

A variation of this is a DNA pooling strategy for linkage mapping. A way to search for genomic regions identical by descent in affected individuals is to physically pool DNA samples (Sheffield *et al*, 1995). By pooling equal molar amounts of DNA from related affected individuals, identity by descent can be observed by analysing the pooled DNA sample with polymorphic microsatellite markers using PCR. The number and frequency of alleles at each locus can be compared to a control DNA pool consisting of DNA from unaffected siblings and parents. In this

method, the relative intensity of each allelic band on the polyacrylamide gel of markers amplified from pools of DNA from the affected and unaffected individuals is proportional to the frequency of that allele in the pooled DNA samples. If the disease gene has been inherited by the affected individuals from a common ancestor, the banding pattern of the microsatellite marker that is linked to the disease will show a shift in intensity toward a particular allele in the affected pool, as compared to the unaffected pool. The identification of a locus for autosomal recessive non-syndromic hearing loss in two inbred Bedouin kindreds (Scott *et al*, 1996) demonstrated the use of DNA pooling as an effective means of quickly identifying regions of linkage in inbred families with recessive disease.

Linkage disequilibrium is a phenomenon in which the frequencies of certain marker alleles among affected individuals diverge from the frequencies in the general population. Linkage disequilibrium is seen only when many of the apparently unrelated affected people in the population in fact derive their disease chromosome from a shared ancestor. This phenomenon is observed for markers located close to the disease gene and can therefore help to narrow the disease interval once the general location of the disease gene has been identified by conventional linkage. The gene causing diastrophic dysplasia was fine mapped and subsequently identified using linkage disequilibrium data (Hästbacka *et al*, 1992; Hästbacka *et al* 1994).

1.6.2.3. Physical mapping

Following assignment of a gene to a particular chromosome, the primary goal of physical mapping is to assemble a comprehensive series of DNA clones with overlapping inserts, known as a clone contig. This is necessary to start physical mapping and as a source of polymorphic markers which are used to generate a high resolution genetic map of the region. The clones used may be YACs (Yeast artificial chromosomes) which are able to maintain large fragments of DNA. YAC contigs are constructed by screening publicly available YAC clone libraries to find YACs that contain markers known to map to the candidate region. Such contigs are being defined as part of the ongoing work of the Human Genome Project. Due to the large insert size (up to 1Mb), YACs are very unstable, often showing rearrangements. Other vectors such as PACs (P1 artificial chromosomes) or BACs (Bacterial artificial chromosomes) with insert sizes of 100-200Kb are often more applicable.

1.6.2.4. Identification of coding sequences

Once a contig is established across the candidate region, the clones are searched for genes via the detection of expressed sequences. Common methods used for identifying genes in cloned DNA include exon trapping, cDNA selection and computer analysis of DNA sequences.

Exon trapping

Exon trapping detects the presence of exons flanked by functional splice sites in a clone, via an artificial RNA splicing assay (Auch and Reth,

1990; Buckler et al, 1991). This approach was successful in the identification of the gene for Opitz G/BBB syndrome (Quaderi *et al*, 1997).

cDNA selection

In this technique, cloned DNA contained in a vector, such as a YAC from the critical region, is used to directly screen a cDNA library. YAC DNA is immobilised on a filter and hybridised with an entire library of cDNA inserts. cDNAs corresponding to any gene contained in the YAC insert should preferentially bind, and can be amplified using vector primers for further analysis (Reviewed in Brennan and Hochgeschwender, 1995).

Computer analysis

The goal of the Human Genome project is the sequencing of the entire human genome and the identification of all human genes. With the accumulation of information from large-scale sequence projects, computer analysis of genomic sequence data is invaluable. Sequence data is available from public databases on the World Wide web (Borsani *et al*, 1998) and a large number of programs exist to predict potential coding exons, splice junctions, promoter and regulatory sequences and predict the overall gene structure from genomic sequence (Claverie, 1997)

Nucleic acid sequences can be used in homology similarity searches using programmes such as BLAST (**B**asic **L**ocal **A**lignment **S**earch **T**ool).

This programme is designed to search for significant sequence homology to known genes or expressed sequences, between a sequence under investigation and any sequence in the database.

1.6.2.5. Mutation screening

The candidate region for a particular disease is thus defined using linkage analysis, and can be denoted as being between two polymorphic markers shown to be linked to the disease. All the transcripts in this region are potential candidate genes depending on pattern of expression or function if known, and have to be examined for mutations.

For a candidate gene to be implicated in a particular disease, it must be shown to be mutated in affected individuals. A distinction between a change which is the pathogenic mutation and a change which is a polymorphic variant needs to be addressed. A polymorphism is defined as a change anywhere in DNA structure, usually without phenotypic effect and present at 0.01 frequency or higher in the population (Cotton and Scriver, 1998). In order to exclude the nucleotide change as a polymorphic variant, 100 chromosomes from unrelated individuals, in addition to affected and unaffected members of the pedigree if the disorder is familial, can be tested for the particular change. Various methods for mutation screening can be used.

Southern blotting

In Southern blotting, genomic DNA is digested with a restriction endonuclease, electrophoresed, then denatured and transferred to a nylon membrane for hybridisation. A region of the candidate gene is radiolabelled and used as a probe to hybridise to the fragments in the gel blot. Large deletions and rearrangements are detectable by the pattern of bands compared to the wild type DNA, or by different intensities of the bands.

Heteroduplex analysis

Conformation based methods of mutation detection rely on the fact that DNA containing a sequence change has altered mobility under certain gel electrophoresis conditions.

Heteroduplex analysis relies on detecting mismatched bases formed when complementary strands of a mutant and a wild type allele are allowed to hybridise to form a heteroduplex. This occurs naturally when a PCR product from a heterozygous person is denatured and cooled slowly, which allows single mutant strands to base-pair with complementary wild type strands. The electrophoretic mobility of heteroduplexes can be detected as extra slow moving bands. For detecting homozygous mutations or X-linked mutations in males, wild type DNA is added to the mutant fragment. This method can be used to screen for mutations in fragments up to 1 kilobase in size (Reviewed in Cotton, 1997).

Single-strand conformation polymorphism (SSC) analysis.

This strategy exploits the phenomenon that the electrophoretic mobility of single-stranded DNA on non-denaturing gels depends not only on length but also on their conformation, which is dictated by the DNA sequence. Control samples are run alongside patient samples, so that differences between the wild type pattern are noticed and polymorphisms excluded. The overall sensitivity of this method is between 70% and 90% for fragments no longer than 300bp, under multiple gel conditions of temperature and percentage of glycerol (Reviewed in Cotton, 1997).

Other methods of mutation detection, such as mismatch cleavage methods, not only detect a mutation in a fragment but also can locate a mutation precisely after cleavage of a heteroduplex. These methods can scan much larger fragments than SSC analysis and heteroduplex analysis.

Ultimately, DNA sequencing defines the precise nucleotide change involved in the mutant phenotype. Confirmation of mutation is achieved by prediction of the effect of the sequence change on the structure or function of the predicted protein, and where possible, expression of the mutant protein to demonstrate any loss or alteration of function.

1.6.2.6. Identification of genes by positional cloning

A number of genes have been identified by positional cloning including those causing Duchenne and Becker muscular dystrophies, Cystic fibrosis, Huntington's disease and many others (Reviewed in Collins,

1995). With respect to deafness, this approach, in conjunction with information arising form large scale sequencing projects, has been successful in the identification of genes for Pendred syndrome/DFNB4, DFNA1 and DFNA5 (Everett *et al*, 1997; Li *et al*, 1998; Lynch *et al*, 1997; Van Laer *et al*, 1998).

The isolation of the Pendred syndrome gene, *PDS*, took advantage of the Human Genome Project's sequencing of human chromosome 7 at the Washington University Genome Sequencing Centre. A novel gene was identified and mutations demonstrated in individuals with Pendred syndrome (Everett *et al*, 1997). On the basis of homology, it was originally postulated that *PDS* encodes a putative sulphate transporter (Everett *et al*, 1997). However, functional studies in *Xenopus laevis* oocytes suggests that Pendrin, encoded by *PDS*, functions as an iodine/chloride transporter (Scott *et al*, 1998a), therefore its precise role in hearing loss remains to be confirmed.

The effort to sequence the human genome also contributed to the identification of the DFNA5 gene (Van Laer *et al*, 1998). The DFNA5 locus was first mapped to chromosome 7p15 (Van Camp *et al*, 1995). Subsequent analysis of additional family members and the development of new polymorphic markers from the genomic sequence generated for chromosome 7 refined the candidate region to 600-850kb. Genes were identified from within the DFNA5 candidate region using the sequence data available on the World Wide Web, one of which was a novel gene

expressed in the cochlea. A mutation segregating with the deafness in the family was identified (Van Laer *et al*, 1998). The DFNA5 gene encodes a completely novel protein with no homology to previously identified protein families, thus its role in progressive high frequency hearing loss remains to be established.

Another gene identified using the positional cloning approach is the gene underlying DFNA1, *Diaphanous* (Lynch *et al*, 1997). DFNA1 is defined by autosomal dominant, non-syndromic, fully penetrant sensorineural hearing loss, and was mapped in a large Costa Rican kindred (Leon *et al*, 1992). The locus, the first for an autosomal form of deafness, was mapped to a 1cM interval on chromosome 5q, and a complete BAC contig constructed. In order to identify the genes in the region, the BACs were sequenced and potential coding regions identified. Genomic sequencing revealed a previously unidentified gene homologous to the *Drosophila* gene *diaphanous* and to the mouse gene encoding p140mDia. The human *Diaphanous* gene was isolated and a mutation identified in the affected members of the DFNA1 kindred (Lynch *et al*, 1997). This gene is ubiquitously expressed. A role for *diaphanous* in the regulation of actin polymerisation in hair cells has been suggested (Lynch *et al*, 1997), since products of its yeast and *Drosophila* homologues interact with proteins known to polymerise actin.

1.6.3. Candidate genes and positional candidates

An initial genome-wide search for linkage will use microsatellite markers spaced at relatively wide intervals, for example 10cM, and so define a broad candidate region; the candidate locus is too large to consider a positional cloning approach. In such cases the candidate gene approach is the most appropriate cloning strategy. The candidate gene approach relies on partial knowledge of the disease gene function. A candidate gene can be suggested from an appropriate expression pattern or function, its homology to a gene implicated in an animal model of the disease, or from functional relatedness to a gene implicated in a similar human disease phenotype. Due to a limited knowledge of the genes involved in normal auditory development and function, there are difficulties in suggesting suitable candidate genes for this approach. Genes may be expressed exclusively in the inner ear, or more widely expressed but mutation in which is only detrimental to the inner ear.

Recent successes in disease gene identification have relied on the positional candidate approach (Reviewed in Collins, 1995), a strategy which combines knowledge of the map position of the disease locus with the availability of candidate genes mapping to the same chromosomal region.

The first gene to be identified for an autosomal non-syndromic form of deafness, the gene encoding the gap junction protein connexin 26, involved a positional candidate gene approach (Kelsell *et al*, 1997). Initial studies centred on a family in which autosomal dominant palmoplantar

keratoderma and congenital deafness was segregating. Linkage analysis showed the disease locus to be on chromosome 13q11-12, a region previously implicated in two forms of non-syndromic deafness, DFNB1 (Guilford *et al*, 1994a) and DFNA3 (Chaib *et al*, 1994) and an autosomal dominant skin disease - Clouston hidrotic ectodermal dysplasia. Based on its expression pattern and chromosomal localisation, *GJB2* (connexin 26; Cx26) was a positional candidate gene for the skin disorder in this family. *GJB2* was screened for mutations and a substitution of threonine for methionine at codon 34 (M34T) was found segregating with the deafness in this family and not the skin disease. Mutations in *GJB2* were also identified in DFNB1-linked families (Kelsell *et al*, 1997).

After the initial identification of the DFNB1 locus on chromosome 13 (Guilford *et al*, 1994a), studies on collections of families has suggested that this locus might be a major contributor to prelingual deafness (Maw *et al*, 1995; Gasparini *et al*, 1997). Since the identification of *GJB2* as the causative gene, there is the opportunity to assess the contribution of mutations in this gene in autosomal recessive prelingual deafness. In particular, the frequency of one specific mutation, 30delG or 35delG, a deletion of a single G in a sequence of six guanine residues starting at position 30, is very significant in familial and sporadic cases of prelingual deafness (Zelante *et al*, 1997; Denoyelle *et al*, 1997; Estivill *et al*, 1998a; Lench *et al*, 1998). A carrier frequency for the mutation of up to 1 in 31 has been suggested in certain European populations (Denoyelle *et al*, 1997; Estivill *et al*, 1998a) making it one of the most common disease-

causing mutations described to date. In addition to the 35delG mutation, another mutation in *GJB2* was commonly found in Ashkenazi Jews. The mutation, 167delT, was detected in more than 4% of the control population of Ashkenazi Jews analysed in the study (Morell *et al*, 1998).

Controversy exists over the original M34T mutation with respect to its involvement in autosomal dominant non-syndromic deafness, as this mutation has been found in normal hearing individuals (Scott *et al*, 1998; Rabionet *et al*, 1998). Functional data suggests that the M34T mutation acts through a dominant-negative mechanism (White *et al*, 1998). The involvement of connexin 26 in autosomal dominant non-syndromic deafness has recently been confirmed (Denoyelle *et al*, 1998).

Expression of connexin 26 has been demonstrated in the inner ear in the spiral limbus, the spiral ligament, the stria vascularis and between the supporting cells of the organ of Corti of the rat cochlea (Kikuchi *et al*, 1995; Lautermann *et al*, 1998). A role for connexin 26 in forming the cell-to-cell pathway for recycling potassium ions back to the endolymph following auditory transduction has been suggested (Kelsell *et al*, 1997) and a loss of connexin 26 would be expected to cause hearing loss due to disruption of this potassium flow.

To study the possible involvement of other connexin molecules in deafness, Xia and colleagues cloned and mapped human *GJB3* (Connexin 31) to chromosome 1p33-p35 (Xia *et al*, 1998). This is an

example of how a positional candidate subsequently suggests other candidate genes. The *GJB3* gene mapped to a previously defined locus for autosomal dominant non-syndromic deafness, DFNA2 (Van Camp *et al*, 1997) thus suggesting Cx31 as a good positional candidate gene for high frequency sensorineural hearing loss characteristic of DFNA2. Mutation analysis revealed mutations associated with high frequency hearing loss in two families (Xia *et al*, 1998). Expression of rat *Gjb3* was demonstrated in the inner ear by RT-PCR (Xia *et al*, 1998), although it is not fully understood how mutation in *GJB3* causes deafness. Interestingly, mutations in *GJB3* (connexin 31) have also been found in families with autosomal dominant Erythrokeratodermia Variabilis (Richard *et al*, 1998), illustrating that mutation in Connexin 31 results in two distinct phenotypes. Interestingly a second "DFNA2" gene on chromosome 1p34 has recently been identified. A mutation in the novel potassium channel gene, KCNQ4, was observed segregating with dominant hearing loss in a small french family (Kubisch *et al*, 1999). It remains to be confirmed which is the true "DFNA2" gene (Van Hauwe *et al*, 1999).

1.6.3.1. Mouse models for human hearing impairment.

A number of mouse mutants have been identified with defects in the auditory system (Reviewed in Steel, 1995), providing a rich source of models for human deafness. The mouse has proved to be an invaluable model for identification of genes for human deafness due to similarities in inner ear structure, range of inner ear defects and range of associated

abnormalities (Steel, 1991). Conserved linkage groups between man and mouse allow the identification of homologous genes. In addition, studies of the mouse also allow access to the inner ear at various developmental stages to study disease pathology.

Deaf mouse mutants in conjunction with linkage analysis of families with deafness have speeded the identification of two human genes MYO7A and MYO15.

Mice homozygous for the recessive *shaker-1* mutation show dysfunction and degeneration of the organ of Corti, and shaker/waltzer behaviour typical of vestibular dysfunction. This mouse mutant represented an excellent model for non-syndromal hearing loss in humans (Reviewed in Steel and Brown, 1996). The *shaker-1* mutation mapped to mouse chromosome 7, near the *omp* gene (Brown *et al*, 1992). A physical map of the region was constructed and genes in the region identified, including an unconventional myosin, myosin VII, which was subsequently shown to encode *shaker-1* (Gibson *et al*, 1995). OMP in the human genome was mapped to 11q13 (Evans *et al*, 1993), in the vicinity of the locus for Usher syndrome type 1B (Kimberling *et al*, 1992). A locus for autosomal recessive non-syndromic deafness, DFNB2, also mapped to the same interval (Guilford *et al*, 1994b). This indicated that either or both of these mutant loci represented potential homologues to the mouse *shaker-1* gene. Mutations in Myosin 7A have now been found to be responsible for non-syndromic deafness in humans (Liu *et al*, 1997a;

Weil *et al*, 1997; Liu *et al*, 1997b) as well as Usher syndrome 1B (Weil *et al*, 1995) and Atypical Usher syndrome (Liu *et al*, 1998).

Unconventional myosins, such as myosin VIIA, share structurally conserved heads and have divergent tails. The head region is thought to be used in moving along actin filaments using actin-activated ATPase activity, whereas the tail region is presumed to be involved in moving different macromolecular structures relative to actin filaments (Reviewed in Hasson 1997). In the ear Myosin VIIA is present in both inner and outer hair cells, expressed along the stereocilia of the hair cell (Hasson *et al*, 1995; Hasson *et al*, 1997). Its location suggests that it is the intracellular anchor of the basal links that connect each stereocilium to its neighbour (Hasson, 1997) thus maintaining the rigidity of the stereocilia bundle.

DFNB3, a locus for autosomal recessive non-syndromal deafness, was first mapped to a 12cM interval on human chromosome 17p11.2 in a population of 1200 villagers of Bengkala, Bali, in which 45 individuals are deaf (Friedman *et al*, 1995). The identification of new polymorphic markers in the region and analysis of additional individuals unavailable for the initial mapping studies refined the interval to 3cM (Liang *et al*, 1998). On the basis of conserved synteny and similar phenotype of profound deafness, the mouse autosomal recessive mutation *shaker-2* (*sh-2*) had been proposed as the homologue of DFNB3 (Friedman *et al*, 1995). Genetic analyses and co-localisations of human and mouse ESTs

near DFNB3 and *shaker-2* strengthened the hypothesis that *shaker-2* is likely to be the homologue of DFNB3 (Liang *et al*, 1998). The strategies to clone the DFNB3 gene were the identification of the *shaker-2* gene in the mouse by positional cloning and BAC rescue and screening of candidate genes in the DFNB3/*sh-2* intervals. BAC-transgene rescue in the shaker-2 mouse identified a novel unconventional myosin, *myo15*, as the *sh-2* gene (Probst *et al*, 1998). The identification of *myo15* as the *sh-2* gene led to the isolation of the human homologue and the demonstration of mutations in *MYO15* in DFNB3-linked families (Wang *et al*, 1998).

The stereocilia in the inner ear of the *sh-2* mouse are abnormally short but arranged in a nearly normal pattern. A long actin-containing structure was found to be associated with the mutant inner hair cells (Probst *et al*, 1998). This evidence suggests that the *sh-2* gene, myo15, is critical for normal cytoskeletal morphology and actin organisation.

The mutations identified in unconventional myosins in deafness have demonstrated a crucial role for these proteins in hearing. The defects illustrated in the mouse mutants *shaker-1*, *Snell's waltzer* (Avraham *et al*, 1995) and *shaker-2* suggest a role for unconventional myosins in anchoring or controlling the actin based structures of the hair cell, which are vital for their function.

Once the chromosomal intervals for the DFNA15 and DFNA8/12 loci were identified by linkage analysis (Vahava *et al*, 1998; Kirschhofer *et al*, 1998; Verhoeven *et al*, 1998), examination of the homologous regions on mouse chromosomes revealed excellent candidate genes. Cloning and sequencing of the human orthologues led to the identification of mutations in *POU4F3 and TECTA* genes (Vahava *et al*, 1998; Verhoeven *et al*, 1998).

Linkage analysis of a family with autosomal dominant hearing loss defined a 25cM interval of chromosome 5q. An 8 base pair deletion in the *POU4F3* gene was found in affected individuals of this family (Vahava *et al*, 1998). *POU4F3* is a member of the POU transcription factors, a group of proteins identified by well-characterised POU-specific domain and POU homeodomain, both of which participate in DNA binding (Reviewed in Wegner *et al*, 1993). *POU4F3* was an excellent candidate for a gene causing human deafness, as targeted deletion of both alleles of *pou4f3* causes complete deafness in mice (Erkman *et al*, 1996; Xiang *et al*, 1997). *Pou3f4* is expressed in adult hair cells of mice, supporting its requirement for continued maintenance of these structures.

The contribution of mutations in POU4F3 was assessed in a comprehensive screen in families with progressive hearing loss. This failed to identify any mutations apart from the one observed in the DFNA15 family (Avraham *et al*, 1998).

The identification of mutations in *TECTA* implicated a new type of protein in the pathogenesis of deafness. *TECTA* encodes α-tectorin, one of the major non-collagenous components of the tectorial membrane in the inner ear. Although not identified in a deaf-mouse mutant, this gene was first described as an inner-ear specific protein in mice. The gene encoding mouse α-tectorin was mapped to mouse chromosome 9, to a region which shows evolutionary conservation with human chromosome 11q (Hughes *et al*, 1998). The gene encoding human α-tectorin maps within the genetic interval of DFNA12 (Verhoeven *et al*, 1997; Hughes *et al*, 1998). Subsequent cloning and mutation analysis of human *TECTA* has implicated α-tectorin in autosomal dominant non-syndromic deafness (Verhoeven *et al*, 1998). Missense mutations in conserved regions of the *TECTA* coding sequence are thought to reduce both the structural integrity of the tectorial membrane and its ability to stimulate the hair cells (Verhoeven *et al*, 1998). More recently, a splice site mutation has been identified in a DFNB21-linked family (Mustapha et al, 1999), establishing that α-tectorin mutations are responsible for both dominant and recessive forms of deafness.

1.6.3.2. Cochlea-specific approaches

A cochlear cDNA library will contain copies of mRNA of most of the genes in the cells of the cochlea. A cDNA library can be enriched for tissue-specific messages by subtraction techniques, to eliminate housekeeping genes. Genes preferentially and genes specifically

expressed in the inner ear can therefore be effectively isolated and characterised (Robertson *et al*, 1994). Selected cDNA clones from a cochlea-subtracted library can be individually examined to confirm that they are specifically expressed in the cochlea. Once these cDNAs are mapped, they are excellent candidates for any deafness disorder mapping to the same chromosomal interval. This approach was successful in the identification of the gene for DFNA9, an autosomal dominant, non-syndromic deafness with vestibular dysfunction (Robertson *et al*, 1998). A human fetal cochlear cDNA library was constructed and a novel cochlear gene, *COCH*, was isolated (Robertson *et al*, 1994; Robertson *et al*, 1997). COCH mapped to human chromosome 14q11.2-q13 (Robertson *et al*, 1997), within the locus for DFNA9 (Manolis *et al*, 1996) and mutation was demonstrated in affected individuals (Robertson *et al*, 1998).

cDNA libraries need not be of human origin. A novel approach by Heller and colleagues have identified 120 cDNA clones in a cDNA library constructed from chicken auditory epithelia that code for 12 genes that are ear-specific or highly-expressed in the ear (Heller *et al*, 1998), implicating their human homologues as candidate genes for deafness. Advances in these techniques should identify more candidate genes for human hearing disorders.

1.6.4. Mitochondrial genes

The human mitochondrial genome is a circular, extrachromosomal DNA molecule, inherited uniquely through the maternal line (Jacobs, 1997). Mitochondria serve a variety of metabolic functions, the most important being the synthesis of ATP by oxidative phosphorylation.

Hearing loss occurs as an additional symptom in a number of syndromic diseases caused by mitochondrial DNA defects. Mitochondrial syndromes associated with hearing loss include Kearns Sayre syndrome, Myoclonic epilepsy and ragged red fibres (MERRF), Mitochondrial encephalopathy, lactic acidosis and stroke-like episodes (MELAS) and Diabetes Mellitus (Reviewed in Fischel-Ghodsian, 1998).

Some sensorineural non-syndromic and antibiotic-induced hearing losses show a mitochondrial mode of inheritance. The first homoplasmic mutation associated with non syndromic deafness was identified in an Arab Israeli pedigree. An A1555G mutation in the mitochondrial 12S rRNA gene was identified as the pathogenic mutation, and the same mutation was also found to predispose individuals to aminoglycoside-induced hearing loss (Prezant *et al*, 1993). The postulated mechanism of aminoglycoside susceptibility is that the mutation makes the rRNA more similar to the bacterial rRNA, which is involved in aminoglycoside-induced bactericidal activity (Prezant *et al*, 1993). The role of the A1555G mutation in hereditary deafness and its relationship with aminoglycoside treatment was investigated in 70 unrelated Spanish families with sensorineural hearing loss (Estivill *et al*, 1998b). The

A1555G mutation was observed in 19 families with progressive and maternally transmitted deafness, making this mutation the most common cause of late-onset familial sensorineural deafness in the families studied. The same study also showed that aminoglycosides accelerated the development of deafness. The onset of deafness in patients treated with aminoglycosides was lower than the onset in those individuals who did not receive antibiotics (Estivill *et al*, 1998b). It has been suggested that the A1555G mutation alone is not severe enough to cause hearing loss. Not all the patients with the mutation became deaf, suggesting the involvement of other factors in the development of the hearing loss in affected individuals. A second mutation in the gene encoding tRNA ser(UCN) has been identified in a family with maternally inherited sensorineural deafness (Reid *et al*, 1994). The same mutation, A7445G, has also been associated with progressive hearing loss and palmoplantar keratoderma (Sevior *et al*, 1998).

In the case of the A1555G mutation, it was postulated that the mutation, which is in a highly conserved region of the mitochondrial 12S rRNA gene, elongates the tRNA binding region on the ribosome, with an adverse effect on the accuracy of the translation of the mRNA, leading to hair cell death (Prezant *et al*, 1993).

1.7. Syndromic deafness

The association of hearing loss with additional clinical features outside of the auditory system, account for approximately 30% of inherited forms of

deafness. Hundreds of syndromes have been described in which hearing loss is associated with a variety of anomalies such as eye, renal, nervous and pigmentary disorders (Winter and Baraitser, 1998). A large number of causative genes have been identified and, as is the case for non-syndromic deafness genes, the genes responsible for syndromic forms of deafness encode for a diverse range of molecules including extracellular matrix components, transcription factors and cytoskeletal components (Reviewed in Petit, 1996; Kalatzis and Petit, 1998).

Genetic mapping and gene identification in a rare syndromic form of deafness, the Jervell and Lange-Nielsen syndrome forms the basis of part of this thesis.

1.7.1. The Jervell and Lange-Nielsen syndrome (JLNS)

Jervell and Lange-Nielsen syndrome (JLNS) was first reported in 1957 in a Norwegian family (Jervell and Lange-Nielsen, 1957). Four of six children born to unrelated parents suffered from profound congenital deafness. The affected children had multiple fainting attacks from 3 to 5 years of age. There were no signs of heart disease clinically or on x-ray, the only pathologic finding was a prolongation of the QT interval on electrocardiogram (ECG). Three of the four children died suddenly following syncopal episodes.

Untreated, the syndrome has a very high mortality. Although the condition is very rare with an estimated prevalence of up to 10 per

million, a number of other cases have been reported since the original description, and autosomal recessive inheritance has been confirmed (Fraser, 1976).

1.7.1.2. Ear pathology in JLNS

The primary mechanism of hearing loss in patients with Jervell and Lange-Nielsen syndrome is thought to be cochleosaccular. Developmental abnormalities of the stria vascularis in mice and in humans may result in reduction of the normal osmotic pressure of the endolymphatic duct resulting in collapse of Reissner's membrane. The collapse of Reissner's membrane was one of the observations noted by Freidmann in 1966 on post-mortem examination of the inner ear of patients diagnosed with JLNS (Freidmann *et al*, 1966; Freidmann *et al*, 1968). Observations strikingly similar to those observed by Freidmann, were noted in isk-knockout mice (Vetter *et al*, 1996). Behaviourally, mice homozygous for a complete targeted disruption of the IsK gene exhibit hyperactivity, bi-directional circling, head tilt and head bobbing, classically described as shaker/waltzer phenotype. This behaviour is indicative of inner ear dysfunction. Examination of the inner ear of these mice showed the collapse of the Reissner's membrane and degeneration of the organ of Corti (Vetter *et al*, 1996); an inner ear pathology closely resembling that seen on post-mortem examination of human subjects who have died from JLNS (Friedmann *et al*, 1966; Friedmann *et al*, 1968). Controversy exists over the cardiac phenotype of this mouse. In some instances surface electrocardiogram (ECG) recordings of IsK

knockout mice showed a longer QT interval, and hence cardiac repolarisation, at slow heart rates (Drici *et al*, 1998), but additional investigations at the cellular level showed that ventricular repolarisation of IsK knockout mice was not prolonged and indistinguishable from control mice (Charpentier *et al*, 1998). The discrepancies over the cardiac phenotype in this mouse means it may not be the most appropriate model to study repolarisation abnormalities associated with the long QT syndromes, but the inner ear pathology of the IsK-knockout mouse suggests it as a model for the hearing loss associated with JLNS.

1.7.2. Romano Ward syndrome (RWS)

Phenotypically JLNS has similarities with Romano Ward syndrome. Romano and Ward independently described a condition of isolated cardiac syncope, not associated with deafness, inherited in an autosomal dominant manner (Ward, 1964; Reviewed in Ackerman, 1998a). Three individuals were described with prolonged QT intervals on electrocardiogram. The two affected children had syncopal attacks, with documented ventricular fibrillation. One of the children died at 18 months (Ward, 1964). This form of long QT syndrome is more common than Jervell and Lange-Nielsen, with an estimated incidence of 1 in 10000 (Reviewed in Wang, Q. *et al*, 1998).

Fraser speculated that the two conditions, JLNS and RWS, might have a common pathogenesis and the connection between the cardiac and auditory defect in JLNS might be due to electrolyte imbalance (Fraser,

1976). It was also suggested that individuals with RWS might be heterozygous for a mutant allele and those with recessive JLNS homozygous for the same allele or a different allele at the same locus. Against this hypothesis was the absence of syncope and sudden death in normal hearing relatives of individuals with JLNS.

The progress in the molecular genetics of Romano Ward syndrome has been very rapid. Four genes have been implicated in causing isolated long QT syndrome: HERG, SCN5A, KVLQT1, ISK and a fifth locus on chromosome 4 for which the gene has not yet been identified (Curran *et al*, 1995; Wang *et al*, 1995; Wang *et al*, 1996; Splawski *et al*, 1997a; Schott *et al*, 1995). The known genes all encode components of ion channels. HERG encodes a potassium channel, which underlies I_{kr}, the rapidly-activating component of the delayed rectifier current (Sanguinetti *et al*, 1995). SCN5A encodes an α-subunit of a cardiac sodium channel, KVLQT1 encodes an α-subunit of a cardiac potassium channel and ISK (minK) encodes a unique transmembrane β-subunit. KVLQT1, the product of the KVLQT1 gene has been shown to associate with IsK, to form a channel reproducing the properties of I_{ks}, the slowly-activating component of the delayed rectifier current (Barhanin *et al*, 1996; Sanguinetti *et al*, 1996a).

Besides the genetic factors, long QT syndrome can be caused by acquired factors such as cardiac ischaemia, metabolic abnormalities and

medications including antiarrhythmic drugs, antidepressants and antihistamines (Reviewed in Ackerman, 1998a).

1.7.3. Ion channels

Ion channels are macromolecular protein tunnels that span the lipid bilayer of cell membranes. They form pores that allow the passage of millions of ions per second. Ion channels are classified according to the type of ion they allow to pass, for example potassium, sodium, chloride and calcium, and according to how they are gated, for example, changes in transmembrane voltage, extracellular ligand or intracellular secondary messenger (Hebert, 1998). Ion channels regulate a wide variety of cellular functions. Two critical roles are the generation of electrical impulses and the maintenance of salt balance in fluids.

1.7.4. The cardiac action potential

A crucial role for ion channels in the heart is the orchestration of the cardiac action potential. Voltage-activated sodium, calcium and potassium ion channels are the principal ion channels responsible for the cardiac action potential in the ventricular myocyte. The action potential is due to a sequence of permeability changes to sodium and potassium, and can be divided into 5 phases, as illustrated in figure 1.9.

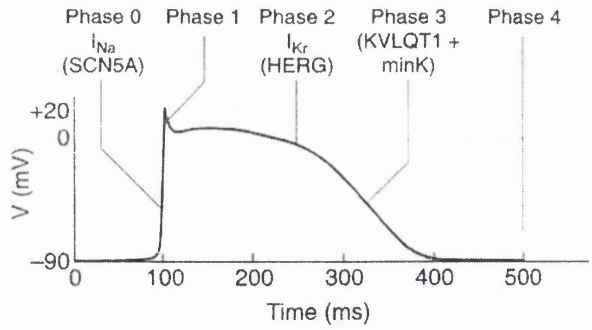

Figure 1.9.

The five phases of the cardiac action potential. Reproduced from Wang, Q. et al, 1998.

The underlying defect in Long QT syndrome is aberrant cardiac repolarisation, affecting phases 2 and most commonly phase 3 (figure 1.9). Cardiac repolarisation requires the action of a specific potassium current, the delayed rectifier current. This current has two components: a rapidly-activating component, I_{kr}, and a slowly-activating component, I_{ks}.

1.7.5. The electrocardiogram (ECG)

The electrocardiogram (ECG) is the summation on the surface of the body of the individual action potentials from throughout the heart. The spread of the cardiac impulse through the heart gives rise to the main deflections of the ECG: P, QRS, T, as illustrated in figure 1.10. The PR interval represents the time taken for the cardiac impulse to spread over the atrium and through the AV node and His-Purkinje system. The QRS complex represents the spread of depolarisation through the ventricles and the QT interval represents the total time from the onset of ventricular depolarisation to the completion of repolarisation. The QT interval is measured from the beginning of the Q wave to the end of the T wave.

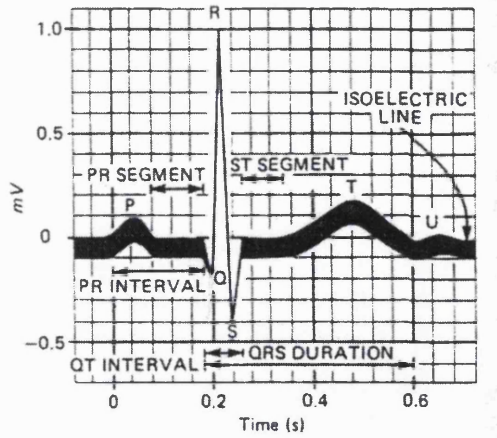

Figure 1.10.

Waves of the ECG. From "Review of Medical Physiology by WF Ganong.

The registration on the ECG of electrical disturbances of the heart plays an essential diagnostic role.

1.7.5.1. Prolonged QT interval

The ECG defect observed in patients with long QT syndrome is a prolonged QT interval. Figure 1.11 illustrates a normal and prolonged QT interval. The QT interval represents the total time from the onset of ventricular depolarisation to the completion of repolarisation; a prolonged QT interval is an indication of abnormal cardiac repolarisation.

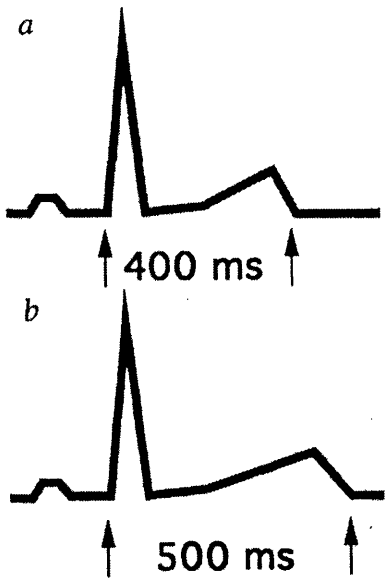

Figure 1.11.
Representation of a normal (Top) and prolonged (bottom) QT interval. Reproduced from Schwartz, 1994.

The importance of a prolonged QT interval is its association with a risk of ventricular tachycardias, in particular "Torsade de Pointes". "Torsade de Pointes" describes a form of polymorphic ventricular arrhythmia which can degenerate into ventricular fibrillation. Ventricular fibrillation is a rapid uncoordinated, fluttering contraction of the ventricles resulting in the loss of cardiac output. This in turn causes syncope (fainting attack with loss of consciousness), and if not defibrillated, sudden death. This form of ventricular fibrillation is responsible for the symptoms of syncope and sudden death in long QT syndrome patients.

1.7.6. Diagnosis of Long QT syndrome.

The diagnosis of long QT syndrome is primarily based on QT interval corrected for heart rate, QTc, which is calculated using Bazett's formula

(QTc= QT/√RR). Two major factors for diagnosis are considered. One is clinical symptoms, which include the presence of syncope, the age of onset of symptoms and the occurrence of family history and the other is the length of the QT interval and appearance of the T waves (Schwartz *et al*, 1993; Ackerman, 1998a). A QTc of greater than 440 milliseconds (ms) is considered to be abnormal (Schwartz *et al*, 1993). In addition, affected persons with Jervell and Lange-Nielsen syndrome also suffer from profound, congenital, sensorineural deafness.

CHAPTER 2: MATERIALS AND METHODS

2.1. MATERIALS

All chemicals were obtained from Sigma, except for the following;

Restriction enzymes were obtained from New England Biolabs.

Polynucleotide kinase was supplied by Promega.

Taq polymerase, 10x buffer and 50mM $MgCl_2$ were supplied by Bioline.

α-^{32}P-dCTP and γ-^{32}P dATP, Qiagen plasmid DNA extraction kit and Hybond N+ membrane were supplied by Amersham International.

Protogel™ and Sequagel™ was supplied by National Diagnostics.

MDE™ was supplied by Flowgen.

dRhodamine cycle-sequencing kit was supplied by Perkin Elmer Applied Biosystems.

Agarose, 100bp ladder, Superscript II, DNase I, NZY broth, LB broth and TRIZOL™ were supplied by GibcoBRL.

Quikchange™ site-directed mutagenesis kit was supplied by Stratagene.

dNTPs, Ficoll-Paque and Ready-To-Go™ DNA labelling kit was supplied by Pharmacia Biotech.

2.1.1. Primers

All primers were synthesised by MWG and Genosys with the exception of those used in site-directed mutatgenesis, which were synthesised by PE Applied Biosystems. PCR reactions were carried out at an annealing temperature of 55°C with 1.5mM $MgCl_2$, unless stated otherwise. Primers used in the genome search and for linkage on the X-chromsome were

microsatellite markers part of Research Genetics mapping set 6.0, designed by the Co-operative Human Linkage Centre (CHLC) (http://www.chlc.org).

Primer sequences for the additional microsatellites analysed are listed below. Sequences were obtained from GDB (http://www.hgmp.mrc.ac.uk) or published sources where indicated.

2.1.1.1. X chromosome

DXS995

Forward 5' AAGGGGCTGCTGATGATTAT 3' 58°C

Reverse 5' AATGCGTTCCCCAAATGT 3'

DXS1002

Forward 5' CTGCTACCCTTTAGTTCTCTC 3' 56°C

Reverse 5' TCCATGTTGCTGCGAA 3'

DXS986

Forward 5' CCTAAGTGCTCATCATCCCA 3' 58°C

Reverse 5' AGCTCAATCCAAGTTGCTGA 3'

DXS990

Forward 5' AGCTATATGACCAGTACAAACATAC 3' 56°C

Reverse 5' GACAGAAGGGACATCAACTC 3'

DXS1106

Forward 5' TATGAGAACTCCCTAAACAAA 3'

Reverse 5' TGATGCACCAAATACCA 3'

CA-PLP

Forward 5'	CAACAGCATCTGGACTATCTTG 3'	58°C
Reverse 5'	CCCAATGCTTGCACATAAATTG 3'	

DXS1230

Forward 5'	TATTGGGCAGAGCCTGT 3'	
Reverse 5'	TCCCGTTGTGGCATAAA 3'	

COL4A5, Barker *et al*, 1992

Forward 5'	TATAATGGAAGTTATTCATGTAGAC 3'	57°C
Reverse 5'	GTGATTCAGATGTTACTTAAGGAC 3'	

DXS1210

Forward 5'	TCATGTGAAACTCCAGAACCAGTA 3'	59°C
Reverse 5'	GCCCTCAAATCTTCAGAGAGTGTA 3'	

DXS1231

Forward 5'	AAAAGCACCCTCATAGGAACC 3'	59°C
Reverse 5'	GGCTCTCTGCACCAGCAT 3'	

DXS1220

Forward 5'	AGCGAGAGTCTGACCCAC 3'	58°C
Reverse 5'	GGGGCCTATAAAATGGAG 3'	

DXS1001

Forward 5'	TACAAGTAACCCTCGTGACA 3'	53°C
Reverse 5'	GTTATGGAATCAATCCAAGTG 3'	

DXS178

Forward 5'	AGTTCCAAACAAAATCCCAAGA 3'	52°C
Reverse 5'	ATTGTAAAACTTGATATTTGCT 3'	

DXS8020

Forward 5'	CTAATGGCCCTGGATG 3'	

Reverse 5' ACAATTCTGTATAGACTTTGTGTG 3'

DXS6809

Forward 5' TGAACCTTCCTAGCTCAGGA 3'

Reverse 5' TCTGGAGAATCCAATTTTGC 3'

5' DYS I

Forward 5' ATAAATGGATAAAAAAGTGG 3' 50^0C

Reverse 5' TTATATAAATGAATATTCCG 3'

DMD Intron 44

Forward 5' TCCAACATTGGAAATCACATTTCAA 3' 54°C

Reverse 5' TCATCACAAATAGATGTTTCACAG 3'

DMD intron 45

Forward 5' GAGGCTATAATTCTTTAACTTTGGC 3' 54°C

Reverse 5' CTCTTTCCCTCTTTATTCATGTTAC 3'

DMD Intron 49

Forward 5' CGTTTACCAGCTCAAAATCTCAAC 3' 54°C

Reverse 5' CATATGATACGATTCGTGTTTTGC 3'

DMD Intron 50

Forward 5' AAGGTTCCTCCAGTAACAGATTTGG 3' 54°C

Reverse 5' TATGCTACATAGTATGTCCTCAGAC 3'

DMD Intron 62/63

Forward 5' TTCTTCGTCGATACCCCCATTCCA 3' 60°C

Reverse 5' CTCTTTGAGTTTGAAGTTACCTGA 3'

3' STR HI

Forward 5' ACGACAAGAGTGAGACTCTAG 3' 51°C

Reverse 5' ATATATCAAATATAGTCACTTAGG 3'

2.1.1.2. Chromosome 1

D1S255

Forward 5' TTAGCAAATCCCAAGCAATA 3'

Reverse 5' GTGATGGTGGTAAAGGCAGA 3'

D1S193

Forward 5' ACTCTAGCCTGGGTGACAAG 3'

Reverse 5' AGACTGGGAAAATGCAAATG 3'

D1S194

Forward 5' AGCTAGGCTGTAAGTTTTCTGCTC 3'

Reverse 5' GTCTCTTGCTGGACTGGGA 3'

D1S 196

Forward 5' GGCTGTGGGTGTTTCTCCTA 3'

Reverse 5' AGCCCTCATGNCTTTACATTCT 3'

D1S210

Forward 5' CCTCAGTTCATTCCCCATAA 3'

Reverse 5' AGCTGAATCTCACCCAATAACTA 3'

2.1.1.3. Chromosome 2

D2S144

Forward 5' TCTCCCTGACAGACTCTGCG 3' 60 °C

Reverse 5' GCTGCATAGGCCGTACTGAG 3'

D2S171

Forward 5' TGGCAGGCAGAGGTTA 3'

Reverse 5' GTGCAAAGGCCCAGAG 3'

D2S158

Forward 5' CCACCATATTCCAGTCTGAGC 3'

Reverse 5' ATGAAACAACCAACCTGAGAATA 3'

2.1.1.4. Chromosome 3

D3S1298

Forward 5' AGCTCTCAGTGCCACCCC 3'

Reverse 5' GAAAAATCCCCTGTGAAGCG 3'

D3S1100

Forward 5' GGTTTCATATACCATCAATCCCAC 3'

Reverse 5' GTACACCATCATGAGGAGTCTGG 3'

D3S1211

Forward 5' CAGGGCTTGTGGGATTAGAA 3'

Reverse 5' ATTTCAGATTTCAGGACAAGGG 3'

D3S1767

Forward 5' ATGCTGTATTTCAACACACAGG 3'

Reverse 5' AATTAGGCACGGTAGCACAC 3'

D3S1289

Forward 5' AAAGCAACTTGTAAGAGAGCA 3'

Reverse 5' CTCCTAGATATAATCACTGGCA 3'

D3S1582

Forward 5' CAGCAGGTACTATGAAAGCCTGT 3' 61 °C

Reverse 5' GGAACAGCCCTATGGTTCAC 3'

2.1.1.5. Chromosome 4

D4S402

Forward 5' CTTACTGTGTTGCCCAAGGT 3'

Reverse 5' AGCTCTATGATTCATTTCAAGTTTG 3'

D4S430

Forward 5' TAACCCTGTATATGTTAATGTGC 3'

Reverse 5' GGACCCAGTCTTGCTATG 3'

D4S406

Forward 5' CTGGTTTTAAGGCATGTTTG 3'

Reverse 5' TCCTCAGGGAGGTCTAATCA 3'

D4S1614

Forward 5' CATCTAGGAGAATCAGTACTTGG 3'

Reverse 5' TTACCATGAGCATATTTCCA 3'

D4S412

Forward 5' ACT ACCGCCAGGCACT 3'

Reverse 5' CTAAGATATGAAAACCTAAGGGA 3'

D4S432

Forward 5' ACTCTGAAGGCTGAGATGGG 3'

Reverse 5' CTGAACCGCAGATCCCC 3'

2.1.1.6. Chromosome 5

D5S640

Forward 5' CCCACATAGCACTCACAGC 3'

Reverse 5' GCCCAGTTGCCACCTT 3'

D5S410

Forward 5' TTCTGCTAGTTTATCCCACTG 3'

Reverse 5' TCATGCCACACATTGTTT 3'

D5S412

Forward 5' GCTGGGGAATGTTACAGTAT 3'

Reverse 5' CCCATGAGAACTTCCACATA 3'

2.1.1.7. Chromosome 7

D7S483

Forward 5' AGTGGTCATTAGCCTTGGCAAAATC 3' 56°C

Reverse 5' AACCAGAGTTGTAAGCCATGAAAGT 3'

D7S636

Forward 5' GGAGTGACTGGGCAGGAA 3' 56°C

Reverse 5' AGCTTGTGTGGGGTTTCA 3'

D7S505

Forward 5' ACTGGCCTGGCAGAGTCT 3' 56°C

Reverse 5' CAGCCATTCGAGAGGTGT 3'

D7S629

Forward 5' ATTTCTGATTCAAAATGCCG 3'

Reverse 5' AATGTTATACCCAAGGATTTCTGT 3'

D7S673

Forward 5' GGGGNCCTTGAGAAGT 3'

Reverse 5' TCCCAGTCCTGTGGCTAC 3'

D7S529

Forward 5' AAATTCTAGACATCGCCTGTAA 3'

Reverse 5' GGTACCATCACCACAATCAA 3'

D7S501

Forward 5' CACCGTTGTGATGGCAGAG 3'

Reverse 5' ATTTCTTACCAGGCAGACTGCT 3'

D7S523

Forward 5' CTGATTCATAGCAGCACTTG 3'

Reverse 5' AAAACATTTCCATTACCACTG 3'

D7S496

Forward 5' AACAACAGTCAACCCACAAT 3' 53 °C

Reverse 5' GCTATAACCTCATAANAAACCAAAA 3'

2.1.1.8. Chromosome 9

D9S50

Forward 5' GATCCTTTTCATCTTCTGAC 3'

Reverse 5' GAGGGACGGAGCAACTGAT 3'

D9S301

Forward 5' AGTTTTCATAACACAAAAGAGAACA 3'

Reverse 5' ACCTAAATGTTCATCAAAAGAGG 3'

D9S166

Forward 5' AAATCATGCAATTCATTTCA 3'

Reverse 5' TCCTAATTCACTGGGAAAAC 3'

D9S175

Forward 5' GTAATGTGCTAAATACCAGAGTTG 3'

Reverse 5' CCCTTACCTAGAATGCCC 3'

D9S43

Forward 5' TTCTGATATCAAAACCTGGC 3'

Reverse 5' AAGGATATTGTCCTGAGGA 3'

D9S1862

Forward 5' CATGAGAGCACTGTATGAGGCC 3'

Reverse 5' ACATCAGGATTGTGGGTTC 3'

2.1.1.9. Chromosome 10

D10S193

Forward 5' TATATGCAGTTTGGGATGGG 3'

Reverse 5' ATTGGGCTGTGCCTACACTT 3'

D10S537

Forward 5' CCTACTGTGCCTGGCTAGA 3'

Reverse 5' ATTTGGATGAAACCCACG 3'

2.1.1.10. Chromosome 11

D11S922

Forward 5' GGGGCATCTTTGGCTA 3'

Reverse 5' TCCGGTTTGGTTCAGG 3'

D11S4046

Forward 5' ACTCCAGCCTGGGAAAC 3' 56°C

Reverse 5' TGATAGACACACCCATTGC 3'

D11S131

Forward 5' CCCGTATGGCAACAGG 3' 56°C

Reverse 5' TGTGCATGTNCATGAGTG 3'

D11S4088

Forward 5' GGGCAGAGGCAGTGGAG 3' 56°C

Reverse 5' GCATGTTTCGGGGGTG 3'

D11S4146

Forward 5' AACACGAGGTTAAGCAGAG 3' 56°C

Reverse 5' GAATGAAGAATTTTCCAAACTAC 3'

D11S1345

Forward 5' TGCCACAGTAATACATGTGTGTAAT 3'

Reverse 5' TAGTCAGTGCTGAGCCCATA 3'

D11S934

Forward 5' GCTGTCCCTGACAACTACATGC 3'

Reverse 5' TTCCATCAGAACTGGGAATGAG 3'

D11S1320

Forward 5' AACATTACTAAAAGGTTAAATGAGC 3'

Reverse 5' ATTAAGGCACCAAATGGG 3'

D11S911

Forward 5' CTTCTCATGCTTGACCATTT 3'

Reverse 5' CTTCTGAACAATTGCCACAT 3'

D11S937

Forward 5' CTAATAAACAAATCCCTCTACCTCC 3'

Reverse 5' TAGTCAGTCAGGGACCCAAGT 3'

D11S925

Forward 5' AGAACCAAGGTCGTAAGTCCTG 3'

Reverse 5' TTAGACCATTATGGGGGCAA 3'

D11S1347

Forward 5' CAGCCTGGGCAATAGT 3'

Reverse 5' GCAGCAACAACAACAATAA 3'

D11S527

Forward 5' GCCCCTCTACTTGTCTGGAG 3'

Reverse 5' ATGCGGCTCCAAGACAAGTTC 3'

2.1.1.11. Chromosome 13

D13S115

Forward 5' TGTAAGGAGAGAGAGATTTCGACA 3' 57 °C

Reverse 5' TCTTAGCTGCTGGTGGTGG 3'

D13S175

Forward 5' TATTGGATACTTGAATCTGCTG 3'

Reverse 5' TGCATCACCTCACATAGGTTA 3'

OMP

Forward 5' CTGAAAGGTAAAACAATAATGC 3' 56 °C

Reverse 5' TGTCCTCCTACCACTAATGC 3'

D13S292

Forward 5' TAATGGCGGACCATGC 3' labelled with FAM 53°C

Reverse 5' TTTGACACTTTCCAAGTTGC 3'

D13S141

Forward 5' GTCCTCCCGGCCTAGTCTTA 3' 57°C

Reverse 5' ACCACGGAGCAAAGAACAGA 3' labelled with FAM

D13S143

Forward 5' CTCATGGGCAGTAACAACAAAA 3' labelled with TET

Reverse 5' CTTATTTCTCTAGGGGCCAGCT 3'

D13S232

Forward 5' TGCTCACTGCTCTTGTGATT 3' labelled with HEX

Reverse 5' GGCACAGAAATAAATGTTGATG 3'

2.1.1.12. Chromosome 14

D14S70

Forward 5' ATCAATTTGCTAGTTTGGCA 3'

Reverse 5' AGCTAATGACTTAGACACGTTGTAG 3'

D14S253

Forward 5' CCAGCATAAAAAACAGACAT 3'

Reverse 5' TGTGCCCGGACAGATT 3'

D14S286

Forward 5' CATTAAGCGAAATTGGAGAA 3' 53 °C

Reverse 5' TTGTTTGGCCTTTGTTTATG 3'

2.1.1.13. Chromosome 15

D15S132

Forward 5' CTGATAATAAAACCAGGAAGACAC 3'

Reverse 5' TATTGGCCTGAAGTGGTG 3'

D15S123

Forward 5' AGCTGAACCCAATGGACT 3'

Reverse 5' TTTCATGCCACCAACAAA 3'

2.1.1.14. Chromosome 17

D17S122

Forward 5' CAGAACCACAAAATGTCTTGCATTC 3'

Reverse 5' GGCCAGACAGACCAGGCTCTGC 3'

D17S805

Forward 5' ATCACTTGAACCTGAGGGG 3' 60 °C

Reverse 5' AATGAGATACCGATCCATGC 3'

D17S842

Forward 5' AGCTCACTGTAGCCTATCCTC 3' 60 °C

Reverse 5' AAATGCAGAGTCAAACTTGTAGA 3'

2.1.1.15. Chromosome 19

D19S208

Forward 5' CCCAGTGGGCCTTAGAGATA 3'

Reverse 5' GGATGCCTGACGGTGTTTAC 3'

D19S224

Forward 5' AACACCATTCCTCATCTTCC 3'

Reverse 5' CCCAGGCCCTATCTGA 3'

APOC2

Forward 5' CATAGCGAGACTCCATCTCC 3'

Reverse 5' GGGAGAGGGCAAAGATCGAT 3'

2.1.1.16. Chromosome 21

D21S212

Forward 5' CATTTTAATGAACACCGCTC 3'

Reverse 5' GGCCTCCTGGAATAATTCTC 3'

D21S1225

Forward 5' AGAAGTGCCTGGATTCAGC 3' 58 °C

Reverse 5' AGGTTTTACAAATAAGCAGAAAGG 3'

D21S1575

Forward 5' GAAACCCATCTCACATGCAG 3' 57 °C

Reverse 5' GAAGTGCTCTAAGAACTTGC 3'

D21S261

Forward 5' AAAACACCTTACCTAAAACAGCA 3'

Reverse 5' AGATGATGGTGAGTCCTGAG 3'

D21S1895

Forward 5' AGTCCTACTGATAAACTGTGGGC 3' 56°C

Reverse 5' CTGTCTCATAAGAACCTACCTGG 3'

D21S1252

Forward 5' TCTGTCTTTGTCTCACTATCTG 3' 56°C

Reverse 5' GCAATGCTCTGTGGCT 3'

D21S1254

Forward 5' AAATACTGATGATCCTTAATTTTGG 3' 56°C

Reverse 5' GGTGGCTGAGCGAGAC 3'

D21S268

Forward 5' GGGAGGCTGAAGCGAGG 3'

Reverse 5' CCCCGCTGGCAGTGTA 3'

D21S265

Forward 5' TTAAAGCAATCAATCATGG 3'

Reverse 5' GGGTTCTGTGAATATGGG 3'

D21S1253

Forward 5' GAAGAATCTCCCGAACCAGG 3'

Reverse 5' AAGACCAGTGTTATTCAGAGCC 3'

D21S269

Forward 5' AAAAAGTCTCCCATTATACAATAG 3'

Reverse 5' CCCTTTGCTTTACAAATCT 3'

D21S1258

Forward 5' CGTTTCAATATAGACCAGATAAAGG 3'

Reverse 5' AGGTCAACTGCCAAAATCTAAG 3'

D21S263

Forward 5' TTGGCTTTGGAACCAG 3'

Reverse 5' CATCAGCAAGGGTCCTC 3'

2.1.1.17. DDP (Jin *et al*, 1996)

Exon1

Forward 5' GCGGAGTTCGTCTCTGCAAGC 3' 62°C

Reverse 5' GTAGGTACAGTGTTTAGGTC 3'

Exon 2

Forward 5' GTTCACTGGCTAGATTCC 3' 62°C

Reverse 5' CTAAGCAACAAAAAGGGAC 3'

2.1.1.18. POU3F4 (de Kok *et al*, 1995)

Primer set 1a and 1b

Forward 5'	ACTAGTAGGGGATCCTCACCG 3'	61°C
Reverse 5'	CCGTCGCTCAGACTGGTCAC 3'	

Primer Vb

Reverse 5'	GCCTCCTCGCTTCCTCCA 3'	61°C

2.1.1.19. ISK (Tesson *et al*, 1996)

1F	5' GATCCTGTCTAACACCAC 3'	56°C
2R	5' AATGGGTCGTTCGAGTGC 3'	
3F	5' TACATCCGCTCCAAGAAG 3'	56°C
4R	5' TCGTCTCAGGAAGGTGTG 3'	

2.1.1.20. KVLQT1 cDNA (Lee *et al*, 1997)

LQT109	5' AGCAAGCGCGGAAGCCTTACGATGTGC 3'	64°C
LQT209	5' AGCTGCGTCACCTTGTCTTCTACTCGG 3'	

2.1.1.21. HPRT (Jolly *et al*, 1983)

Forward	5' CCACGAAAGTGTTGGATATAAGC 3'	58°C
Reverse	5' GGCGATGTCAATAGGACTCCAGATG 3'	

2.1.2. Solutions

TE: 10mM Tris (tris(hydroxymethyl)aminomethane)
1mM EDTA pH adjusted to 8.0 with HCl.

TAE: 0.38M Tris

0.12M NaAc

0.02M EDTA

pH adjusted to 7.7 with glacial acetic acid

5 x TBE: 0.089M Tris

0.089M Boric acid

2mM EDTA pH 8.0

20 x SSC: 2.9M NaCl

0.3M sodium citrate

pH adjusted to 7.0 with sodium hydroxide

Loading dye: 50% glycerol

10mm EDTA

0.05% bromophenol blue

0.05% xylene cyanol

Formamide dye: 95% Formamide

20mM EDTA

0.05% bromophenol blue

0.05% xylene cyanol

Loading dye for the ABI 377:

17% Loading dye (PE Applied Biosystems)

83% Formamide

Loading dye for Heteroduplex gels:

50% sucrose

0.2% bromophenol blue

0.3% xylene cyanol

2.1.2.1. DNA extraction solutions

Nuclei lysis buffer: 10mM tris pH8.0

400mM NaCl/ 2mM Na-EDTA

Proteinase K solution:

2mM Na-EDTA/ 1%SDS

2mg/ml Proteinase K

STE buffer:

100mM MaCl

10mM Tris (pH 8.0)

10mM EDTA

Storage buffer:

482.5µl STE buffer

0.2mg/ml Proteinase K

0.5% SDS

2.1.2.2. Qiagen DNA preparation buffers

Buffer P1: 50mM Tris-HCl

10mM EDTA

100μg RNaseA/ml

Buffer P2: 0.2M NaOH

1% SDS

Buffer P3: 3.0M potassium acetate pH 5.5 at 4°C

Buffer QBT: 750mM NaCl

50mM MOPS

15% ethanol

0.15% Triton X-100 pH 7.0

Buffer QC: 1.0mM NaCl

50mM MOPS

15% ethanol pH7 .0

Buffer QF: 1.25mM NaCl

50mM tris-HCl

15% ethanol pH 8.5

2.1.2.3. Southern blotting solutions

PEG Hybridisation buffer:

0.125M Na_2HPO_4, pH 7.2 with NaH_2PO_4

0.25M NaCl

1.0mM EDTA

7% SDS

10% PEG 8000 (BDH Chemicals Ltd.)

50μg/ml denatured salmon sperm DNA

Denaturation solution:

1.5M NaCl

0.5M NaOH

2.1.2.4. Media solutions

LB (Luria-Bertani) medium:

10g/l Bactotryptone

5g/l Bacto-yeast extract

10g/l NaCl

LB agar: 1 litre of LB broth with 15g bacto-agar added before autoclaving

NZY broth: 5g/l NaCl

2g/l $MgSO_4.7H_2O$

5g/l yeast extract

10g/l NZ amine (casein hydrolysate)

2.1.2.5. Solutions in supplied kits

ABI PRISM™ dRhodamine Terminator cycle sequencing

Terminator ready reaction mix:

A-dye Terminator labeled with dichloro[R6G]

C-dye Terminator labeled with dichloro[TAMRA]

G-dye Terminator labeled with dichloro[R110]

T-dye Terminator labeled with dichloro[ROX]

deoxynucleoside triphosphates (dATP, dCTP, dITP, dTTP)

AmpliTaq DNA polymerase, FS, with thermally stable pyrophosphatase

$MgCl_2$

Tris-HCl buffer, pH 9.0

DNA labelling

Reaction mix: dATP, dGTP, dTTP, FPL*pure*® klenow fragment and random oligodeoxyribonuclotides

Site-directed mutagenesis

Reaction mix: 100mM KCl

100mM $(NH_4)_2SO_4$

200mM Tris-HCl pH8.8)

20mM $MgSO_4$

1% Triton X-100

1mg/ml nuclease-free bovine serum albumin (BSA)

2.2. METHODS

2.2.1. Preparation of DNA and RNA

2.2.1.1. Extraction of human DNA from blood

DNA was extracted from 10ml venous blood, stored at -70°C in EDTA-containing tubes. EDTA tubes were defrosted by removing the caps and inverting inside a 50ml plastic falcon tube. Ice cold distilled water was added to each blood sample to a final volume of 50ml. Tubes were inverted gently to mix and centrifuged at 900*g* at 4°C for 20 minutes. The supernatant was discarded into chloros, leaving the nuclear pellet. 25ml of 0.1% NP40 was added, and the pellet broken by vortexing. Tubes were centrifuged at 900*g*, 4°C for a further 20 minutes. The supernatant was discarded, 3ml of cold nuclei lysis buffer was added and the pellet resuspended by vortexing. 200µl of 10% SDS and 600µl fresh proteinase K solution was added to this, and the sample incubated at 60°C for 1 hour. Protein was precipitated by adding 1ml of saturated ammonium acetate solution and shaking vigorously for 15 seconds. After allowing to stand for 15 minutes, the sample was centrifuged at 900*g* for 15 minutes. The supernatant was removed to a falcon tube and to this was added 2 volumes of absolute ethanol to precipitate the DNA. DNA was spooled out using a sealed glass pipette and dissolved in 300µl of TE.

2.2.1.2. Extraction of DNA from lymphoblastoid cell lines and urine

Cell suspension was centrifuged at 900*g* for 20 minutes at 4°C. The supernatant was discarded, leaving the cell pellet. 25ml of 0.1% NP40 was added, and the pellet broken by vortexing. DNA was extracted as described in section 2.2.1.1.

2.2.1.3. DNA isolation from a mouth swab (Muelenbelt *et al*, 1995)

The inside of the mouth, especially cheek and gums, were wiped using one end of a clean cotton bud. This bud was then placed sample end first in a plastic 50ml falcon tube containing 10ml of storage buffer. A maximum of 10 cotton buds were placed in each falcon tube. The sample was then stored at room temperature prior to isolation of DNA.

In order to lyse the buccal cells, the falcon tube containing the cotton buds in storage buffer was placed in a waterbath at 65°C for 2 hours. The cotton buds were then placed in a 20ml syringe upside down in a falcon tube and centrifuged at 400*g* for 1 minute. The syringe containing the dry cotton buds was removed and the lysation product transferred to 1.5ml eppendorf tubes. To this was added 1 volume of phenol/chloroform/isoamyl alcohol (24:24:1) to each tube, and mixed gently by rotation. Tubes were then centrifuged at 14000 rpm for 5 minutes. The aqueous upper layer was removed to a clean 1.5ml eppendorf, to which was added 1 volume of chloroform/isoamyl alcohol (24:1). The sample was mixed gently by rotation and the tubes centrifuged at 14000 rpm for 5 minutes. The aqueous layer was removed to a clean 1.5ml eppendorf tube. To this was added 0.1 volume of 3M NaAc (pH 5.2) and 1 volume of 98% isopropanol. Tubes were then placed at -20°C for a minimum of 30 minutes, after which the tubes were centrifuged at 14000 rpm for 30 minutes. The 98% isopropanol was removed and discarded, and the pellet washed with 500µl of 70% ethanol. Tubes were centrifuged for 5 minutes at 14000 rpm. This washing step was repeated. The 70% ethanol was removed and

discarded, and the pellet was allowed to air-dry before re-dissolving in 100μl TE.

2.2.1.4. Preparation of Plasmid DNA

DNA was extracted using the Qiagen "maxi-prep" kit and the solutions and protocol supplied.

A single bacterial colony grown on LB plates was inoculated into 5ml of LB, and ampicillin added to a final concentration of 50μg/ml. This was incubated overnight at 37°C. The next day, the 5ml culture was added to 500ml of LB in a 2L conical flask with a final concentration of ampicillin of 50μg/ml. This was incubated overnight in a shaking incubator at 37°C. The next day, the culture was centrifuged at 6000*g* for 15 minutes at 4°C. The bacterial pellet was re-suspended in 10ml of buffer P1. 10ml of buffer P2 was added, the tube inverted gently to mix and left to stand at room temperature for 5 minutes. 10ml of ice cold buffer P3 was then added and the sample placed on ice for 20 minutes. The sample was then centrifuged at 20000*g* for 30 minutes at 4°C. The supernatant was removed to a clean tube and re-centrifuged for 15 minutes. This supernatant was applied to a Qiagen maxi-prep column that had been equilibrated with 10 ml of buffer QB. 2x30ml of buffer QC was then added to the column, and the DNA eluted into a clean tube on addition of 15ml of buffer QF. 0.7 volumes of isopropanol was added, the sample mixed and immediately centrifuged at 15000*g* for 30 minutes at 4°C. The DNA pellet was washed with 70% ethanol, and centrifuged at 15000*g* for

10 minutes. The supernatant was discarded, and the pellet allowed to air-dry before being re-suspended in 200μl of TE.

2.2.1.5. Isolation of RNA from lymphoblastoid cell lines, urine and fetal tissues

Human tissues were provided by the Medical Research Council-funded Human Embryo bank maintained at the Institute of Child Health. Fetal tissue samples were homogenised in 1ml (or 10x volume) of TRIZOL using a DEPC-treated glass homogeniser. For urine samples and lymphoblastoid cell lines, cells were pelleted by centrifugation and lysed with 1ml of TRIZOL reagent per 5-10 x 10^6 cells. The homogenised samples were incubated for 5 minutes at room temperature to allow the nucleoprotein complexes to completely dissociate. 0.2ml chloroform per 1ml TRIZOL used in the initial homogenisation was added and the sample shaken vigorously for 15 seconds. After incubation at room temperature for 3 minutes, the tubes were centrifuged at 12000*g* for 15 minutes at 2 to 8°C. Following centrifugation, the colourless upper aqueous phase was transferred to a clean tube. To this was added 0.5ml of isopropanol per 1ml TRIZOL reagent used for the initial homogenisation, to precipitate the RNA. Samples were incubated at room temperature for 10 minutes, then centrifuged at 12000*g* for 10 minutes at 2 to 8°C. The supernatant was discarded and the pellet washed in 1ml 75% ethanol. The sample was allowed to air-dry before resuspending in 100-500μl of Rnase-free water.

2.2.1.6. RNA extraction from whole blood

2ml fresh venous blood was diluted with an equal amount of PBS. The diluted blood sample was carefully layered upon 3ml Ficoll Paque in a clear plastic falcon tube and centrifuged at 400*g* for 40 minutes. Without disturbing the interface, the upper layer was drawn off using a pasteur pipette, and discarded. The interface (lymphocyte layer) was then transferred to a clean falcon tube. The cells were gently suspended in 6ml of PBS and centrifuged at 100*g* for 10 minutes. The supernatant was removed and discarded, and the cells gently re-suspended in 6ml of PBS. The sample was centrifuged at 100*g* for 10 minutes. The supernatant was removed and discarded. 500µl TRIZOL reagent was added to the cells and RNA extracted as described in section 2.2.1.5.

2.2.2. Polymerase chain reaction (PCR)

25-250ng of DNA was amplified in the polymerase chain reaction (PCR). Reaction mix consisted of DNA, 50pmol of each primer, 5µl of 10 X Buffer consisting of 160mM $(NH4)_2SO_4$, 670mM Tris-HCl pH8.8 at 25°C (Bioline), 1.5mM $MgCl_2$, 0.2mM dGTP, dATP, dTTP and dCTP and 1 unit of Taq polymerase (Bioline) in a reaction volume of 50µl. Each sample was overlaid with one drop of mineral oil to reduce evaporation. PCR was carried out in 0.5ml eppendorf tubes using a Hybaid Omn-E or Biometra thermal cycler.

All genotyping performed as part of the genome search was performed in 96-well Omniplates (Hybaid) under oil. PCR was performed with 25ng of

DNA in a 10μl volume containing 10pmol 3'-primer, 1 X buffer (Bioline), 1.5mM $MgCl_2$, 0.2mM dGTP, dATP, dTTP and dCTP and 0.2U Taq polymerase (Bioline). Prior to amplification, 10pmol 5'-primer per 10μl reaction was end-labelled with 0.5μl [γ-^{32}P]dATP (3000Ci/mmol) with 0.5 units of polynucleotide kinase (Promega), 1 x PNK buffer (10 x buffer = 500mM Tris-HCl, pH7.6; 100mMMgCl2; 50mM DTT), distilled water to a volume of 10μl and incubated at 37°C for 30 minutes.

For dinucleotide repeat analysis and radioactive SSC analysis, radiolabelled ^{32}P-dCTP was used as well as dCTP. The final concentrations of the nucleotides used were 0.2mM dGTP, dATP and dTTP, 0.02mM dCTP and 1μl of ^{32}P-dCTP (3000Ci/mmol; 1mCi = 100μl) per 1ml of reaction mix.

Conditions for thermal cycling consisted of denaturation at 95°C for 5 minutes, followed by 30 or 35 cycles at 95°C for 30 seconds- 1 minute, 30 seconds- 1 minute at the annealing temperature of the individual primer pair, extension at 72°C for 45 seconds - 1 minute, followed by a final extension step of 72°C for 10 minutes.

2.2.2.1. Reverse transcriptase (RT) PCR

1st strand cDNA synthesis was carried out in duplicate. Prior to 1st strand cDNA synthesis, 5μg RNA was treated with *DNase* I. 2 units of enzyme and 1 X buffer was added to the RNA sample and made up to a final volume of 20μl with DEPC-treated water. The sample was incubated

for 15 minutes at room temperature. In order to stop the reaction, 50 mM EDTA pH 8.0 was added and the sample placed at 65°C for 10 minutes.

DNase-treated RNA was used in the synthesis of 1st strand cDNA. To the RNA sample was added 7μl 5 x First strand buffer (Gibco BRL), 3.5μl 0.1M DDT, 2μl 20mM dNTPs, 100pmol oligo dT, 100pmol 9mer, 40 units rRNAsin Ribonuclease inhibitor and DEPC-treated water to a final volume of 60μl. The sample was incubated at 65°C for 10 minutes then plunged on ice. The sample was pre-warmed for 2 minutes at 42°C prior to the addition of 200 units of Superscript II to one of the samples. The conditions for 1st strand synthesis consisted of 42°C for 90 minutes, followed by 15 minutes at 72°C. 4μl Ist strand cDNA was subsequently used in PCR.

2.2.3. Restriction endonuclease digestion

For digestion of human DNA, 5μg of DNA was added to 4μl of the appropriate restriction enzyme buffer, 10-20 units of restriction enzyme, and the volume made up to 40μl with distilled water. For *EcoR* I digests, the sample was incubated at 37°C for 4 hours, with a further 1μl of enzyme added after 2 hours.

For digestion of PCR products, 10μl PCR product, 3μl appropriate restriction buffer, 10-20 units of restriction enzyme and the volume made up to 30μl with distilled water. The sample was then incubated for 2

hours at the appropriate temperature; 37°C for *Bfa* I, *Dde* I, *EcoR* I, *Hha* I and *Hinf* I; 60°C for *BsiE* I, 65°C for *Taq* I.

2.2.4. Electrophoresis

Agarose gel electrophoresis

2.2.4.1. Separation of PCR products in agarose gels

2g agarose in 100ml 1 x TBE was boiled in the microwave. On cooling, 5μl of ethidium bromide (10mg/ml) was added and the gel poured in to a BRL midi gel tray. After setting, 10μl of PCR product was diluted with 5μl of loading buffer, loaded onto the gel and the gel electrophoresed at 100 volts for 20-40 minutes. The gel was transilluminated and photographed under ultraviolet (UV) light. The size of the amplified product was compared to a 100 base pair ladder loaded at the same time as the PCR product.

PCR products which had been digested by restriction enzymes were separated on 3% Nusieve/1% agarose gels.

2.2.4.2. Separation of restriction enzyme fragments of human DNA for Southern blotting.

2.4g agarose in 300ml 1 x TAE buffer was boiled in the microwave. On cooling, 15μl of ethidium bromide (10mg/ml) was added and the gel poured in to a 20cm x 20cm NBL tray. Once set, 10μl loading buffer was added to each 40μl digest and the total volume loaded into a well. Molecular weight marker, 1μg of lambda DNA digested with *BstE* II, was

also loaded. Gels were electrophoresed at 50 volts for 16 hours, and photographed under UV light next to a fluorescent ruler.

Polyacrylamide gel electrophoresis.

2.2.4.3. Microsatellite analysis.

^{32}P-labelled dinucleotide repeat polymorphisms.

A pair of BRL sequencing plates were washed in detergent, rinsed with water, dried and wiped with 70% ethanol. The smaller plate was coated in Sigmacote (Sigma). Two 0.4mm spacers were placed along the edges of the two opposed plates and these were then clipped together using bulldog clips. Gel mix consisted of 70ml Sequagel (6%, 19:1 Acrylamide:Bisacrylamide, 1 x TBE), to which was added 560µl 10% APS. The gel was quickly poured using a 50ml syringe, with the gel plates lying horizontally. Two vinyl sharks tooth combs were placed beside each other with the flat surface approximately 0.5cm into the gel. Clips were placed across the top of the plates until the gel was set.

Once set, the gel was placed in a vertical BRL tanked and clamped into place. The combs were removed and the gel was pre-run in 1 x TBE at 65W for 1 hour. Following this the combs were inverted so that the teeth just penetrated the gel to form wells. The wells were washed out with 1 x TBE prior to loading.

PCR amplification was performed using direct incorporation of α-^{32}P-dCTP as described in section 2.2.2. 5µl of PCR product was diluted in

5μl formamide dye, denatured for 3 minutes at 95°C, held on ice and 3.5μl loaded onto the gel. The gel was run at 65W for about 2-3 hours at depending on the size of the PCR product. Following this, the gel plates were prised apart and the gel blotted onto a piece of 3MM Whatman paper, covered with cling film and dried at 80°C for 1 hour. The dried gel was exposed to X-ray film, overnight at room temperature.

Microsatellite markers labelled with fluorescent dyes

PCR reaction was carried out in a 25μl volume as described in section 2.2.2. Gel plates were washed in alconox, rinsed thoroughly in milliQ water and left to air-dry. Once dry the plates were then assembled in the cassette with 0.2mm spacers and the plates clamped. Polyacrylamide gel electrophoresis was carried out on the ABI 377. Gel mix consisted of 37ml diluent (Sequagel), 8ml concentrate (Sequagel), and 5ml of 10x TBE. Prior to pouring, 400μl 10% APS and 20μl TEMED was added. The gel was quickly poured using a 50ml syringe, with the gel plates lying horizontally, and left to set for 1 hour prior to running. A 1 in 10 dilution of each PCR product was made, and 2μl of this diluted product was added to 2μl of size standard, GS350 (PE Applied Biosystems). These samples were denatured at 95°C for 3 minutes and held on ice prior to loading 2.5μl per lane. The gel was electrophoresed for 2.5 hours under the parameters stipulated by Genescan programme GS2400C. Following this, the data was collected and analysed using the Genescan version 2.0 and Genotyper software, supplied by the manufacturer (PE Applied Biosystems).

2.2.4.4. Sequencing products

Direct sequencing was performed on an ABI 377 automated DNA sequencer (PE Applied Biosystems). Gel plates were prepared as described for microsatellite markers labelled with fluorescent dyes, in section 2.2.4.3. Gel mix consisted of 18g ultrapure urea, 5.2ml acrylamide [19:1], 25ml milliQ water and 0.5g Amberlite in order to deionise the solution. Once dissolved, 5ml of 10 x TBE was added and the gel mix filtered and de-gassed using a 0.2μM cellulose nitrate filter. Prior to pouring, 250μl freshly-made 10% APS and 35μl TEMED was added. The gel was quickly poured using a 50ml syringe, with the gel plates lying horizontally. Once set, the gel was wrapped in cling film and allowed to stand for 2 hours prior to running.

The gel was electrophoresed for 7 hours using the following parameters: Dye set: DT dRset-Any; Matrix: dRHOD; Plate check: Plate check A; Pre-run module: Seq PR 36A-1200 and Run module: Seq run 36E-1200. The following day, the sequence run was analysed using the Sequence Analysis version 3.0 and Sequence Navigator f software (PE Applied Biosystems).

2.2.4.5. Single Stranded conformation (SSC) analysis

2.2.4.5.1. Silver Staining SSC analysis

Gel mix consisted of 30ml Mutation Detection Enhancement (MDE) gel, 6ml of 5 x TBE, with or without 7ml 87% glycerol and made up to a final volume of 60ml with distilled water. To this was added 30μl of TEMED

and 300μl 10% APS. 3μl non-radioactive PCR product was diluted with 5μl of formamide dye, denatured for 3 minutes at 95°C, and loaded on 1 X MDE gel at room temperature with and without 10% glycerol and electrophoresed at 45W for 4 hours in 0.5 x TBE. Additional gels were electrophoresed at 15W, overnight at 4°C. Following electrophoresis, the glass plates were prised apart and the gel blotted onto 3MM Whatman paper and then floated gel-side down in a tray containing 500ml of 10% ethanol. A further 500ml of 10% ethanol was poured onto the gel and the 3MM Whatman paper peeled away. The gel was washed in 10% ethanol for 5 minutes. Following this, the gel was oxidised in 1% nitric acid for 3 minutes then washed briefly in distilled water. The gel was then impregnated with 0.012M silver nitrate solution for 20 min and rinsed again with distilled water for a few seconds. After developing the bands to optimum intensity with 0.028M N_2CO_3 in 0.019% formaldehyde, the reaction was stopped with 10% acetic acid for 2 minutes. After a final rinse step with distilled water, the gel was shrunk by immersing it in 50% ethanol for up to 30 minutes. Finally the gel was blotted onto 3MM Whatman paper and dried at 80°C for 1 hour.

2.2.4.5.2. Radioactive SSC analysis

PCR amplification was performed using direct incorporation of α-^{32}P-dCTP as described in section 2.2.2. 5μl of PCR product was diluted in 5μl formamide dye, denatured for 3 minutes at 95°C and 3.5μl loaded onto a non-denaturing gel. This consisted of 6% polyacrylamide (Protogel: 30% acrylamide to 0.8% bis acrylamide; 5% glycerol, 1 x

TBE). The gel was electrophoresed at 360 volts overnight at either room temperature or at 4°C. Following this, the gel plates were prised apart and the gel blotted onto a piece of 3MM Whatman paper, covered with cling film and dried at 80°C for 1 hour. The dried gel was exposed to X-ray film, overnight at room temperature.

2.2.4.6. Heteroduplex analysis

Gel plates were prepared as described for ^{32}P-labelled dinucleotide repeat polymorphisms in section 2.2.4.3, with the exception that 1mm spacers were used. The gel mix consisted of 75ml MDE, 18ml 5 x TBE and 22.5g of urea, and made up to a final volume of 150ml with distilled water. To this was added 600μl 10% APS and 60μl TEMED, and the gel poured quickly using a 50ml syringe, with the gel plates horizontal. 4μl PCR product was diluted with 1μl sucrose loading dye, and denatured under the following conditions: 95°C for 5 minutes, 75°C for 5 minutes, 55°C for 5 minutes and held at 37°C until loading. This allows the strands to separate and reanneal slowly to form heteroduplexes. For detection of autosomal recessive mutations and X-linked mutations in males, 2μl mutant PCR product was diluted with 2μl control PCR product and 1μl sucrose loading dye prior to denaturation, in order to force the formation of a heteroduplex. Gels were electrophoresed in 0.6 x TBE at 700 volts for 16 hours. Following this, the gels were stained in 1 litre of 0.6 x TBE containing 100μl ethidium bromide (10mg/ml) for 5-10 minutes. Bands were visualised and photographed under UV light. Alternatively, the gels

were stained with 0.012M Silver nitrate solution as described in section 2.2.4.5.1.

2.2.5. Southern blotting and hybridisation

2.2.5.1. Southern blotting

DNA digests were separated by electrophoresis in 20cm x 20cm, 0.8% agarose gels overnight in 1 x TAE buffer as described in section 2.2.4.2.

The gel was soaked in denaturation solution for 30-60 minutes, with shaking. The gel was then inverted and placed onto the blotting apparatus. This consisted of a sponge soaked in 20 x SSC placed in a tray containing 20 x SSC, and covered with two pieces of 3MM Whatman paper lying across the sponge to act as wicks.

A piece of nylon membrane (Hybond N+), cut to the same size of the gel, was soaked in 2 x SSC and then placed on top of the gel. On top of this was placed two pieces of 3MM Whatman paper soaked in 2 x SSC. Clingfilm was placed along the edge of the gel to prevent absorption of 20 x SSC by any other route other than through the gel. Three paper towels were unfolded and placed on top of the gel/filter/Whatman paper. Finally, paper towels were stacked to a height of approximately 10cm and a glass plate and weight were placed on the top.

The gel was blotted overnight, or during the day with frequent changing of the paper towels. Following this, the apparatus was disassembled,

leaving the Hybond N+. The position of the wells was marked and the filter washed in 2 x SSC. DNA was then fixed to the filter by soaking in 0.4M NaOH for 10 minutes after which the filter was repeatedly rinsed in 2 x SSC to neutralise it.

2.2.5.2. Oligolabelling

This was performed using the Ready-To-Go™ DNA labelling kit (Pharmacia Biotech) with the solutions and protocol supplied.

20μl distilled water was added to the reaction mix tube supplied to reconstitute its contents, and incubated on ice for 15 minutes. 25-50ng probe DNA was placed in an eppendorf tube and a hole pierced in the lid. The DNA was denatured for 3 minutes at 95-100°C, then placed on ice for 2 minutes to prevent renaturation. After pulse centrifugation, the DNA was added to the reaction mix and to this was added 5μl α-^{32}P-dCTP (3000Ci/mmol) and distilled water to a final volume of 50μl. The sample was gently mixed and pulse centrifuged prior to incubation at 37°C for 15 minutes.

Labelled DNA was separated from unincorporated nucleotides by filtration through a Sephadex G-50 column in a 1ml syringe plugged with an autoclaved glass bead. The column was equilibrated with 300μl of TE. The volume of the probe sample was made up to 300μl with TE and then added to the column. The elute was discarded. The radiolabelled DNA was eluted by adding a further 300μl of TE to the column. The

radioactivity of the eluted DNA was counted in a 4μl aliquot using a calibrated Bioscan bench top beta counter. 1 x 10^6 dpm of probe per ml of hybridisation solution was added to pre-hybridising filters.

2.2.5.3. Hybridisation of ^{32}P labelled DNA to filters

Hybond N+ filters were soaked in 2 x SSC. These were then rolled and placed in a Hybaid bottle with 15ml of prehybridisation solution, and incubated in a Hybaid rotary oven at 65°C for 3 hours. Denatured, radiolabelled DNA probe was added to a final concentration of 1 x 10^6 dpm/ml hybridisation solution and the filters hybridised overnight at 65°C in the rotary oven.

Following hybridisation, the filters were washed twice in 3 x SSC/0.1% SDS at room temperature for 20 minutes. Depending on the signal detected with a beta emission counter, filters were then washed in 1 x SSC/0.1% SDS at 65°C for 20 minutes. Filters were then dried on 3MM Whatman paper, wrapped in cling film and exposed to X-ray film at -70°C with intensifying screens for 1-7 days.

2.2.6. DNA Sequencing

2.2.6.1. Cycle sequencing on ABI 377

Purification of PCR products

PCR products demonstrating SSCP variants were eluted through Microspin S-400 HR columns (Pharmacia Biotech). Each column was

vortexed gently to resuspend the resin. The cap was loosened and the bottom closure snapped off. The column was placed in a 1.5ml eppendorf, which had had its lid removed, and centrifuged for 1 minute at 13000 rpm in a MSE micro centaur centrifuge. The column was then transferred to a clean 1.5ml eppendorf and 40μl product carefully applied to the column, and centrifuged at 13000 rpm for 2 minutes. 5μl of the cleaned PCR product was diluted with 3μl of loading dye and electrophoresed on a 2% agarose gel, with a 100bp ladder, to estimate the volume of product required for the sequencing reaction.

Cycle sequencing

Direct sequencing was performed on both strands using ABI Prism dRhodamine Terminator cycle-sequencing kits (PE Applied Biosystems). The cycle sequencing reaction mixture consisted of 2-5μl PCR product, 4μl Terminator Ready Reaction mix, 3.2pmol primer, made up to a final volume of 10μl with MilliQ water, in a 0.5ml eppendorf. The sample was mixed, centrifuged and overlaid with 30μl of mineral oil. The tubes were placed on a Techne Gene-E thermal cycler. Cycling conditions consisted of 25 cycles of 96°C for 30 seconds, 50°C for 15 seconds and 60°C for 4 minutes. Tubes were held at room temperature until ready to purify.

Purification of sequenced products

10μl of sequenced product was removed from under the mineral oil and placed on a piece of parafilm. The parafilm was gently tipped, in order to separate the product from any residual oil. The product was then placed

in a clean eppendorf tube on ice and to this was added 2μl 3M NaAc (pH 4.6) and 50μl 95% ethanol. The sample was mixed by vortexing and left on ice for 15 minutes under foil to prevent any light degradation of the fluorescent product. After this time, the samples were centrifuged at 13000 rpm for 30 minutes. The supernatant was removed, the pellet washed with 200μl 70% ethanol further centrifuged for 5 minutes. The pellet was allowed to air-dry, under foil and was re-suspended in 4μl loading dye prior to loading the gel.

Sequencing conditions

The samples were denatured at 94°C for 3 minutes and held on ice. The lanes were washed with 1 x TBE and 2μl of sample was loaded in alternate lanes, and the samples allowed to run into the gel for 3 minutes. The wells were rinsed again, and the second batch of samples loaded. The gel was electrophoresed for 7 hours in 1 x TBE as described in section 2.2.4.4.

2.2.7. Site-directed mutagenesis

This was performed using the Quikchange™ site-directed mutagenesis kit (Stratagene) with the solutions and protocol supplied.

2.2.7.1. Primer design.

PCR primers for site-directed mutagenesis were designed using the following criteria:

1. Both mutagenic primers must contain the desired mutation and anneal to the same sequence on opposite strands of the plasmid.

2. Primer length between 25 and 45 bases.

3. Melting temperature (Tm) of the primer greater than or equal to 78°C

4. Desired mutation in the middle of the primer, with 10-15 bases of correct sequence on either side.

5. Minimum GC content of 50%.

6. Each primer must terminate in one or more C or G bases.

These primers were ordered from PE Applied Biosystems, with Readypure™ purification.

2.2.7.2. Temperature cycling.

Four sample reactions with varying concentrations of template were prepared in 0.5ml thin-walled eppendorf tubes using 5ng, 10ng, 20ng and 50ng of human IsK clone as template. Primers were added in excess. The reaction mix consisted of 5µl of 10 x reaction buffer, 5-50ng of double-stranded DNA template, 125ng of each mutagenesis primer, 1µl dNTP mix, made up to a final volume of 50µl with distilled water. To this was added 2.5 units of *PfuTurbo* DNA polymerase, and the sample overlaid with 30µl of mineral oil. Cycling parameters consisted of 95°C for 30 seconds, followed by 18 cycles of 95°C for 30 seconds, 55°C for 1 minute and 68°C for 7 minutes and 36 seconds (2 minutes per Kb plamid length). 18 cycles were chosen due to the complex nature of the desired mutation. Following this, the samples were placed on ice for 2 minutes to cool the reaction to 37°C. In order to check for sufficient amplification,

10µl of the PCR product was electrophoresed on a 1% gel, as described in section 2.2.4.1.

2.2.7.3. *Dpn* I digestion

10 units of *Dpn* I was added directly to each amplification reaction underneath the oil. The sample was mixed gently and incubated at 37°C for 1 hour to digest the methylated, nonmutated parental DNA template.

2.2.7.4. Transformation

Following *Dpn* I digestion, the double stranded DNA template was transformed into E.Coli XL-1 blue competent cells. 1µl of *Dpn* I-digested DNA from each reaction was added to separate 50µl aliquots of competent cells contained in pre-chilled 15ml falcon tubes, and the reaction heat pulsed for 45 seconds at 42°C. These were then placed on ice for 2 minutes.

500µl pre-warmed NZY^+ broth was added to each transformation reaction and incubated at 37°C for 1 hour with shaking at 225-250rpm. Immediately following this, the entire volume of each sample transformation was plated on LB-ampicillin plates and incubated at 37°C for 16 hours. The following day, single colonies were used to inoculate 5ml LB and ampicillin added to a final concentration of 50µg/ml. This was incubated overnight at 37°C.

2.2.7.5. Characterisation of mutation.

In order to check for the creation of the desired mutation, the next day 5µl of the 5ml culture was removed and diluted with 50µl of distilled water in a 0.5ml eppendorf. This was heated at 95°C for 5 minutes, after which 5µl was removed to use as a template in a PCR reaction. Direct sequencing, as described in section 2.2.4.4., was used to check for the mutation. DNA was prepared from the 5ml cultures as described in section 2.2.1.4.

2.3. CLINICAL DETAILS OF PATIENTS STUDIED

2.3.1. X-linked deafness families

2.3.1.1. Family CN

Affected males in this family suffer from a severe/profound pure sensorineural hearing loss which is prelingual in onset. Re-evaluation of Family CN, figure 2.1, revealed that individual IV_{12} has congenital profound sensorineural hearing loss and also suffers from Downs Syndrome. In the past this individual was typed as unaffected, as little was known about him. Individual II_4, previously shown to be affected with hearing loss but with no other family history, is shown as unaffected here since the sudden onset of her hearing loss was revealed to have dated from a severe head injury sustained in her teens. A CT scan of the petrous temporal bone in affected males showed no abnormality. All of the obligate female carriers have shown a mild/moderate hearing loss, more pronounced in the higher frequencies but none has complained of a subjective hearing loss. There was no family history of renal disease and urinalysis was normal. Ophthalmic evaluation was also normal.

2.3.1.2. Family FP

Affected males in Family FP have a moderate to severe sensorineural hearing loss of childhood onset (age 3-9 years at diagnosis) and all have developed speech. Obligate female carriers have a mild hearing loss. CT

scan of the petrous temporal bone of an affected male showed no abnormality. Family FP is shown in figure 2.2.

2.3.2. Deafness/Dystonia affected males

Individual NB

This individual was diagnosed as profoundly deaf at 8 months of age. He suffers from progressive dystonia. There is no family history of deafness and/or dystonia.

Individual GF

This individual was diagnosed as profoundly deaf at 12 months of age although hearing loss was suspected within the first 4 months of life. He was diagnosed with Dystonia at the age of 17. Symptoms are progressive. There is no family history of deafness and/or dystonia.

2.3.3. Jervell and Lange Nielsen syndrome

Individuals were considered to have JLNS if they had profound sensorineural deafness and a prolonged QTc interval. Most individuals were ascertained following syncopal episodes (although families N5B and N8A were ascertained following ECG screening of deaf children). QTc intervals were calculated using Bazett's formula and a QTc interval of greater than 440ms is generally considered to be prolonged (Schwartz *et al*, 1993). Some gene carriers fulfil the criteria for a prolonged QT interval.

2.3.3.1. British families

Pedigrees are shown in figure 2.3.

Family UK1S

Family UK1S is a British family. II_1 and II_2 have congenital profound sensorineural hearing loss with absent vestibular function. II_2 has a QTc interval of 488ms and II_1 a QTc interval of 478ms. II_2 had 3 episodes of syncope on exertion prior to diagnosis and treatment, one of which required resuscitation. Both parents have normal QTc intervals. II_2 has retinal pigmentation of unknown origin but both boys have normal electroretinograms, excluding a diagnosis of Usher syndrome.

Family UK2T

Family UK2T comes from Turkey but is resident in the U.K. Parents are first cousins. The proband has prelingual deafness and suffered from syncope. His QTc is 480ms and that of his sister is 374ms. The QTc of the parents are within the normal range.

Family UK3C

Family UK3C is a British family. II_1 was diagnosed as having a congenital long QT syndrome at 15 months when he had an episodic loss of consciousness. An ECG confirmed a long QT interval in sinus rhythm and typical Torsades de pointes were seen during attacks. He and his brother (II_2) were both known to have bilateral sensorineural deafness since early infancy and a subsequent ECG confirmed that II_2 also had a long QT interval. Neither parent has a long QT interval in sinus rhythm. The QTc of the mother is 428ms, that of the father is 430ms and

individual II_2 is 456ms. The proband, individual II_1 has a QT interval of 520-560ms.

2.3.3.2. Norwegian families

Pedigrees are shown in figure 2.4.

Family N1H

Family N1H originates from Norway and has been previously reported (Jervell *et al*, 1966). The parents are not related. The QTc of the proband is 646ms. Her mother has a QTc of 430ms and her father's is 400ms. No QTc are available for the unaffected siblings.

Family N2S

Family N2S originates from Norway and has been previously reported (Jervell *et al*, 1966). The proband is congenitally deaf and suffered from syncopal episodes provoked by exercise and fear. DNA was available from the parents and unaffected sibling. DNA was not available from the proband.

Family N3S

Family N3S originates from Norway. The proband is congenitally deaf and suffered from syncopal episodes elicited by stress. His QT interval is 600ms, but no other information is available.

Family N4O

This family originates from Norway. The proband was diagnosed with congenital deafness at 18 months, and had three syncopal attacks, after which an ECG was requested and showed a prolonged QT interval of 500ms. No QTc intervals are available for the parents and the unaffected child.

Family N5B originates from Norway. The proband is congenitally deaf and the diagnosis was made on ECG examination (customary practice for all deaf children in Norway). The affected girl's QTc is 540ms, her father's is 410ms, her brother's is 370ms and that of her mother is 470ms at rest increasing to 540ms on exercise.

Family N6K. The proband in Family N6K is congenitally deaf, and comes from the same geographical region in Norway as Family N7J. No QTc intervals are available.

Family N7J formed the basis of the original description of this condition by Jervell and Lange-Nielsen in 1957 (Jervell and Lange-Nielsen, 1957). The QTc of the proband, individual II_1, is 533ms. The parents are not related and have QTc values in the normal range.

Family N8A comes from Pakistan but is resident in Norway. The parents are first cousins. The diagnosis was made neonatally based on the family history and finding of a QTc of 650ms in the proband. She is congenitally deaf. The QTc of the mother is 450ms, that of the father is

410ms, that of the proband's older sibling is 430ms and that of the younger sister is 400ms.

Family N9A originates from Norway. The proband is congenitally deaf and has suffered from episodes of syncope. No QTc intervals are available for the proband or her mother.

Family N10D originates from Norway. The proband is congenitally deaf and has suffered from episodes of syncope. The proband, individual IV_1 has a QTc of 500ms, that of her father is 470ms, her mother's is 430ms and her sister's is 360ms. Individual IV_5 was independently ascertained with Romano-Ward syndrome following a syncopal episode. This individual has a QTc of 500ms.

2.3.4. Autosomal recessive Long QT syndrome

2.3.4.1. Family N16O

This family originates from Norway. The parents are first cousins. The proband was diagnosed with Romano Ward syndrome, following the identification of a prolonged QT interval on ECG. Her hearing is normal. The QTc of the parents and unaffected sibling are normal. Family N16O is shown in figure 2.5.

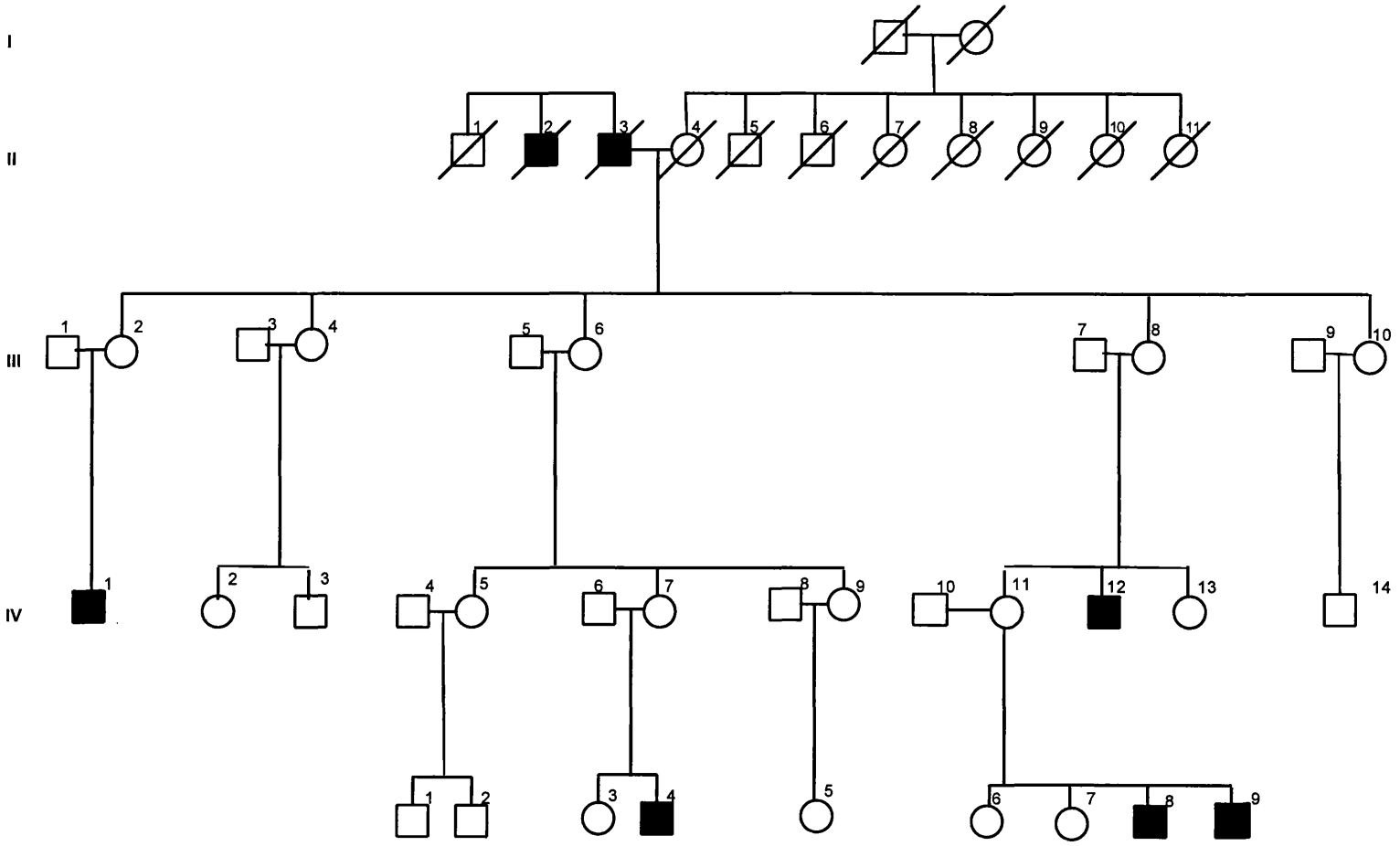

Figure 2.1. Pedigree of X-linked deafness family, Family CN.

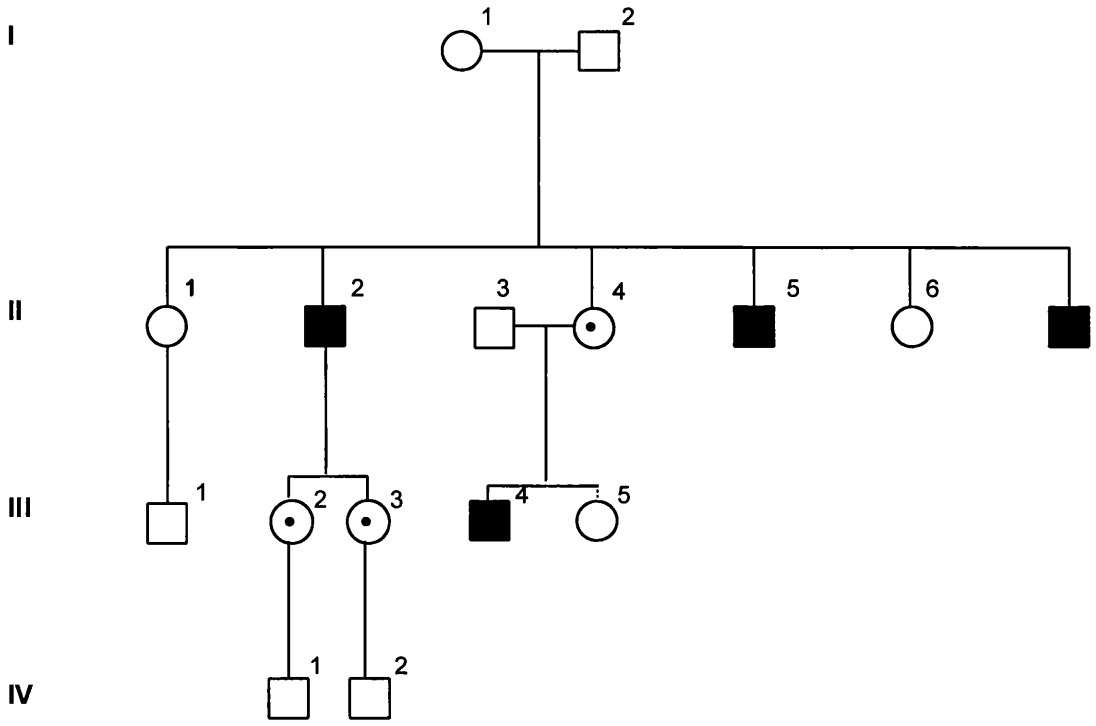

Figure 2.2.

Pedigree of X-linked deafness family, Family FP

Family UK1S

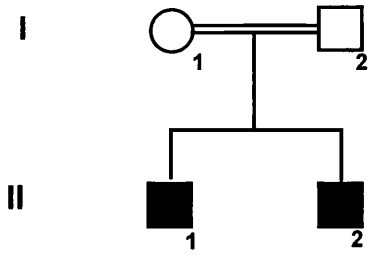

Family UK2T

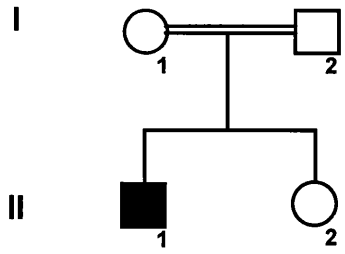

Family UK3C

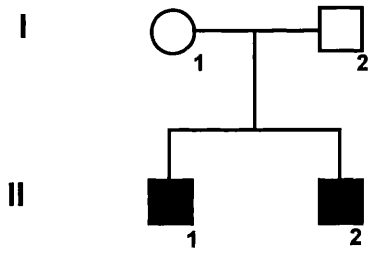

Figure 2.3.

Pedigrees of British Jervell and Lange-Nielsen families described in this study. Double line denotes consaguinity.

Family N1H

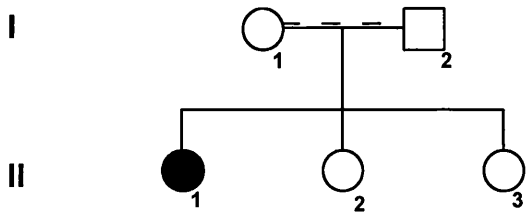

Family N2S

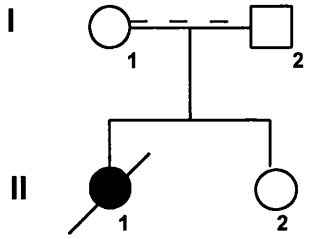

Family N3S

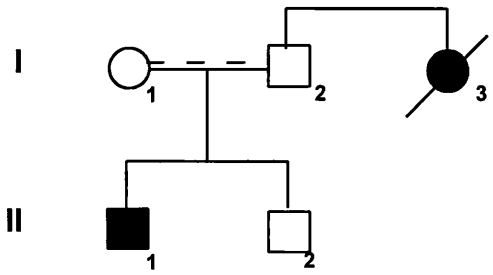

Family N4O

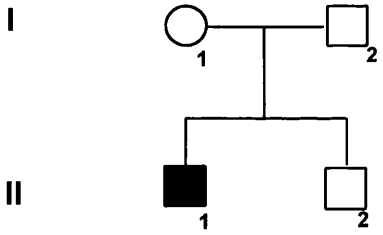

Family N5B

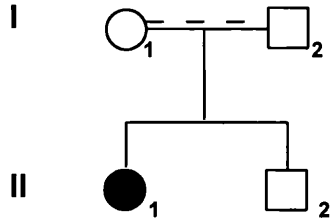

Figure 2.4.

Pedigrees of Norwegian Jervell and Lange-Nielsen families described in this study. Double line denotes consanguinity, dashed line indicates suspected consanguinity.

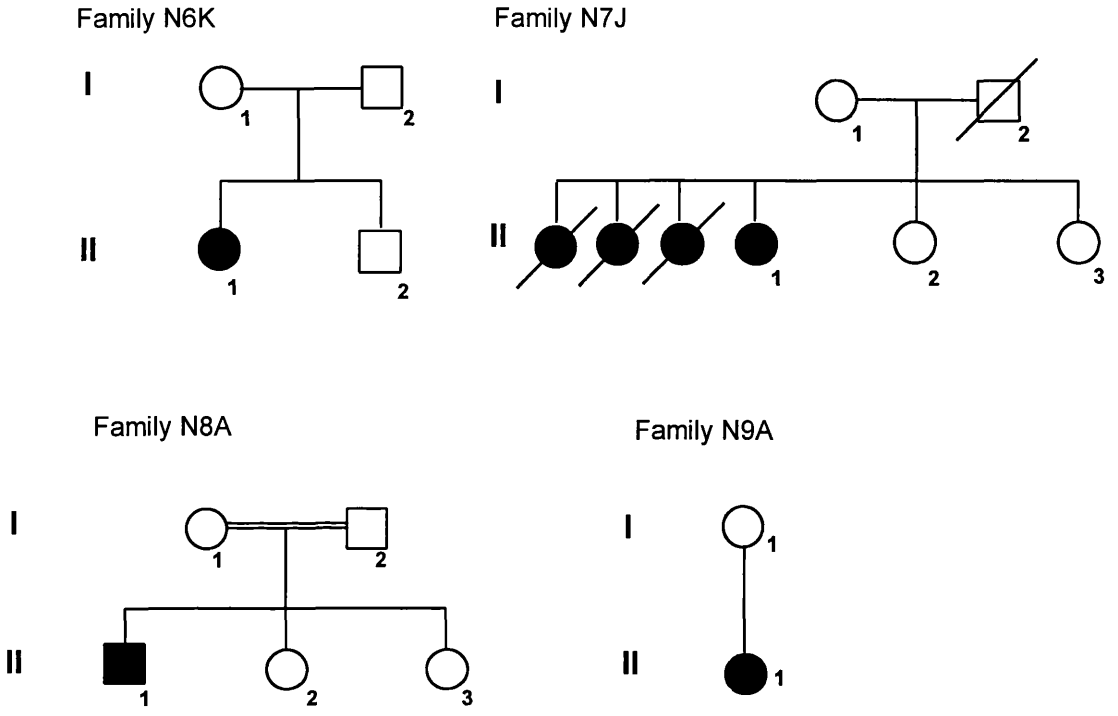

Figure 2.4. continued.

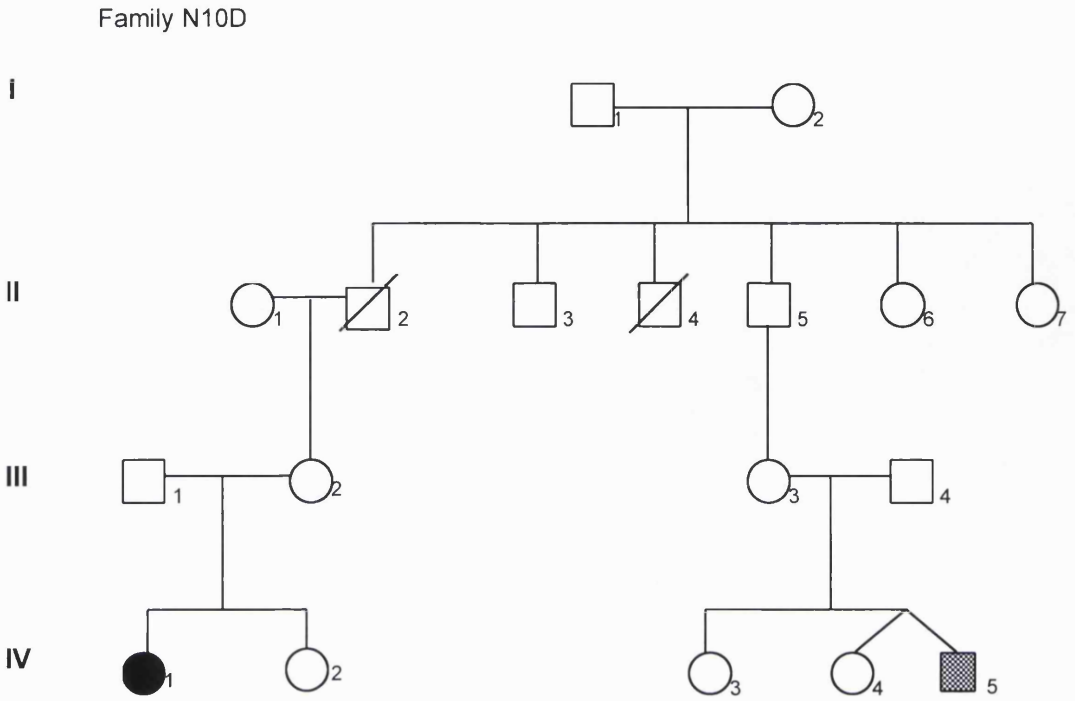

Figure 2.4. continued

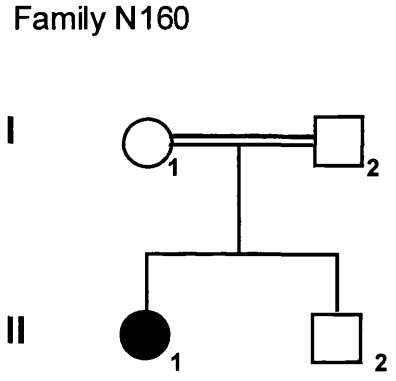

Figure 2.5.

Pedigree of Family N16O segregating autosomal recessive Long QT syndrome. Double line indicates consanguinity.

CHAPTER 3: RESULTS

3.1. X-LINKED DEAFNESS

The work on X-linked deafness is divided into two sections. The first part addresses the issue of locus heterogeneity in X-linked deafness. From one of the first publications on the mapping of genes for X-linked deafness, (Reardon *et al*, 1991), it has been known that, despite accounting for a small percentage of inherited forms of deafness, X-linked deafness is genetically heterogeneous. Analysis of seven families segregating X-linked deafness confirmed the existence of a locus at Xq13-q21 in the majority of these families with one exception; Family CN represents the family which originally suggested genetic heterogeneity (Reardon *et al*, 1991). The aim of this part of the study on X-linked deafness was to perform linkage analysis and map the disease locus in Family CN and another family with X-linked deafness, Family FP, and work towards the identification of the causative gene.

The second part of this study on X-linked deafness, section 3.1.5, examines the DFN3 locus at Xq13-q21 and the question of heterogeneity at this locus, since not all families mapping to DFN3 have mutation in POU3F4.

3.1.1. Analysis of published loci in Family CN

Two loci for X-linked deafness, DFN3 at Xq13-q21, and DFN4 at Xp21.1, were initially analysed in Family CN.

3.1.1.1. Microsatellite analysis at DXS995 and DXS1002

Since DFN3 accounts for the majority of cases of X-linked deafness, Family CN was analysed for the markers DXS995 and DXS1002 at this locus on Xq13-q21 to confirm whether or not DFN3 is the disease locus in this family. DXS995 and DXS1002 are known to flank the POU3F4 gene at DFN3 (Nelson *et al*,1995). DXS995 lies within 5cM of DFN3 (Bitner-Glindzicz *et al*,1994) and physical data has shown that it actually lies within 20kb of the POU3F4 gene (de Kok *et al*,1995). The affected individuals of this family have not inherited the same alleles for the markers DXS995 and DXS1002, as shown in figures 3.1 and 3.2 respectively. Affected individual IV_1 has inherited allele c, as has the unaffected individual IV_{14} for the marker DXS995, whereas the affected males V_8 and V_9, have inherited allele d. Assuming the least number of recombination events, a cross over has probably occurred between individuals IV_7 and V_4, and individuals III_8 and IV_{11}, with DXS995 and between III_8 and IV_{11} with DXS1002. These multiple recombinations effectively exclude DFN3 as the causative locus.

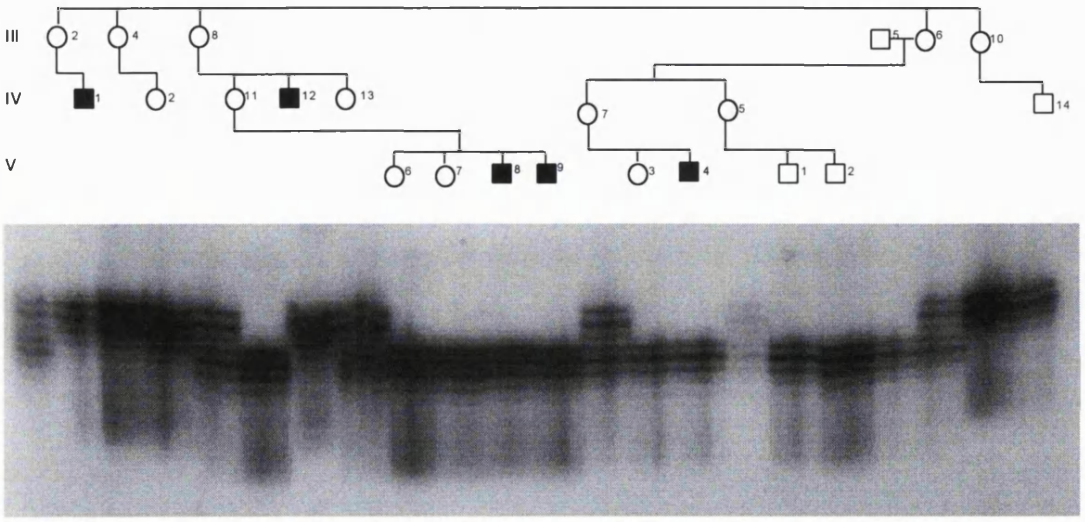

Figure 3.1.

Microsatellite analysis of Family CN at DXS995. Individuals analysed for this marker are indicated. Individual numbers correspond to the original pedigree, figure 2.1.

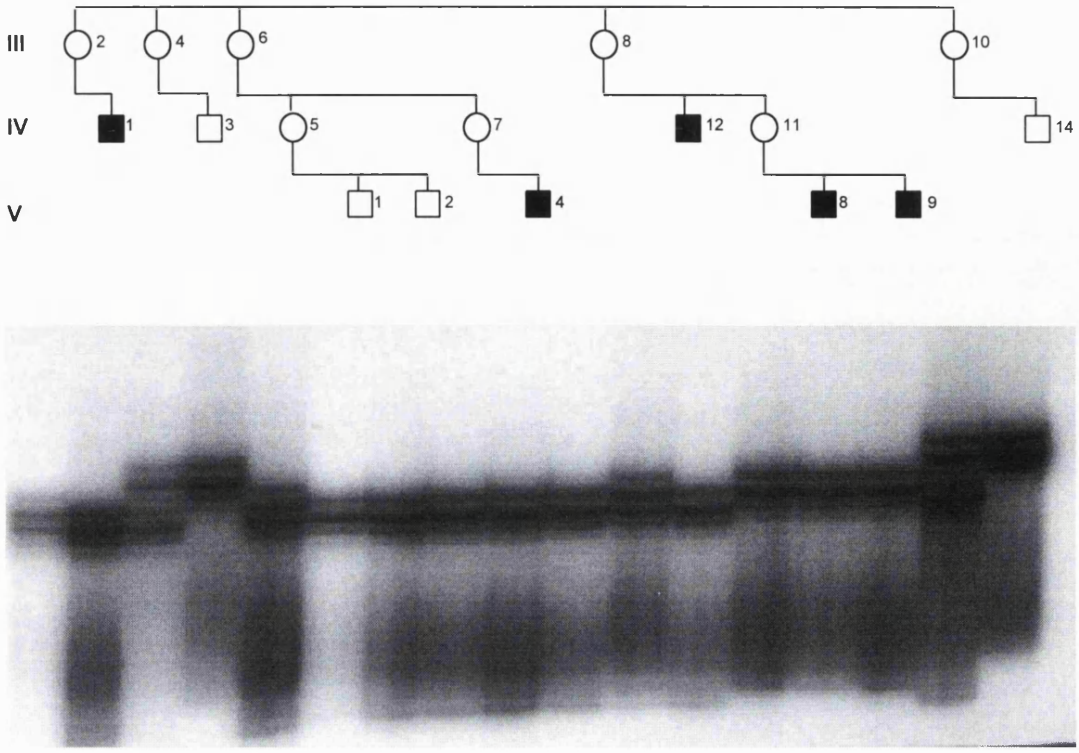

Figure 3.2.

Microsatellite analysis of Family CN at DXS1002. Individuals analysed for this marker are indicated. Individual numbers correspond to the original pedigree, figure 2.1.

3.1.1.2. Microsatellite analysis at the Duchenne Muscular Dystrophy (DMD) locus

Family CN was also typed for microsatellite markers which span the Duchenne muscular dystrophy gene located in Xp21.1 in order to analyse the DFN4 locus. The DFN4 locus included 10cM of 5' end of DMD locus and 1.6cM centromeric to DMD. Physically, the region corresponds to 1.5Mb both within and centromeric to DMD (Lalwani *et al*,1994). Linkage of a second family to the DMD locus at Xp21.1 refined DFN4 to entirely within the DMD locus (Pfister *et al*, 1998). The following markers, which span the DMD gene from the 5' promoter to the 3' untranslated region in Xp21.1, were typed in Family CN in order to exclude or establish linkage to DFN4: 5' Dys I, intron 44, intron 45, intron 49, intron 50, introns 62/63 and 3' STR HI. Typing of Family CN for these markers revealed different haplotypes across the entire DMD locus, thus effectively excluding DFN4 as the causative locus in this family (Personal communication, Dr. M. Bitner-Glindzicz).

3.1.2. Linkage analysis

With the exclusion of DFN3 and DFN4 as the disease loci in Family CN, further genetic heterogeneity in X-linked deafness was established. The next stage was to map the disease locus in Family CN.

3.1.2.1. Microsatellite analysis of markers at Xq22

Typing with polymorphic microsatellite markers along the long arm of the X-chromosome from Xq21 to Xq24, revealed a region of linkage at Xq22.

Microsatellite markers analysed were DXS995, DXS1002, DXS990, DXS1106, PLP, DXS17, DXS1230, COL4A5, DXS1210, DXS1220, and DXS1001. The dinucleotide repeat marker at COL4A5 was fully informative in Family CN. Allele c of this marker faithfully co-inherits with the deafness in this family. Results of microsatellite analysis at COL4A5 are shown in figure 3.3.

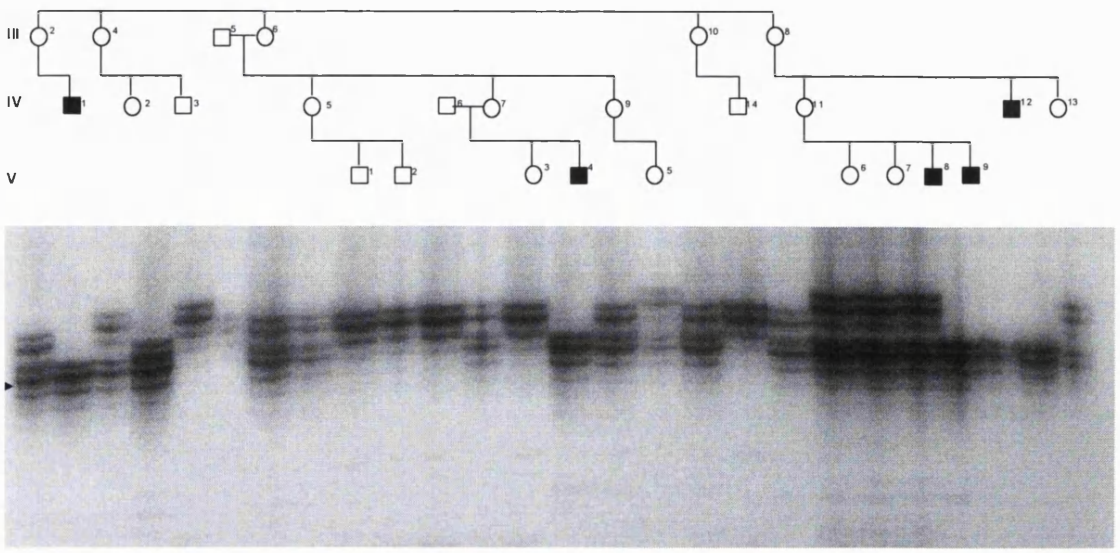

Figure 3.3.

Microsatellite analysis of Family CN at the dinucleotide repeat marker at COL4A5. Individuals analysed for this marker are indicated. Individual numbers correspond to the original pedigree, figure 2.1. Arrow indicates allele c, which co-inherits with the deafness in this family.

3.1.2.2. Linkage of DFN2 to Xq21-q23

Family CN is shown in Figure 3.4 with haplotype data for X chromosome polymorphic markers. Two-point lod scores between the disease gene and marker loci were generated by LIPED. These are shown in Table 3.1. A maximum two-point lod score of 2.91 at zero recombination was observed with dinucleotide repeats at COL4A5 and DXS1106. For X-linked diseases, the two loci, the disease locus and the microsatellite marker, are already known to map to the same chromosome. The prior probability of odds against linkage are reduced so that a lod score of 2 is considered as evidence of linkage. Likely recombinations occurred between individuals III_8 and IV_{11} between the markers DXS990 and DXS1106, and between individual IV_{11} and her sons V_8 and V_9 between DXS1220 and DXS1001. A recombination between DXS990 and DXS1106 places the disease allele telomeric to DXS990, and a recombination between DXS1001 and DXS1220 places the disease allele centromeric to DXS1001. This work demonstrates that the mutant deafness gene in this family maps to Xq22, with a significant lod score of 2.91, between the microsatellite markers DXS990 and DXS1001. The approximate size of the candidate region in Family CN is 20-25cM (Nelson *et al*, 1995; Dib *et al*, 1996).

Analysis of Family CN identified a new locus for X-linked deafness on Xq22, the nomenclature assigned for this locus is DFN2.

	Lod score at θ =								
	0	**.05**	**.1**	**.2**	**.3**	**.4**	**.5**	θ_{max}	**Max lod score**
DXS1002	-99.99	0.057	0.293	0.429	0.380	0.243	0	0.2	0.429
DXS990	-99.99	0.057	0.293	0.429	0.380	0.243	0	0.2	0.429
DXS1106	2.913	2.671	2.42	1.894	1.327	0.706	0	0	2.913
PLP	1.408	1.297	1.182	0.934	0.661	0.353	0	0	1.408
DXS17	1.12	1.002	0.869	0.562	0.230	-0.016	0	0	1.12
DXS1230	0.505	0.461	0.416	0.322	0.222	0.116	0	0	0.505
COL4A5	2.913	2.671	2.42	1.894	1.327	0.706	0	0	2.913
DXS1210	1.408	1.297	1.182	0.934	0.661	0.353	0	0	1.408
DXS1220	1.138	1.046	0.951	0.749	0.527	0.280	0	0	1.138
DXS1001	-99.99	-0.148	0.284	0.504	0.412	0.166	0	0	0.504

Table 3.1.

Pairwise Lod scores between the disease locus and Xq chromosome markers for Family CN.

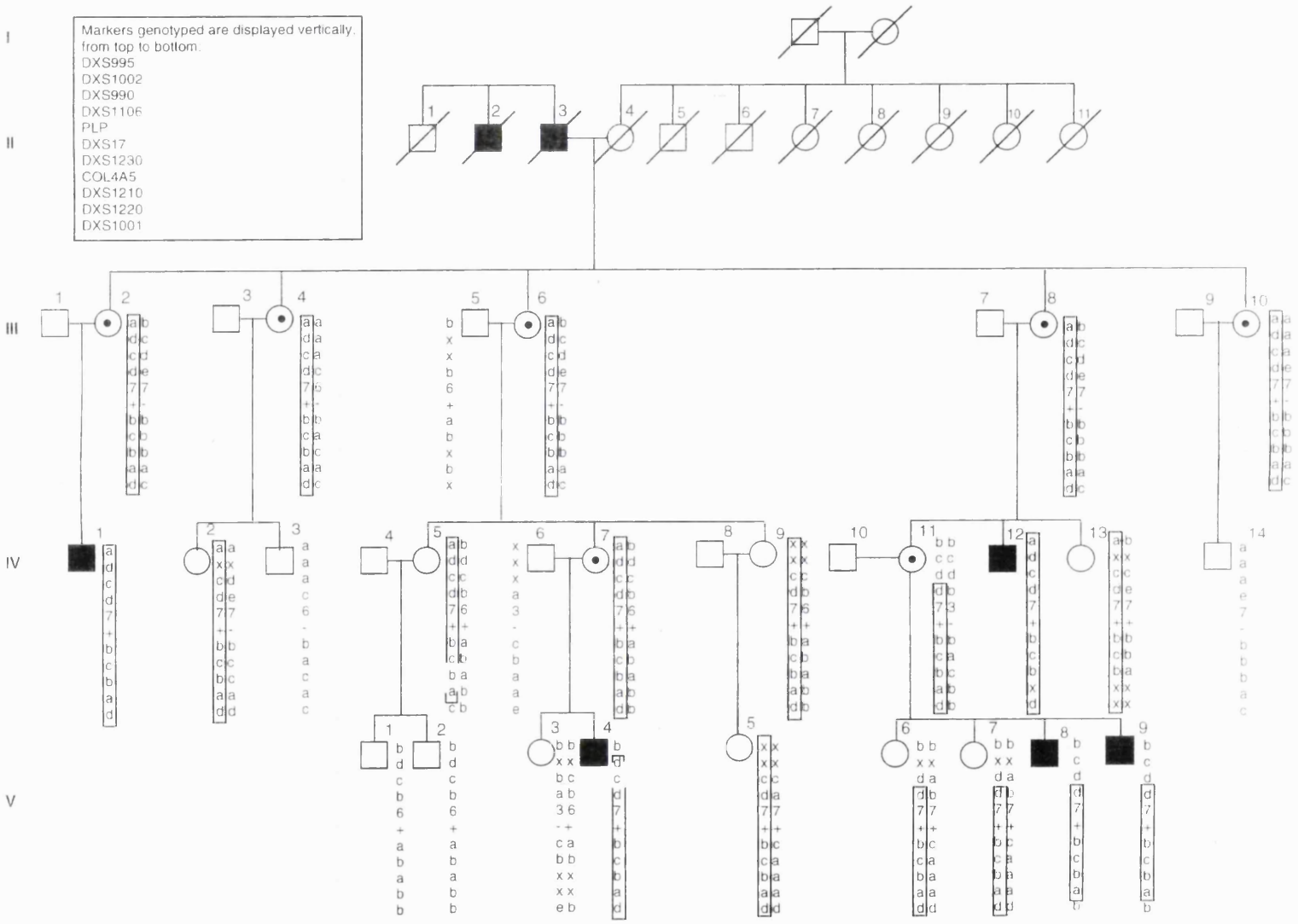

Figure 2.4. Pedigree of Family CN, showing probable haplotypes across Xq21-q24.

3.1.3. Analysis of candidate genes in Xq22.

The DFN2 candidate region is approximately 20-25cM (Nelson *et al*, 1995; Dib *et al*, 1996). Without additional recombinations in Family CN and other families with X-linked deafness mapping to the same interval, the DFN2 region is too large to consider a positional cloning approach. A positional candidate gene approach was undertaken to identify the causative gene.

Several syndromic forms of deafness map to Xq22, including Alport syndrome (Barker *et al*, 1990) and Mohr-Tranebjærg syndrome (MTS) (Tranebjærg *et al*,1995). The aim of this work was to investigate whether or not the deafness in Family CN represents an allelic form of one of these conditions. The genes screened as part of this work were Deafness/Dystonia peptide (*DDP*), *COL4A5* and a novel human homologue to the *Drosophila* gene *diaphanous*, DiaX.

3.1.3.1. Mutation analysis of DDP (Deafness/Dystonia peptide)

Mutation in DDP results in a rare syndromic form of deafness, the Mohr-Tranebjærg syndrome (Jin *et al*, 1996). The Mohr-Tranebjærg syndrome was originally described by Mohr and Magerøy in 1960 in a family with a non-syndromic form of progressive sensorineural deafness (Mohr and Magerøy, 1960). However re-evaluation of the family revealed additional clinical symptoms which include progressive dystonia, spasticity, mental deterioration and visual symptoms leading to blindness (Tranebjærg *et al*, 1995). On SSC analysis of DDP in Family CN, no aberrant shifts were

observed in the affected males of this family, as compared to control individuals. No mutation was identified on direct sequencing of the DDP gene in individual V_4 of Family CN, making it unlikely that mutation in *DDP* is responsible for this form of non-syndromic X-linked deafness.

3.1.3.1.1. Further analysis of DDP in affected males with Deafness and dystonia

The DDP gene was screened by SSC analysis and direct sequencing in two affected males with isolated deafness and dystonia. A **g** to **a** transition at the invariant **gt** of the 5' splice donor site of exon 1 was identified in patient NB. A donor consensus splice site consists of C**AGgt**aagt; an AG, or less commonly CG or GG, dinucleotide at the end of the exon followed immediately by a gt dinucleotide sequence in the intron (Shapiro and Senapathy, 1987). The mutation is depicted in figure 3.5, the sequence change is shown in figure 3.6.

	Exonic sequence	Intronic sequence
Wild type	CTT TGT TGG	**g**tgaggagc
Mutant	CTT TGT TGG	**a**tgaggagc
Consensus splice site	CAG	gtaagt

Figure 3.5.
Illustration of the DDP mutation identified in individual NB. The g to a transition is shown in bold. Upper case lettering denotes coding sequence, lower case denotes intronic sequence.

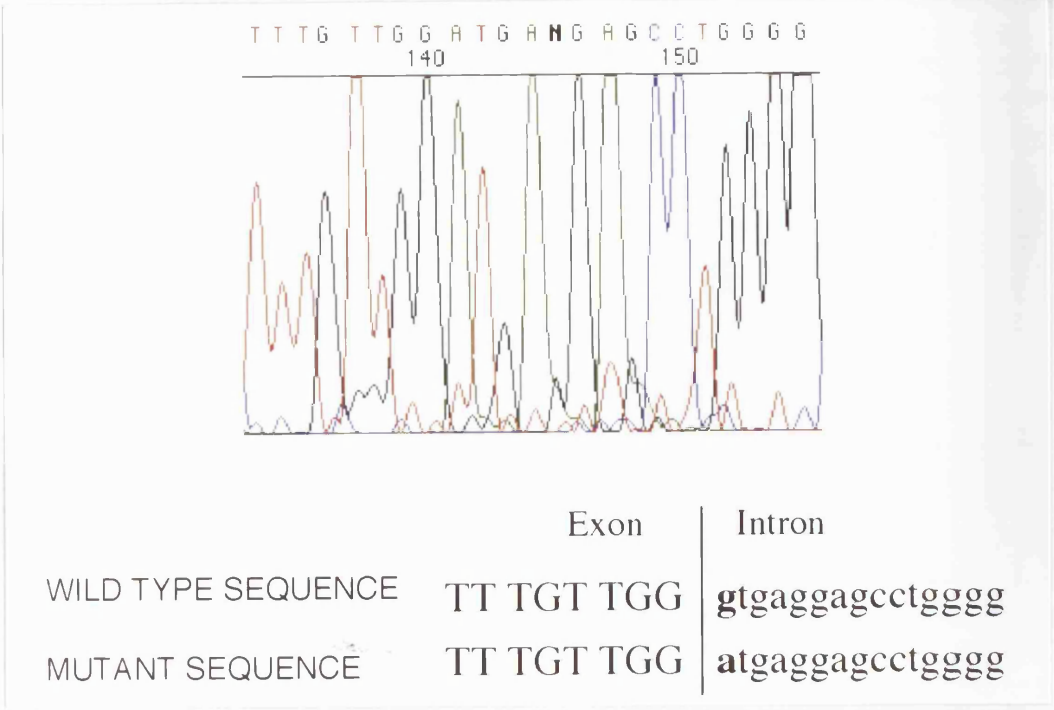

Figure 3.6. Sequence analysis of DDP in individual NB. Sequence of mutation is illustrated. DNA sequence of wild type and mutation is displayed beneath the electropherogram, with the g to a transition highlighted in bold.

In order to predict the effect of this mutation on splicing, the wild type and mutant DNA sequences of DDP were submitted for analysis by a Neural Network available on the World Wide Web (http://www-hgc.lbl.gov/projects/splice.html). Analysis of the wild type sequence by Neural Network identifies all the splice sites in the sequence, and assigns a score (maximum 1.0) according to the suitability of that site as a potential 5' splice donor. The wild type 5' donor site for exon 1 is given a score of 0.8. Analysis of the mutant sequence reveals abolition of this splice donor site. A new donor splice site is suggested, 60 nucleotides proximal to this site within the coding region of exon 1, with a score of 0.57. The use of this site would result in the in frame deletion of 20 amino acid residues and hence a truncated protein. The consequence of this mutation at the RNA level needs to be confirmed.

No mutation was identified by SSC analysis or direct sequencing of the DDP gene in individual GF.

3.1.3.2. X-linked diaphanous

DFNA1 encompasses an autosomal dominant, fully penetrant non-syndromic sensorineural progressive hearing loss, which was localised in a large Costa Rican kindred to chromosome 5q31 (Leon *et al*, 1992). During the cloning of the gene for DFNA1, a human homologue of *Drosophila* gene Diaphanous (Lynch *et al*, 1997), work by Eric Lynch and Mary-Claire King at the University of Washington School of Medicine identified a second human homologue, related to but not identical to the autosomal homologue. This homologue was partially sequenced and it was demonstrated to map to Xq22. Mapping data was on the basis that the homologue is represented by several IMAGE clones, including IMAGE clone consortium number 626664, a 3.1Kb cDNA clone from a HeLa cDNA library. When searched against the GenBank database, a portion of the Diaphanous clone was identical to genomic DNA from PAC 117P19. This PAC had been sequenced and mapped by the Sanger Centre to Xq21.3. This homologue is denoted Diaphanous X (DiaX). Since the deafness in Family CN localises to Xq22, we were approached by Eric Lynch and Mary-Claire King to test DiaX as a candidate gene for the deafness in Family CN. Several strategies were undertaken.

3.1.3.2.1. Mutation analysis of Diaphanous X

From the partial sequence generated by Eric Lynch of the 3.1Kb DiaX cDNA clone, overlapping PCR primers were designed using a primer design programme at HGMP. The primers were checked for specificity to DiaX using a BLAST search programme. These were then used to amplify cDNA generated from total RNA isolated from a lymphoblastoid cell line of individual V_4 (Family CN) and from lymphoblastoid cell lines of 5 control individuals. PCR primers are shown in table 3.2. 812bp of sequence was available from the 5' end of the 3.1Kb clone, and 829bp of sequence was available from the 3'end of the clone, leaving 1459bp of unknown sequence, the middle portion of the clone. Partial sequence and position of PCR primers is shown in figure 3.7.

Radioactive single stranded conformation polymorphism (SSC) analysis was used to screen for mutations in the portion of DiaX for which the sequence was known. No shifts were observed in cDNA from individual V_4 as compared to cDNA from 5 control individuals. A representation of this is shown in figure 3.8.

Southern blots were prepared from *EcoR*I-digested genomic DNA of affected males of Family CN, Family FP and control individuals. A DiaX PCR product, using PCR primers 5'4F and 3'4F (PCR product ~1.5Kb), generated from the clone was radiolabelled and used as a probe for Southern blotting to detect any gross rearrangements of Diaphanous X in these families. No altered bands were observed, as indicated in figure

3.9, indicating that no deletions or rearrangements of DiaX was detected in these families.

In order to screen the middle portion of DiaX cDNA without prior knowledge of the sequence, a PCR product was generated using the PCR primers 5'4F and 3'4F from cDNA of individual V_4 and 5 control individuals. Since the size of the product is approximately 1.5Kb, it was digested with the restriction enzymes *Hha*I, *Hinf*I and *EcoR*I to generate products less than 1Kb in order to perform heteroduplex analysis. No heteroduplex bands were observed.

These three experiments, SSC analysis, Southern blotting and heteroduplex analysis, did not identify a mutation in DiaX in Family CN.

PRIMER NAME	PRIMER SEQUENCE, 5' TO 3'	ANNEALING TEMPERATURE (^{O}C)
5' 1F	GCA CGA GCC TTA ACG AAG AG	
5' 1R	GAA ACC CTG AGG GAT TCT AGG	57 ^{O}C
5' 2F	TCG GGT ATA TCA GAT GAG AAA CTT C	
5' 2R	TCC TAG AAT CCT TTG TAA GCC AA	53 ^{O}C
5' 3F	GCC TCA AAG CAT TTA TGA ATA ATA AG	
5' 3R	CGG TCC ACA AGT GGT GAA A	58 ^{O}C
5' 4F	ACG AAG AAA TAA CAC GGA ACG	
5' 4R	CAA TTG CAG AAG AGG GTG AAA	55 ^{O}C
3' 1F	CCA CTA GAA ACT TTT ACT ACT TGA TTA TC	
3'1R	GAT GGA TAA TCT TCT AGA AGC CC	54 ^{O}C
3' 2F	GTC TCT GAA TGC TGC ACC TG	
3' 2R	TCT CAA CAA CTT CCG AAC TTT G	55 ^{O}C
3' 3F	ATA TTG TTT TCT CTC ACT GCT TCC A	
3' 3R	CAG AAA TCA ACA CGA TAG GTG TGT	53 ^{O}C
3' 4F	GGG CAG TCT TTG TAA ACT GGT C	
3' 4R	GGT TAA ACA ATC CGT AAA ATC GA	57 ^{O}C

Table 3.2. PCR primers used to amplify DiaX.

```
   5'1F
   GCACGAGCCTTAACGAAGAGAAAAAAGCTCCTTTACgAAACAAAGACTTTACCACCAAAC
  1---------+---------+---------+---------+---------+---------+
60
   CGTGCTCGGAATTGCTTCTCTTTTTTCGAGGAAATGcTTTGTTTCTGAAATGGTGGTTTG


   GTGAGATGGTTGTCCAGTATATTTCTGCCACTGCCAAATCTGGTGGGCTGAAAAACAGCA
 61---------+---------+---------+---------+---------+---------+
120
   CACTCTACCAACAGGTCATATAAAGACGGTGACGGTTTAGACCACCCGACTTTTTGTCGT


                                                        5'2F
   AACATGAATGCACCCTGTCTTCACAAGAATATGTTCATGAATTACGATCGGGTATATCAG
121---------+---------+---------+---------+---------+---------+
180
   TTGTACTTACGTGGGACAGAAGTGTTCTTATACAAGTACTTAATGCTAGCCCATATAGTC


   ATGAGAAACTTCTTAATTGCCTAGAATCCCTCAGGGTTTCTTTAACCAGCAATCCGGTCA
181---------+---------+---------+---------+---------+---------+
240
   TACTCTTTGAAGAATTAACGGATCTTAGGGAGTCCCAAAGAAATTGGTCGTTAGGCCAGT
                      5'1R


   GCTGGGTTAACAACTTTGGCCATGAAGGTCTTGGACTCTTATTGGATGAGCTGGAAAAGC
241---------+---------+---------+---------+---------+---------+
300
   CGACCCAATTGTTGAAACCGGTACTTCCAGAACCTGAGAATAACCTACTCGACCTTTTCG


   TTCTGGACAAAAAACAGCAAGAAAATATTGACAAGAAGAATCAGTATAAACTTATTCAAT
301---------+---------+---------+---------+---------+---------+
360
   AAGACCTGTTTTTTGTCGTTCTTTTATAACTGTTCTTCTTAGTCATATTTGAATAAGTTA


   5'3F
   GCCTCAAAGCATTTATGAATAATAAGTTTGGCTTACAAAGGATTCTAGGAGATGAAAGAA
361---------+---------+---------+---------+---------+---------+
420
   CGGAGTTTCGTAAATACTTATTATTCAAACCGAATGTTTCCTAAGATCCTCTACTTTCTT
                              5'2R
```

Figure 3.7.

Sequence of 5' and 3' ends Diaphanous X cDNA clone, generated by Eric Lynch, at the University of Washington School of Medicine. The position of primers designed at ICH is indicated by an underlined, bold sequence.

```
   GTCTTTTGCTATTGGCAAGAGCAATTGACCCCAAACAACCCAACATGATGACTGAAATAG
421---------+---------+---------+---------+---------+---------+
480
   CAGAAAACGATAACCGTTCTCGTTAACTGGGGTTTGTTGGGTTGTACTACTGACTTTATC


   TAAAAATACTTTCGGCAATTGCATTGTTGGAGAAGAGACACTCTAGATAAACTTTTACGG
481---------+---------+---------+---------+---------+---------+
540
   ATTTTTATGAAAGCCGTTAACGTAACAACCTCTTCTCTGTGAGATCTATTTGAAAATGCC

                    5'4F
   GGCTACAACACAGCAGCACGAAGAAATAACACGGAACGACTTTCACCACTTGTGGACCGT
541  ---------+---------+---------+---------+---------+---------+
600
   CCGATGTTGTGTCGTCGTGCTTCTTTATTGTGCCTTGCTGAAAGTGGTGAACACCTGGCA
                                           5'3R


   TTACAAATCANGAATCCTTGCATTACAGGTGGCTGCATGCACTTTATAATGCCCATGTAC
601---------+---------+---------+---------+---------+---------+
660
   AATGTTTAGTNCTTAGGAACGTAATGTCCACCGACGTACGTGAAATATTACGGGTACATG


   TTCTCCTTAGAGCTGCATTTCGACACTTTACGGATGATTCCTCGTCACGACTAAACACAG
661  ---------+---------+---------+---------+---------+---------+
720
   AAGAGGAATCTCGACGTAAAGCTGTGAAATGCCTACTAAGGAGCAGTGCTGATTTGTGTC


   TACAGATGATAGCAAAGAGATGTGAGCTGACATCACTTGACGTATTTGTAACACAAAAAT
721  ---------+---------+---------+---------+---------+---------+
780
   ATGTCTACTATCGTTTCTCTACACTCGACTGTAGTGAACTGCATAAACATTGTGTTTTTA


   GCCTACCGCATTTCACCCTCTTCTGCAATTG
781 ---------+---------+---------+- 811
   CGGATGGCGTAAAGTGGGAGAAGACGTTAAC
             5'4R

3'end of clone

                              3'1F
   TTTTTTTTTTTTTTTTTTTCATGTTTCCACTAGAAACTTTTACTACTTGATTATCTTAAA
  1---------+---------+---------+---------+---------+---------+
60
   AAAAAAAAAAAAAAAAAAAGTACAAAGGTGATCTTTGAAAATGATGAACTAATAGAATTT


   AAGTCATGTTGTACCATCACCCAATCCTGTTTAAAACAGCACTCAGGCCGTTTATGTAGC
 61---------+---------+---------+---------+---------+---------+
120
   TTCAGTACAACATGGTAGTGGGTTAGGACAAATTTTGTCGTGAGTCCGGCAAATACATCG
```

Figure 3.7 continued.

```
   TGATCTTGGATTAGCCCTTGTTGCACAGGGATGATTTACCACTGGATTCCTTGGAATCCG
121---------+---------+---------+---------+---------+---------+
180
   ACTAGAACCTAATCGGGAACAACGTGTCCCTACTAAATGGTGACCTAAGGAACCTTAGGC

            3'2F
   CTTTCGACGGTCTCTGAATGCTGCACCTGATTGTAGGGCTTCTAGAAGATTATCCATCAC
181---------+---------+---------+---------+---------+---------+
240
   GAAAGCTGCCAGAGACTTACGACGTGGACTAACATCCCGAAGATCTTCTAATAGGTAGTG
                                       3'1R

   ACCAGTCTCATCACCCTCTTTGTTTATATCAATGAGTTGTTTCTTTTTCTTCTGGCGTTC
241---------+---------+---------+---------+---------+---------+
300
   TGGTCAGAGTAGTGGGAGAAACAAATATAGTTACTCAACAAAGAAAAAGAAGACCGCAAG

   TAACTTTTCTTGTTCAGCTTTCTCTTTTGCAAGTTTTGCCCTCCTGGTCTTCTCTTCCAT
301---------+---------+---------+---------+---------+---------+
360
   ATTGAAAAGAACAAGTCGAAAGAGAAAACGTTCAAAACGGGAGGACCAGAAGAGAAGGTA

             3'3F
   TTCTCTTCTCATATTGTTTTCTCTCACTGCTTCCAAAAACAAAGTTCGGAAGTTGTTGAG
361---------+---------+---------+---------+---------+---------+
420
   AAGAGAAGAGTATAACAAAAGAGAGTGACGAAGGTTTTTGTTTCAAGCCTTCAACAACTC
                                          3'2R

   ATCACCAAAGAACTCTTCTATGCTCACTGTCTTTGAGTCAAAAATGAAGTATTCTCCAAG
421---------+---------+---------+---------+---------+---------+
480
   TAGTGGTTTCTTGAGAAGATACGAGTGACAGAAACTCAGTTTTTACTTCATAAGAGGTTC


   ATTCTCATAGAGCTTCATCATGTTGTTGTGCATGGTTGGACAGTTTTTCATACAGTTCTC
481---------+---------+---------+---------+---------+---------+
540
   TAAGAGTATCTCGAAGTAGTACAACAACACGTACCAACCTGTCAAAAAGTATGTCAAGAG

   3'4F
   GGGCAGTCTTTGTAAACTGGTCATCTTTTCACACACCTATCGTGTTGATTTCTGCTTGGC
541---------+---------+---------+---------+---------+---------+
600
   CCCGTCAGAAACATTTGACCAGTAGAAAAGTGTGTGGATAGCACAACTAAAGACGAACCG
                                       3'3R

   GGAATTTCTTGATGTCACTTCCAGATGAACAATTGTTGTTCCATGATGCAGGGTGCTCTG
601---------+---------+---------+---------+---------+---------+
660
   CCTTAAAGAACTACAGTGAAGGTCTACTTGTTAACAACAAGGTACTACGTCCCACGAGAC
```

Figure 3.7 continued.

```
   ACAACTTGGGCTGAACTTGCTTGCACTTCAACGTGTTCACATTCTTAGGACATTTTAGAA
661---------+---------+---------+---------+---------+---------+
720
   TGTTGAACCCGACTTGAACGAACGTGAAGTTGCACAAGTGTAAGAATCCTGTAAAATCTT



   TCTCAATTTTCCTCCAAAGTCGGCATAATCGAACGGTTGTTTTAATCGCGAATAAAACCT
721---------+---------+---------+---------+---------+---------+
780
   AGAGTTAAAAGGAGGTTTCAGCCGTATTAGCTTGCCAACAAAATTAGCGCTTATTTTGGA



   CGATTTTACGGATTGTTTAACCCAACCGGGATTTTGACCGCTTACTTTC
781---------+---------+---------+---------+--------- 829
   GCTAAAATGCCTAACAAATTGGGTTGGCCCTAAAACTGGCGAATGAAAG
   3'4R
```

Figure 3.7 continued.

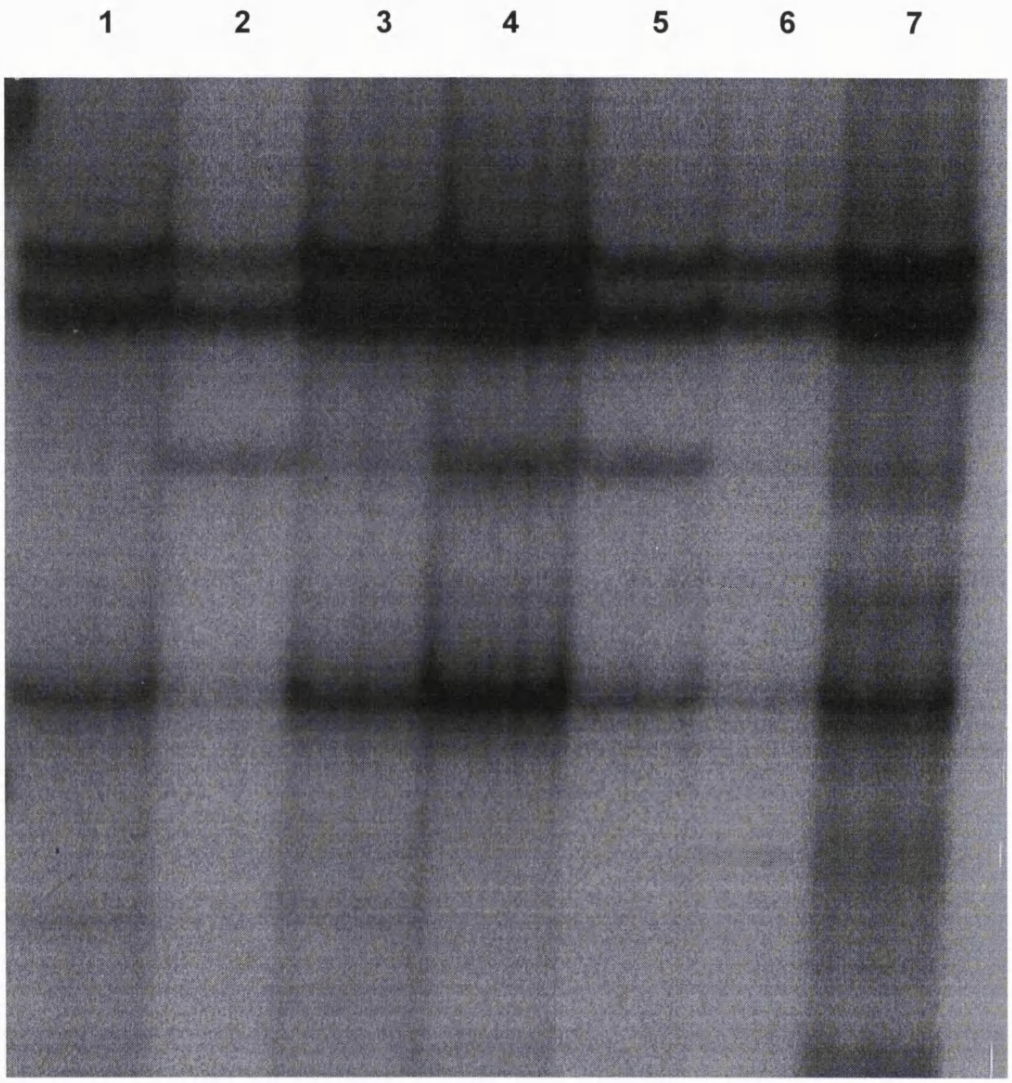

Figure 3.8.

Radioactive SSC analysis of DiaX, using primers 3' 3F and 3' 3R. No aberrant shifts were observed in individual V4, family CN (lane 3) as compared to control individuals (lanes 1,2,4-7).

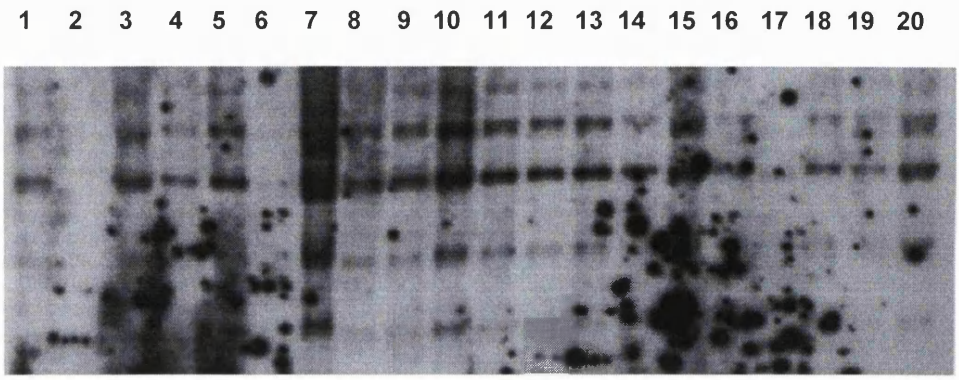

Figure 3.9.

Southern blot analysis of DiaX. *Eco*RI-digested DNA, probed with radiolabelled DiaX PCR product (primers 5' 4F and 3'4F), illustrating the same pattern of bands in individual V_4, family CN (lanes 1 and 9) and in individual III_4, family FP (lanes 3 and 10) as compared to control individuals (lanes 4-8, 11-20).

3.1.3.2.2. Deletions of Xq21.1-q22

Individual MBU

A DNA sample and lymphoblastoid cell line were available from this patient. This individual has a characterised deletion of Xq21.1-22, from DXS33 to pF1 (Bach *et al*, 1992; Clark *et al*, 1994), and clinically has choroideremia and mental retardation, but normal hearing. PCR analysis of microsatellite markers in Xq21-q24 was performed to further refine the extent of the deletion and establish whether or not patient MBU is deleted for DiaX.

The microsatellite markers analysed were DXS986, DXS1002, DXS990, PLP, DXS1231, DXS8096, DXS1230, DXS1106, DXS1210, DXS1220 and DXS1001. Individual MBU is deleted for the following markers; DXS1002, DXS990, DXS1231, and not deleted for the following markers; DXS986, DXS1106, DXS1230, PLP, DXS1210, DXS1220 and DXS1001. The minimum deletion of Xq21-q22 in individual MBU is between DXS1002 and DXS1231. Diagrammatic representation of MBU deletion is shown in figure 3.10.

Southern blotting, using the radiolabelled PCR products 5'4F and 3'4F (PCR product ~1.5Kb) 5'1F and 5'3R (PCR product ~600bp) and 3'1F and 3'3R (PCR product ~ 560bp) generated from the clone as probes, was used to detect any gross rearrangements of DiaX in patient MBU. On Southern blot analysis (figure 3.11), MBU is deleted for several bands, indicating a possible deletion of DiaX. The presence of some

bands on Southern blot analysis due to cross hybridisation of the autosomal homologue could not be ruled out.

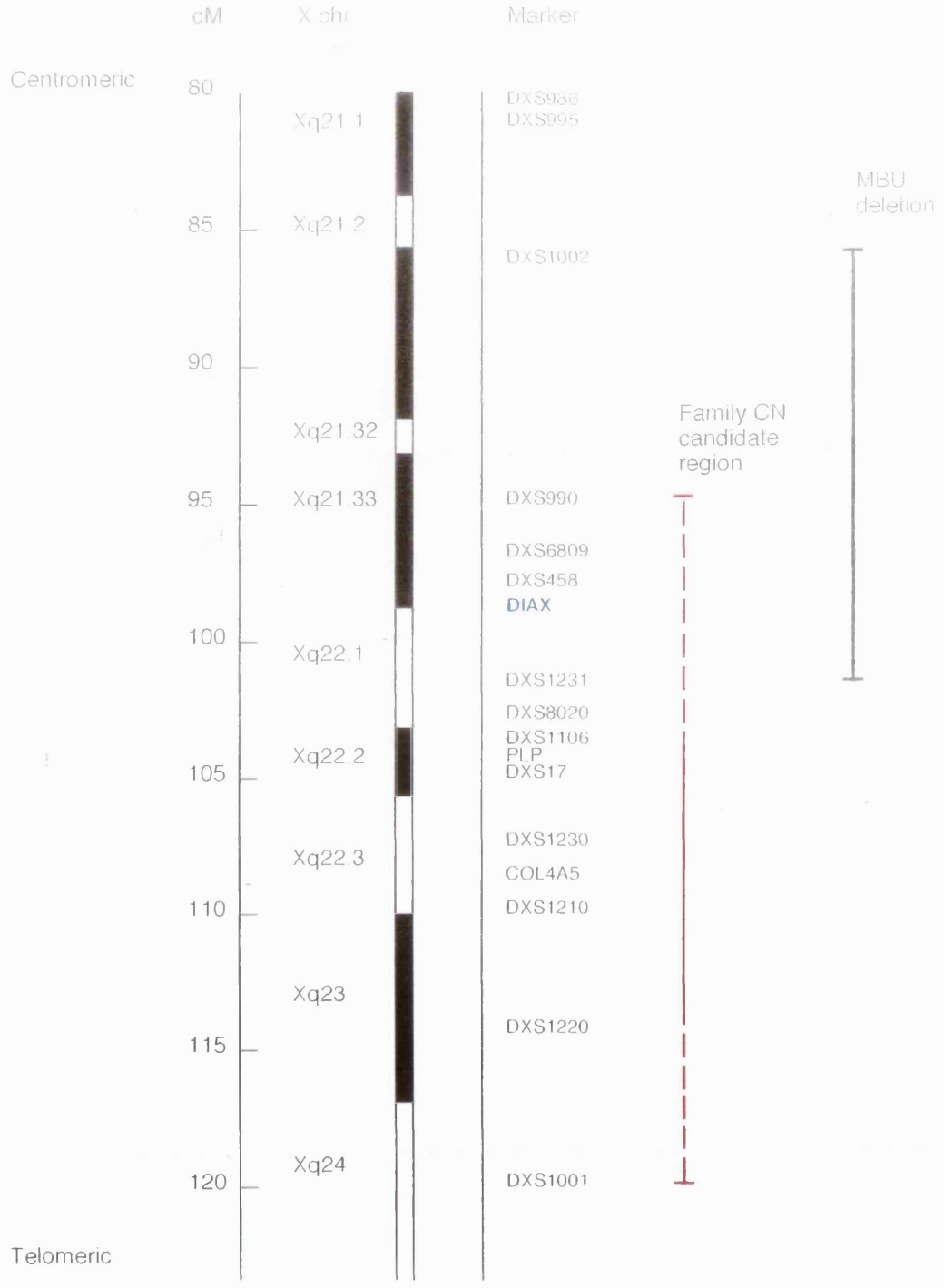

Figure 3.10.

Diagrammatic representation of MBU deletion in relation to the microsatellite markers analysed in this study, the DFN2 candidate region, and the approximate position of DiaX. The deletion is represented by a solid black line. The DFN2 candidate region is defined by a solid red line, a dashed line indicates the markers between which a recombination has been observed in Family CN.

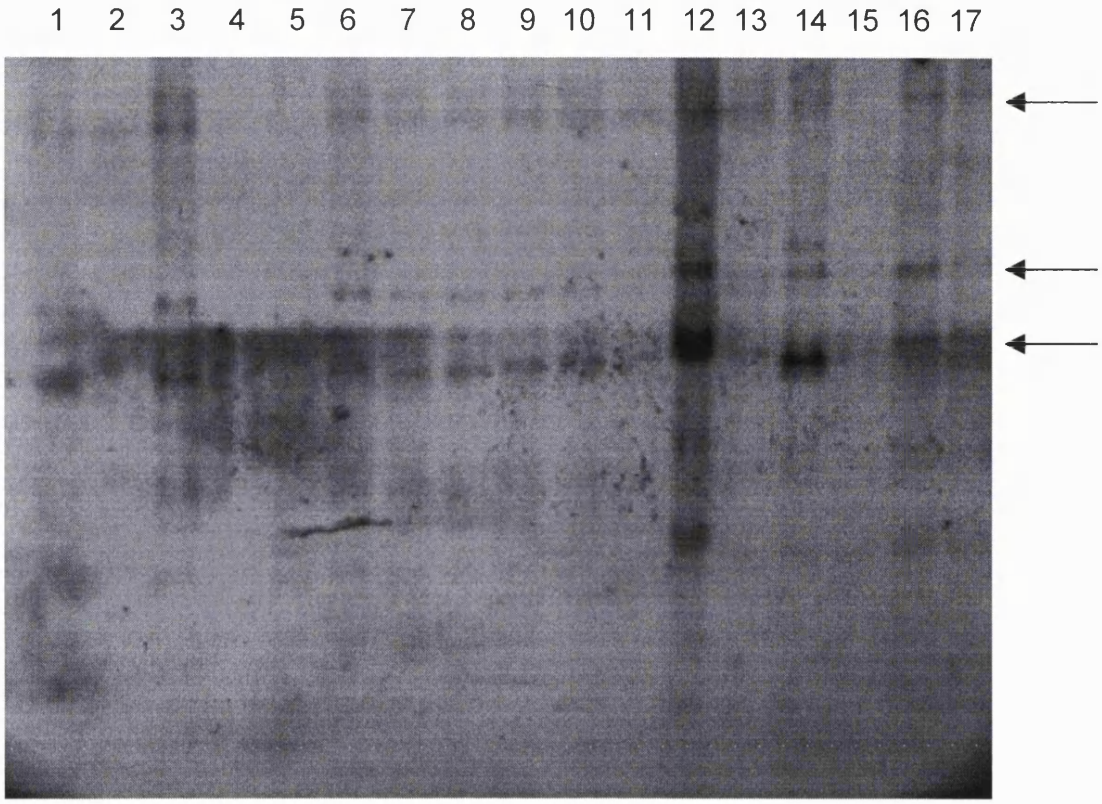

Figure 3.11.

Southern blot analysis of DiaX in individual MBU. *Eco*RI-digested DNA, probed with radiolabelled DiaX PCR product (primers 5' 4F and 3'4F), illustrating deletion of bands observed in individual MBU (lanes 5 and 15, indicated by arrows) as compared to control individuals (lanes 1, 3-4, 6-14, 17)

3.1.3.2.3. Mapping of Diaphanous X cDNA on a YAC contig encompassing Xq21-q22

This work was carried out in collaboration with Drs. David Vetrie and Elaine Kendall at Guy's Hospital, London. The purpose of this work was to map more precisely the position of DiaX. PCR products 5'4F and 3'4F (PCR product ~1.5Kb) 5'1F and 5'3R (PCR product ~600bp) and 3'1F and 3'3R (PCR product ~ 560bp) generated from the clone at ICH, were used by Elaine Kendall as probes to map DiaX cDNA onto a complete YAC contig and cosmid interval map covering human Xq21.33 to Xq22.3 from DXS3 to DXS287 (Kendall *et al*, 1997). These results localised the entire DiaX gene just telomeric to DXS458. The position of DiaX and DXS458 with respect to the DFN2 candidate region and deletion observed in MBU is illustrated in figure 3.10.

3.1.3.2.4. Further microsatellite analysis of Xq22 in Family CN.

The recombination defining the centromeric boundary of the DFN2 candidate region is between the markers DXS990 and DXS1106. In order to define more precisely the position of this recombination in Family CN, additional microsatellite markers located between DXS990 and DXS1106 were analysed. The results of which would hope to establish whether DiaX still mapped within the candidate region for the deafness in this family. Additional microsatellite markers analysed were DXS6809, DXS8020 and DXS178. The order of markers in relation to DXS458 and DiaX is as indicated: DXS990, DXS458, DXS6809, DiaX, DXS178, DXS8020 and DXS1106 (Collins *et al*, 1996). These markers

were not fully informative in this family, hence the recombination between DXS990 and DXS1106 could not be more finely mapped. DiaX still maps within the candidate region.

Compilation of these results makes it unlikely that the deafness in Family CN is caused by mutation in DiaX. It was demonstrated that DiaX maps just telomeric to DXS458, within the minimum deleted region of Xq22 observed in individual MBU. This mapping data combined with Southern blot and microsatellite analysis indicates that MBU is deleted for DiaX. Since MBU is not deaf, this suggests that complete deletions of DiaX do not result in hearing loss. DiaX maps within the DFN2 candidate region, but a mutation in DiaX was not identified by SSC and heteroduplex analysis in Family CN.

3.1.3.2.5. Expression of Diaphanous X in fetal tissues

Human autosomal diaphanous is ubiquitously expressed as demonstrated by Northern blot analysis (Lynch *et al*, 1997). In order to establish expression of DiaX, total RNA was extracted from tissues dissected from a 72 day old fetus. Expression of DiaX was demonstrated in fetal ear, gut, kidney and adrenal, stomach and hindbrain using RT-PCR, as shown in figure 3.12. The primers used were 3' 1F and 3'1R, giving a PCR product of 211 bp. Since the genomic structure of the gene is unknown, primers could not be designed to specifically cross an intron. Therefore in order to rule out the possibility of genomic DNA contamination, controls were set up in which no reverse transcriptase

enzyme had been added to the 1st strand cDNA reaction. This demonstrated that DiaX is widely expressed in fetal tissues including the ear.

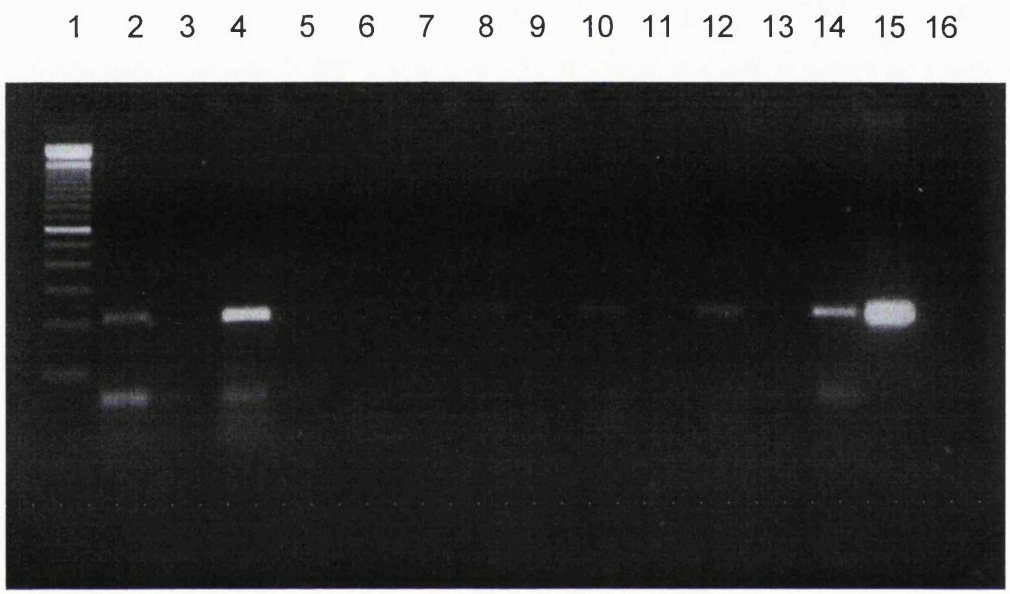

Figure 3.12.

PCR amplification of cDNA samples prepared from human fetal tissues, illustrating DiaX expression in fetal ear (lanes 2 and 12), gut (lane 4), kidney and adrenal (lane 6), stomach (lane 8) and hindbrain (lane 10). Lane 1, 100bp ladder. Lane 14, genomic control. Lane 15, IMAGE clone626664, 1/20 dilution. Lane 16, blank.
Lanes 3, 5, 7, 9,11 and 13 are RT minus controls.

3.1.4. Family FP

A second family with X-linked deafness, Family FP, was analysed for markers at the known XLD loci, DFN3, DFN4 and the new locus identified in Family CN (DFN2).

3.1.4.1. Microsatellite analysis at the DFN3 locus

Analysis of this family with the markers DXS986 and DXS1002, from Xq13-q21 showed multiple recombinations and excluded POU3F4 (DFN3) as the disease gene. Two-point lod scores generated by Liped are shown in table 3.3. DFN3 can be excluded as the disease gene if a lod score of -2 is taken as evidence against linkage.

Locus	Lod score at θ =						
	0.0	0.001	0.05	0.1	0.2	0.3	0.4
DXS986	-99.99	-7.371	-2.339	-1.505	-0.744	-0.365	-0.142
DXS1002	-99.99	-7.371	-2.339	-1.505	-0.744	-0.365	-0.142

Table 3.3.
Two point lod scores between the disease gene and marker loci for Family FP.

3.1.4.2. Microsatellite analysis at the DFN4 locus

Family FP was typed for the following microsatellite markers which span the DMD gene in order to exclude linkage to DFN4: 5' DYS I, intron 44, intron 45, intron 49, intron 50, introns 62/63 and 3' STR-HI. Typing

revealed different haplotypes in affected males across the entire DMD locus, excluding DFN4 as the causative locus in Family FP. The haplotypes are shown in figure 3.13 and show that the affected males, II_2, II_5, II_7 and III_4 do not share a common haplotype in this region, effectively excluding linkage.

3.1.4.3. Microsatellite analysis at the DFN2 locus

Subsequent to the observation of linkage of Family CN to Xq22, Family FP was typed for the dinucleotide repeat marker at COL4A5. As shown in figure 3.14, three of the affected males, II_5, II_7 and III_4, have different alleles, indicating that the COL4A5 gene is an unlikely candidate for the deafness in this family

3.1.4.4. Microsatellite analysis of X chromosome markers

Family FP was typed for the following markers shown in table 3.4, as part of the Research Genetics mapping set 6.0. These markers are spaced approximately at 10.75cM intervals along the X-chromosome, with an average heterozygosity of 0.75. Typing of these markers in Family FP failed to identify an informative marker consistent with linkage.

Microsatellite analysis of Family CN identified a novel locus for X-linked deafness, DFN2. The causative gene remains to be identified. Although it is unlikely that Family FP maps to either DFN2, DFN3 or DFN4, if new X-linked deafness genes are identified, then this family can be analysed for exclusion of a candidate gene. At the present time the small family

size precludes the possibility of independently establishing or refuting linkage.

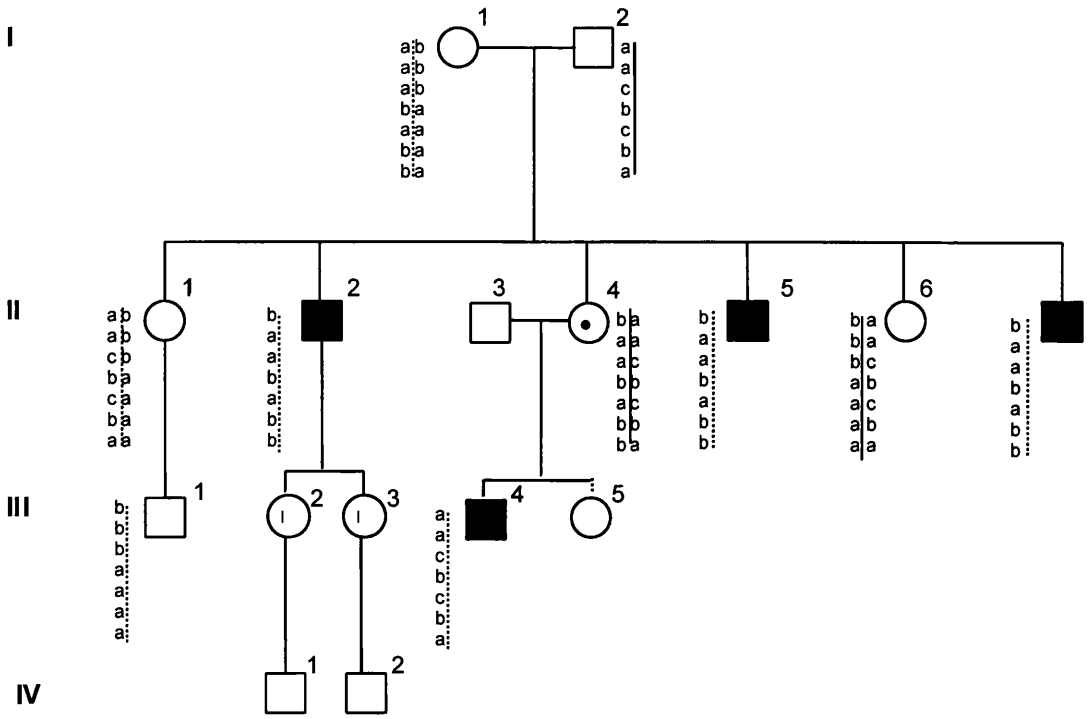

Order of Markers
5' DYS I
STR 44
STR 45
STR 49
STR 50
STR 62/63
3' STR HI

Figure 3.13.

Family FP. Probable haplotypes across the DFN4 locus at Xp21.1 assuming the least number of recombinations. The affected males do not share a common haplotype in this region. Individuals III_2, III_3, III_5, IV_1 and IV_2 were not typed for this marker since DNA was not available.

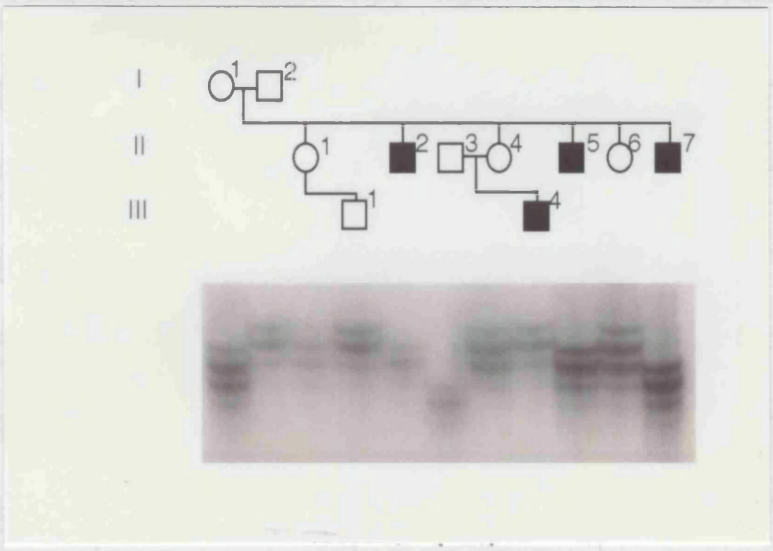

Figure 3.14.

Microsatellite analysis of Family FP with the diducleotide repeat at COL4A5. The three affected males II_5, II_7 and III_4 have different alleles effectively excluding this as the disease gene. Individuals III_2, III_3, III_5, IV_1 and IV_2 were not typed for this marker since DNA was not available.

Marker	Heterozygosity	cM between	Total cM along chromosome
DXS6807	0.68	0	
DXS987	0.83	14	14
DXS989	0.80	17	31
DXS1068	0.79	17	48
DXS6810	0.66	6	54
DXS1003	0.81	13	67
DXS7132	0.73	9	76
DXS6800	0.76	10	86
DXS6789	0.76	14	100
DXS6799	0.70	5	105
DXS6797	0.76	6	111
DXS6804	0.66	6	117
DXS1001	0.82	14	131
DXS1047	0.81	12	143
DXS1193	0.75	27	170

Table 3.4.

Microsatellite markers analysed as part of Research Genetics mapping set 6.0. Average heterozygosity and spacing of the markers along the X chromosome is indicated in centimorgans (cM).

3.1.5 DFN3 and POU3F4

The second part of the work on X-linked deafness addresses the clinical heterogeneity in DFN3. The majority of DFN3 families are accounted for by mutation in the *POU3F4* gene (de Kok *et al*, 1995; Bitner-Glindzicz *et al*, 1995). However in some X-linked deafness families which map to Xq12-q21, *POU3F4* mutations have not been identified. In some of these cases, microdeletions proximal to the *POU3F4* gene have been characterised (de Kok *et al*, 1995; de Kok *et al*, 1996).

The aim of this work was to analyse individuals with X-linked deafness who have characterised microdeletions proximal to *POU3F4* in order to study the effect of the deletion on *POU3F4* expression. From whether or not the expression of POU3F4 is altered in these individuals, it would provide evidence for the presence of another gene in the commonly-deleted region shared by these individuals, mutation in which results in deafness, or a position effect on the expression of the POU3F4 gene.

3.1.5.1. Expression system

The first task was to find an accessible tissue in which to study POU3F4 (BRN-4) expression. Ideally, one where POU3F4 is expressed at a detectable level, in order to look for a difference in level of expression between control individuals and individuals with the proximal deletion. Brn-4 (pou3f4) expression has been demonstrated in the developing and adult brain (Wegner *et al*, 1993) and the developing inner ear of the mouse (Phippard *et al*, 1998). RT PCR detects expression in human fetal

kidney at 6 and 8 weeks, and in an embryonic kidney cell line (M. Bitner-Glindzicz, 1996, PhD thesis). For this reason, urothelial cells sloughed into the urine were chosen as a source of RNA to examine POU3F4 expression.

3.5.1.1.1. POU3F4 expression in urine

Total RNA was extracted from urine from control individuals. First strand cDNA was used to amplify, by PCR, the region of BRN-4 using the primers Ia and Ib. cDNA amplification was not observed in urine as shown in figure 3.15. A band of approximately 220bp in the genomic control lane indicated that the PCR was successful. In order to check the integrity of cDNA from the urine sample, the 1st strand cDNA was used to amplify, by PCR, the region of HPRT between exon 7 and exon 9 (Jolly *et al*, 1983). The presence of a cDNA amplification product is indicated by a product size of approximately 200bp. Any genomic DNA contribution is indicated by a band of approximately 1.5kb. This PCR demonstrated the presence of cDNA in the sample. Having established this, the BRN-4 PCR product was electrophoresed on a 0.8% agarose gel, and a Southern blot generated. The presence of BRN-4 product was demonstrated using a radiolabelled BRN-4 PCR product as a probe (primers Ia and Vb, product size 1.1Kb). A diffuse band (lane 1) was observed on overnight exposure, as shown in figure 3.16. Lanes 3 and 4 show strong hybridisation to the genomic control.

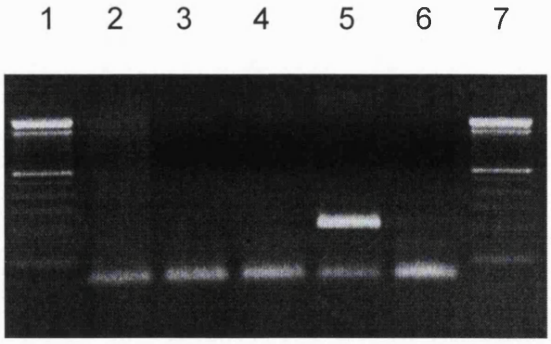

Figure 3.15.

cDNA amplification of POU3F4 from urothelial cells from adult urine. Lanes 2 and 4, cDNA from urine. Lane 3, RT minus control, Lane 5, genomic DNA. Lane 6, blank. Lanes 1 and 7, 100bp ladder.

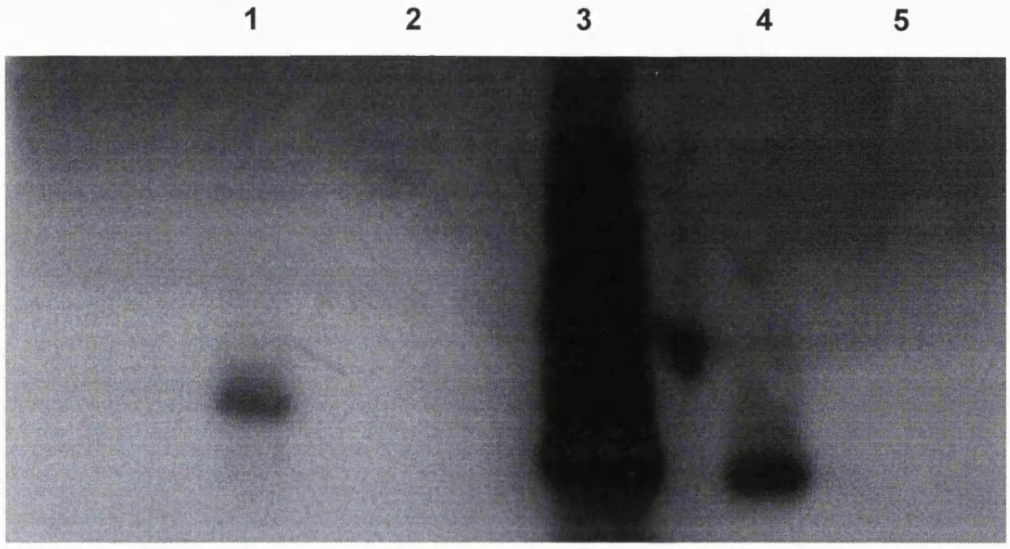

Figure 3.16.

Autoradiograph demonstrating POU3F4 expression in cells obtained from urine (Lane 1). Lane 2, RT minus control, Lanes 3 and 4, genomic control, lane 5, blank.

This work demonstrated low level expression of POU3F4 in urine. Due to doubts whether differences in expression of POU3F4 between individuals with the proximal deletion and control individuals could be accurately detected using this method and the problem of susceptibility to DNA contamination at such low levels of expression, another source of RNA was sought.

3.5.1.1.2. POU3F4 expression in lymphoblastoid cell lines

Total RNA was extracted from lymphoblastoid cell lines of control individuals and individuals with characterised deletions. PCR analysis showed that BRN-4 is not expressed in lymphoblastoid cell lines, an observation in keeping with published data (de Kok *et al*, 1996). HPRT control reaction demonstrated the integrity of the cDNA in the sample, as shown in figure 3.17.

Despite the demonstration of POU3F4 expression in cells obtained from urine, it was thought that this method would not be sensitive enough to detect changes in expression of POU3F4. Further experiments need to be performed to address the problem of whether the deletions cause a position effect on the POU3F4 gene, or whether the presence of a another transcript in the commonly-deleted region is responsible for the hearing loss in these individuals.

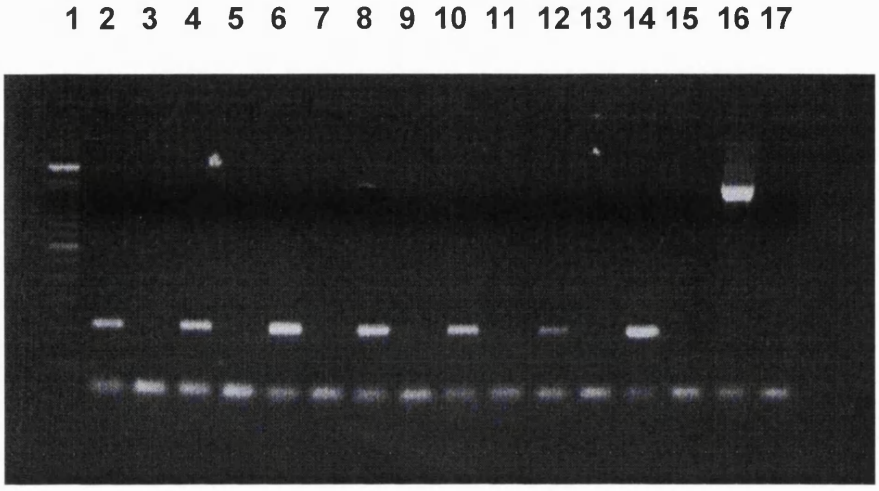

Figure 3.17.

PCR amplification of cDNA samples prepared from lymphoblastoid cell lines, demonstrating HPRT expression in lanes 2, 4, 6, 8, 10, 12 and 14. Lane 16, genomic control. Lane 17, blank.

Lanes 3, 5, 7, 9, 11, 13 and 15 are RT minus controls.

3.2. JERVELL AND LANGE-NIELSEN SYNDROME

3.2.1. Genetic mapping

At the start of this work, Jervell and Lange-Nielsen syndrome had not been mapped. The aim was to map this syndrome using homozygosity mapping and work towards the identification of the causative gene. The mapping strategy employed was a genome search in combination with microsatellite analysis of candidate loci. Very few families were available at the time, thus the mapping of JLNS centred around a single consanguineous British family, Family UK1S (Figure 2.3). Only affected members of the family were typed initially for each microsatellite marker. Once homozygosity for a single marker was observed, the entire family was then analysed at that locus. If homozygosity-by-descent was found for Family UK1S, then these regions were checked in other families with JLNS, which became available at a later stage of the work. During the course of this work, Neyroud *et al* described homozygosity for a single mutation in the potassium channel gene KVLQT1 in two families with JLNS (Neyroud *et al*, 1997).

3.2.1.1. Microsatellite analysis at candidate loci

Due to the clinical overlap between Romano Ward syndrome and Jervell and Lange-Nielsen syndrome, ion channels genes and loci implicated in Romano Ward syndrome were chosen as candidate regions (Wang *et al*, 1996; Curran *et al*, 1995; Wang *et al*, 1995; Schott *et al*, 1995). At least three highly polymorphic microsatellite markers were typed for each

candidate locus, as indicated in table 3.5. Additional markers within the chosen candidate locus were analysed if the results for a particular microsatellite marker was uninformative. Loci for autosomal recessive and autosomal dominant non-syndromic deafness were also chosen as candidate regions, information for which are shown in tables 3.6 and 3.7. These were chosen on the basis that syndromic and non-syndromic forms of deafness map to the same chromosomal location and could therefore be allelic (Everett *et al*, 1997: Li *et al*, 1998; Weil *et al*, 1995a; Liu *et al*, 1997a; Weil *et al*, 1997; Liu *et al*, 1997b)

3.2.1.2. Exclusion of candidate loci

Analysis of Family UK1S excluded the KVLQT1 gene as the disease locus, homozygosity for the microsatellite markers typed was not observed in the affected boys of Family UK1S. Initially, the markers D11S922, D11S1318 and D11S4146 were typed in Family UK1S. Additional markers were analysed due to the re-positioning of the KVLQT1 gene with respect to these microsatellite markers (Dausse *et al*, 1995). The exclusion of KVLQT1 as the disease locus provided evidence for genetic heterogeneity in Jervell and Lange-Nielsen syndrome. Microsatellite analysis of Family UK1S at this locus is shown in figure 3.18 and haplotype data is shown in figure 3.19.

All other candidate loci, loci for LQT2-LQT4, DFNA1-12 and DFNB1-12, and DFNB16, were excluded as the disease locus in Family UK1S on the basis that homozygosity by descent was not observed with any of the

microsatellite markers analysed. A genome search was initiated, typing microsatellite markers as part of the Research Genetics mapping set 6.0, spaced at approximately 10cM intervals.

Locus name	Location	Gene	Microsatellite markers	Reference
LQT1	11p15.5	KVLQT1	D11S922, D11S4046, D11S1318, D22S4088, D11S4146	Wang *et al*, 1996
LQT2	7q35-36	HERG	D7S483, D7S636, D7S505	Curran *et al*, 1995
LQT3	3p21-24	SCN5A	D3S1298, D3S1100, D3S1211	Wang *et al*, 1995
LQT4	4q25-27	unknown	D4S402, D4S430, D4S406	Schott *et al*, 1995

Table 3.5.

Microsatellite markers for Ion channel genes and loci implicated in Romano Ward syndrome, screened as part of genome search.

Locus name	Location	Microsatellite markers	Reference
DFNA1	5q31	D5S640, D5S410, D5S412	Leon *et al*, 1992
DFNA2	1p32	D1S255, MYCL1, D1S193	Coucke *et al*, 1994
DFNA3	13q12	D13S143, D13S175, D13S292	Chaib *et al*, 1994
DFNA4	19q13	D19S208, D19S224,ApoC2	Chen *et al*, 1995
DFNA5	7p15	D7S629, D7S673,D7S529	Van Camp *et al*, 1995
DFNA6	4p16.3	D4S1614, D4S412, D4S432	Lesperance *et al*, 1995
DFNA7	1q21-q23	D1S194, D1S196, D1S210	Fagerheim *et al*, 1996
DFNA8	11q22-24	D11S1345, D11S934, D11S1320	Kirschhofer *et al*, 1998
DFNA9	14q12-q13	D14S70, D14S121,D14S290	Manolis *et al*, 1996
DFNA10	6q22-q23	D6S267, D6S407, D6S472	O 'Neill *et al*, 1996
DFNA11	11q13.5	D11S911, D11S937	Tamagawa *et al*, 1996
DFNA12	11q22-24	D11S925, D11S1347, D11S934	Verhoeven *et al*, 1997

Table 3.6.

Microsatellite markers for autosomal dominant non-syndromic deafness loci screened as part of genome search.

Locus name	Location	Microsatellite markers	Reference
DFNB1	13q12	D13S143, D13S175, D13S292	Guilford *et al*, 1994a
DFNB2	11q13.5	D11S911, D11S527, D11S937	Guilford *et al*, 1994b
DFNB3	17p11.2-q12	D17S122, D17S805, D17S842	Friedman *et al*, 1995
DFNB4	7q31	D7S501, D7S496, D7S523	Baldwin *et al*, 1995
DFNB5	14q12	D14S79, D14S253, D14S286	Fukushima *et al*, 1995a
DFNB6	3p14-p21	D3S1767, D3S1289, D3S1582	Fukushima *et al*, 1995b
DFNB7	9q13-q21	D9S50, D9S301, D9S166	Jain *et al*, 1995
DFNB8	21q22	D21S212, D21S1225, D21S1575	Veske *et al*, 1996
DFNB9	2p22-p23	D2S144, D2S171, D2S158	Chaib *et al*, 1996a
DFNB10	21q22	D21S1225, D21S212, D21S1575	Bonné-Tamir *et al*, 1996
DFNB11	9q12-q21	D9S166, D9S175, D9S43, D9S1862	Scott *et al*, 1996
DFNB12	10q21-q22	D10S193, D10S537	Chaib *et al*, 1996b
DFNB16	15q21-q22	D15S132, D15S123	Campbell *et al*, 1997

Table 3.7.

Microsatellite markers for autosomal recessive non-syndromic deafness loci screened as part of genome search.

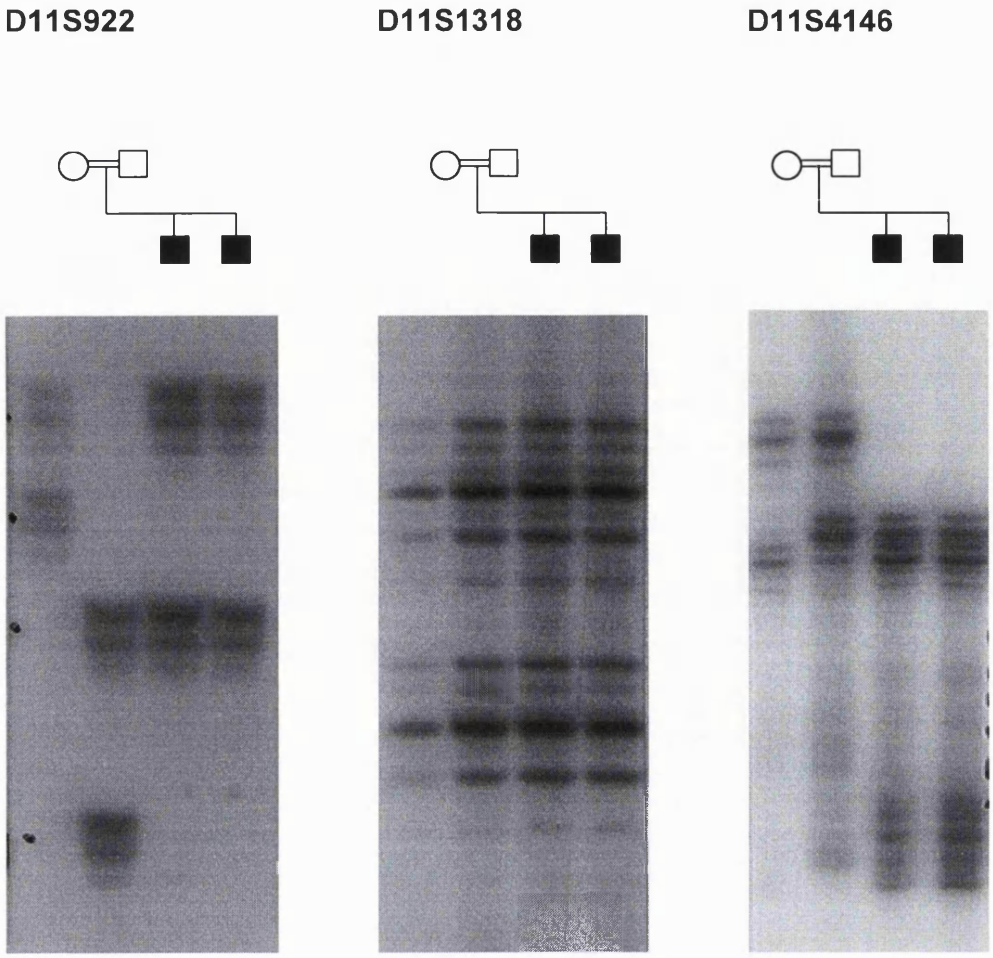

Figure 3.18.

Microsatellite analysis of Family UK1S at the KVLQT1 locus on 11p15.5. Markers shown are D11S922, D11S1318 and D11S4146.

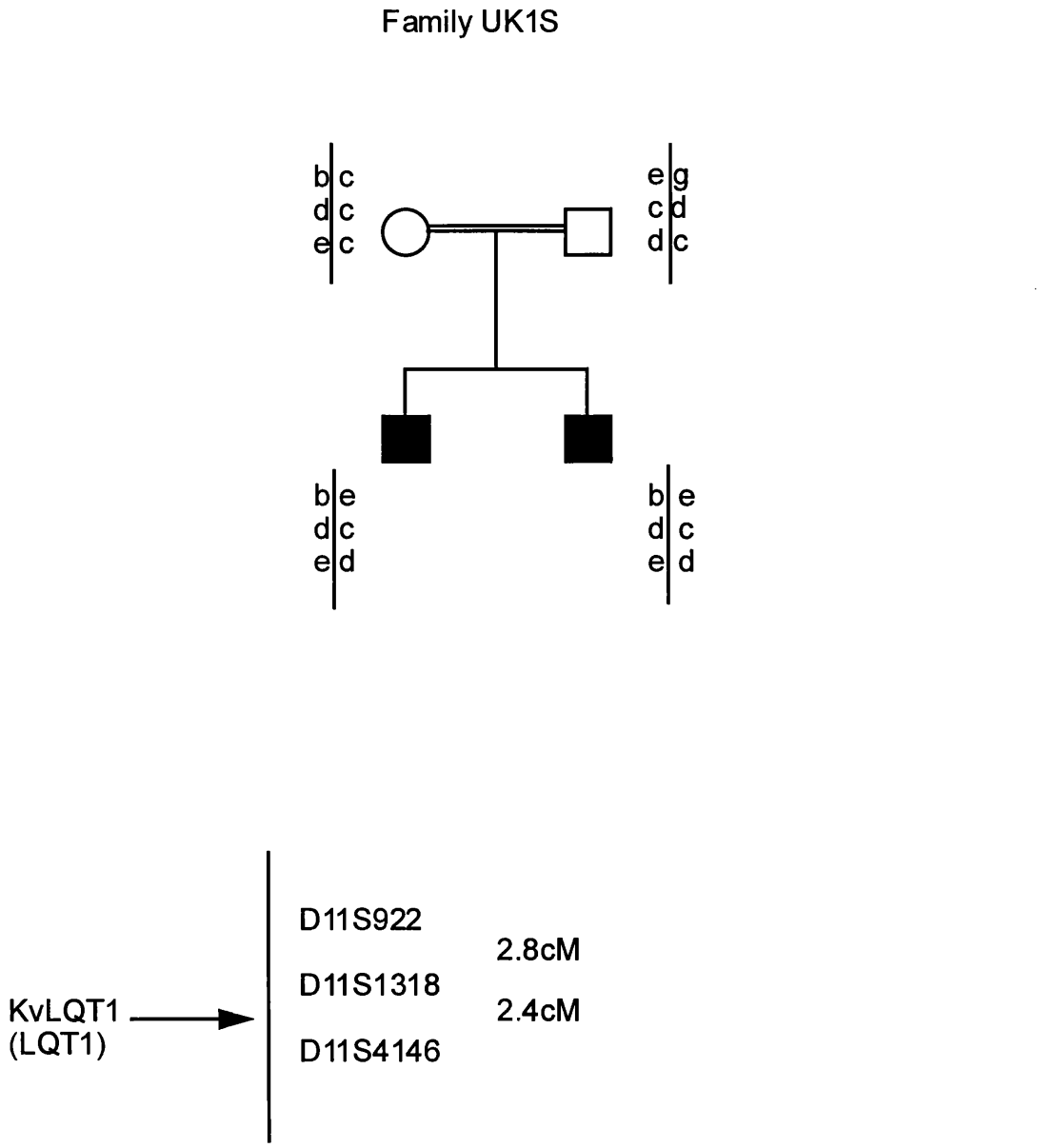

Figure 3.19.

Results of haplotyping for three markers, D11S922, D11S1318 and D11S4146 on chromosome 11 around the LQT1 locus in Family UK1S. The double line between the parents denotes consanguinity. The results show that although the two boys in this family have inherited the same alleles flanking this locus, they are not homozygous for any of the markers.

3.2.1.3. Genome search

A region of homozygosity by descent in Family UK1S was found on chromosome 21q22 with D21S261 after 50 microsatellite markers had been genotyped. Other markers which showed homozygosity are D21S1895 and D21S1252 but not D21S268 (D21S1254 was uninformative). Markers are in the order cen-D21S261, D21S1254, D21S1895, D21S1252, D21S268-tel. The minimum region of homozygosity is between the markers D21S263 and D21S1252, corresponding to an approximate genetic distance of 7cM (Dib *et al*, 1996). Microsatellite analysis of these markers is shown in figure 3.20, marker haplotypes are shown in Figure 3.21.

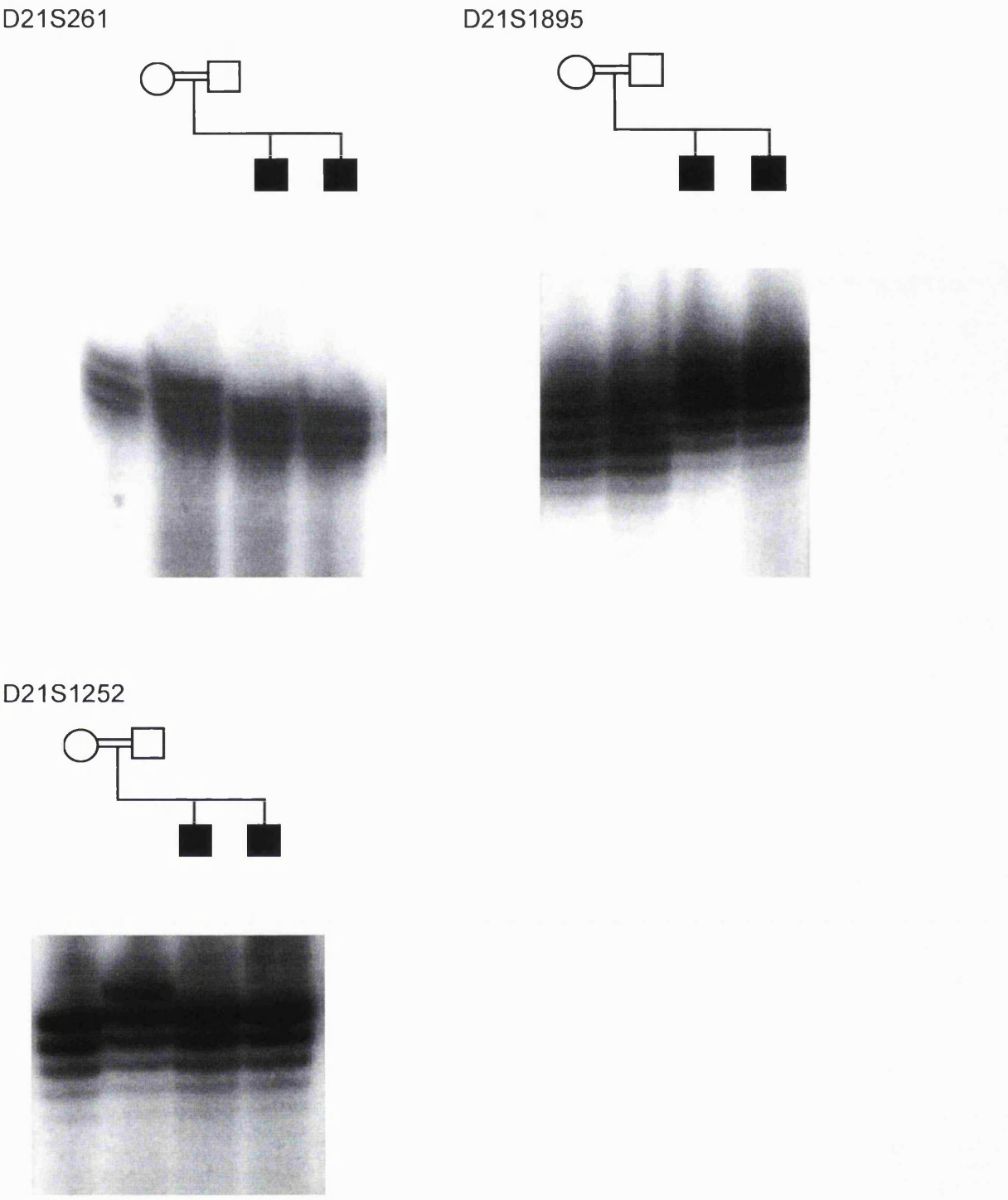

Figure 3.20.

Microsatellite analysis of Family UK1S at D21S261, D21S1895, and D21S1252.

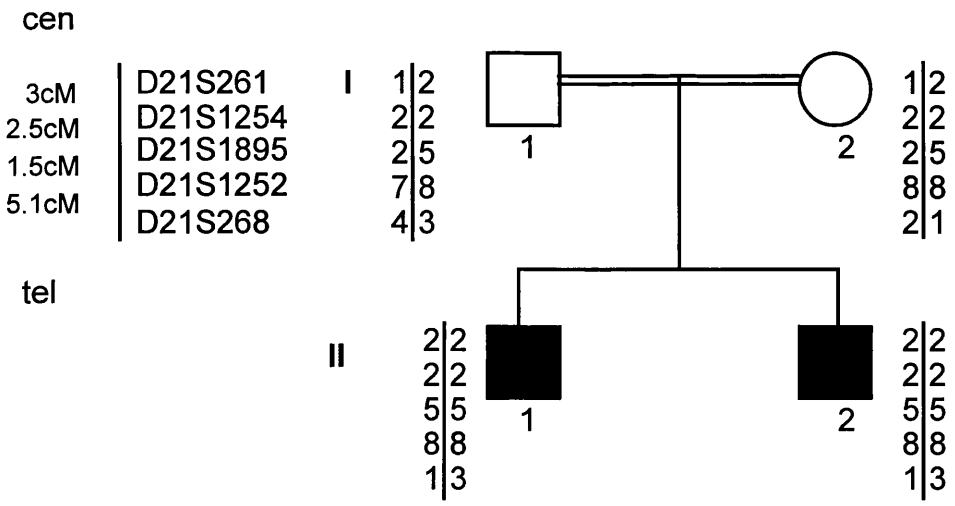

Figure 3.21.

Family UK1S with haplotype data for chromosome 21 markers, indicating homozygosity for the markers D21S261, D21S1254, D21S1895 and D21S1252.

Analysis of additional microsatellite markers on chromosome 21, D21S265 ~~D2S265~~, D21S1253, D21S269, D21S1258, D21S263, D21S1255, and D21S1259, demonstrated that the region of homozygosity observed in Family UK1S does not overlap with the autosomal recessive non-syndromic locus DFNB8 or DFNB10 (Veske *et al*, 1996; Bonné-Tamir *et al*, 1996), or the locus for Usher syndrome type 1E (Chaib *et al*, 1997).

3.2.2. Analysis of candidate gene, IsK

A candidate gene, IsK (minK), maps to the homozygous region observed in Family UK1S (Shimizu *et al,* 1995). The IsK gene is placed between the microsatellite markers D21S1254 and D21S1895 (Collins *et al*, 1996). The coding sequence of the IsK gene was analysed in Family UK1S and in 11 other families with JLNS using SSC analysis. Previously described intragenic polymorphisms were detected (Lai *et al*, 1994; Tesson *et al*, 1996) but no novel shifts were seen in single stranded DNA in the affected boys of Family UK1S or their parents or in any other JLNS families. However, novel heteroduplexes were observed in both parents in Family UK1S in double stranded DNA, neither of which were seen in over 60 control individuals (120 chromosomes) or in any other individuals with JLNS, as shown in figure 3.22.

Sequencing of the PCR products IsK gene showed the changes illustrated in figure 3.23, in which three separate nucleotides have been altered. The mutation identified is an A to C transition at nucleotide position 172, an insertion of C and a deletion of G within a stretch of 6

nucleotides, resulting in the overall change from ACCCTG to CCCCCT. The mutation described here causes Thr_{58} and Leu_{59} each to be replaced by Proline in the transmembrane region of the predicted protein.

Molecular analysis of Family UK1S excluded the KVLQT1 gene as the disease gene in this family, identified a new locus for Jervell and Lange-Nielsen syndrome, and implicated IsK as the causative gene. This is the first report of mutations in IsK associated with a human disease. This work demonstrated that more than one gene underlies the cardio-auditory syndrome, JLNS.

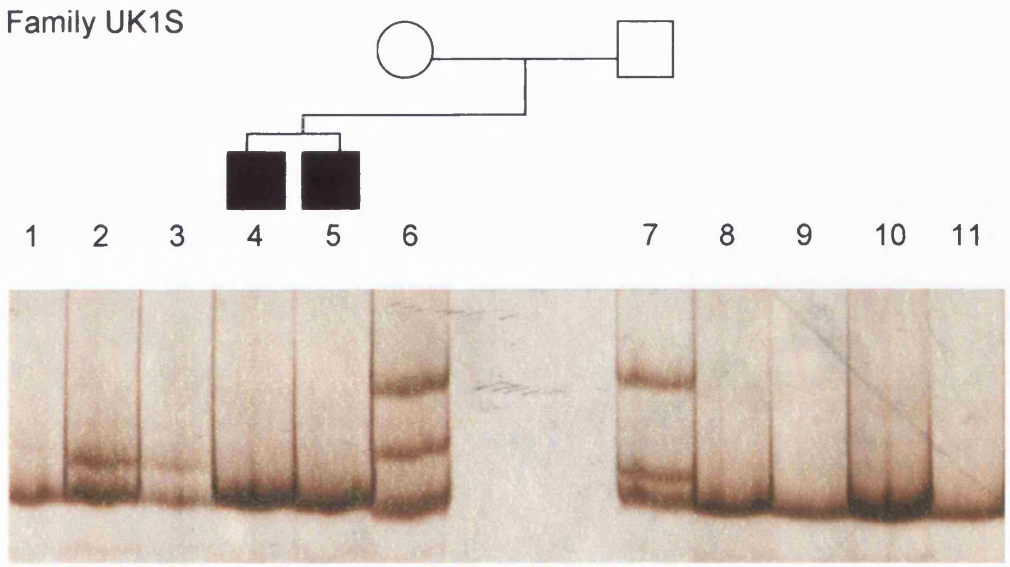

Figure 3.22.

SSC analysis of the IsK coding region in Family UK1S. Novel heteroduplexes were observed in individuals I_1 and I_2 (lanes 6 and 7). No aberrant bands were observed in the affected boys (lanes 4 and 5). Lanes 1-3, and 8-11 are control individuals.

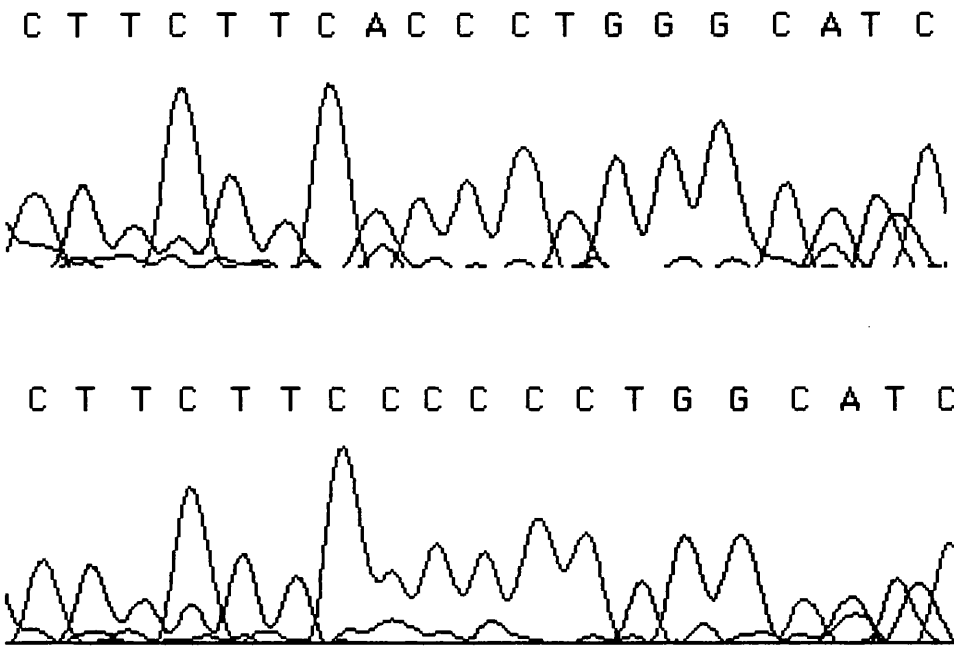

		Phe	Thr	Leu	Gly	Ile
WILD TYPE SEQUENCE	TC	TTC	ACC	CTG	GGC	ATC
MUTANT SEQUENCE	TC	TTC	C*CC	C**CT	GGC	ATC
		Phe	Pro	Pro	Gly	Ile

Figure 3.23.

Sequencing of mutation in Family UK1S. Top panel shows the wild type IsK sequence, lower panel the homozygous mutation. The DNA and protein sequences of the normal and mutant IsK alleles are displayed underneath the electropherograms. The base pair changes are indicated with an asterix.

3.2.3. Microsatellite analysis of JLNS families at the IsK locus on chromosome 21q22

Two additional families with Jervell and Lange-Nielsen syndrome were ascertained, families UK2T and UK3C, and in collaboration with Professor Lisbeth Tranebjærg in Norway, a further ten families were obtained, including the original JLNS family described in 1957 (Jervell and Lange-Nielsen, 1957).

DNA was initially available from three Norwegian families, families N3S, N5B and N8A, for mapping purposes. N8A is a small, consanguineous family, and in families N3S and N5B, consanguinity is suspected, but cannot be confirmed. Results of microsatellite analysis at the IsK locus for these families showed that the affected individuals of these families were not homozygous-by-descent for the microsatellite markers D21S1254, D21S1895 and D21S1252. Figure 3.24 illustrates results of haplotyping for three markers on chromosome 21, demonstrating that the IsK locus on chromosome 21 is not the disease locus in these families.

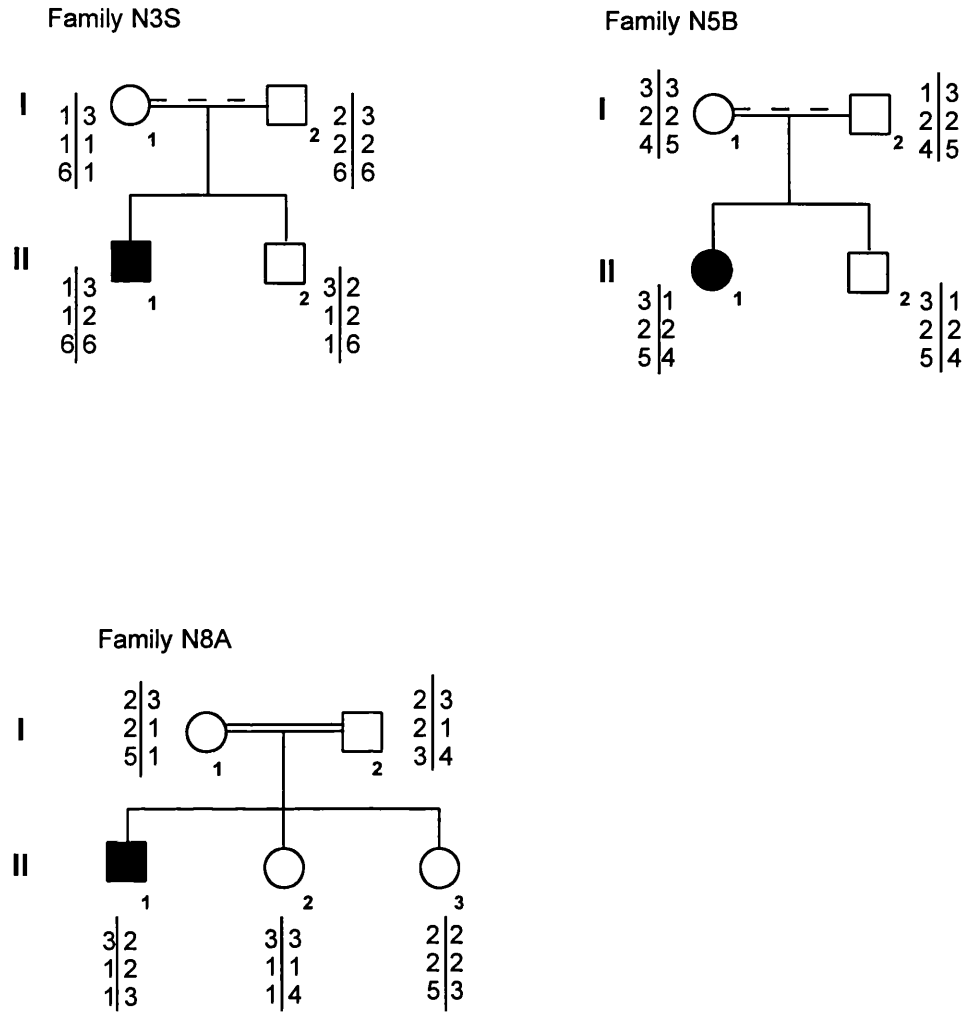

Figure 3.24.

Haplotype analysis at the IsK locus in families N3S, N5B and N8A, demonstrating lack of homozygosity-by-descent for microsatellite markers at this locus.

3.2.4. Microsatellite analysis of additional JLNS families at the KVLQT1 locus on chromosome 11p15.5

3.2.4.1. Norwegian families

Families N1H, N2S, N3S, N4O, N5B, N6K, N7J, N8A and N10D were typed with microsatellite markers flanking and within the KVLQT1 locus on chromosome 11p15.5. Mapping data in these additional families is consistent with linkage to chromosome 11 and the KVLQT1 locus. Haplotypes are shown in Figure 3.25. Families N1H and N10D were homozygous for markers D11S4046 and D11S1318, in Family N3S and N7J homozygosity by descent was seen for all the markers typed, D11S1318, D11S4088 and D11S4146. In Family N8A and N5B markers distal to D11S1318 were homozygous whereas in Family N6K homozygosity was observed for the markers D11S1318 and D11S4088.

There has been some debate on the position of the KVLQT1 gene with respect to these microsatellite markers. Previous analysis of recombinants in families with JLNS had indicated that the KVLQT1 gene is placed between the microsatellite markers D11S922 and D11S4146 (Neyroud *et al*, 1997) with the presumed order being D11S922, D11S4046, D11S1318, D11S4088, D11S4146 (Dib *et al*, 1996). The mapping of 12 recombinants in eight French families with autosomal dominant Long QT syndrome placed the gene distal to D11S1318 (Dausse *et al*, 1995). Correlation of the haplotype data for these Norwegian families shows the markers consistently homozygous are

D11S1318 and D11S4088. This suggests that the mutant gene is located between the markers D11S1318 and D11S4088, but given that the KVLQT1 gene covers a large genomic region (at least 300Kb), it is possible that some of these markers may lie within the gene itself (Lee *et al*, 1997).

3.2.4.2. British families

UK2T

The proband of Family UK2T is homozygous by descent for all the markers typed, D11S4046, D11S1318, D11S4088 and D11S4146, and therefore consistent with KVLQT1 as the disease locus in this family. Haplotypes are shown in figure 3.26.

UK3C

Family UK3C was first reported by Jeffrey *et al* (Jeffrey *et al*, 1992) as being excluded from the KVLQT1 locus. The affected sibs in this family were found to have inherited different parental alleles for a marker closely linked to the LQT1 locus (Harvey-ras) (Jeffrey *et al*, 1992). The Harvey-ras marker had not previously shown any recombinations with the disease locus in Romano-Ward families (Keating *et al*, 1991a: Keating *et al*, 1991b), until a report in 1994 excluded Harvey-ras from the Long QT locus (Roy *et al*, 1994). Refined mapping of the LQT1 locus (Neyroud *et al*, 1997; Dausse *et al*, 1995) and the availability of polymorphic markers closer to the KVLQT1 gene, prompted re-analysis

of this family. Haplotyping showed that recombination has occurred distal to Harvey-ras on the paternal chromosome, the two affected have inherited different paternal alleles for the marker D11S922. Both boys have inherited the same parental alleles for the markers D11S1318 and D11S4146, which are now known to flank the disease gene (Figure 3.27). Therefore the data in this family are now consistent with mutation at the LQT1 locus.

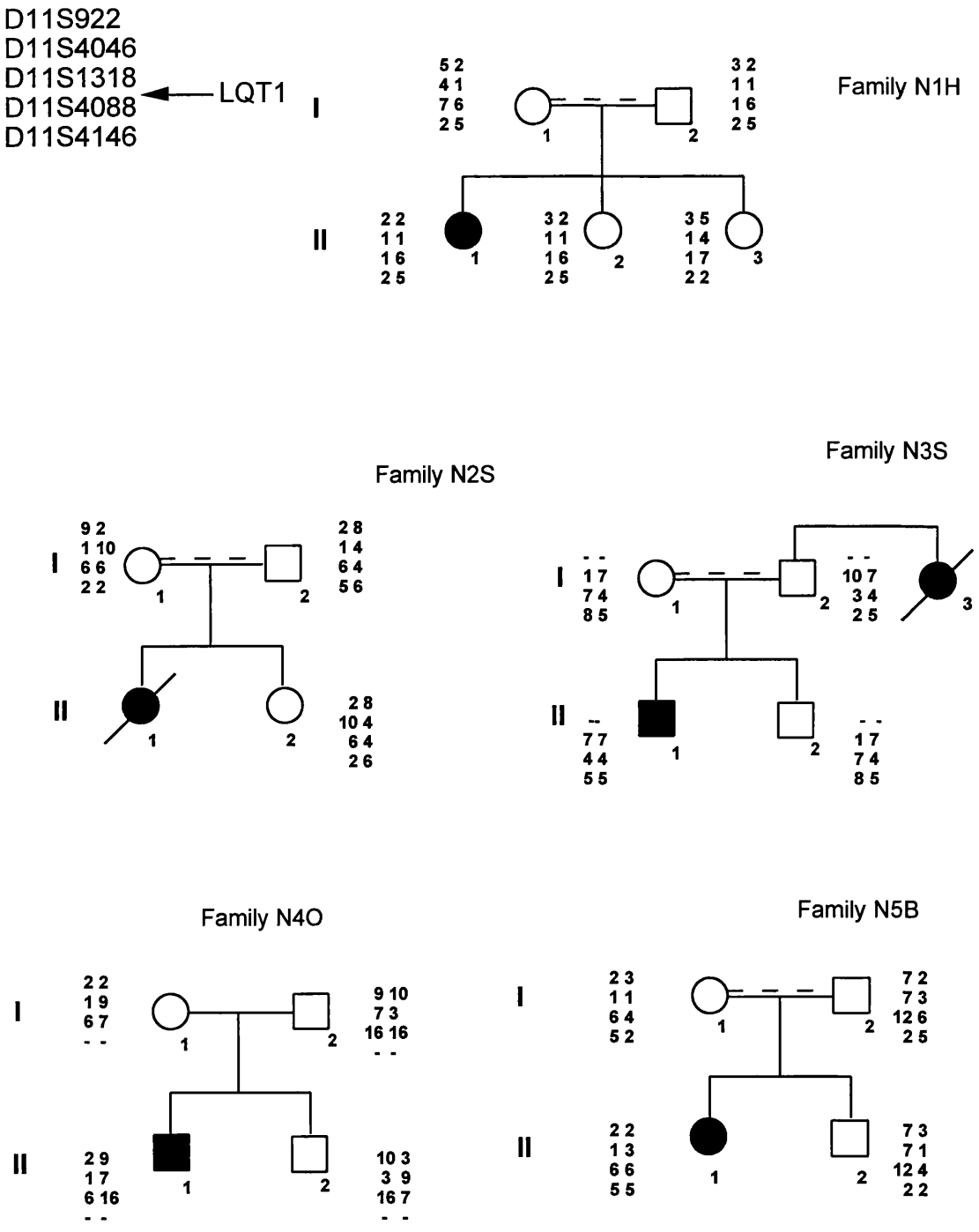

Figure 3.25.

Results of haplotyping for markers on chromosome 11 around the KVLQT1 locus in Norwegian JLNS families. Double line indicates consanguinity, dashed line indicates suspected consanguinity. Order of markers is as indicated in the key.

Family N6K

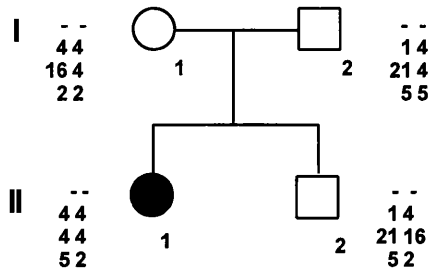

Family N7J

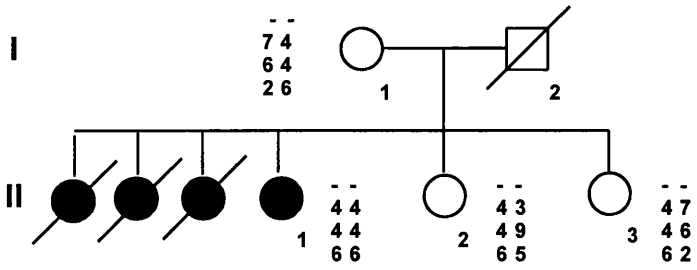

Family N8A

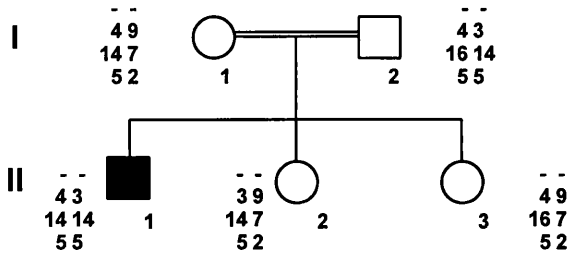

Family N10D

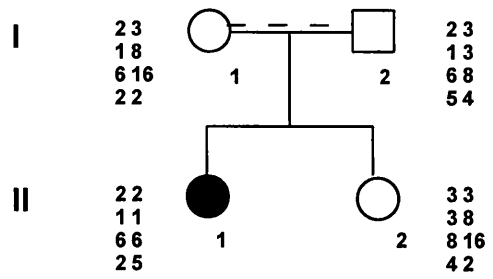

Figure 3.25 continued.

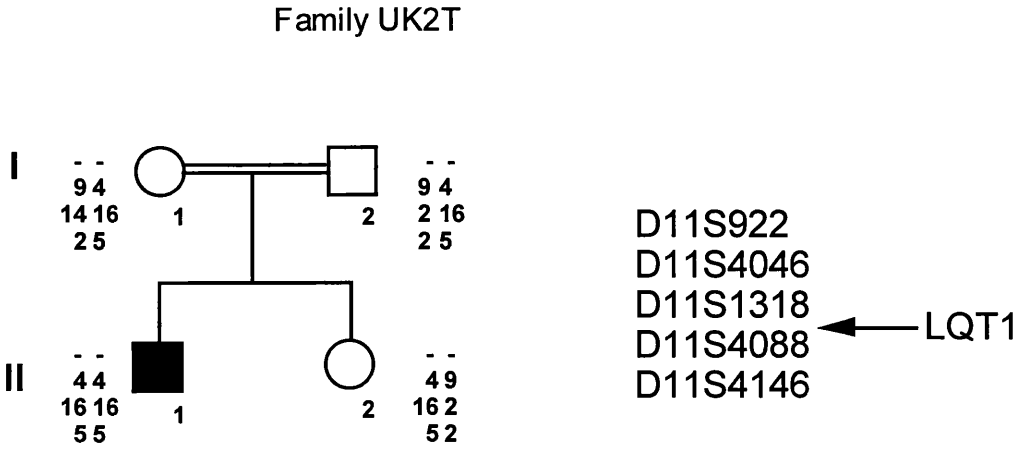

Figure 3.26.

Results of haplotyping for markers on chromosome 11 around the KVLQT1 locus in family UK2T. Double line indicates consanguinity. Order of markers is as indicated in the key.

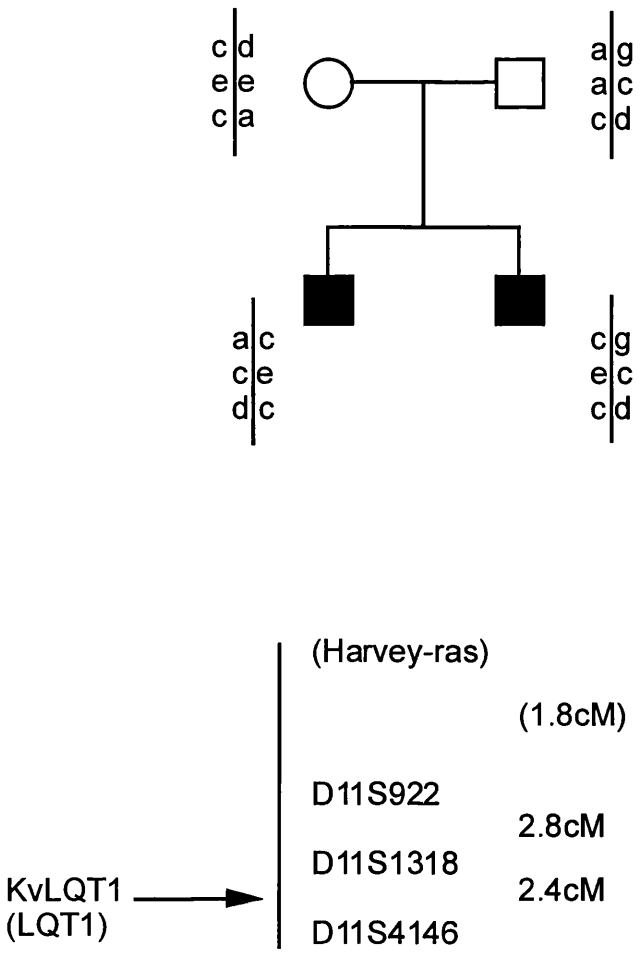

Figure 3.27.

Results of haplotyping for three markers, D11S922, D11S1318 and D11S4146 on chromosome 11 around the LQT1 locus in Family UK3C. The position of the Harvey-ras locus and its distance from D11S922 is shown in parentheses. Re-analysis of this family shows that a recombination has occurred on the paternal chromosome and that both sons have inherited the same parental alleles flanking the LQT1 locus.

3.2.5. PCR analysis of KVLQT1

The coding region of the KVLQT1 gene was amplified in the polymerase chain reaction (PCR) by intronic primers. Initially, only 40% of the genomic structure of KVLQT1 was known, exons 2 to 7 encoding the S2 to S6 transmembane domains (Wang *et al*, 1996). Primers designed by Wang were used to amplify KVLQT1 from genomic DNA between the S2 and S6 transmembrane segments (Wang *et al*, 1996).

Additional intron sequences were obtained from raw sequence data available on the world wide web at the University of Texas Southwestern Medical Centre at Dallas Genome Science and Technology Centre (GESTEC) (http://gestec.swmed.edu/sequence.htm). The GESTEC project efforts include the mapping and sequencing of human chromosome 11 and human chromosome 15. The policy is to release pre-analysed and analysed sequence information into a public database on the World Wide Web. From this sequence information, it was possible to obtain genomic structure for the KVLQT1 gene. Using information regarding the intron/exon boundaries (Lee *et al*, 1997) and the cDNA sequence of KVLQT1 (Wang *et al*, 1996), exons were identified from raw sequence data available for PACs 5541, pDJ74K15, pDJ608B4; BAC 70I6 and clone 6959, using a BLAST (**B**asic **L**ocal **A**lignment **S**earch **T**ool) programme. The position of these clones in relation to the KVLQT1 coding region is illustrated in figure 3.28. Primers were designed from the intronic sequence using a primer design programme at HGMP. PCR primers designed at HGMP were checked for specificity to KVLQT1

using a BLAST programme. No other significant homology was found. Exon 11 was screened in two parts A and B. From the raw sequence data analysed, it was evident that there was an additional intron, splitting the exon 11 coding sequence. Exon 11 had previously been published as one exon (Lee et al, 1997). This was the first set of primers to screen the C-terminal region of KVLQT1 from genomic DNA. Primer sequences are shown in Table 3.8.

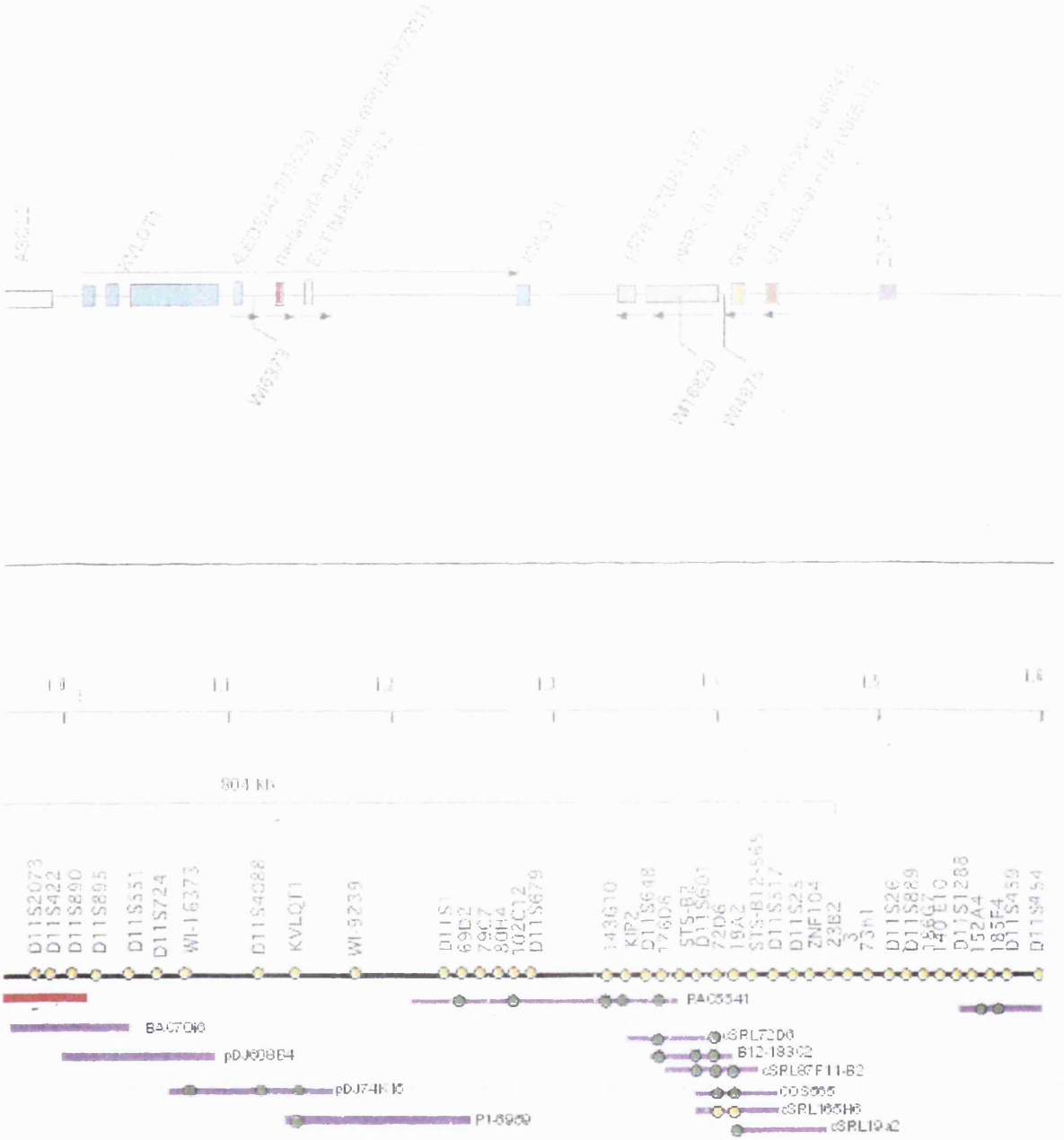

Figure 3.28.

Chromosome 11p15.5 contig, reproduced from the University of Texas Southwestern Medical Centre World Wide Web homepage (http://gestec.swmed.edu/sequence.htm), indicating the position of the KVLQT1 coding region with respect to clones analysed in this study.

Exon	Primer sequence	Product size	Annealing temperature (°C)
1	For. 5' TAATGGATGACTGGGTTTTCG 3' Rev. 5' AGGGAGATGCCAGCTTCC 3'	291bp	60°C
2	Wang *et al*, 1996		
3	Wang *et al*, 1996		
4	For. 5' CCCACACCATCTCCTTCG 3' Rev. 5' CCCGTTCAGGTACCCCTG 3'	258bp	57.5°C
5	Wang *et al*, 1996		
6	Wang *et al*, 1996		
7	Wang *et al*, 1996		
8	For. 5' AGCTGTAGCTTCCATAAGGGC 3' Rev. 5' ATGGTGAGATCCCAGCCTC 3'	286bp	62°C
9	Larsen *et al*, 1997		
10	For. 5' CTCCTTGAGCTCCAGTCCC 3' Rev. 5' CACAGCACTGGCAGGTTG 3'	236bp	58°C
11A	For. 5' CAGGTCTCAGATAGGCCTGC 3' Rev. 5' CCACTCACAATCTCCTCTCCTC 3'	260bp	62°C
11B	For. 5' GAGGCAAGAACTCAGGGTCTC 3' Rev. 5' GTCACTGCCTGCACTTTGAG 3'	284bp	62°C
12	For. 5' GGGCACGTCAAGCTGTCT 3' Rev. 5' GCAATGGCCCATTCTGAC 3'	239bp	56°C
13	For. 5' CAGGACGCTAACCAGAACCAC 3' Rev. 5' TTTTGACTCTCAGCTACCTCCC 3'	218bp	62°C
14	For. 5' GCTTCCCACCACTGACTCTC 3' Rev. 5' TCTCACTCAGGCCCATCC 3'	315bp	60°C

Table 3.8. PCR primers used to amplify KVLQT1.

3.2.5.1. Mutation screening of KVLQT1

Non-radioactive single-strand conformation polymorphism (SSC) analysis was used to screen for mutations in KVLQT1.

3.2.5.2. SSC analysis results

Single-strand conformation polymorphism (SSC) analysis of KVLQT1 demonstrated aberrant bands in exon 2 (Families N1H, N2S, N4O, N5B and N10D), exon 4 (Family UK2T), exon 6 (Family UK3C) and exon 11A (Families N2S, N3S, N4O, N6K and N7J). SSC analysis results for exon 11A is shown in figure 3.29. Both single stranded and heteroduplex bands are represented on the single gel. Interestingly, the mutations identified in exon 11A were only seen as heteroduplexes, no shifts were seen in the single-stranded DNA.

Figure 3.29.

SSC analysis of KVLQT1 exon 11A, for families N2S (lane 2), N3S (lanes3-5, 9), N4O (lanes 6-8, 10), N6K (lanes 11-14), N7J (lanes 15-18) and N8A (lanes 19-23). Lane 31 represents a control individual demonstrating a novel polymorphism. Both single- and double-stranded DNA is represented on the same gel. Arrows indicate the shifts observed as heteroduplexes.

3.2.5.3. Sequencing and confirmation of mutations

Direct sequencing was performed on PCR products demonstrating SSCP variants on both strands on an ABI 377 automated DNA sequencer. Novel KVLQT1 mutations were identified. Figure 3.30 illustrates a single KVLQT1 α-subunit, showing the position of each mutation with its corresponding premature stop codon.

Mutation 1, 572-576 delTGCGC.

A 5bp deletion in exon 2, 572-576 delTGCGC, was identified in six families from Norway; homozygous in the probands of families N1H, N5B and N10D, and heterozygous in the probands of families N2S, N4O and N9A. Sequence data is shown in figure 3.31. This 5bp deletion results in a frameshift, disrupting the coding sequence of KVLQT1 after the second putative transmembrane domain. It is predicted to lead to premature termination of the transcript at codon 282, the final amino acid residue of the fifth transmembrane domain. The predicted protein will lack the pore region, the S6 transmembrane domain and the entire intracellular C-terminal region.

This mutation and all subsequent mutations identified were confirmed, by either SSC analysis or restriction enzyme digest, in affected and unaffected members of the family, and in at least 50 control individuals (100 chromosomes) to rule out the possibility of the nucleotide change being a polymorphic variant.

The mutation 572-576 delTGCGC abolishes the cut site for the enzyme *Hha*I (cut site 5'...GCGC...3'). In normal controls, digestion with *Hha*I yields fragments of 98bp and approximately 80bp. In the homozygous affected individual, the 5bp deletion abolishes the cut site for the enzyme in the PCR fragment for exon 2, resulting in a single fragment of approximately 180bp as demonstrated in figure 3.32. In heterozygotes after *Hha*I digestion there are fragments of ~180bp, 98bp and ~80bp and an additional fainter band at 200bp. This faint band at 200bp probably represents heteroduplexes, partially resistant to *Hha*I digestion. This band, which is not present in controls or homozygous affected individuals, can be created by mixing PCR products from a normal and a homozygous affected individual, and then digesting with *Hha*I. This mutation was not observed in 120 normal chromosomes examined by restriction analysis.

Mutation 2, 728 G>A.

Direct sequencing of exon 4 revealed a homozygous substitution of G to A at position 728 in the proband of Family UK2T as illustrated in figure 3.33. This missense mutation results in an arginine being replaced by histidine at codon 243, a highly conserved residue in the S4 transmembrane domain. Both parents and sister are carriers for this mutation.

The mutation 728G>A disrupts a *BsiE*I restriction site in the exon 4 PCR fragment. This mutation destroys a single *BsiE*I site in this PCR

fragment. In unaffected individuals and controls digestion with *BsiE*I yields fragments of 194bp and 64bp. In the homozygous affected individual, the mutation abolishes the cut site for the enzyme, leaving intact a single fragment of 258bp as demonstrated in lane 2, figure 3.34. In heterozygotes after *BsiE*I digestion, there are fragments of 258bp, 194bp and 64bp. This mutation was not observed in 80 normal chromosomes examined by restriction analysis.

Mutation 3, 1008delC.

An aberrant band was noted in the PCR product of exon 6 in Family UK3C. The affected boys of this family and their mother were heterozygous for this shift. Direct sequencing showed a deletion of a single C nucleotide at position 1008, which results in a frameshift (Figure 3.35). This deletion of C nucleotide leads to a frameshift at codon 337 within the S6 domain, and the introduction of a premature stop codon at position 354. The protein, if produced, is predicted to lack the entire intracellular C-terminal portion of KVLQT1.

This shift was not seen in 50 Caucasian control individuals by SSC analysis.

Mutation 4, 1552C>T.

Two different mutations were identified in part A of exon 11. The aberrant SSCP band observed in families N2S, N3S and N4O corresponds to a substitution of C to T at position 1552 (1552C>T) (Figure 3.36) This

mutation changes an arginine residue at position 518 to a stop codon (TGA). The proband of families N2S, N4O and N9A are heterozygous for this nonsense mutation, the proband of Family N3S is homozygous.

The mutation 1552C>T abolishes the cut site for the enzyme *Taq*I (cut site 5'..TCGA...3') in the exon 11A PCR fragment. Figure 3.37 demonstrates that the enzyme site is abolished in individuals homozygous for this mutation leaving intact a single fragment of 260bp. In unaffected individuals and controls, digestion yields fragments of 189bp and 71bp and in heterozygotes, after *Taq*I digestion, there are fragments of 260bp, 189bp and 71bp.

Mutation 5, 1588C>T.

A second mutation in exon 11A was identified in families N6K and N7J. The affected individuals of both families are homozygous for this mutation. Electropherograms are shown in figure 3.38. This mutation is a C to T transition at position 1588, causing a substitution of glutamine at position 530 for a stop codon (TAG).

The mutation 1588C>T creates a cutting site for the restriction enzyme *Bfa*I (cut site 5'...CTAG...3') in the exon 11A PCR fragment. *Bfa*I does not cut in unaffected individuals, leaving intact the 260bp fragment as shown in figure 3.39 In the homozygous affected individuals, this mutation creates the cut site for the enzyme, resulting in two fragments

of 153bp and 107bp. In heterozygotes, after *Bfa*I digestion, there are three fragments of 260bp, 153bp and 107bp.

A summary of mutations in KVLQT1 identified in this study is shown in table 3.9. Numbering for all the mutations starts at the A nucleotide in the ATG initiation codon (Yang *et al*, 1997; Chouabe *et al*, 1997).

With the exception of the missense mutation identified in Family UK2T, the novel KVLQT1 mutations identified in these JLNS families are frameshift and nonsense mutations, resulting in the premature truncation of the predicted protein. The missense mutation of a highly conserved amino acid in the S4 transmembrane domain appears to be an exception.

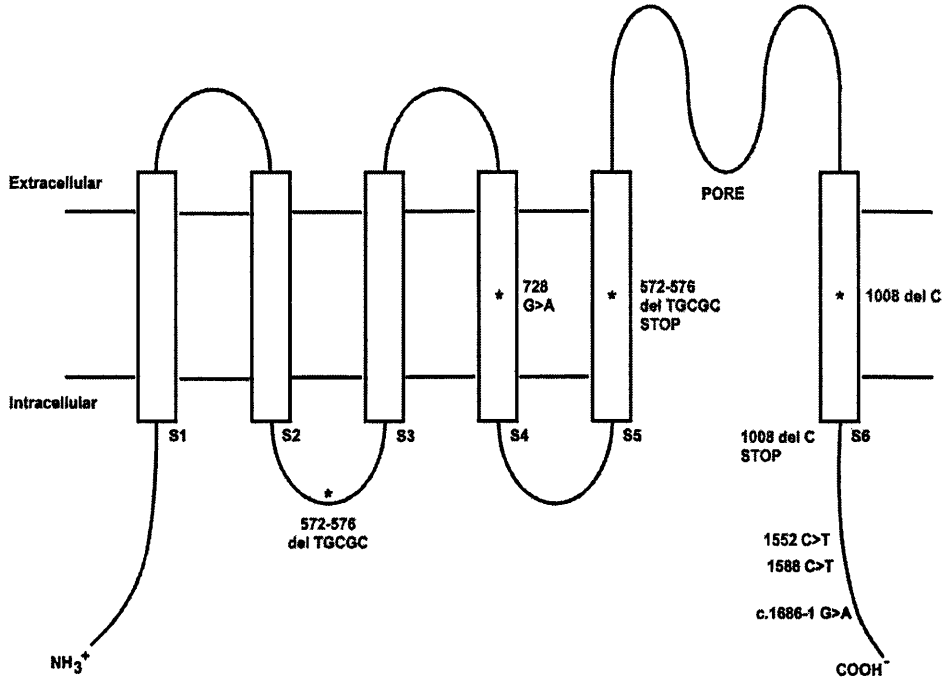

Figure 3.30.

Diagrammatic representation of a single KVLQT1 alpha-subunit. The "rectangles" represent transmembrane alpha-helices, numbered S1 to S6. The pore of the channel is formed by the loops between segments S5 and S6. The position of the novel mutations identified in this study is indicated. For the frameshift mutations, 572-576 delTGCGC and 1008 delC, the predicted position of protein termination is also indicated.

572-576 delTGCGC

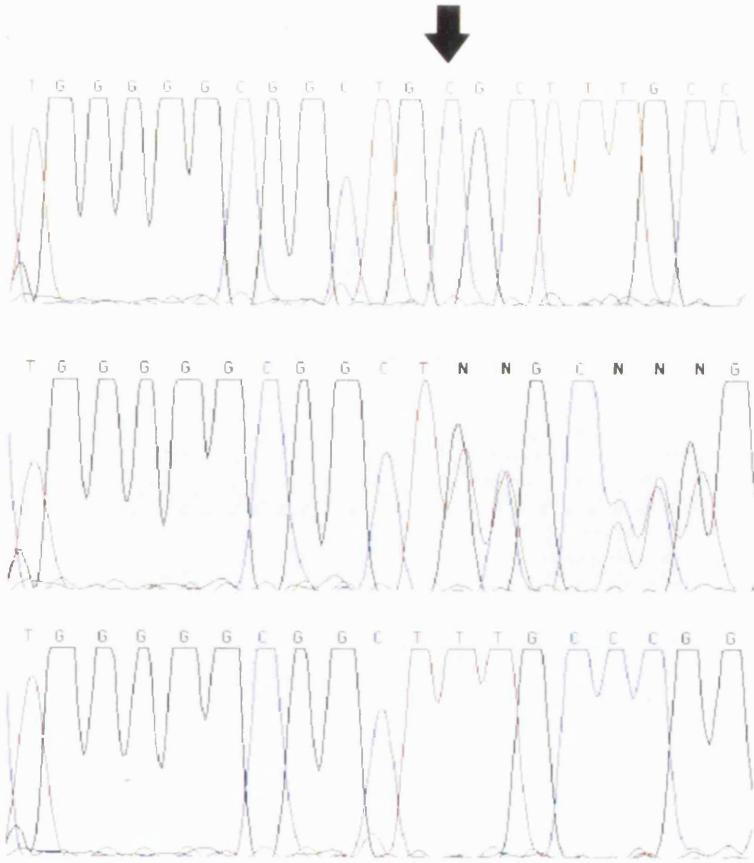

	Trp	Gly	Arg	Leu	Arg	Phe	Ala
WT	TGG	GGG	CGG	CTG	CGC	TTT	GCC...$Stop_{676}$
MUTN	TGG	GGG	CGG	CTT	TGC	CCG	GAA...$Stop_{284}$
	Trp	Gly	Arg	Leu	Cys	Pro	Glu

Figure 3.3.1.

Sequence analysis of KVLQT1: mutation 1, 572-576 delTGCGC. Sequence is shown for a control individual (top panel), a carrier (middle panel) and the affected individual (lower panel). An arrow indicates the site of the mutation. The DNA and polypeptide sequence of the normal and mutant KVLQT1 allele is displayed underneath the electropherograms.

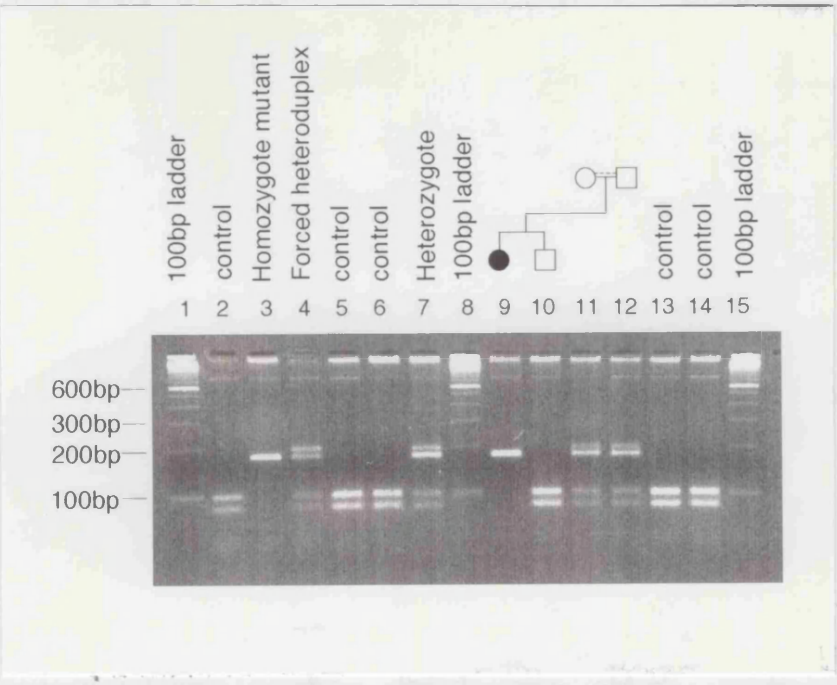

Figure 3.32.

Confirmation of mutation 1, 572-576 delTGCGC. PCR amplification products of exon 2 after digestion with the enzyme *Hha*I. In control individuals digestion yields fragments of 98 and 80bp (lanes 2, 5, 6, 13,and 14). In heterozygotes, after digestion there are fragments of 180, 98 and 80bp (lanes 7, 11 and 12) and in the homozygous affected individuals, the mutation abolishes the cut site for the enzyme, resulting in a single fragment of 180bp (lanes 3 and 9).

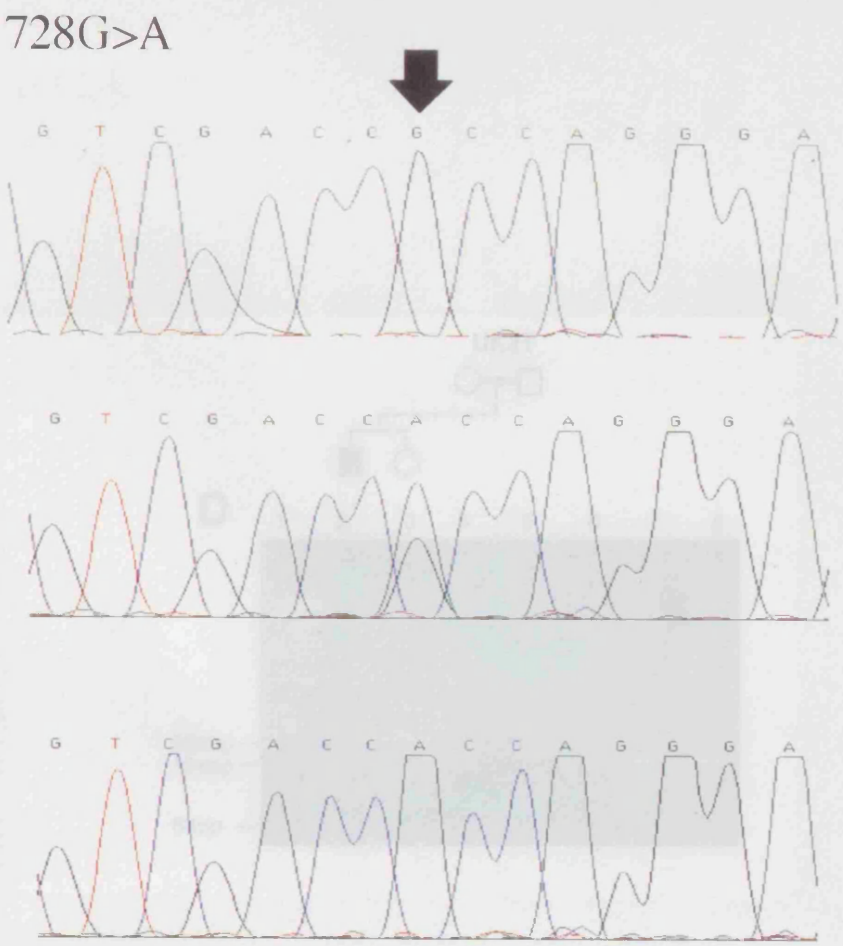

	Val	Asp	Arg	Gln	Gly
WT	GTC	GAC	CGC	CAG	GGA
MUTN	GTC	GAC	CAC	CAG	GGA
	Val	Asp	His	Gln	Gly

Figure 3.33.

Sequence analysis of KVLQT1: mutation 2, 728 G>A. Sequence is shown for a control individual (top panel), a carrier (middle panel) and the affected individual (lower panel). An arrow indicates the site of the mutation. The DNA and polypeptide sequence of the normal and mutant KVLQT1 allele is displayed underneath the electropherograms.

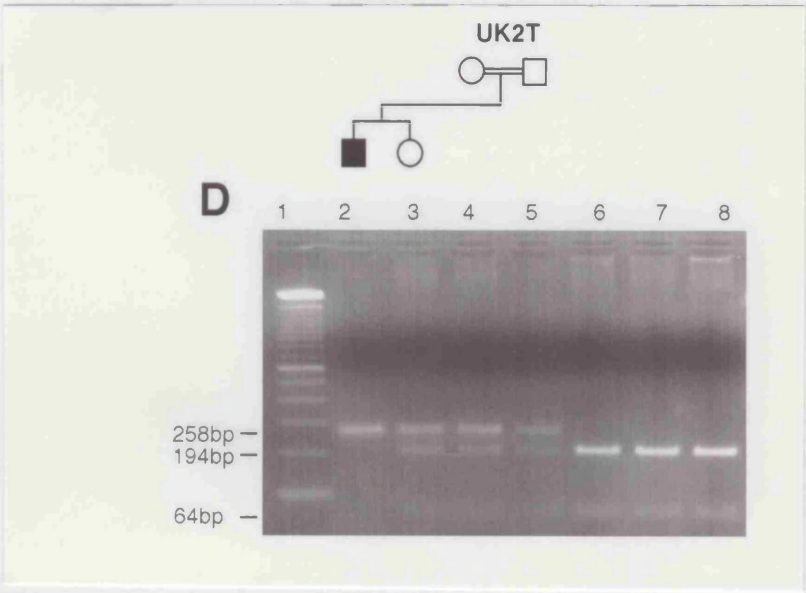

Figure 3.34.

Confirmation of mutation 2, 728 G>A. PCR amplification of exon 4 of the KVLQT1 gene after digestion with BsiEI. Results are shown below the pedigree. This mutation destroys a single BsiEI site in this PCR fragment. In unaffected individuals and controls, digestion yields fragments of 194bp and 64bp (lanes 6, 7 and 8). In the homozygous affected individual, the mutation abolishes the cut site for the enzyme, leaving intact a single fragment of 258bp (lane 2). In heterozygotes after BsiEI digestion, there are fragments of 258bp, 194bp and 64bp (lanes 3,4 and 5). Lane 1 shows 100bp ladder (Gibco BRL).

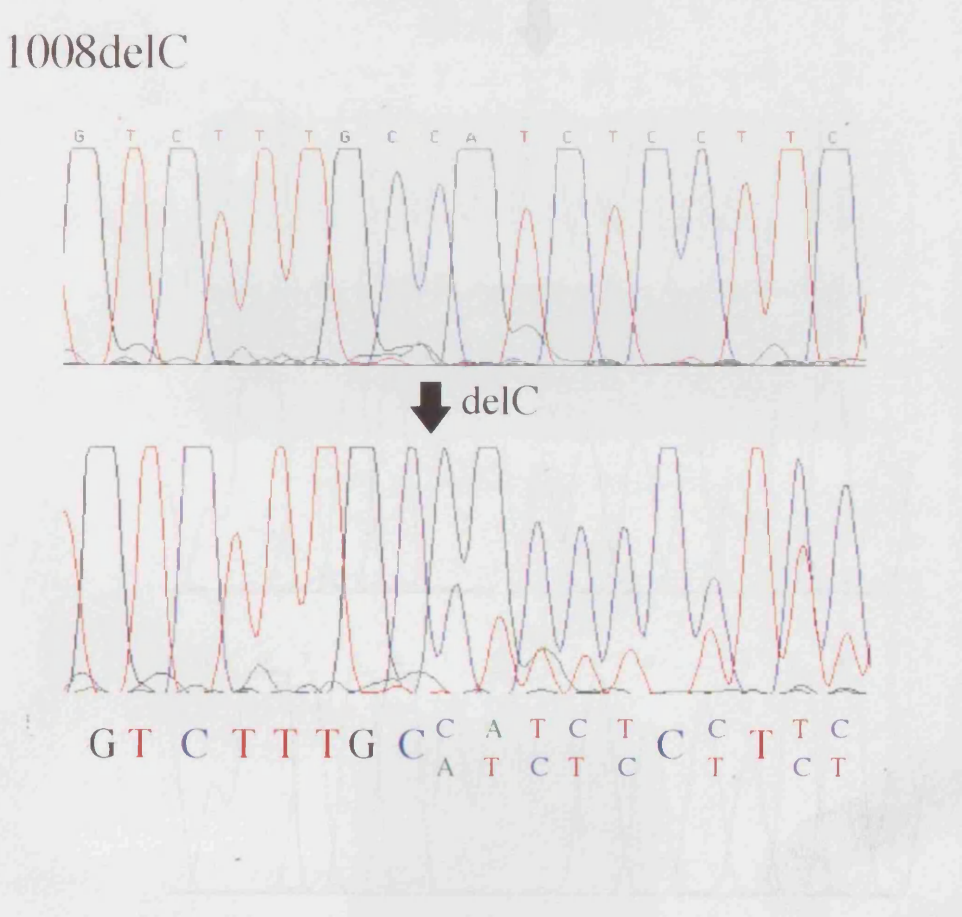

Val Phe Ala Ile Ser Phe

WT GTC TTT GCC ATC TCC TTC.....$stop_{676}$

MUTN GTC TTT GCA TCT CCT TCT.....$stop_{354}$

Val Phe Ala Ser Pro Ser

Figure 3.35.

Sequence analysis of KVLQT1: mutation 3, 1008 delC. Sequence is shown for a control individual (top panel) and a heterozygote (middle panel). This mutation was found only in the heterozygote form. An arrow indicates the site of the mutation. The DNA and polypeptide sequence of the normal and mutant KVLQT1 allele is displayed underneath the electropherograms.

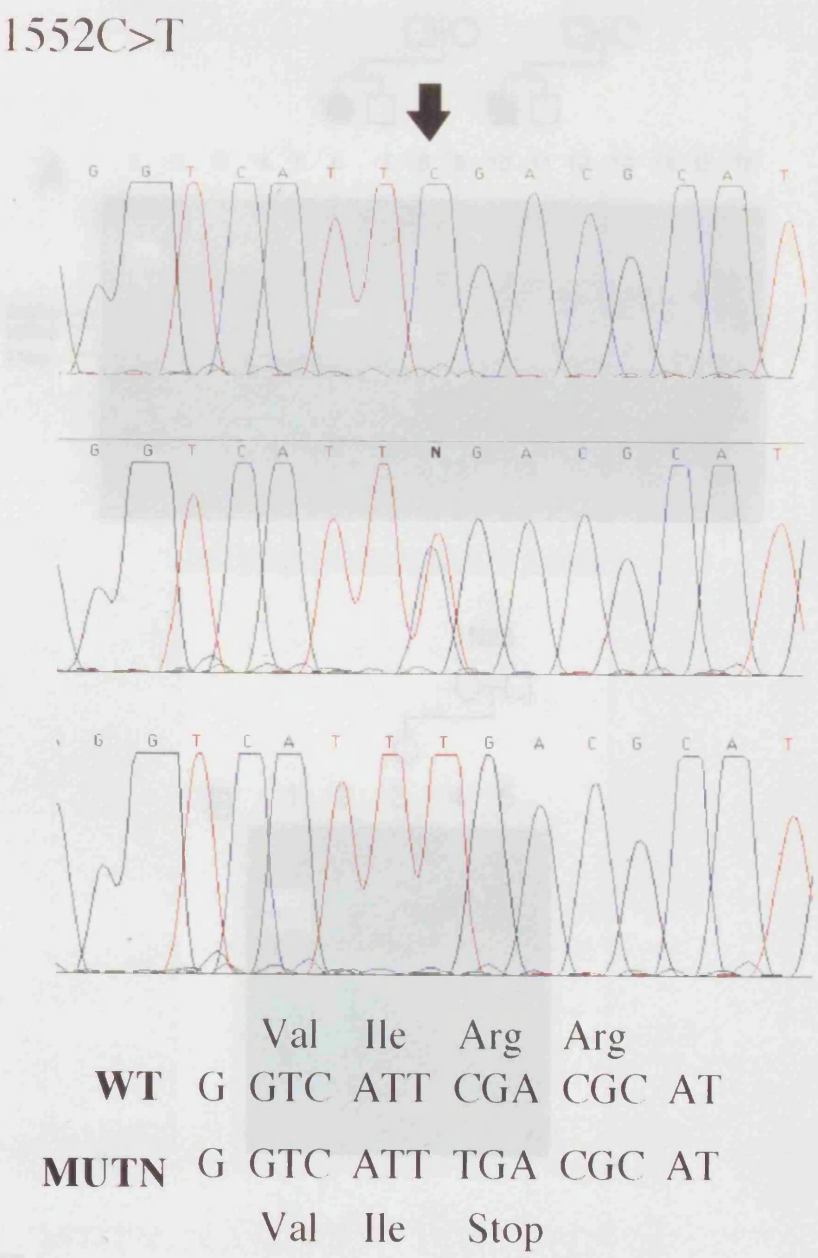

Figure 3.36.

Sequence analysis of KVLQT1: mutation 4, 1552 C>T. Sequence is shown for a control individual (top panel), a carrier (middle panel) and the affected individual (lower panel). An arrow indicates the site of the mutation. The DNA and polypeptide sequence of the normal and mutant KVLQT1 allele is displayed underneath the electropherograms.

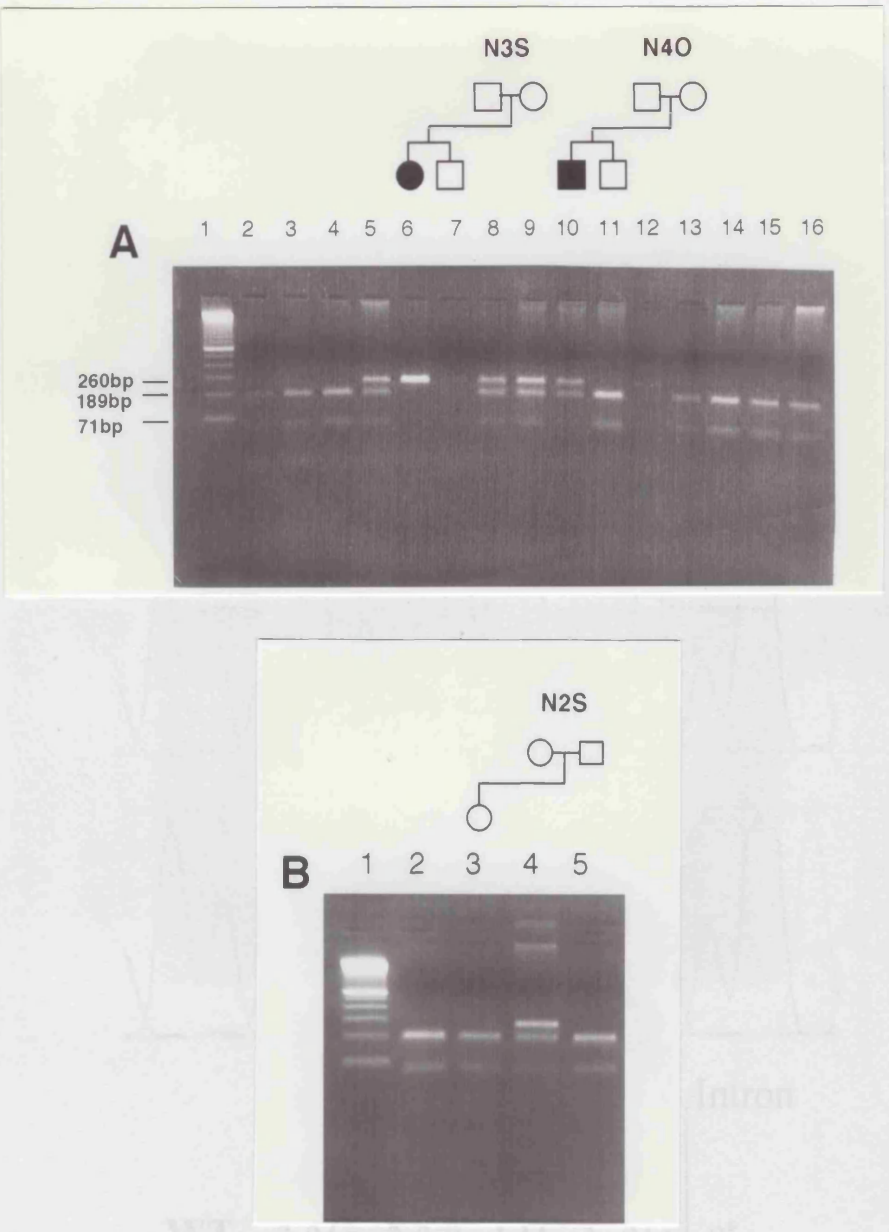

Figure 3.37.

Confirmation of mutation 4, 1552 C>T. PCR amplification products of exon 11 of the KVLQT1 gene after digestion with TaqI. Results are shown below each pedigree. In unaffected individuals and controls, digestion yields fragments of 189bp and 71bp (Panel A; lanes 2-4, 14-16: Panel B; lanes 2,3,5). In the homozygous affected individual, the mutation abolishes the cut site for the enzyme, resulting in a single fragment of 260bp (Panel A; lane 6). In heterozygotes, after TaqI digestion, there are fragments of 260bp, 189bp and 71bp (Panel A; lanes 5,7,8,9,12: Panel B; lane 4). Lane 1 of each panel shows 100bp ladder (Gibco BRL).

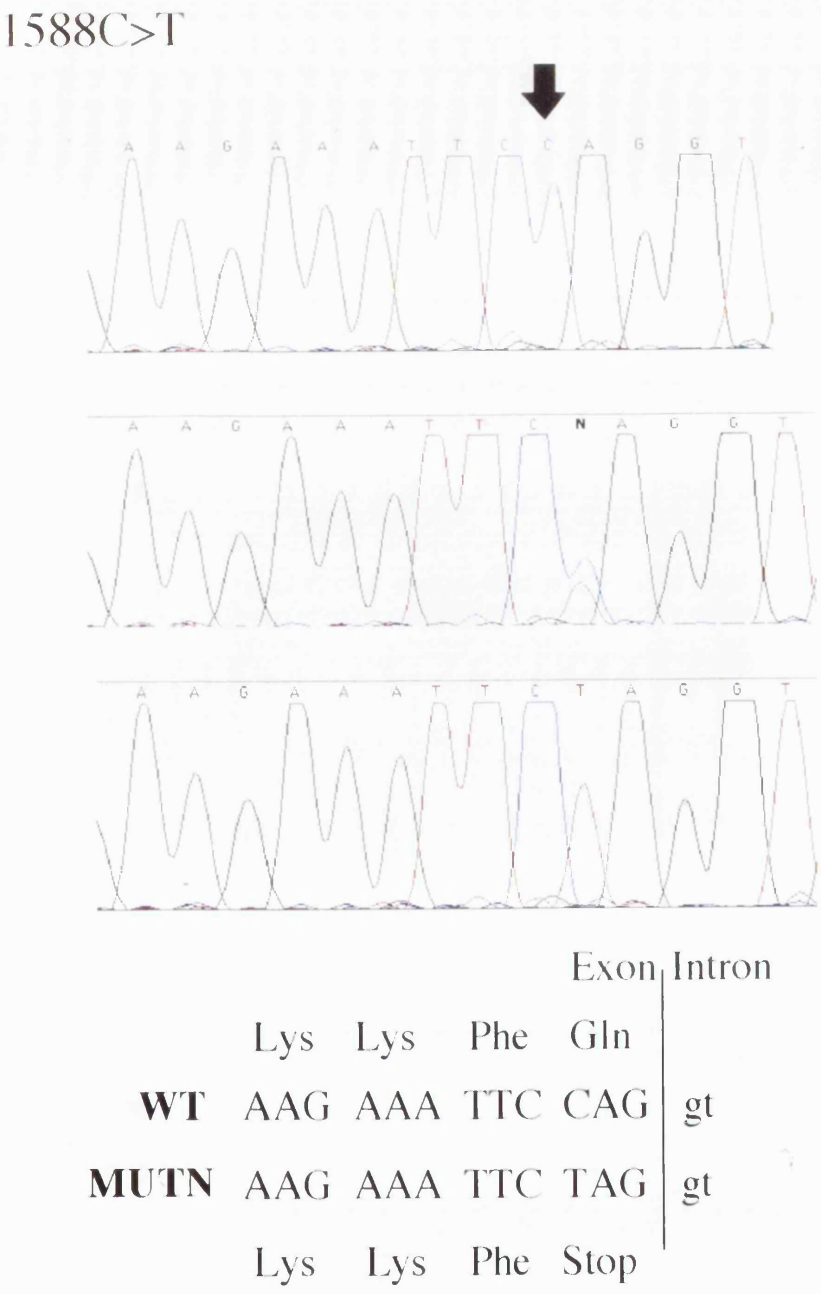

Figure 3.38.

Sequence analysis of KVLQT1: mutation 5, 1588 C>T. Sequence is shown for a control individual (top panel), a carrier (middle panel) and the affected individual (lower panel). An arrow indicates the site of the mutation. The DNA and polypeptide sequence of the normal and mutant KVLQT1 allele is displayed underneath the electropherograms.

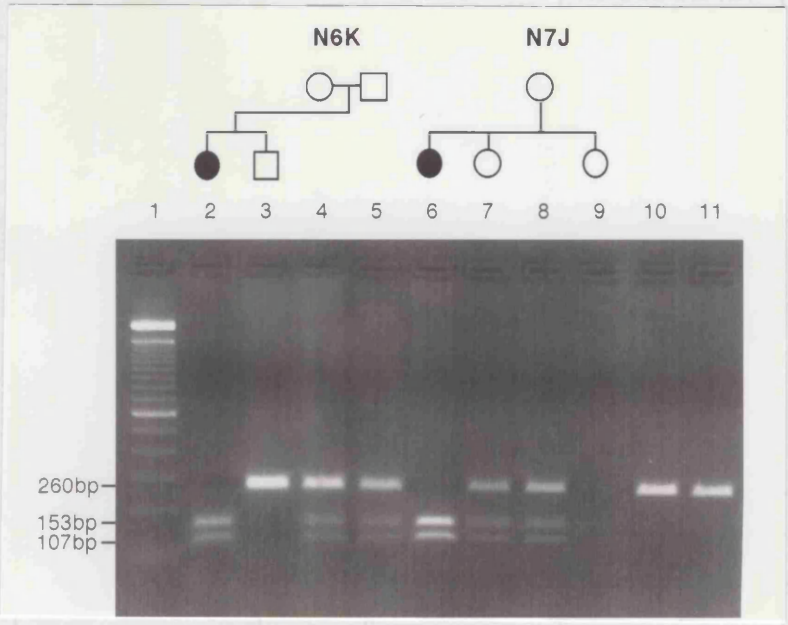

Figure 3.39.

Confirmation of mutation 5, 1588 C>T. PCR amplification products of exon 11 of the KVLQT1 gene after digestion with Bfal. Results are shown below each pedigree. This mutation introduces a single Bfal site in this PCR fragment. Bfal does not cut in unaffected individuals, leaving intact the 260bp fragment (control individuals lanes 10, 11; Family N6K, lane 3). In the homozygous affected individual, this mutation creates the cut site for the enzyme, resulting in two fragments of 153bp and 107bp (lanes 2 and 6). In heterozygotes, after Bfal digestion, there are three fragments of 260bp, 153bp and 107bp (Lanes 4,5,7 and 8). Lane 1 shows 100bp ladder (Gibco BRL).

FAMILY	PROBAND	EXON	NUCLEOTIDE CHANGE	AMINO ACID CHANGE	PREDICTED PROTEIN
N1H	HOMOZYGOUS	2	572-576 del TGCGC	FRAMESHIFT AT CODON 191	TRUNCATED AT CODON 282, S5 DOMAIN
N2S	HETEROZYGOUS	2	572-576 del TGCGC	FRAMESHIFT AT CODON 191	TRUNCATED AT CODON 282, S5 DOMAIN
	HETEROZYGOUS	11A	1552 C>T	ARG 518 STOP	TRUNCATED AT CODON 518, C-TERMINUS
N3S	HOMOZYGOUS	11A	1552 C>T	ARG 518 STOP	TRUNCATED AT CODON 518, C-TERMINUS
N4O	HETEROZYGOUS	2	572-576 del TGCGC	FRAMESHIFT AT CODON 191	TRUNCATED AT CODON 282, S5 DOMAIN
	HETEROZYGOUS	11A	1552 C>T	ARG 518 STOP	TRUNCATED AT CODON 518, C-TERMINUS
N5B	HOMOZYGOUS	2	572-576 del TGCGC	FRAMESHIFT AT CODON 191	TRUNCATED AT CODON 282, S5 DOMAIN
N6K	HOMOZYGOUS	11A	1588 C>T	GLN 530 STOP	TRUNCATED AT CODON 530, C-TERMINUS
N7J	HOMOZYGOUS	11A	1588 C>T	GLN 530 STOP	TRUNCATED AT CODON 530, C-TERMINUS
N9A	HETEROZYGOUS	2	572-576 del TGCGC	FRAMESHIFT AT CODON 191	TRUNCATED AT CODON 282, S5 DOMAIN
	HETEROZYGOUS	11A	1552 C>T	ARG 518 STOP	TRUNCATED AT CODON 518, C-TERMINUS
N10D	HOMOZYGOUS	2	572-576 del TGCGC	FRAMESHIFT AT CODON 191	TRUNCATED AT CODON 282, S5 DOMAIN
UK2T	HOMOZYGOUS	4	728 G>A	ARG243HIS	FULL LENGTH
UK3C	HETEROZYGOUS	6	1008delC	FRAMESHIFT AT CODON 337	TRUNCATED AT CODON 354, S6 DOMAIN

Table 3.9.

Summary of KVLQT1 mutations identified in families with JLNS in this study.

3.2.5.4. Polymorphisms

A novel intronic polymorphism, a T to C transition 14 nucleotides downstream of the end of exon 11A, was identified. This change was confirmed in control individuals by restriction digest with *Dde*I.

3.2.6. Family N10D

The proband of Family N10D with Jervell and Lange-Nielsen syndrome, individual IV_1, is homozygous for the mutation 572-576 delTGCGC. In the same family, Individual IV_5 was independently ascertained with Romano Ward syndrome, and is heterozygous for the same 5 base pair deletion. Identification of the mutation in this family allowed the characterisation of additional carriers of this mutation by restriction analysis. This is shown in figure 3.40. Where available the QTc values are indicated, showing that a number of asymptomatic carriers of this mutation have QTc values within the normal range (< 440ms).

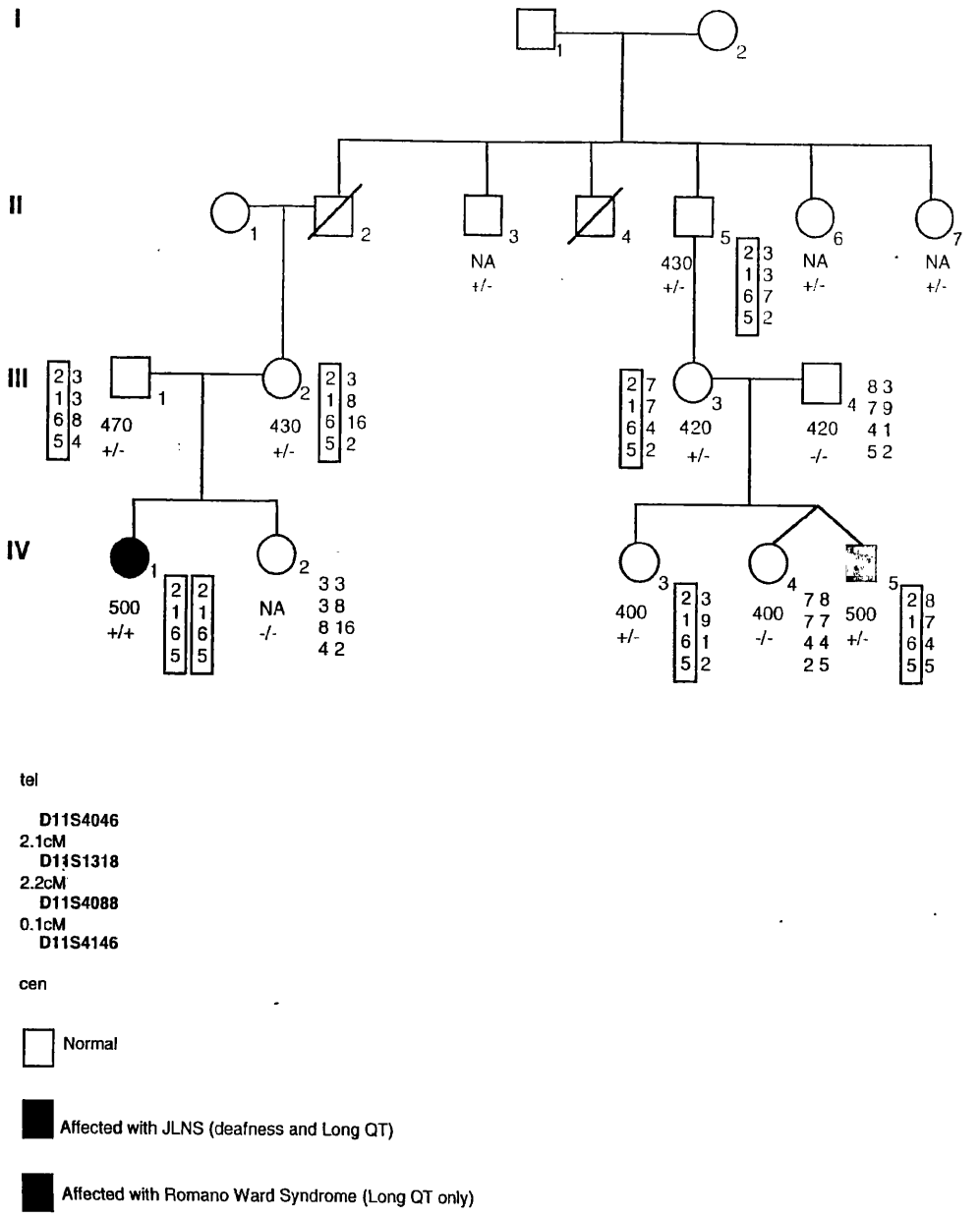

Figure 3.40.

Haplotype and mutation analysis of Family N10D. This is a large extended family with the 5bp deletion, 572-576 delTGCGC, in which only a single individual heterozygous for this mutation suffered from syncope (individual IV_5). Genotypes are shown next to each individual. The subject's QTc intervals (milliseconds) are shown below, NA denotes not available. Where applicable, below the QTc intervals for each individual, is their mutation status, annotated as follows: +/-, heterozygous for 5bp deletion, +/+, homozygous for 5bp deletion and -/-, no mutation. Order of markers is as indicated in the key.

3.2.7. Expression of KVLQT1

Previously, expression of mouse kvlqt1 had been demonstrated in the inner ear by in situ hybridisation (Neyroud et al, 1997). In order to investigate KVLQT1 expression in human tissues, total RNA was extracted from ear and heart of a 72 day old fetus. RT-PCR analysis was performed using cDNA primers LQT109 and LQT209. These primers amplify KVLQT1 between exons 11B and 14 (Lee *et al*, 1997), the cDNA product size is 220bp, and that of genomic DNA is greater than 2kb. Figure 3.41 shows that KVLQT1 is expressed in the fetal heart and fetal ear.

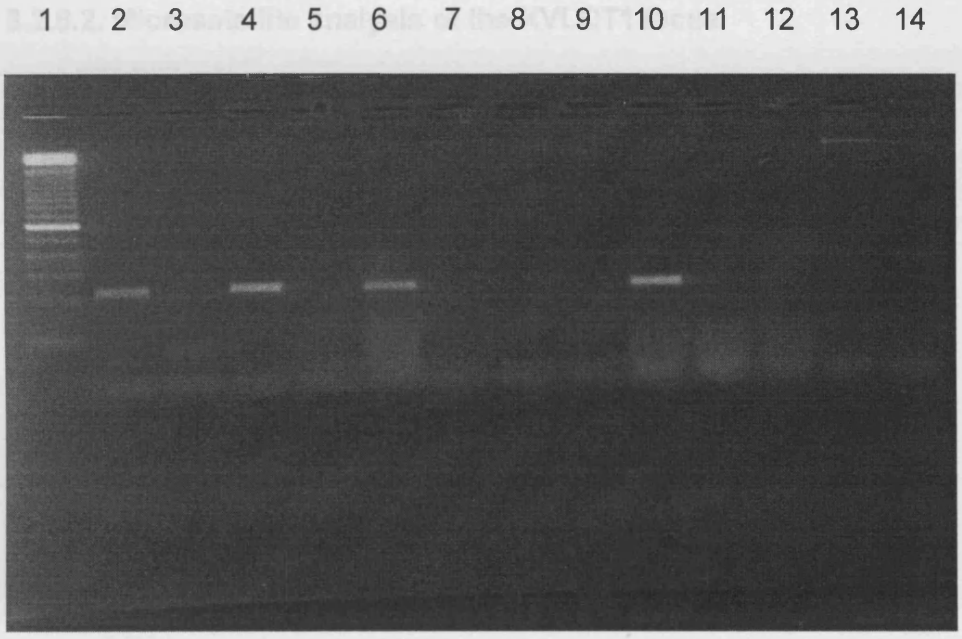

Figure 3.41.

PCR amplification of cDNA samples prepared from human fetal tissues, demonstrating expression of KVLQT1 in lymphoblastoid cell lines (lanes 2 and 4), fetal ear (lane 6 and 12) and fetal heart (lane 10). Lane 13, genomic control. Lane 14, blank. Low level expression was observed in the kidney (lane 8).

3.2.8. Further analysis of the KVLQT1 gene in Autosomal recessive Long QT syndrome

A report of a single family with autosomal recessive long QT (Priori *et al*, 1998) prompted the analysis of KVLQT1 in Family N16O, a consanguineous Norwegian family with autosomal recessive long QT

3.2.8.1. Mutation analysis of KVLQT1

Single stranded conformation polymorphism (SSC) analysis was used to screen for mutations in KVLQT1 in Family N16O. No aberrant shifts were observed.

3.2.8.2. Microsatellite analysis of the KVLQT1 iocus.

Family N16O was typed for microsatellite markers at the KVLQT1 locus to establish whether or not KVLQT1 could still be the causative gene in this family, despite normal analysis of the coding region. Analysis of Family N16O excluded the KVLQT1 gene as the disease locus since homozygosity by descent was not observed with the microsatellite markers D11S4046, D11S1318, D11S4088 and D11S4146, thus providing evidence for genetic heterogeneity in autosomal recessive long QT syndrome. Microsatellite analysis of Family N16O at this locus is shown in figure 3.42. Haplotype data is shown in figure 3.43.

3.2.8.3. Microsatellite analysis of the IsK locus

Exclusion of KVLQT1 as the disease locus in Family N16O prompted the analysis of the IsK locus on chromosome 21q22. Family N16O was

typed for the microsatellite markers D21S1254, D21S1895 and D21S1252. Analysis of Family N16O excluded the IsK gene as the disease locus since homozygosity by descent was not observed with any of the microsatellite markers analysed in the proband of this family. Microsatellite analysis of Family N16O at this locus is shown in figure 3.44. Haplotype data is shown in figure 3.45.

This work excluded both the KVLQT1 and the IsK loci as the disease locus in Family N16O, providing evidence for genetic heterogeneity in autosomal recessive long QT syndrome. Further haplotype analysis at the other RWS loci, the HERG locus on chromosome 7, the SCN5A locus on chromosome 3 and the locus on chromosome 4, may identify a new locus for this form of inherited long QT syndrome.

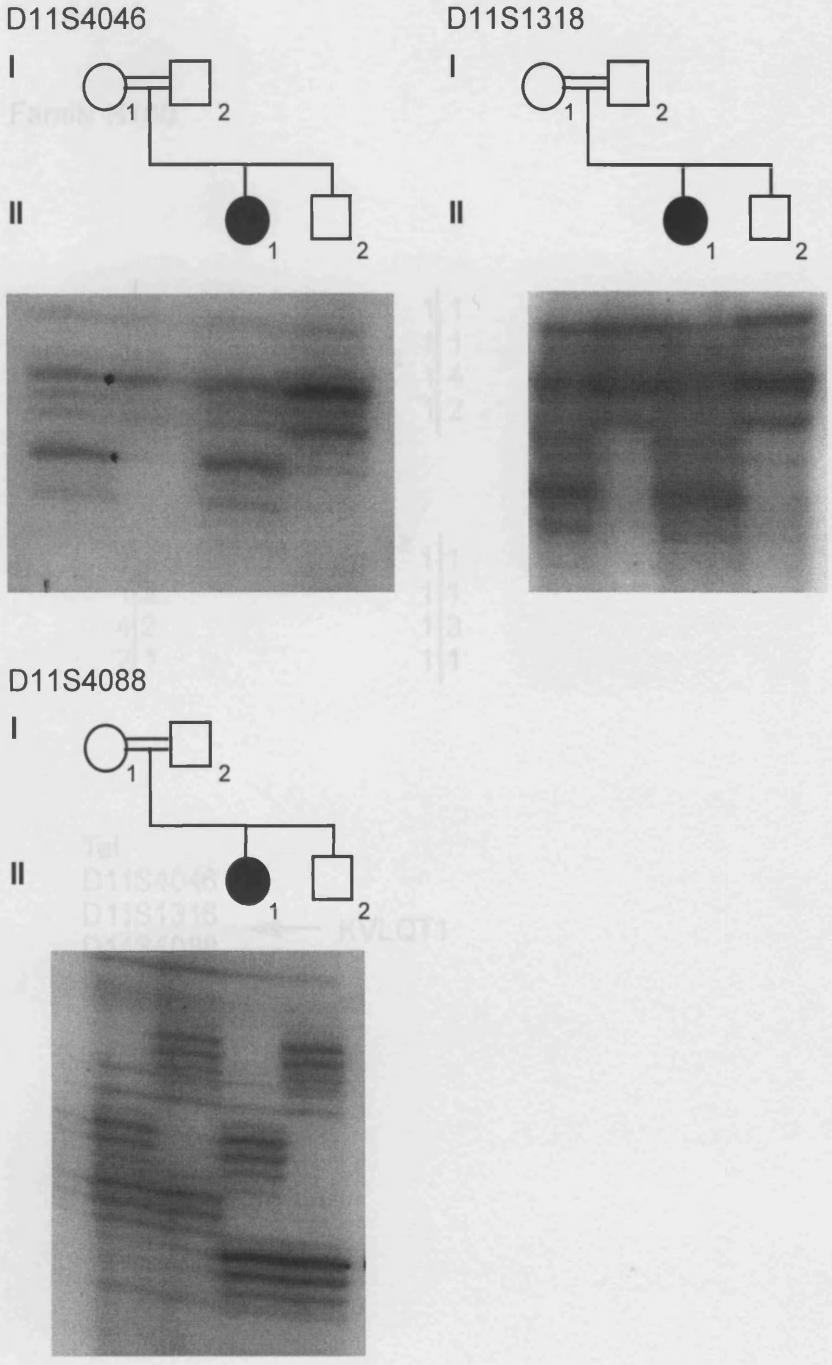

Figure 3.42.

Microsatellite analysis of Family N16O at the KVLQT1 locus on chromosome 11. Microsatellite markers analysed were D11S4046, D11S1318 and D11S4088.

Family N160

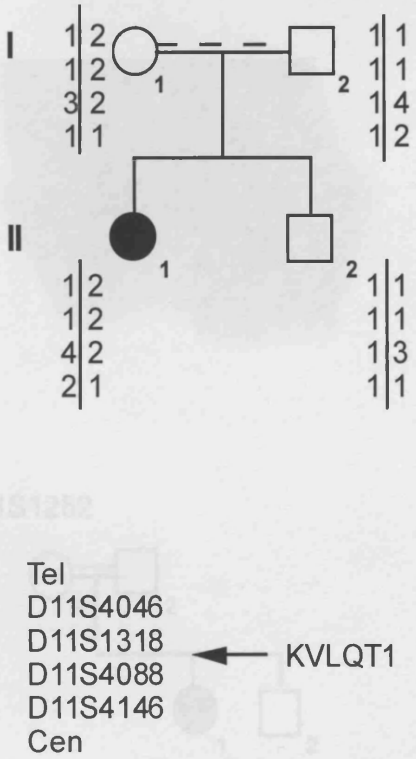

Figure 3.43.

Haplotype analysis of Family N16O at the KVLQT1 locus on chromosome 11, demonstrating lack of homozygosity for the markers analysed in individual II_1. Order of markers and position of the KVLQT1 gene is as indicated in the key.

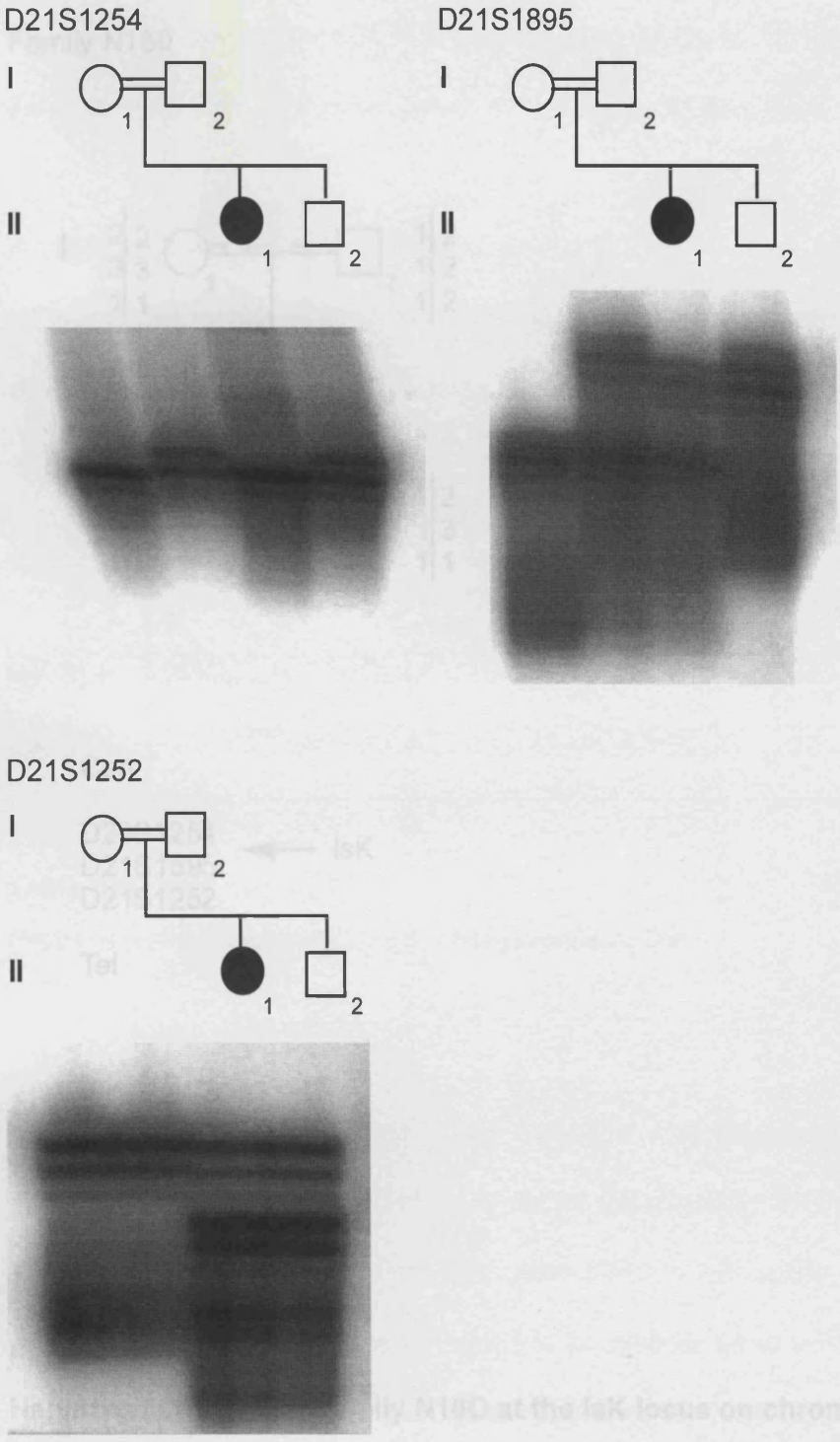

Figure 3.44.

Microsatellite analysis of Family N16O at the IsK locus on chromosome 21. Microsatellite markers analysed were D21S1254, D21S1895 and D21S1252.

Family N160

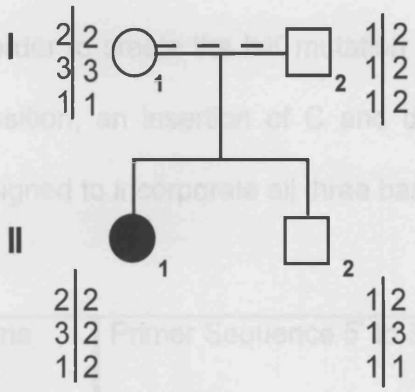

Cen

D21S1254
D21S1895
D21S1252 ← IsK

Tel

Figure 3.45.

Haplotype analysis of Family N16O at the IsK locus on chromosome 21, demonstrating lack of homozygosity for the markers analysed in individual II_1. Order of markers and position of the IsK gene is as indicated in the key.

3.2.9. Site-directed mutagenesis of ISK

Human IsK in the vector pGEM A was supplied by Dr. M. Sanguinetti at the Eccles Institute of Human Genetics, University of Utah, USA.

In order to create the IsK mutation observed in Family UK1S, an A to C transition, an insertion of C and deletion of G, a pair of primers was designed to incorporate all three base changes as detailed in table 3.10.

Name	Primer Sequence 5' to 3'	Length (bases)	Tm (°C)
IsK SDF	CGGCTTCTTCCCCCCTGGCATCATGCTG	28	67.1°C
IsK SDR	CAGCATGATGCCAGGGGGGAAGAAGCCG	28	67.1°C

Table 3.10.
Primers used for site-directed mutagenesis of IsK.

Following temperature cycling, *Dpn*I digestion and transformation, 6 single colonies were picked and analysed for the mutation. The genomic sequence of IsK and that of the IsK clone differ in nucleotide, but not amino acid, composition. The IsK clone is an artificial gene synthesised for expression efficiency. Hence, the enzyme sites for confirmation of the mutation in genomic DNA were not available in the clone. In order to confirm the presence of the mutation, each clone was sequenced. Direct sequencing indicated that 3 of the 6 clones contained all three base changes. The remainder of the clones were wild type. Sequence data is

shown in figure 3.46. On sequencing of the entire IsK clone, no other base changes apart from the desired mutation were observed. This work produced the IsK mutant for future *in vitro* functional work.

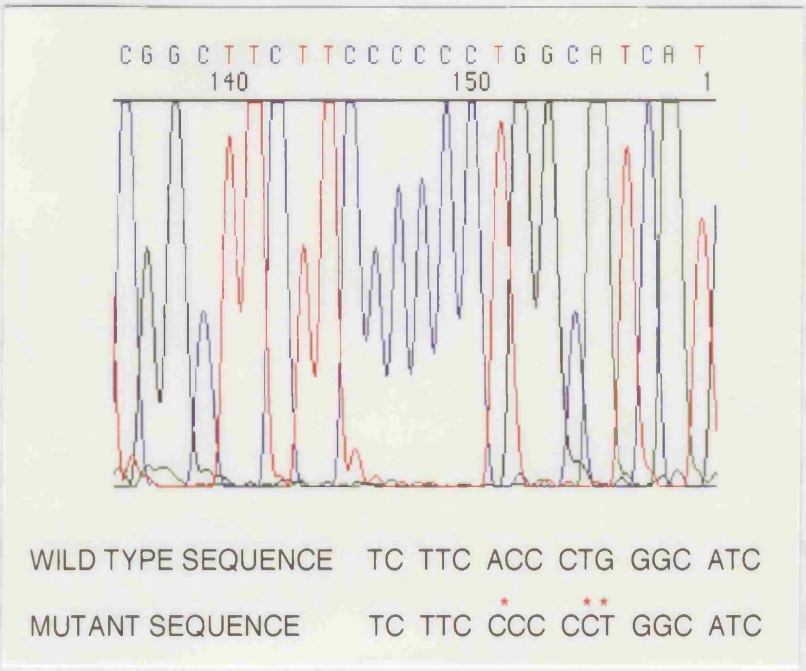

Figure 3.46.

Sequence analysis of IsK clone, illustrating the creation of the desired mutation. DNA sequence of wild type and mutation is displayed beneath the electropherogram; nucleotide changes are indicated with an asterix.

CHAPTER 4: DISCUSSION

4.1. X-LINKED DEAFNESS

At the start of this research, it was known that X-linked deafness is genetically heterogeneous and that there was a major locus, DFN3, at Xq13-q21. The work on X-linked deafness is divided into two parts; the first is the mapping of a novel locus for X-linked deafness, DFN2, and the second section addresses heterogeneity at the major locus DFN3.

4.1.1. DFN2

Linkage analysis of Family CN defined a new locus for X-linked deafness, DFN2, introducing further genetic heterogeneity in this form of inherited hearing loss. Since no additional families have been found that mapped to the same locus, refinement of the DFN2 locus seems unlikely. Due to the large size of the candidate region, a positional candidate gene approach was used to work towards the identification of the causative gene. As several syndromic forms of deafness map to Xq22, including Alport syndrome and Mohr-Tranebjærg syndrome (MTS), it was investigated whether or not the deafness in Family CN represented an allelic form of one of these conditions.

The first positional candidate gene chosen was COL4A5, mutations in which cause Alport syndrome (Barker *et al*, 1990). Screening of the COL4A5 gene in Family CN was undertaken by Dr. Frances Flinter at Guy's Hospital, London, to exclude an unusual allelic variant, as mutation in the COL4A5 gene has been described in a family with

characteristic renal disease but without hearing loss (Kawai *et al*, 1996). No mutations in the COL4A5 gene were identified in Family CN by SSC analysis or by Southern blotting. Normal ophthalmic examination, normal urinalysis and lack of family history of renal disease, as well as the age of onset and pattern of hearing loss made Alport syndrome unlikely. The gene COL4A6, which lies in a head to head configuration with COL4A5, remains a possible candidate, although deletions of the 5' end of this gene and part of the neighbouring COL4A5 gene are reported to cause diffuse leiomyomatosis (DL) and Alport syndrome (Heidet *et al*, 1995). However, no mutations in COL4A6 alone have yet been described, so the phenotype associated with mutations in this gene alone are unknown.

The locus DFN1 was originally described in a family with X-linked non-syndromic progressive sensorineural hearing loss (Mohr and Magerøy, 1960), but recent restudy of the same family revealed additional clinical features of late-onset which now define this clinical entity as a new syndrome, Mohr-Tranebjærg Syndrome (Tranebjærg *et al*, 1995). The Mohr-Tranebjærg syndrome (MTS) comprises progressive sensorineural deafness, progressive dystonia, spasticity, mental deterioration and visual symptoms leading to blindness (Tranebjærg *et al*, 1995) and is caused by mutation in the gene *DDP*, Deafness/dystonia peptide (Jin *et al*, 1996). The *DDP* gene was identified through the molecular analysis of an individual with a deletion of the X-linked agammaglobulinaemia (XLA) gene, *BTK*. This individual has an apparent contiguous gene deletion

syndrome of XLA, progressive sensorineural deafness and dystonia. The deletion was shown to extend into a second gene. Since the deletion of *BTK* accounted for the immunodeficiency, the deletion of the second gene prompted the analysis of this gene as a candidate for deafness and dystonia. The gene, named *DDP*, was isolated and characterised (Jin et al, 1996). Although the role of this gene remains to be determined, the *DDP* protein is evolutionarily conserved since it shows striking similarity to a predicted *Schizosaccharomyces pombe* protein of no known function.

No mutations in this gene were identified in Family CN making it unlikely that *DDP* is the deafness gene in this family. None of the clinical features associated with MTS, dystonia, mental deterioration and blindness, have been observed in the affected males IV_1 and IV_{12} who are now in their thirties and forties, nor have such features been reported in previous generations. Additionally, there is no evidence of progression of the deafness in Family CN.

A splice mutation in the *DDP* gene was identified in this study in an affected male with progressive deafness and dystonia, individual NB. This is only the fourth mutation to be identified in this gene. In addition to the individual with XLA and the deletion of *DDP*, mutations in *DDP* have been identified in only 2 families, the original DFN1/MTS family and a second family with deafness, dystonia, mental deficiency but not blindness (Jin *et al*, 1996). These mutations in *DDP* are small deletions

resulting in a frameshift and premature truncation of the predicted protein. A complete deletion of the *DDP* gene, as observed in the individual with the contiguous gene deletion appears to have the milder phenotype of deafness and dystonia. The consequence of the splice mutation identified in individual NB needs to be confirmed at the RNA level. A mutation of a splice site can result in one of a combination of splicing defects. The defects include (i) the failure to recognise the affected exon, so that it is skipped; (ii) the activation of a cryptic splice site; and (iii) the failure to recognise the intron, so it is retained (Maquat, 1996). The predicted effect of the mutation identified in NB is the abolishment of the wild type 5' donor splice site (refer to section 3.1.3.1.1.). If indeed, on abolishing the wild type donor splice site of exon 1, splicing occurs within exon 1, the consequence of the mutation would be an in-frame deleted transcript. In frame deleted transcripts may be stable and indeed translated into protein, as shown recently for the dystrophin gene underlying X-linked Duchenne and Becker muscular dystrophies (Dunkley *et al*, 1998).

A third candidate gene screened in this study was Diaphanous X (DiaX), a human homologue of the *Drosophila* gene *diaphanous.* Two human homologues of this gene have now been identified, one mapping to human chromosome 5q31, the other to human Xq22. Mutation in human diaphanous 1, mapping to 5q31, is associated with a form of autosomal dominant non-syndromic deafness, DFNA1 (Lynch *et al*, 1997).

Human Diaphanous 1, *Drosophila diaphanous* and mouse p140mDia are homologues of the *S.cervisiae* protein Bni1p. They are all members of the formin gene family which are involved in cytokinesis and the establishment of cell polarity. Cytokinesis is the division of the entire cell and it is believed to be mediated by contraction of a structure, the contracile ring, the contraction of which is brought about by force generated by actin and myosin (Castrillon and Wasserman, 1994). Members of the formin gene family interact with the protein profilin, which in turn binds actin monomers and is a regulator of actin polymerisation (Castrillon and Wasserman, 1994).

A proposed role for Diaphanous in hearing is the regulation of actin polymerisation (Lynch *et al*, 1997). Actin is a major component of the cytoskeleton of hair cells. Hair cell stereocilia may be the site affected by the aberrant protein. Stereocilia are membrane-enclosed rigid structures that contain hundreds of bundled actin filaments which serve to provide structural support to this structure. One can imagine that if organisation of the actin is disrupted by mutation in a gene crucial to its regulation, then the maintenance of the rigidity of this structure and hence its function will be impaired.

The second human homologue, mapping to Xq22, was isolated during the cloning of DFNA1, and because of the implication of diaphanous 1 in a form of hearing loss, Diaphanous X (DiaX) became an attractive candidate gene for the deafness in Family CN. No mutations, deletions

or rearrangements of DiaX were found in the affected individuals in Family CN. In addition it was shown that deletion of DiaX does not result in deafness, as illustrated by characterisation of the deletion observed in individual MBU and refined mapping of DiaX (section 3.1.3.2.2.). Individual MBU is deleted for a region of the X chromosome between the microsatellite markers DXS1002 and DXS1231. Since deletion of this region does not result in deafness, the DFN2 candidate region can be narrowed to between the microsatellite markers DXS1231 and the centromeric recombination, between DXS1220 and DXS1001. This has narrowed the region by 5cM to approximately less than 20cM, in which to look for positional candidate genes.

Subsequent to the work on DiaX, a report has implicated DiaX in premature ovarian failure (POF) (Sala *et al*, 1997; Bione *et al*, 1998). The last intron of the DiaX gene is interrupted by a balanced translocation in a patient with POF. Previous cytogenetic analysis of Xq rearrangements defined a critical region on human Xq from Xq13 to Xq26 as the "critical region" for normal ovarian function and although it is thought that several genes may be involved in normal ovarian development and/or oogenesis, the role of diaphanous is strengthened by the fact that mutant alleles of *diaphanous* are responsible for sterility in male and female fruit flies (Castrillon *et al*, 1993; Castrillon and Wasserman, 1994). In addition there is no evidence of hearing loss in the individual with POF. Since translocations do not necessarily disrupt a structural gene (Reviewed in

Kleinjan and van Heyningen, 1998), the role of DiaX in POF remains to be substantiated.

It is therefore possible that the deafness in Family CN is caused by mutation in an unknown gene in Xq22. In order to identify candidate genes for human hearing disorders, Skvorak and colleagues have submitted an aliquot of an unsubtracted human fetal cochlear cDNA library to the IMAGE consortium for the generation of expressed sequence tags (ESTs) (Skvorak *et al*, 1999). The analysis of ESTs has proven useful in identifying positional candidate genes for human disease. ESTs are short, unique nucleotide sequences that are identifiers of both novel and known genes. Map positions of ESTs form cDNA libraries are a crucial resource for determining positional candidates for disease genes, and amongst the ESTs generated from the Morton fetal cochlear cDNA library, 437 of the cochlear-specific ESTs have now been mapped, providing candidate genes for non-syndromic hearing disorders. Three such cochlear-specific ESTs have been mapped, using radiation hybrids, to Xq22 and the DFN2 candidate region (http://www.bwh.partners.org/pathology). These ESTs do not match the nucleotide or protein sequence of any previously identified genes but such ESTs will be considered as potential positional candidate genes during the course of future work.

If new X-linked deafness genes are identified, Family FP can be analysed for exclusion of a candidate gene. At the present time the small

family size precludes the possibility of independently establishing or refuting linkage.

4.1.2. DFN3

Since most families with X-linked deafness map to Xq13-q21 (Reardon *et al*, 1991), DFN3 is considered a major locus for X-linked deafness, with the majority of DFN3 families accounted for by mutation in POU3F4. The aim of this work was to study individuals with X-linked deafness, known to map to this locus at Xq13-q21, but in which no mutation in the POU3F4 gene has been identified. Families with no mutation in the POU3F4 fall broadly into three groups. The first group includes patients with the developmental abnormality of the ear characteristic of DFN3, who have microdeletions or other aberrations proximal to the POU3F4 coding region. These microdeletions, which do not disrupt the POU3F4 gene, are located 15-800Kb 5' to the POU3F4 coding region (de Kok *et al*, 1995; de Kok *et al*, 1996). The second group includes patients who have the developmental abnormality of the ear, but have no DNA rearrangements or mutations in the POU3F4 gene and the final group include patients from pedigrees which appear map to this locus, but have normal ear morphology.

The work on DFN3 centred around patients in the first group, with previously characterised microdeletions proximal to the gene (de Kok et al, 1995; de Kok et al, 1996). Possible explanations for the phenotype observed in these individuals include

(i) The presence of another gene in this region, mutation in which causes deafness, or

(ii) a position effect on the expression of the POU3F4 gene.

By studying the effect of the deletion on the expression of POU3F4 in this group of individuals, it was hoped it would provide evidence for either of the above explanations. If the phenotype observed in these individuals is a result of a deleterious change in the level of expression of POU3F4, one would hope to see a difference in expression of POU3F4 between control individuals and individuals with proximal microdeletions. The problem in studying a position effect is accessibility to a tissue in which the gene is normally expressed, and then to measure levels of expression accurately. A normal level of expression of POU3F4 in patients with microdeletions would favour the argument of the presence of another gene or indeed more coding region of the POU3F4 gene. Since the only tissues known to express POU3F4 in humans are fetal brain, fetal kidney and adult brain, examining factors that influence expression levels of this gene would not be straightforward. Since POU3F4 expression in lymphoblastoid cell lines has not been observed (de Kok et al, 1996 and this study), urothelial cells obtained from adult urine was chosen as a source of RNA. Unfortunately, at the level of expression of POU3F4 in the cells obtained from urine, it would not be accurate to quantitatively determine POU3F4 expression. In addition, the experiment is too susceptible to DNA contamination at such low levels of expression. Thus it remains to be proven whether a second gene at the

DFN3 locus or a position effect on the POU3F4 accounts for the DFN3 cases in which no mutation in the POU3F4 gene has been identified.

Evidence for a position effect comes from a variety of human diseases. Position effects are mutations that alter gene expression through long range effects on chromatin structure or by disrupting distal regulatory elements of a gene. These mutations can be located several hundred kilobases from the affected gene, from 85 to 185Kb in Aniridia and 50 to 850Kb upstream of SOX9 (Reviewed in Bedell *et al*, 1996; Kleinjan and van Heyningen, 1998). It is possible that the chromosomal rearrangements observed in these DFN3 individuals influence POU3F4 expression. In patients with microdeletions around Xq21, the POU3F4 gene may become repositioned to a different chromatin environment, rendering the gene transcriptionally silent. Alternatively, the deletion could separate the promoter/transcription unit from an essential distant regulatory element, removing the effect of this regulator on the gene. For example, if a deletion removes an enhancer, a sequence which increases transcriptional activity from the promoter of a gene, the absence of this element would lead to reduction or absence of transcription from the gene.

Position effects have been associated with a number of human genetic diseases (reviewed in Kleinjan and van Heyningen, 1998). The PAX6 gene, mutations in which underlie Aniridia, (Jordan *et al*, 1992) was one of the first to provide evidence that a position effect could play a role in

human genetic disease. Aniridia is a congenital malformation of the eye which typically features severe hypoplasia of the iris. It is caused by loss of function of one copy of the PAX6 gene (PAX6 haploinsufficiency) as illustrated by deletion cases and the identification of loss of function mutations (Davis and Cowell, 1993). Two aniridia patients have been described in which translocation breakpoints map 85Kb and 125-185Kb distal to the PAX6 gene (Fantes *et al*, 1995). An example of a position effect involved in deafness in mammals is the deaf-mouse mutant *Snell's waltzer*. A paracentric inversion that does not disrupt the coding region of myosin VI causes the same phenotype as an intragenic deletion (Avraham *et al*, 1995). The inversion reduces mRNA and protein levels, suggesting that the chromosomal rearrangement results in the alteration in a regulatory element.

It is also possible that there is more than one gene in the DFN3 region, mutation in which causes deafness and the temporal bone abnormality. The molecular characterisation of the region 600-1200Kb proximal to the POU3F4 gene identified a hotspot for DFN3-associated microdeletions proximal to the POU3F4 gene. These microdeletions overlap in an 8Kb fragment (de Kok et al, 1996). A YAC or cosmid contig of this region would allow the search for potential coding sequences by exon trapping, cDNA selection or GRAIL analysis. It remains to be shown whether mutation in one gene can account for all the remaining DFN3 patients with and without the inner ear abnormality.

Finding out which of the factors, a second gene or a position effect on the POU3F4 gene, is responsible for the unexplained cases of DFN3 may not be a simple task. The study of a knockout mouse may provide some useful information. It may be possible to generate mouse mutants with deletions proximal to the pou3f4 gene, to study the phenotype observed and see if the phenotype is correctable with BAC-transgene rescue, a procedure employed in the identification of the gene *myo15* underlying the deafness in the mouse mutant *shaker-2* (Probst *et al*, 1998). This is a similar scenario to that being planned for investigating the position effect on the PAX6 gene. The importance of the region distal to PAX6 has been investigated by introducing human YAC clones containing different amounts of 3' flanking DNA to see if the small eye phenotype, caused by mutation in the murine homologue of PAX6, can be corrected (Fantes *et al*, 1995).

4.2. JERVELL AND LANGE-NIELSEN SYNDROME (JLNS).

The efficiency of mapping disease phenotypes using conventional linkage strategies is limited by the acquisition of appropriate families and genotyping using genetic markers which span the genome. With the availability of a large number of highly polymorphic microsatellite markers, a genome wide search for linkage has become a feasible task. The employment of novel mapping strategies, such as homozygosity mapping, has allowed significant lod scores to be obtained from single small families thus dispensing with the requirement for large families, and minimising the problems of genetic heterogeneity. The work presented here on the cardioauditory syndrome JLNS represents a success of homozygosity mapping and the candidate gene approach. The powerful nature of the technique is illustrated in that evidence for both genetic heterogeneity in JLNS and the involvement of a new gene was suggested on analysis of a single consanguineous family with two affected individuals.

4.2.1. Mutation in IsK causes Jervell and Lange-Nielsen syndrome.

A genome search in association with screening of candidate loci identified a region homozygous-by-descent on chromosome 21q22 in Family UK1S. A candidate gene, IsK, mapped to this homozygous interval. Several lines of evidence including predicted function and expression data rendered IsK an excellent candidate gene for the disorder in Family UK1S.

IsK cDNA was first isolated from a rat kidney library, by expression cloning in *Xenopus* oocytes of a slow potassium current strikingly similar to IKs (Takumi *et al*, 1988). In "expression cloning" *in vitro* transcripts of mRNA from a cDNA library derived from a tissue known to be rich in a particular ion channel, are injected into individual *Xenopus* oocytes. The currents in these oocytes are measured by two-electrode voltage clamp techniques. The mRNA from a single cDNA clone that confers the desired ion channel activity can be isolated. IsK encodes a small protein of 129 amino acids, with one putative α-helical transmembrane domain and no pore region, as found in other voltage-sensitive channels (Takumi *et al*, 1988; Murai *et al*, 1989).

Recent physiological studies suggest that IsK interacts with KVLQT1 to form a channel reproducing the properties of IKs, the slowly activating component of the delayed rectifier potassium current in the heart (Barhanin *et al*, 1996; Sanguinetti *et al*, 1996a). KVLQT1 encodes an α-subunit of a voltage-gated potassium channel, with the characteristic six membrane-spanning domains, pore region, and intracellular N- and C-termini (Wang *et al*, 1996; Hebert, 1998). KVLQT1 alone expresses a fast-activating current of small amplitude with no equivalent current described in the heart. Co-expression of the IsK protein dramatically increases current amplitude but decreases activation rate and shifts the voltage-dependence of activation to more positive potentials, producing a current closely resembling IKs (Barhanin *et al*, 1996; Sanguinetti *et al*, 1996a). IsK appears to be a regulatory protein that modulates KVLQT1

channel activity. An interaction of IsK with HERG, a potassium channel gene, has also been demonstrated (McDonald *et al*, 1997).

The mechanism of interaction of KVLQT1 and IsK subunits has recently been elucidated (Wang, K-W., *et al*, 1996; Romey *et al*, 1997; Tai *et al*, 1998). Biochemical studies have shown that there is a physical association between the C-terminal domain of IsK with the pore region of KVLQT1. Voltage-gated potassium channels, such as KVLQT1, are tetrameric proteins, i.e. four α-subunits assemble to form the functional channel (Ackerman and Clapham, 1997). The number of IsK subunits per KVLQT1 channel is unknown, however a correlation between level of IsK expression and the slowing down of the current has been observed (Romey *et al*, 1997).

IsK is expressed in many mammalian tissues (Barhanin *et al*, 1998). Expression in the ear and the heart has been demonstrated. Immunohistochemical studies in the rat and mouse inner ear have localised IsK to the endolymphatic surface of the marginal cells and in the vestibular dark cells (Sakagami *et al*, 1991; Vetter *et al*, 1996). Staining was not observed for the Reissner's membrane, the spiral ligament nor the organ of Corti. Mouse kvlqt1 is expressed in the marginal cells of the stria vascularis (Neyroud *et al*, 1997). Human KVLQT1 expression has also been demonstrated in heart, kidney, lung and placenta (Wang *et al*, 1996). The co-localisation of the two proteins, KVLQT1 and IsK, in both heart and inner ear provides a clear

explanation for the main clinical symptoms observed in patients with JLNS.

In the heart, IsK associates with KVLQT1, reproducing the properties of IKs, the slow component of the delayed rectifier current in the heart (Barhanin *et al*, 1996; Sanguinetti *et al*, 1996a). This current is responsible for the repolarisation phase of the cardiac action potential.

In the ear, the marginal cells of the stria vascularis are known to secrete endolymph, a potassium rich fluid of the inner ear, which bathes the stereocilia of the sensory hair cells. IsK appears to be responsible for transporting high concentrations of potassium into the endolymph, thus establishing the ionic environment necessary for normal hair cell transduction (Wangemann *et al*, 1995). Any disruption to this potassium environment would ultimately lead to hearing loss.

In conjunction with mapping data, the function and expression pattern of IsK in the ear and the heart rendered IsK an excellent positional candidate gene.

Mutation in IsK in Family UK1S.

A mutation in IsK was demonstrated in Family UK1S. The mutation identified is and A to C transition at nucleotide position 172, an insertion of C and a deletion of G, within a stretch of 6 nucleotides, resulting in the overall change from ACCCCC to CTGCCT. A survey of the Human Gene

mutation database illustrates that complex mutations such as the one described here are rare (Krawczak and Cooper, 1997). A proposed mechanism of how the mutation may have arisen is outlined in figure 4.1. Approximately 60 bases upstream of the mutation is a small region of sequence similarity sufficient to allow transient mispairing of the two regions in the germline of an ancestor (figure 4.1c). This would be followed by attempted correction of the 3' sequence, based on the template of the upstream 5' sequence. Certainly the base changes that have arisen as a result of the mutation, create greater homology between these two regions.

The mutation causes threonine at position 58 and leucine at position 59 each to be replaced by proline in the transmembrane region of the predicted protein. The cyclical structure of proline is expected to influence the resulting protein structure since it causes bending of folded protein chains (Stryer, 1988). Observations of the relative occurrence of amino acids in α-helices show that proline is the least likely of all the amino acids to be found in this secondary structure (Stryer, 1988).

Site-directed mutagenesis of the IsK gene has also contributed insight into the functional domains of this small protein. Amino acid substitutions at a number of positions within and outside the transmembrane region were found to have varying effects on the functional activity of the channel. Mutation of the threonine residue at position 58 to a structurally related amino acid, valine, was shown to cause a reduction in channel

activity as observed by electrophysiological measurements in oocyte systems (Takumi *et al*, 1991). The mutation in Family UK1S alters both this amino acid, Thr_{58} and the one adjacent to it, Leu_{59} and is therefore very likely to be of functional significance and disease-causing.

Site-directed mutagenesis to create the IsK mutation identified in Family UK1S has been completed. The next step is the synthesis of complementary RNA to inject into *Xenopus* oocytes to evaluate the functional significance of this mutation *in vitro*. From this work it will be interesting to establish if the mutant IsK protein is localised to the membrane, or if it associates with KVLQT1 or whether insertion or assembly with KVLQT1 is prevented by the cyclical nature of the proline residues in the transmembrane region. Furthermore, it is important to establish if the mutation in IsK results in a stable protein. This could be demonstrated *in vitro* by placing an epitope tag on the IsK clone. If the subsequent mutant transcript was degraded, this would manifest as a reduction or absence of protein on a western blot probed with antibodies to the epitope tag. Functional data is available for the two mutations in IsK underlying autosomal dominant long QT syndrome. These are missense mutations in the intracellular C-terminus (Splawski *et al*, 1997a). The mutant IsK subunits form heteromultimeric channels with wild type IsK and KVLQT1, and reduce IKs by a strong dominant negative mechanism. Reduction of this outward current during the repolarisation phase of the cardiac action potential lengthens this phase and hence increases the risk of arrhythmias.

In summary, the following are evidence that mutation in the IsK gene causes JLNS in Family UK1S. Mutation in KVLQT1 has been excluded in this family due to lack of homozygosity for markers on chromosome 11p15.5, but homozygosity-by-descent for markers flanking the IsK gene was observed. The interaction of the IsK gene product with that of KVLQT1, provides a plausible biological mechanism for the disease pathology. Finally, the identification of IsK as a gene underlying JLNS in humans is strongly supported by observations in IsK-knockout mice (Vetter *et al*, 1996; Drici *et al*, 1998; Charpentier *et al*, 1998).

The involvement of IsK in JLNS has now been confirmed by other reports (Schulze-Bahr *et al*, 1997; Duggal *et al*, 1998), although it remains a rare cause of this syndrome. Mutation in IsK has now been identified in two families with autosomal dominant isolated long QT syndrome or Romano Ward syndrome (Splawski *et al*, 1997a), demonstrating that mutation in IsK can give rise to both recessive and dominant phenotypes.

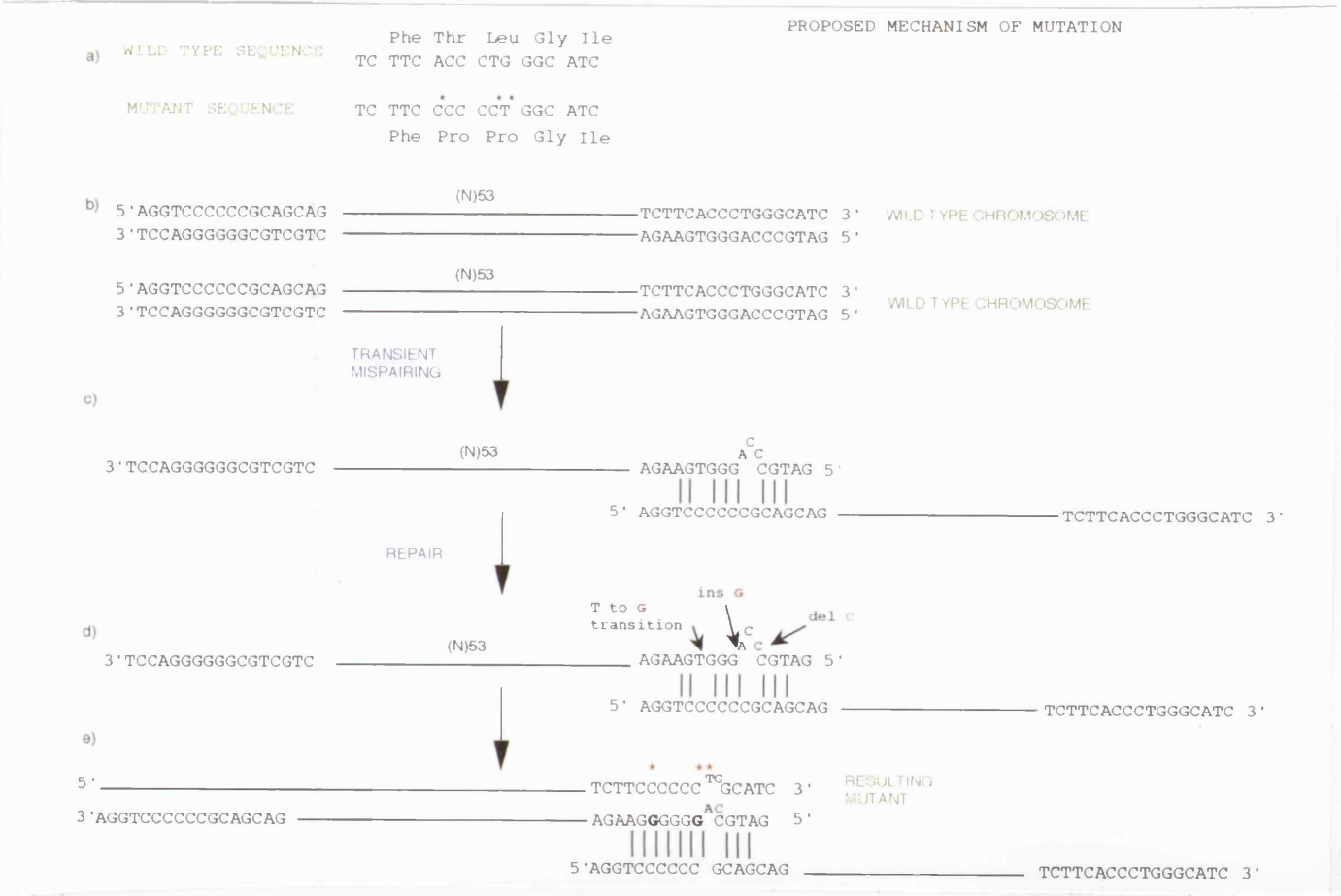

Figure 4.1.

(a)The wild type and mutant sequences. There are three nucleotide substitutions which are indicated by * in the mutant sequence. (b-d), A proposed mechanism for the complex mutation. There are two regions of sequence similarity, approximately 60 bases apart in the gene. Transient mispairing between these two regions is shown in (c). Attempted correction of the 3'-sequence based on the template of the 5'-sequence is shown in (d). partial correction results in the changes observed in the mutant sequence.

4.2.2. Mutation in KVLQT1 causes Jervell and Lange-Nielsen syndrome

After the initial identification of a mutation in IsK, analysis of 12 unrelated families with JLNS failed to identify another mutation in IsK. During the course of this work, Neyroud *et al* published two families with JLNS homozygous for a single mutation in KVLQT1 (Neyroud *et al*, 1997), a gene previously implicated in autosomal dominant Romano Ward syndrome (Wang *et al*, 1996). Haplotype data for the additional families described in this study is consistent with mutation in KVLQT1. Exons of the KVLQT1 gene were identified and primers designed in order to screen the entire gene from genomic DNA. Novel mutations were identified, thus analysis of these additional JLNS families confirmed the role of KVLQT1 in JLNS and also demonstrated that KVLQT1 is the major locus for this syndrome.

It is now shown that an indistinguishable phenotype arises from mutation in either IsK or KVLQT1 the two subunits of the slow component of the delayed rectifier current Iks. The interaction of IsK with HERG (McDonald *et al*, 1997) implicates mutations in HERG as a cause of JLNS, although none have been described to date. Evidence against this is that in this particular study of 13 JLNS families, the molecular basis of the disease is accounted for by either mutation in IsK or KVLQT1. Although, mutations in HERG account are the second most common cause of RWS, mutation in HERG in JLNS would be rare.

Norwegian families

Ten unrelated Norwegian families were ascertained in collaboration with Professor Lisbeth Tranebjærg, including the original JLNS family described in 1957 (Jervell and Lange-Nielsen, 1957).

SSC analysis and direct sequencing of KVLQT1 identified three common mutations in this subset of families; a 5 base pair deletion, denoted 572-576 delTGCGC, and two nonsense mutations, 1552C>T (Arg518Stop) and 1588C>T (Gln530Stop).

The 5 base pair deletion was identified in six families from Norway, in both the homozygous and heterozygous form. The consequence of this mutation is the premature truncation of the predicted protein in the S5 transmembrane domain. The predicted protein, if produced, will lack the pore region, the S6 transmembrane domain and the entire intracellular C-terminus. Since interaction of KVLQT1 with IsK involves the pore region of KVLQT1, it is unlikely that this mutant subunit would retain the ability to interact with IsK.

A founder effect, which is the introduction of a mutation into a small population by one member, leading to a relatively high prevalence of that mutation in the population in future generations, is likely since a common haplotype for markers spanning the KVLQT1 gene was observed in these families, figure 3.26. These families are not known to be related, but do originate from the same county in Norway.

Two novel nonsense mutations were identified in exon 11A of the KVLQT1 gene, which encodes part of the C-terminus of the predicted protein. The same nonsense mutation, 1552C>T, was identified in three Norwegian JLNS families. The mutation occurred on two different haplotypes for markers around the KVLQT1 gene on chromosome 11p15.5, figure 3.26, suggesting that these are independent mutation events. However, further refinement with markers closer to the KVLQT1 gene needs to be performed, since the interval at present spans a region of 6cM.

Another nonsense mutation in exon 11A, 1588C>T, was found in two Norwegian families, N6K and N7J. These families share a common haplotype for polymorphic markers at the KVLQT1 locus.

No mutation has been identified by SSC analysis in Family N8A. There is no suggestion of the involvement of another gene; the proband is homozygous-by-descent for markers flanking the KVLQT1 gene, and there remains a small area of the gene unscreened. Direct sequencing of the entire KVLQT1 gene, and southern blot analysis to examine the gene for rearrangements, would hope to identify the mutation in this family.

British families

The mutation identified in Family UK2T results in a histidine replacing an arginine at position 243 in the S4 transmembrane domain of the

predicted protein. The S4 transmembrane domain contains a cluster of positively-charged amino acids such as arginines and lysines, and is the major voltage sensor of the ion channel (Hebert, 1998). A mutation of an arginine to a different residue may affect the function of this domain. Neutralisation of the four positively charged residues in the S4 segment of a sodium channel by site-directed mutagenesis has been shown to have major effects on the voltage dependence of activation (Catterall, 1995). The mutation described in Family UK2T, a histidine replacing an arginine, may affect the voltage dependence of activation of the channel, in turn affecting the IKs current, although histidine also carries a positive charge, albeit a weaker one. Additionally, in the KVLQT1 gene, this arginine residue is highly conserved in human, mouse, *xenopus* and *C. elegans* (Chouabe *et al*, 1997).

Family UK3C was originally published as being excluded from the KVLQT1 locus (Jeffrey et al, 1992). However, subsequent recombinations between Harvey-ras and Romano Ward syndrome (RWS) and the repositioning of the KVLQT1 gene with respect to microsatellite markers prompted the re-analysis of this family which showed that they are consistent with mapping to the KVLQT1 locus. Evidence of genetic heterogeneity is provided by the molecular analysis of Family UK1S. Both the affected boys of Family UK3C and their mother are heterozygous for a 1 bp deletion at position 1008 of the KVLQT1 gene. The father does not have this particular mutation; his mutation and hence the second mutation in these boys has not yet been identified.

Direct sequencing of the entire KVLQT1 gene, including a previously unscreened exon, would hopefully identify the mutation in this family.

Each of the mutations identified, with the exception of Family UK2T, are nonsense and frameshift mutations prematurely truncating the predicted protein in the C-terminus.

4.2.3. Molecular mechanism of KVLQT1 mutations in JLNS

A mutation of a gene might cause a phenotypic change in either of two ways; the product may have reduced or no function (loss-of-function mutation) or the product may function in an abnormal way. The majority of mutations in KVLQT1 identified in JLNS in this study are predicted to result in the translation of an aberrant or truncated protein, which is unlikely to act as a functional channel subunit. The domains involved in the assembly of the KVLQT1 tetrameric channel are not known. If co-assembly requires an intact C-terminus, then mutant subunits truncated in this domain cannot interact with other subunits, hence the molecular mechanism of these mutations is likely to be loss of function. The homozygous missense mutation, Arg243His, of a highly conserved residue, identified in one of the 12 families studied, appears to be an exception, but functional studies of HERG, mutations in which cause chromosome-7 linked RWS, have shown that missense mutations can act as loss of function mutations (Sanguinetti *et al*, 1996b). Additionally, low penetrance missense mutations in the S4 domain of KVLQT1 have recently been described (Priori *et al*, 1999). An alternative explanation is

that since IsK associates with the pore region of KVLQT1 (Wang, K-W., *et al*, 1996; Romey *et al*, 1997; Tai *et al*, 1998), then mutant subunits truncated before the pore region, for example the 572-576 delTGCGC and 1008 delC mutations, would lack the ability to physically assemble with IsK, producing an aberrant IKs.

The functional significance of mutations in ion channels can be assayed using *Xenopus* oocytes. These oocytes are large enough to be injected with exogenous mRNA and are capable of synthesising the resulting foreign proteins. After microinjection of the mRNA and incubation, the activity of the channel protein can be determined by patch-clamping techniques (Ackerman and Clapham, 1997). By measuring the electrophysiological properties of the reconstituted channel in the oocyte it is possible to elucidate the mechanisms by which mutations in KVLQT1 cause disease. Analysis of the properties of mutant alleles of KVLQT1 are performed in the presence of IsK in order to reproduce, as far as possible, the IKs current in patients. By examining whole cell currents and comparing with control conditions (wild type KVLQT1 with and without IsK), it should be possible to tell if mutations produce functional channels. If mutant subunits do not interact with wild type subunits, then one would expect a 50% wild type current, on a 1:1 expression of wild type and mutant subunits, the equivalent of injecting half the amount of wild type subunit alone. This was subsequently observed for the first homozygous KVLQT1 mutation described in families with JLNS, an insertion/deletion mutation resulting in a frameshift, disrupting the coding

region after the S6 transmembrane domain and premature truncation of the predicted protein in the cytoplasmic C-terminus (Neyroud *et al*, 1997). Expression of the mutant subunit alone did not show novel currents, nor did it assemble with wild type subunits, demonstrating that this mutation acts as a loss of function mutation (Wollnik *et al*, 1997). It remains to be seen if this is the molecular mechanism by which all truncating mutations act. Transcripts with premature translational termination are often degraded by mechanisms not fully understood (Maquat, 1996). This could be demonstrated *in vitro* by placing an epitope tag on the KVLQT1 clone. If the subsequent mutant transcript was degraded, this would manifest as a reduction or absence of protein on a western blot probed with antibodies to the epitope tag.

4.2.4. Significance

From the clinical data available for the families in this study, the majority of mutation carriers do not have prolonged QTc (section 2.3.3). The parents of children with JLNS may occasionally have prolonged QTc and some gene carriers may even be symptomatic (Splawski *et al*, 1997b), but a family history of syncope and sudden death is rare in individuals with JLNS and has not been reported in the literature until recently (Neyroud et al, 1997; Splawski et al, 1997b). These mutations appear to be low penetrance in the heterozygous state, in contrast to the higher penetrance traditionally described in RWS (Vincent *et al*, 1992). In the case of the 5 base pair deletion, 572-576 delTGCGC, only a single carrier from a total of 16 suffered from syncope, a penetrance much

lower than that seen in RWS, even "forme fruste" long QT syndrome (Donger *et al*, 1998). Furthermore, an apparently normal phenotype has been described for a heterozygous missense mutation in the pore region of KVLQT1, individuals homozygous for this mutation suffered from JLNS (Neyroud *et al*, 1998). An important consequence of the identification of low penetrance mutations, is that so called "sporadic" cases of long QT, thought to out number the genetic cases, may have mutations of low pentrance, and therefore appear to have no family history. The finding that QTc intervals may be prolonged in infants subsequently dying of SIDS (Schwartz *et al*, 1998) may now be accounted for at the molecular level; some infants may have new missense mutations in KVLQT1 but some may be heterozygous for low penetrance ("loss of function") mutations in KVLQT1 such as those identified in this study, which are not clinically manifest in their parents and rarely give rise to familial recurrences.

It is interesting to speculate what determines whether these "low penetrance" mutations do become clinically apparent in the heterozygous state. The intrafamilial variation of penetrance and disease severity in the long QT syndromes may be influenced in part by common polymorphisms in the IsK gene (Lai *et al*, 1994; Tesson *et al*, 1996), which have an effect on the function of the KVLQT1/IsK complex. The sequence variations, harmless by themselves may influence the phenotype of heterozygous carriers of KVLQT1 mutations. It is only by correlating genotype, phenotype and functional effects of mutations and

polymorphisms that such an interaction could be determined. Environmental or hormonal factors may also influence the phenotype of carriers.

4.2.5. Mutations in KVLQT1 in Romano Ward syndrome.

Romano Ward or autosomal dominant long QT syndrome is characterised by isolated cardiac syncope and prolongation of the QT interval on electrocardiogram. Of the four genes implicated in RWS, mutations in KVLQT1 account for approximately 40% of cases of inherited long QT (Ackerman, 1998a).

Of the 30 different mutations in KVLQT1 that underlie dominant Long QT syndrome 26 are missense mutations (Reviewed in Wang, Q. *et al*, 1998).

An exception to this rule appears to be the 3bp deletion described by Wang (Wang *et al*, 1996), the 3bp deletion described by Ackerman (Ackerman *et al*, 1998b), and the novel mutations identified by Li (Li, H., *et al*, 1998).

However, the 3bp deletion described by Wang (Wang *et al*, 1996), results in the deletion of an amino acid, and a substitution of a phenylalanine residue for a tryptophan residue in the second putative transmembrane domain of the predicted protein. Essentially, this mutation can be considered to be a missense, since the effect of the

mutation is localised, there is no major frameshift or premature truncation. The 3bp deletion reported by Ackerman also results in the in-frame deletion of a single phenylalanine residue without frameshift (Ackerman *et al*, 1998b).

Li and colleagues have recently identified novel mutations in KVLQT1 in families with Romano-Ward syndrome (Li, H. *et al*, 1998) which they propose both cause a frameshift, disrupt splicing and lead to premature truncation of the KVLQT1 protein. However, this may not be the only explanation of the effect of these mutations. A splice site mutation, SP/A249/g-a was identified in 4 families. Most commonly, a mammalian spice site mutation results in exon skipping (Maquat, 1996). The mutation which is denoted SP/A249 (g-a) occurs at a splice junction and may cause the exon to be skipped with the resulting mRNA, in this particular case, still reading "in frame". Li also identified a novel 3bp deletion which spans an exon-intron boundary. However, the 5' donor splice consensus sequence seems to be intact (Shapiro and Senapathy, 1987) and splicing may still occur at this position, 3 nucleotides proximal to the wild type splice site. The consequence of this mutation may therefore be a mutant protein with a deletion of a single amino acid, valine. If this is the case, these mutations may have a localised effect and are not necessarily null alleles as proposed.

In summary, the type of mutation in KVLQT1 that predominates in RWS is missense or small in-frame deletions with localised effects.

Molecular mechanism of KVLQT1 mutations in RWS

The missense mutations identified in KVLQT1 underlying autosomal dominant long QT syndrome (RWS), that have been functionally assessed to date, result in a dominant-negative suppression of potassium channel activity as judged by electrophysiological studies in *Xenopus* oocytes (Russell *et al*, 1996; Wollnik *et al*, 1997; Shalaby *et al*, 1997; Chouabe *et al*, 1997). A dominant-negative effect occurs when the mutant product not only loses its own function but prevents the product of the normal allele from functioning in a heterozygous person. This effect is often seen with proteins that work as dimers or multimers. The mutant protein retains the ability to assemble, sequestering the wild-type subunit into dysfunctional channels. By co-injecting oocytes with mutant and wild-type mRNA it is possible to determine these effects.

4.2.6. Mutation in KVLQT1 in autosomal recessive Long QT syndrome

Homozygosity for a mutation in KVLQT1 in an autosomal recessive variant of RWS has recently been described in a single consanguineous family (Priori *et al*, 1998). The affected individual suffered from classic RWS symptoms, characterised by syncope and prolongation of the QT interval on ECG, but did not suffer from hearing loss. His parents, both carriers of the mutation, had normal ECGs. The mutation, a missense mutation of a highly conserved residue in the pore region, only manifests the cardiac phenotype in the homozygous state. In the case of

multimeric complexes, for recessive mutations it requires that the mutated subunit does not interact with the wild type subunit, compromising the function of the mutant/wild type channel, or if it does assemble, the function of the resulting mutant/wild type channel is not compromised sufficiently to cause disease. The mutant allele described here may still interact with wild type subunits, leaving residual channel activity. Hence the heterozygous carrier is asymptomatic. This suggests that the ear is less sensitive than the heart to a dysfunctional potassium current. Interestingly, this mutation is only 5 amino acid residues away from a mutation found in the homozygous state in an individual with JLNS (Neyroud *et al*, 1998).

The molecular analysis of Family N16O in this study provides evidence for genetic heterogeneity in autosomal recessive long QT syndrome, as this family is not consistent with mapping to either KVLQT1 or IsK. The analysis of other loci and genes implicated in Romano Ward syndrome, HERG, SCN5A and the locus on chromosome 4, will be candidate regions for future work.

4.2.7. Recessive versus dominant mutations in KVLQT1.

Now it has now been shown at the molecular level that autosomal recessive JLNS and the autosomal dominant RWS are allelic conditions caused by mutation in the gene KVLQT1, it is interesting to speculate what accounts for the two phenotypes observed.

Analysis of the large number of families with JLNS, allows for comparisons at the molecular level between JLNS and RWS and from this study, it is proposed that different types of mutation and the position of mutations in KVLQT1 differ in JLNS and RWS. Can the different phenotypes can be accounted for by the type and position of the mutation in the KVLQT1 molecule?

The predominance of nonsense and frameshift mutations in KVLQT1 in families with JLNS is a different scenario to that observed in Romano-Ward syndrome. No nonsense mutations have been identified so far in patients ascertained as Romano-Ward syndrome.

The type of mutation in KVLQT1, and hence the molecular mechanism through which it acts may account for the differences in symptoms in heterozygotes for the two conditions, explaining why carriers of missense mutations, acting in a dominant-negative manner, tend to suffer from RWS, characterised by syncopal episodes, whereas nonsense and frameshift "loss of function" mutations only rarely give rise to symptoms except in the homozygous state. The main difference between RWS and JLNS mutations in KVLQT1 could be the presence or absence, respectively, of a dominant-negative effect on the gene product of the wild type allele.

Expression of these mutations in *Xenopus* oocytes should confirm if these different types of mutation have a significant functional difference.

Not only does the type of mutation in KVLQT1 appear to differ between JLNS and RWS, but the position of mutation appears to be different. From this study and that of Neyroud (Neyroud *et al*, 1997) and Splawski (Splawski *et al*, 1997b), mutations in KVLQT1 in families with JLNS appear to truncate the predicted protein in the C-terminus.

Initially, the KVLQT1 mutations identified in RWS appeared to be clustered in the S2-S6 domains of the predicted protein, but this was the only part of the gene for which primers had been designed to amplify genomic DNA (Wang *et al*, 1996), and hence there would have been a bias towards this part of the gene. The C-terminus can now be screened from genomic DNA, analysis of this part of the KVLQT1 gene may reveal additional mutations, since many groups have failed to identify mutations in KVLQT1 in families with RWS consistent with mutation at this locus (Neyroud *et al*, 1997; Saarinen *et al*, 1998).

A mutation in the C-terminal region of KVLQT1 has resulted in "forme fruste" long QT (Donger *et al*, 1997). This C-terminal mutation resulted in a mild clinical phenotype. Of the 44 carriers of the mutation, only 5 suffered from syncope, and 2 died suddenly. The QTc intervals of the mutation carriers were often borderline, but they were significantly lower than seen in individuals with mutations in the transmembrane regions (Donger *et al*, 1997). It remains to be seen whether all C-terminal

mutations in families ascertained with RWS will be mild and whether a phenotype can be predicted from mutation location.

A scenario similar to that seen for mutations in KVLQT1 in JLNS and RWS is the situation with Myotonia Congenita. Both recessive and dominant forms of Myotonia Congenita are due to mutations in the gene CLCN1, encoding the major skeletal muscle chloride channel CIC-1 (Koch *et al*, 1992). More than 30 different mutations have been identified, scattered the entire length of the channel protein. Total loss of function mutations, like those truncating the protein before the cytoplasmic C-terminus always lead to recessive disease, as do some missense mutations. Mutations found in autosomal dominant Myotonia Congenita exert dominant-negative effects on the co-expressed wild type subunits. However, it has also been found that some mutations do not conform to simple "dominant" or "recessive". Some mutations have reduced penetrance, some have been found associated with both dominant and recessive forms of Myotonia. Recent studies on the CIC-1 gene indicate that it is impossible to predict phenotype based on location or type of mutation (Kubisch *et al*, 1998).

4.2.8. KVLQT1 and imprinting

KVLQT1 is in a cluster of imprinted genes at the Beckwith Wiedemann syndrome locus on 11p15.5. The cluster of genes include the maternally expressed genes H19 and $p57^{KIP2}$, and the paternally expressed genes INS and IGF2 (Li *et al*, 1997). Genomic imprinting is an epigenetic

mechanism controlling gene expression in which the transcriptional activity of each allele is dependent on its parental origin. In most tissues, KVLQT1 is preferentially expressed from the maternal allele, however in the heart, it is biallelically expressed (Lee *et al*, 1997). In the mouse during early embryogenesis, expression of kvlqt1 is maternal in origin, the paternal allele only becomes activated later in fetal development. Juvenile and adult animals show complete biallelic expression (Gould and Pfeifer, 1998). Lack of imprinting in the human heart would account for why no parent of origin effect of transmission is seen in RWS.

Beckwith Wiedemann syndrome (BWS) is an overgrowth disorder characterised by developmental anomalies, tissue and organ hyperplasia, and an increased risk of embryonal tumours (Li *et al*, 1997). KVLQT1 is implicated in the aetiology of BWS in that the gene spans translocation breakpoints associated with the disease (Lee *et al*, 1997; Reid *et al*, 1997). KVLQT1 occupies a very large genomic region of at least 300Kb, therefore these translocations may not be of functional consequence; the rearrangements may disrupt the expression of multiple loci nearby by disrupting an imprinting centre or by "position effects". To date there is no known relationship between mutations in the potassium channel gene KVLQT1 and the BWS phenotype.

4.2.9. Future work

Only functional analysis of mutations identified in this study in expression systems such as the *Xenopus* oocyte and mammalian cell lines can try

to establish the functional possibilities that may explain the various clinical phenotypes seen in the heterozygotes and homozygotes in the Romano Ward and Jervell and Lange-Nielsen syndromes. This should provide better clinical insight into the possible range of severity of mutations in the potassium channel gene KVLQT1.

REFERENCES

Ackerman M, Clapham D. (1997). Ion channels-Basic science and clinical disease. New Engl J Med. **336**:1575-1586.

Ackerman M. (1998a). The Long QT syndrome: Ion channel diseases of the heart. Mayo Clinical Proceedings. **73**:250-269.

Ackerman M, Schroeder J, Berry R, Schaid D, Porter C, Michels V, Thibodeau S. (1998b). A novel mutation in KVLQT1 is the molecular basis of inherited long QT syndrome in a near-drowning patients's family. Pediatr Res. **44**:148-153.

Arslan E, Orzan E. (1996). The audiological approach to genetic hearing impairment in children. In: Martini A, Read A, Stephens D (Eds). Genetics and Hearing Impairment. Whurr Publishers. pp82-91.

Auch D, Reth M. (1990). Exon trap cloning: using PCR to rapidly detect and clone exons from genomic DNA fragments. Nucl Acids Res. **18**:6743-6744.

Avraham KB, Hasson T, Steel KP, Kingsley DM, Russell LB, Mooseker MS, Copeland NG, Jenkins NA. (1995). The mouse Snell's waltzer deafness gene encodes an unconventional myosin required for structural integrity of inner ear hair cells. Nat Genet. **11**:369-75.

Avraham KB, Weiss S, Kagan M, Vahava O (1998) The role of the transcription factor *POU4F3* in human hearing loss. Molecular Biology of Hearing and Deafness, Bethesda, MD. USA.pp 8

Bach I, Brunner HG, Beighton P, Ruvalcaba RHA, Reardon W, Pembrey M, van der Velde-Visser SD, Bruns G, Cremers CWRJ, Cremers FPM, Ropers H-H. (1992). Microdeletions in patients with gusher-associated X-linked deafness (DFN3). Am J Hum Genet. **50**:38-44.

Balciuniene J, Dahl N, Borg E, Sameulson E, Koisti M, Pettersson U, Jazin E. (1998). Evidence for digenic inheritance of nonsyndromic hereditary hearing loss in a Swedish family. Am J Hum Genet. **63**:786-793.

Baldwin C, Farrer L, Weiss S, De Stefano A, Adair R, Franklyn B, Kidd K, Korostishevsky M, Bonne-Tamir B. (1995). Linkage of congenital, recessive deafness (DFNB4) to chromosome 7q31 and evidence for genetic heterogeneity in the Middle Eastern Druze population. Hum Mol Genet. **4**:1637-1642.

Barhanin J, Lesage F, Guillemare E, Fink M, Lazdunski M, Romey G. (1996). KVLQT1 and IsK (minK) proteins associate to form the IKs cardiac potassium current. Nature. **384**:78-80.

Barhanin J, Attali B, Lazdunski M. (1998). IKs, a slow and intriguing cardiac K^+ channel and its associated long QT diseases. Trends Cardiovasc Med. **8**:207-214.

Barker D, Hostikka S-L, Zhou J, Chow L, Oliphant A, Gerken S, Gregory M, Skolnick M, Atkin C, Tryggvason K. (1990). Identification of mutations in the COL4A5 collagen gene in Alport syndrome. Science. **148**:1224-1227.

Barker DF, Cleverly J, Fain PR. (1992). Two CA-dinucleotide polymorphisms at the COL4A5 (Alport syndrome) gene in Xq22. Nucl Acids Res. **20**:929.

Bedell M, Jenkins N, Copeland N. (1996). Good genes in bad neighbourhoods. Nat Genet. **12**:229-231.

Bione S, Sala C, Manzini C, Arrigo G, Zuffardi O, Banfi S, Borsani G, Jonveaux P, Phillipe C, Zuccotti M, Ballabio A, Toniolo D. (1998). A human homologue of the *Drosophila melanogaster diaphanous* gene is disrupted in a patient with premature ovarian failure: Evidence for conserved function in oogenesis and implications for human sterility. Am J Hum Genet. **62**:533-541.

Bitner-Glindzicz M, de Kok Y, Summers D, Huber I, Cremers FPM, Ropers H-H, Reardon W, Pembrey M, Malcolm S. (1994). Close linkage of a gene for non-syndromic X-linked deafness to three microsatellite repeats at Xq21 in radiologically normal and abnormal families. J.Med. Genet. **31**:916-921.

Bitner-Glindzicz M, Turnpenny P, Hoglund P, Kaarianen H, Sankila E-M, van der Maarel S, de Kok Y, Ropers H-H, Cremers F, Pembrey M, Malcolm S. (1995). Further mutations in *Brain 4* (*POU3F4*) clarify the phenotype in the X-linked deafness, DFN3. Hum Mol Genet. **4**:1467-1469.

Boensch D, Scheer P, Storch P, Neumann C, Deufel T, Lamprecht-Dinnesen A. (1998). Mapping of a further type of autosomal dominant nonsyndromic hearing impairment (DFNA18) to chromosome 3q22. Am J Hum Genet. **63**:Abs 1628.

Bonne-Tamir B, DeStefano A, Briggs C, Adair R, Franklyn B, Weiss S, Korostishevsky M, Frydman M, Baldwin C, Farrer L. (1996). Linkage of Congenital Recessive Deafness (Gene DFNB10) to Chromosome 21q22.3. Am J Hum Genet. **58**:1254-1259.

Borsani G, Ballabio A, Banfi S. (1998). A practical guide to orient yourself in the labyrinth of genome databases. Hum Mol Genet. **7**:1641-1648.

Brennan MB, Hochgeschwender U. (1995). So many needles so much hay. Hum Mol Genet. **4**:153-156.

Brown K, Sutcliffe M, Steel KP, Brown SDM. (1992). Close linkage of the olfactory marker protein gene to the mouse deafness mutation *shaker-1*. Genomics. **13**:189-93.

Brown M, Tomek M, Van Laer L, Smith S, Kenyon J, Van Camp G, Smith RJH. (1997). A novel locus for autosomal dominant non-syndromic hearing loss, DFNA13, maps to chromosome 6p. Am J Hum Genet. **61**:924-927.

Brunner HG, van Bennekom CA, Lambermen EMM, Lian Oei T, Cremers CWRJ, Wieringa B, Ropers H-H. (1988). The gene for X-linked progressive mixed deafness with preilymphatic gusher during stapes surgery (DFN3) is linked to P.G.K. Hum Genet. **80**:337-340.

Buckler A, Chang D, Graw S, Brook J, Haber D, Sharp P, Housman D. (1991). Exon amplification: A strategy to isolate mammalian genes based on RNA splicing. Proc Natl Acad Sci USA. **88**:4005-4009.

Campbell D, McHale D, Brown K, Moynihan L, Houseman M, Karbani G, Parry G, Janjua A, Newton V, al-Gazali L, Markham A, Lench N, Mueller R. (1997). A new locus for non-syndromal, autosomal recessive, sensorineural hearing loss (DFNB16) maps to human chromosome 15q21-q22. J Med Genet. **34**:1015-1017.

Castrillon D, Gonczy P, Alexander S, Rawson R, Eberhart C, Viswanathan S, DiNardo S, Wasserman S. (1993). Toward a molecular genetic analysis of spermatogenesis in *Drosophila melanogaster*: characterisation of male-sterile mutants generated by single *P* element mutagenesis. Genetics. **135**:489-505.

Castrillon D, Wasserman S. (1994). *diaphanous* is required for cytokinesis in *Drosophila* and shares domains of similarity with the products of the *limb deformity* gene. Development. **120**:3367-3377.

Catterall W. (1995). Structure and function of voltage-gated ion channels. Ann Rev Biochem. **64**:493-531.

Chaib H, Lina-Granade G, Guilford P, Plauchu H, Levilliers J, Morgon A, Petit C. (1994). A gene responsible for a dominant form of neurosensory non-syndromic deafness maps to the NSRD1 recessive deafness gene interval. Hum Mol Genet. **3**:2219-2222.

Chaib H, Place C, Salem N, Chardenoux S, Vincemt C, Weissenbach J, El-Zir E, Loiselet J, Petit C. (1996a). A gene responsible for a sensorineural nonsyndromic deafness maps to chromosome 2p22-23. Hum Mol Genet. **5**:155-158.

Chaib H, Place C, Salem N, Chardenoux S, Vincemt C, Weissenbach J, El-Zir E, Loiselet J, Petit C. (1996b). Mapping of DFNB12, a gene for non-syndromal autosomal recesive deafness, to chromosome 10q21-22. Hum Mol Genet. **5**:1061-1064.

Chaib H, Kaplan J, Gerber S, Vincent C, Ayadi H, Slim R, Munnich A, Weissenbach J, Petit C. (1997). A newly identified locus for Usher syndrome, USH1E, maps to 21q21. Hum Mol Genet. **6**:27-31.

Charpentier F, Merot J, Riochet D, Le Marec H, Escande D. (1998). Adult KCNE1-knockout mice exhibit a mild cardiac cellular phenotype. Biochem Biophys Res Comm. **251**:806-810.

Chen AH, Ni L, Fukushima K, Marietta J, O'Neill M, Coucke P, Willems P, Smith RJH. (1995). Linkage of a gene for dominant non-syndromic deafness to chromosome 19. Hum Mol Genet. **4**:1073-1076.

Chen A, Wayne S, Bell A, Ramesh A, Srisailapathy C, Scott D, Sheffield V, Van Hauwe P, Zbar R, Ashley J, Lovett M, Van Camp G, Smith RJH. (1997). New gene for autosomal recessive non-syndromic hearing loss maps to either chromosome 3q or 19p. Am J Med Genet. **71**:467-471.

Chouabe C, Neyroud N, Guicheney P, Lazdunski M, Romey G, Barhanin J. (1997). Properties of KvLQT1 K^+ channel mutations in Romano-Ward and Jervell and Lange-Nielsen inherited cardiac arrhythmias. EMBO J. **16**:5472-5479.

Clark P, Lester T, Villard L, Fontes M, Kinnon C. (1994). Deletion mapping of the DXS986, DXS995 and DXS1002 loci defines their order within Xq13.2-q21.33. J Med Genet. **31**:344-345.

Claverie J-M. (1997). Computational methods for the identification of genes in vertebrate genomic sequences. Hum Mol Genet. **6**:1735-1744.

Collins F. (1995). Positional cloning moves from perditional to traditional. Nat Genet. **9**:347-350.

Collins A, Frezal J, Teague J, Morton N. (1996). A metric map of humans: 23,500 loci in 850 bands. Proc. Natl. Acad. Sci. USA. **93**:14771-14775.

Cordes SP, Barsh GS. (1994). The mouse segmentation gene, kr, encodes a novel basic domain-leucine zipper transcription factor. Cell. **79**:1025-1034.

Cotton R. (1997). Slowly but surely towards better scanning for mutations. Trends Genet. **13**:43-46.

Cotton R, Scriver C. (1998). Proof of "disease causing" mutation. Hum Mutat. **12**:1-3.

Coucke P, Van Camp G, Djoyodiharjo B, Smith SD, Frants RR, Padberg GW, Darby JK, Huizing EH, Cremers CWRJ, Kimberling WJ, Oostra BA, Van de Heyning PH, Willems PJ. (1994). Linkage of autosomal dominant hearing loss to the short arm of chromosome 1 in two families. New Engl J Med. **331**:425-431.

Coyle B, Coffey R, Armour JA, Gausden E, Hochberg Z, Grossman A, Britton K, Pembrey M, Reardon W, Trembath R. (1996). Pendred syndrome (goitre and sensorineural hearing loss) maps to chromosome 7 in the region containing the nonsyndromic deafness gene DFNB4. Nat Genet. **12**:421-3.

Cremers C, Van Rijn P. (1991). Acquired causes of deafness in childhood. Ann N Y Acad Sci. **630**:197-202.

Curran ME, Splawski I, Timothy KW, Vincent GM, Green ED, Keating MT. (1995). A molecular basis for cardiac arrhythmia: HERG mutations cause long QT syndrome. Cell. **80**:795-803.

Dausse E, Denjoy I, Kahlem P, Bennaceur M, Faure S, Weissenbach J, Coumel P, Schwartz K, Guicheney P. (1995). Readjusting the localization of long QT syndrome gene on chromosome 11p15. C.R. Acad. Sci. **318**:879-885.

Davis A, Cowell J. (1993). Mutations in the PAX6 gene in patients with hereditary aniridia. Hum Mol Genet. **2**:2093-2097.

de Kok YJM, Van der Maarel SM, Bitner-Glindzicz M, Huber I, Monaco AP, Malcolm S, Pembrey ME, Ropers HH, Cremers FPM. (1995). Association between X-linked mixed deafness and mutations in the POU domain gene *POU3F4.* Science. **267**:685-688.

de Kok YJM, Vossenaar ER, Cremers CWRJ, Dahl N, J. L, Hu LJ, Lacombe D, Fischel-Ghodsian N, Friedman RA, Parnes LS, Thorpe P, Bitner-Glindzicz M, Pander H-J, Heilbronner H *et al.* (1996). Identification of a hot spot for microdeletions in patients with X-linked deafness type 3 (DFN3) 900kb proximal to the DFN3 gene POU3F4. Hum Mol Genet. **9**:1229-1235.

del Castillo I, Villamar M, Sarduy M, Romero L, Herraiz C, Hernandez F, Rodriguez M, Borras I, Montero A, Bellon J, Tapia M, Moreno F. (1996). A novel locus for non-syndromic sensorineural deafness (DFN6) maps to chromosome Xp22. Hum Mol Genet. **5**:1383-1387.

Denoyelle F, Weil D, Maw M, Wilcox S, Lench N, Allen-Poweel D, Osborn A, Dahl H-H, Middleton A, Houseman M, Dode C, Marlin S, Boulila-ElGaied A, Grati Met al. (1997). Prelingual deafness: High prevalence of a 30delG mutation in the connexin 26 gene. Hum Mol Genet. **6**:2173-2177.

Denoyelle F, Lina-Granade G, Plauchu H, Bruzzone R, Chaib H, Levi-Acobas F, Weil D, Petit C. (1998). Connexin 26 gene linked to dominant deafness. Nature. **393**:319-320.

Deol M. (1966). Influence of the neural tube on the differentiation of the inner ear in the mammalian embryo. Nature. **209**:219.

Dib C, Faure S, Fizames C, Samson D, Drouot N, Vignal A, Millasseau P, Marc S, Hazan J, Seboun E, Lathrop M, Gyapay G, Morisette J, Weissenbach J. (1996). A comprehensive genetic map of the human genome based on 5,264 microsatellites. Nature. **380**:152-154.

Donger C, Denjoy I, Berthet M, Neyroud N, Cruaud C, Bennaceur M, Chivoret G, Schwartz K, Coumel P, Guicheney P. (1997). KVLQT1 C-Terminal missense mutation causes a "Forme Fruste" Long-QT syndrome. Circulation. **96**:2778-2781.

Drici M-D, Arrighi I, Chouabe C, Mann J, Lazdunski M, Romey G, Barhanin J. (1998). Involvement of IsK-associated K+ channel in heart rate control of repolarisation in a murine engineered model of Jervell and Lange-Nielsen syndrome. Circ Res. **83**:95-102.

Duggal P, Vesely M, Wattanasirichaigoon D, Villafane J, Kaushik V, Beggs A. (1998). Mutation of the gene IsK associated with both Jervell and Lange-Nielsen and Romano-Ward forms of Long-QT syndrome. Circulation. **97**:142-146.

Dunckley MG, Manoharan M, Villiet P, Eperon IC, Dickson G. (1998). Modification of splicing in the dystrophin gene in cultered Mdx muscle cells by antisense oligoribonucleotides. Hum Mol Genet. **7**:1083-1090.

Erkman L, McEvilly RJ, Luo L, Ryan AK, Hooshmand F, SM OC, Keithley EM, Rapaport DH, Ryan AF, Rosenfeld MG. (1996). Role of transcription factors Brn-3.1 and Brn-3.2 in auditory and visual system development. Nature. **381**:603-6.

Estivill X, Fortina P, Surrey S, Rabionet R, Melchionda S, D'Agruma L, Mansfield E, Rappaport E, Govea N, Mila M, Zelante L, Gasparini P. (1998a). Connexin-26 mutations in sporadic and inherited sensorineural deafness. Lancet. **351**:394-398.

Estivill X, Govea N, Barcelo A, Parello E, Badenas C, Romero E, Moral L, Scozzari R, D'Urbano L, Zeviani M, Torroni A. (1998b). Familial progressive sensorineural deafness is mainly due to the mtDNA mutation and is enhanced by treatment with aminoglycosides. Am J Hum Genet. **62**:27-35.

Evans KL, Fantes J, Simpson C, Arveiler B, Muir W, Fletcher J, van Heyningen V, Steel KP, Brown KA, Brown SDM, St. Clair D, Porteous

DJ. (1993). Human olfactory marker protein maps close to tyrosinase and is a candidate gene for Usher syndrome type 1. Hum Mol Genet. **2**:115-118.

Everett L, Glaser B, Beck J, Idol J, Buchs A, Heyman M, Adawi F, Hazani E, Nassir E, Baxevanis A, Sheffield V, Green E. (1997). Pendred syndrome is caused by mutations in a putative sulphate transporter gene (PDS). Nat Genet. **17**:411-422.

Fagerheim T, Nilssen O, Raeymaekers P, Brox V, Moum T, Elverland H, Teig E, Omland H, Fostad G, Tranebjaerg L. (1996). Identification of a new locus for autosomal dominant non-syndromic hearing impairment (DFNA7) in a large Nowegian family. Hum Mol Genet. **5**:1187-1191.

Fantes J, Redeker B, Breen M, Boyle S, Brown J, Fletcher J, Jones S, Bickmore W, Fukushima Y, Mannens M, Danes S, van Heyningen V, Hanson I. (1995). Aniridia-associated cytogenetic rearrangements suggest that a position effect may cause the mutant phenotype. Hum Mol Genet. **4**:415-422.

Fischel-Ghodsian N. (1998). Mitochondrial genetics and hearing loss: The missing link between genotype and phenotype. Proc Soc Expt Biol Med. **218**:1-6.

Fraser G. (1976). The Causes of Profound Deafness in Childhood. John's Hopkins University Press, London, UK.

Friedman TB, Liang Y, Weber JL, Hinnant JT, Barber TD, Winata S, Arhya IN, Asher JH. (1995). A gene for congenital, recessive deafness DFNB3 maps to the pericentromeric region of chromosome 17. Nat Genet. **9**:86-91.

Friedmann I, Fraser GR, Froggatt P. (1966). Pathology of the ear in the cardioauditory syndrome of Jervell and Lange-Nielsen (recessive deafness with electrocardiographic abnormalities). J Laryngol Otol. **80**:451-470.

Friedmann I, Fraser GR, Froggatt P. (1968). Pathology of the ear in the cardio-auditory syndrome of Jervell and Lange-Nielsen syndrome. Laryngol. Otol. **82**:883-896.

Fukushima K, Arabandi R, Srisailapathy C, Ni L, Chen A, O'Neill M, Van Camp G, Coucke P, Smith S, Kenyon J, Jain P, Wilcox E, Zbar R, Smith RJH. (1995a). Consanguineous nuclear families used to identify a new locus for recessive non-syndromic hearing loss on 14q. Hum Mol Genet. **4**:1643-1648.

Fukushima K, Ramesh A, Srisailapathy C, Ni L, Wayne S, O'Neill M, Van Camp G, Coucke P, Jain P, Wilcox E, Smith S, Kenyon J, Zbar R, Smith

RJH. (1995b). An autosomal recessive non-syndromic form of sensorineural hearing loss maps to 3p-DFNB6. Genome Res. **5**:305-308.

Fukushima K, Ueki Y, Nishizaki K, Kasai N, Sugata K, Hirakawa S, Masuda A, Gunduz M, Ninomiya Y, Masuda Y, Chen A, Smith RJH (1998) Autosomal dominant non-syndromic deafness locus (DFNA16) maps to chromosome 2q24 Molecular Biology of Hearing and Deafness, Bethesda, MD. USA.

Ganong WF (1993) Review of Medical Physiology. 16th Edition· London-Prentice Hall. "Hearing and Equilibrium" pp 161-174; "Origin of the heartbeat and eletrical activity of the heart" pp 509-524.

Gasparini P, Estivill X, Volpini V, Totaro A, Castellvi-Bel S, Govea N, Mila M, Della Monica M, Ventruto V, De Benedetto M, Stanziale P, Zelante L, Mansfield E, Sandkuijl L *et al.* (1997). Linkage of DFNB1 to non-syndromic neurosensory autosomal-recessive deafness in Mediterranean families. Eur J Hum Genet. **5**:83-88.

Gibson F, Walsh J, Mburu P, Varela A, Brown KA, Antonio M, Beisel KW, Steel KP, Brown SDM. (1995). A type VII myosin encoded by the mouse deafness gene *shaker-1.* Nature. **374**:62-64.

Gould T, Pfeifer K. (1998). Imprinting of mouse *Kvlqt1* is developmentally regulated. Hum Mol Genet. **7**:483-487.

Green G, Wayne S, Nishtala R, Chen A, Ramesh A, Srisailapathy C, Fukushima K, Van Camp G, Smith RJH. (1998a). Identification of a novel locus (DFNB19) for non-syndromic autosomal rescessive hearing loss in a consanguineous family. Molecular Biology of Hearing and Deafness, Bethesda, MD. USA, pp 108

Green G, Whitehead S, Van Camp G, Smith RJH (1998b) Identification of a new locus-DFNA19-for dominant hearing impairment. Molecular Biology of Hearing and Deafness, Bethesda, MD. USA., pp 107

Greinwald J, Wayne S, Chen A, Scott D, Zbar R, Kraft M, Prasad S, Ramesh A, Coucke P, Srisailapathy C, Lovett M, Van Camp G, Smith RJH. (1998). Localisation of a novel gene for nonsyndromic hearing loss (DFNB17) to chromosome region 7q31. Am J Med Genet. **78**:107-113.

Guilford P, Ben Arab S, Blanchard S, Levilliers J, Weissenbach J, Belkahia A, Petit C. (1994a). A non-syndromic form of neurosensory, recessive deafness maps to the pericentromeric region of chromosome 13. Nat Genet. **6**:24-28.

Guilford P, Ayadi H, Blanchard S, Chaib H, Le PD, Weissenbach J, Drira M, Petit C. (1994b). A human gene responsible for neurosensory, non-syndromic recessive deafness is a candidate homologue of the mouse *sh-1* gene. Hum Mol Genet. **3**:989-993.

Hasson T, Heintzelman M, Santos-Sacchi J, Corey D, Mooseker M. (1995). Expression in cochlea and retina of myosin VIIa, the gene product defective in Usher syndrome type 1B. Proc Natl Acad Sci USA. **92**:9815-9819.

Hasson T, Gillespie P, Garcia J, MacDonald R, Zhao Y-D, Yee A, Mooseker M, Corey D. (1997). Unconventional myosins in inner-ear sensory epithelia. J Cell Biol. **137**:1287-1307.

Hasson T. (1997). Unconventional myosins, the basis for deafness in mouse and man. Am J Hum Genet. **61**:801-805.

Hastbacka J, de la Chapelle A, Kaitila I, Sistonen P, Weaver A, Lander E. (1992). Linkage disequilibrium mapping in isolated founder populations: diastrophic dysplasia in Finland. Nat Genet. **2**:204-211.

Hastbacka J, de ICA, Mahtani M, Clines G, Reeve-Daly M, Daly M, Hamilton B, Kusmi K, Trivedi B, Weaver A, Coloma A, Lovett M, Buckler A, Kaitila I *et al.* (1994). The diastrophic dysplasia gene encodes a novel sulfate transporter: Positional cloning by fine-structure linkage disequilibrium mapping. Cell. **78**:1073-1087.

Hebert S. (1998). General principles of the structure of Ion channels. Am J Med. **104**:87-98.

Heidet L, Dahan K, Zhou J, Xu Z, Cochat P, Gould J, Leppig K, Proesmans W, Guyot C, Guillot M, Roussel B, Tryggvason K, Grunfield J-P, Gubler M-C *et al.* (1995). Deletions of both 5(IV) and 6(IV) collagen genes in Alport syndrome and in Alport syndrome associated with smooth muscle tumours. Hum Mol Genet. **4**:99-108.

Heller S, Sheane C, Javed Z, Hudspeth A. (1998). Molecular markers for cell types of the inner ear and candidate genes for hearing disorders. Proc Natl Acad Sci USA. **95**:11400-11405.

Hughes D, Legan PK, Steel KP, Richardson GP. (1998). Mapping of the alpha-tectorin gene (TECTA) to mouse chromosome 9 and human chromosome 11: A candidate for human autosomal dominant nonsyndromic deafness. Genomics. **48**:46-51.

Jacobs H. (1997). Mitochondrial deafness. Ann Med. **29**:483-491.

Jain P, Fukushima K, Deshmukh D, Arabandi R, Thomas E, Kumar S, Lalwani A, Ploplis B, Skarka H, Srisailapathy C, Wayne S, Zbar R, Verma I, Smith RJH *et al.* (1995). A human recessive neurosensory nonsyndromic hearing impairment locus is a potential homologue of the murine *deafness* (*dn*) locus. Hum Mol Genet. **4**:2391-2394.

Jain P, Lalwani A, Li X, Singleton T, Smith T, Chen A, Deshmukh D, Verma I, Smith RJH, Wilcox ER. (1998). A gene for recessive nonsyndromic sensorineural deafness (DFNB18) maps to the chromosomal region 11p14-p15.1 containing the Usher syndrome type 1C gene. Genomics. **50**:290-292.

Jeffery S, Jamieson R, Patton MA, Till J. (1992). Long QT and Harvey-ras. Lancet. **339**:255.

Jervell A, Lange-Nielsen F. (1957). Congenital deaf-mutism, functional heart disease with prolongation of the QT interval, and sudden death. Am. Heart J. **54**:59-68.

Jervell A, Thingstad R, Endsjo T-O. (1966). The surdo-cardiac syndrome. Am. Heart J. **72**:582-593.

Jin H, May M, Tranebjaerg L, Kendall E, Fontan G, Jackson J, Subramony S, Arena F, Lubs H, Smith S, Stevenson R, Schwartz C, Vetrie D. (1996). A novel X-linked gene, *DDP*, shows mutations in families with deafness (DFN-1), dystonia, mental deficiency and blindness. Nat Genet. **14**:177-180.

Jolly DJ, Okayama H, Berg P, Esty AC, Filpula D, Bohlen P, Johnson GG, Shively JE, Hunkapillar T, Friedmann T. (1983). Isolation and characterisation of a full length expressible cDNA for human hypoxanthine phosphoribosyl transferase. Proc Natl Acad Sci USA. **80**:477-481.

Jordan T, Hanson I, Zaletayev D, Hodgson S, Prosser J, Seawright A, Hastie N, van Heyningen V. (1992). The human PAX6 gene is mutated in two patients with aniridia. Nat Genet. **1**:328-332.

Kajiwara K, Berson EL, Dryja TP. (1994). Digenic retinitis pigmentosa due to mutations at the unlinked peripherin/RDS and ROM1 loci. Science. **264**:1604-1608.

Kalatzis V, Petit C. (1998). The fundamental and medical impacts of recent progress in research on hereditary hearing loss. Hum Mol Genet. **7**:1589-1597.

Kawai S, Nomura S, Harano T, Harano K, Fukushima T, Osawa G,and the Japanese Alport Network. (1996). The COL4A5 gene in Japanese Alport Syndrome patients: Spectrum of mutations of all exons. Kidney Int. **49**:814-822.

Keating M, Atkinson D, Dunn C, Timothy K, Vincent G, Leppert M. (1991a). Linkage of a cardiac arrhythmia, the long QT syndrome, and the Harvey Ras-1 gene. Science. **252**:704-706.

Keating M, Dunn C, Atkinson D, Timothy K, Vincent G, Leppert M. (1991b). Consistent linkage of the long QT syndrome to the Harvey Ras-1 locus on chromosome 11. Am J Hum Genet. **49**:1335-1339.

Kelsell D, Dunlop J, Stevens H, Lench N, Liang J, Parry G, Mueller R, Leigh I. (1997). Connexin 26 mutations in hereditary non-syndromic sensorineural deafness. Nature. **387**:80-83.

Kendall E, Evans W, Jin H, Holland J, Vetrie D. (1997). A complete YAC contig and cosmid interval map covering the entirety of human Xq21.33 to Xq22.3 from DXS3 to DXS287. Genomics. **43**:171-182.

Kikuchi T, Kimar R, Paul D, Adams J. (1995). Gap junctions in the rat cochlea: immunohistochemical and ultrastructural analysis. Anat Embryol. **191**:101-118.

Kimberling W, Moller C, Davenport S, Priluck I, Beighton P, Greenberg J, Reardon W, Weston M, Kenyon J, Grunkemeyer J, Pieke Dahl S, Overbeck L, Blackwood D, Brower A *et al.* (1992). Linkage of Usher Syndrome Type 1 Gene (USH1B) to the long arm of Chromosome 11. Genomics. **14**:988-994.

Kirschhofer K, Kenyon J, Hoover D, Franz P, Weipoltshammer K, Wachtler F, Kimberling W. (1998). Autosomal dominant prelingual, nonprogressive sensorineural hearing loss-localisation of the gene to chromosome 11q by linkage in an Austrian family. Cyto Cell Genet. **82**:126-130.

Kleinjan D-J, van Heyningen V. (1998). Position effect in human genetic disease. Hum Mol Genet. **7**:1611-1618.

Koch M, Steinmeyer K, Lorenz C, Ricker K, Wolf F, Otto M, Zoll B, Lehmann-Horn F, Grzeschik K-H, Jentsch T. (1992). The skeletal muscle chloride channel in dominant and recessive human myotonia. Science. **257**:797-800.

Krawczak M, Cooper D. (1997). The human gene mutation database. Trends Genet. **13**:121-122.

Kubisch C, Schmidt-Rose T, Fontaine B, Bretag A, Jentsch T. (1998). CLC-1 chloride channel mutations in myotonia congenita: variable penetrance of mutations shifting the voltage dependence. Hum Mol Genet. **7**:1753-1760.

Kubisch C, Schroeder BC, Friedrich T, Lutjohann B, El-Amraoui A, Marlin S, Petit C, Jentsch TJ. (1999). KCNQ4, a novel potassium channel expressed in sensory outer hair cells, is mutated in dominant deafness. Cell. **96**:437-446.

Lai L-P, Deng C-L, Moss AJ, Kass RS, Liang C-S. (1994). Polymorphism of the gene encoding a human minimal potassium ion channel (minK). Gene. **151**:339-340.

Lalwani A, Brister R, Fex J, Grundfast K, Pikus AT, Ploplis B, San Agustin T, Skarka H, Wilcox ER. (1994). A new non-syndromic X-linked sensorineural hearing impairment linked to Xp21.2. Am J Hum Genet. **55**:685-694.

Lalwani A, Luxford W, Mhatre A, Attaie A, Wilcox E, Castelein C. (1999). A new locus for nonsyndromic hereditary hearing impairment, DFNA17, maps to chromosome 22 and represents a gene for cochleosaccular degeneration. Am J Hum Genet. **64**:318-322.

Lander E, Botstein D. (1987). Homozygosity mapping: A way to map human recessive traits with the DNA of inbred children. Science. **236**:1567-70.

Larsen LA, Kanters J, Andersson P, Vuust J, Christiansen M. (1997). A method of detection of point mutations in the potassium encoding genes (KVLQT1 and HERG) associated with long QT syndrome and Jervell and Lange-Nielsen syndrome. Am J Hum Genet. **61**:1290 (Abst).

Lautermann J, tenCate W, Altenhoff P, Grummer R, Traub O, Frank H, Jahnke K, Winterhager E. (1998). Expression of the gap junction connexins 26 and 30 in the rat cochlea. Cell Tiss Res. **294**:415-420.

Lee MP, Hu R-J, Johnson LA, Feinberg AP. (1997). Human KVLQT1 gene shows tissue-specific imprinting and encompasses Beckwith-Wiedeman syndrome chromosomal rearrangements. Nat Genet. **15**:181-185.

Lench N, Houseman M, Newton V, Van Camp G, Mueller R. (1998). Connexin-26 mutations in sporadic non-syndromal sensorineural deafness. Lancet. **351**:415.

Leon PE, Raventos H, Lynch E, Morrow J, King MC. (1992). The gene for an inherited form of deafness maps to chromosome 5q31. Proc Natl Acad Sci USA. **89**:5181-4.

Lesperance M, Hall J, Bess F, Fukushima K, Jain P, Ploplis B, San Agustin T, Skarka H, Smith RJH, Wills M, Wilcox ER. (1995). A gene for autosomal dominant nonsyndromic hereditary hearing impairment maps to 4p16.3. Hum Mol Genet. **4**:1967-1972.

Li M, Squire J, Weksberg R. (1997). Molecular genetics of Beckwith-Wiedemann syndrome. Curr Op Pediatrics. **9**:623-629.

Li H, Chen Q, Moss A, Robinson J, Goytia V, Perry J, Vincent G, Priori S, Lehmann M, Denfield S, Duff D, Kaine S, Shimizu W, Schwartz P *et*

al. (1998). New mutations in the KVLQT1 Potassium channel that cause Long-QT Syndrome. Circulation. **97**:1264-1269.

Li X, Everett L, Lalwani A, Desmukh D, Friedman T, Green E, Wilcox ER. (1998). A mutation in PDS causes non-syndromic recessive deafness. Nat Genet. **18**:215-217.

Liang Y, Wang A, Probst F, Arhya N, Barber T, Chen K-S, Deshmukh D, Dolan D, Hinnant J, Carter L, Jain P, Lalwani A, Li A, Lupski Jet al. (1998). Genetic mapping refines DFNB3 to 17p11.2, suggests multiple alleles of DFNB3, and supports homology to the mouse model shaker-2. Am J Hum Genet. **62**:904-915.

Liu X-Z, Walsh J, Mburu P, Kendrick-Jones J, Cope M, Steel KP, Brown SDM. (1997a). Mutations in the myosin VIIA gene cause non-syndromic recessive deafness. Nat Genet. **16**:188-190.

Liu X-Z, Walsh J, Tamagawa Y, Kitamura K, Nishizawa M, Steel KP, Brown SDM. (1997b). Autosomal dominant non-syndromic deafness (DFNA11) caused by mutation in the myosin VIIA gene. Nat Genet. **17**:268-269.

Liu XZ, Hope C, Walsh J, Newton V, Ke X, Liang C, Xu L, Zhou J, Trump D, Steel KP, Bundey S, Brown SDM. (1998). Mutations in the Myosin VIIA gene cause a wide phenotypic spectrum, including atypical Usher syndrome. Am J Hum Genet. **63**:909-912.

Lynch ED, Lee MK, Morrow JE, Welsch PL, Leon P, King M-C. (1997). Nonsyndromic deafness DFNA1 associated with mutation of a human homologue of the Drosophila gene Diaphanous. Science. **278**:1315-1318.

Manolis E, Yandavi N, Nadol J, Eavcy R, McKenna M, Rosenbaum S, Khetarpal U, Halpin C, Merchant S, Duyck G, MacRae C, Seidman C, Seidman J. (1996). A gene for non-syndromic autosommmal dominant progressive postlingual sensorineural deafness maps to chromosome 14q12-13. Hum Mol Genet. **5**:1047-1050.

Maquat LE. (1996). Defects in RNA Splicing and the consequence of shortened translational reading frames. Am J Hum Genet. **59**:279-286.

Maw MA, Allen Powell DR, Goodey RJ, Stewart IA, Nancarrow DJ, Hayward NK, Gardner RJ. (1995). The contribution of the DFNB1 locus to neurosensory deafness in a Caucasian population. Am J Hum Genet. **57**:629-35.

McDonald T, Yu Z, Ming Z, Palma E, Meyers M, Wang K-W, Goldstein S, Fishman G. (1997). A minK-HERG complex regulates the cardiac potassium current I_{Kr}. Nature. **388**:289-292.

Mohr J, Mageroy K. (1960). Sex-linked deafness of a possibly new type. Acta Genet Stat Med (Basel). **10**:54-62.

Moore KL. (1988) The Developing Human-Clinically orientated Embryology. WB Saunders Co.

Morell R, Kim H, Hood L, Goforth L, Fridercic K, Fisher R, Van Camp G, Berlin C, Oddoux C, Ostrer H, Keats B, Friedman T. (1998). Mutations in the connexin 26 gene (GJB2) among Ashkenazi jews with nonsyndromic recessive deafness. New Engl J Med. **339**:1500-1505.

Morton NE. (1991). Genetic Epidemiology of Hearing Impairment. Ann. N.Y. Acad. Sci. **630**:16-31.

Muelenbelt I, Droog S, Trommelen GJM, Boomsa DI, Slagboom EP. (1995). High-yield non-invasive human genomic DNA isolation method for genetic studies in geographically dispersed families and populations. Am J Hum Genet. **57**:1254-1255.

Murai T, Kakizuka A, Takumi T, Ohkubo H, Nakanishi S. (1989). Molecular cloning and sequence analysis of human genomic DNA encoding a novel membrane protein which exhibits a slowly activating potassium channel activity. Biochem. Biophys. Res. Comm. **161**:176-181.

Mustapha M, Chardenous S, Nieder A, Salem N, Weissenbach J, el-Zir E, Petit C. (1998). A sensorineural progressive autosomal recessive form of isolated deafness, DFNB13, maps to chromosome 7q34-q36. Eur J Hum Genet. **6**:245-250.

Mustapha M, Weil D, Chardenoux S, Elias S, El-Zir E, Beckmann J, Loiselet J, Petit C. (1999). An alpha-tectorin gene defect causes a newly identified autosomal recessive form of sensorineural pre-lingual non-syndromic deafness, DFNB21. Hum Mol Genet. **8**:409-412.

Nadol J. (1993). Hearing loss. New Engl J Med. **329**:1092-1102.

Nelson D, Ballabio F, Cremers F, Monaco A, Schlessinger D. (1995). Report of the sixth international workshop on X chromosome mapping 1995. Cytogenetics and Cell Genetics. **71**:308-336.

Neyroud N, Tesson F, Denjoy I, Leibovici M, Donger C, Barhanin J, Faure S, Gary F, Coumel P, Petit C, Schartz K, Guicheney P. (1997). A novel mutation in the potassium channel gene KVLQT1 causes the Jervell and Lange-Nielsen cardioauditory syndrome. Nat Genet. **15**:186-189.

Neyroud N, Denjoy I, Donger C, Gary F, Villain E, Leenhardt A, Benali K, Schwartz K, Coumel P, Guicheney P. (1998). Heterozygous mutation in

the pore of potassium channel gene KVLQT1 causes an apparently normal phenotype in long QT syndrome. Eur J Hum Genet. **6**:129-133.

O'Neill M, Mariette J, Nishimura D, Wayne S, Van Camp G, Van Laer L, Negrini C, Wilcox E, Chen A, Fukushima K, Sheffield V, Smith RJH. (1996). A gene for autosomal dominant late-onset progressive non-syndromic hearing loss maps to chromosome 6-DFNA10. Hum Mol Genet. **5**:853-856.

O'Rahilly R, Muller F. (1996)Human Embryology and Teratology. 2nd Edition. Wiley-Liss

Petit C. (1996). Genes responsible for human hereditary deafness: symphony of a thousand. Nat Genet. **14**:385-391.

Pfister M, Apaydin F, Turan O, Bereketoglu M, Bylgen V, Braendle U, Zenner H, Lalwani A. (1998). A second family with nonsyndromic sensorineural hearing loss linked to Xp21.2: Refinement of the DFN4 locus within DMD. Genomics. **53**:377-382.

Phelps PD, Reardon W, Pembrey ME, Bellman S, Luxon L. (1991). X-linked deafness, stapes gushers and a distinct defect of the inner ear. Neuroradiology. **33**:326-330.

Phippard D, Heydemann A, lechner M, Lu L, Lee D, Kyin T, Crenshaw III E. (1998). Changes in the subcellular localisation of the *Brn4* gene product precede mesenchymal remodeling of the otic capsule. Hearing Res. **120**:77-85.

Pollack M, Chou Y-H, Cerda J, Steinmann B, La Du B, Seidman J, Seidman C. (1993). Homozygosity mapping of the gene for alkaptonuria to chromosome 3q2. Nat Genet. **5**:201-204.

Prezant TR, Agapian JV, Bohlman MC, Bu X, Oztas S, Qiu W-Q, Arnos KS, Cortopassi GA, Jaber L, Rotter JI, Shohat M, Fischel-Ghodsian N. (1993). Mitochondrial ribosomal RNA mutation associated with both antibiotic-induced and non-syndromic deafness. Nat Genet. **4**:289-293.

Priori S, Schwartz PJ, Napolitano C, Bianchi L, Dennis A, De Fusco M, Brown AM, Casari G. (1998). A recessive variant of the Romano-Ward Long-QT syndrome? Circulation. **97**:2420-2425.

Priori S, Napolitano C, Schwartz P. (1999). Low penetrance in the Long QT syndrome. Circulation. **99**:529-533.

Probst FJ, Fridell RA, Raphael Y, Saunders TL, Wang A, Liang Y, Morell RJ, Touchman JW, Lyons RH, Noben-Trauth K, Friedman TB, Camper SA. (1998). Correction of deafness in shaker-2 mice by an unconventional myosin in a BAC transgene. Science. **280**:1444-1451.

Quaderi N, Schweiger S, Gaudenz K, Franco B, Rugarli E, Berger W, Feldman G, Volta M, ndolfi G, Gilgenkrantz S, Marion R, Hennekam R, Opitz J, Muenke M *et al.* (1997). Opitz G/BBB syndrome, a defect of midline development, is due to mutations in a new RING finger gene on Xp22. Nat Genet. **17**:285-291.

Rabionet R, Melchionda S, D'Agruma L, Zelante L, Gasparini P, Estivill X. (1998). Mutations in the connexin 26 gene (GJB2) in Italian and Spanish patients with congenital deafness. Am J Hum Genet. **63**:Abs 2211.

Reardon W, Middleton-Price H, Sandkuijl L, Phelps P, Bellman S, Luxon L, Pembrey M, Malcolm S. (1991). A multipedigree linkage study of X-linked deafness; linkage to Xq13-21 and evidence for genetic heterogeneity. Genomics. **11**:885-894.

Reardon W. (1992). Genetic Deafness. J Med Genet. **29**:521-526.

Reid F, Vernham G, Jacobs H. (1994). A novel mitochondrial point mutation in a maternal pedigree with sensorineural deafness. Hum Mutat. **3**:243-247.

Reid L, Davies C, Cooper P, Crider-Miller S, Sait S, Nowak N, Evans G, Stanbridge E, deJong P, Shows T, Weissman B, Higgins M. (1997). A 1-Mb physical map and PAC contig of the imprinted domain in 11p15.5 that contains TAPA1 and the BWSCR1/WT2 region. Genomics. **43**:366-375.

Richard G, Smith L, Bailey R, Itin P, Hohl D, Epstein Jr E, DiGiovanna J, Compton J, Bale S. (1998). Mutations in the human connexin gene GJB3 cause erythrokeratodermia variabilis. Nat Genet. **20**:366-369.

Robertson N, Khetarpal U, Gutierrez-Espeleta G, Bieber F, Morton CC. (1994). Isolation of novel and known genes from a human fetal cochlear cDNA library using subtractive hybridization and differential screening. Genomics. **23**:42-50.

Robertson N, Skvorak A, Yin Y, Weremowicz S, Johnson K, Kovatch K, Battey J, Bieber F, Morton C. (1997). Mapping and characterisation of a novel cochlear gene in human and in mouse: A positional candidate gene for a deafness disorder, DFNA9. Genomics. **46**:345-354.

Robertson N, Lu L, Heller S, Merchant S, Eavey R, McKenna M, Nadol Jr J, Miyamoto R, Linthicum Jr F, Neto J, Hudspeth A, Seidman C, Morton C, Seidman J. (1998). Mutations in a novel cochlear gene cause DFNA9, a human nonsyndromic deafness with vestibular dysfunction. Nat Genet. **20**:299-303.

Robson KJ, Chandra T, MacGillivray RT, Woo SI. Polysome immunoprecipitation of phenylalanine hydroxylase mRNA from rat liver and cloning of its cDNA. Proc Natl Acad Sci USA. **79**:4701-4705.

Romey G, Attali B, Chouabe C, Abitbol I, Guillemare E, Barhanin J, Lazdunski M. (1997). Molecular Mechanism and functional significance of the MinK control of the KvLQT1 channel activity. J Biol Chem. **272**:16713-16716.

Rose SP, Conneally PM, Nance WE (1977) Genetic Analysis of Childhood Deafness. In: Bess FH (ed) Childhood Deafness. Grune and Stratton, New York, pp 19-36

Rose C, Patel P, Reardon W, Malcolm S, Winter R. (1997). The *TWIST* gene, although not disrupted in Saethre-Chotzen patients with apparently balanced translocations of 7p21, is mutated in familial and sporadic cases. Hum Mol Genet. **6**:1369-1373.

Roy N, Kahlem P, Dausse E, Bennaceur M, Faure S, Weissenbach J, Komajda M, Denjoy I, Coumel P, Schwartz K, Guicheney P. (1994). Exclusion of HRAS from long QT locus. Nat Genet. **8**:113-114.

Russell M, Dick II M, Collins F, Brody L. (1996). KVLQT1 mutations in three families with familial or sporadic long QT syndrome. Hum Mol Genet. **5**:1319-1324.

Saarinen K, Swan H, Kainulainen K, Toivonen L, Viitasalo M, Kontula K. (1998). Molecular Genetics of the long QT Syndrome, Two novel mutations of the KVLQT1 gene and phenotypic expression of the mutant gene in a large kindred. Hum Mutat. **11**:158-165.

Sakagami M, Fukazawa K, Matsunaga T, Fujita H, Mori N, Takumi T, Ohkubo H, Nakaniski S. (1991). Cellular-localisation of Rat *IsK* protein in the Stria Vascularis by Immunohistochemical observation. Hearing Res. **56**:168-172.

Sala C, Arrigo G, Torri G, Martinazzi F, Riva P, Larizza L, Phillipe C, Jonveaux P, Sloan F, Labella T, Toniolo D. (1997). Eleven X chromosome breakpoints associated with premature ovarian failure (POF) map to a 15-Mb YAC contig spanning Xq21. Genomics. **40**:123-131.

Sanguinetti M, Jiang C, Curran M, Keating M. (1995). A mechanistic link between an inherited and an acquired cardiac arrythmia: *HERG* encodes the IKr potassium channel. Cell. **80**:805-811.

Sanguinetti M, Curran M, Zou A, Shen J, Spector P, Atkinson D, Keating M. (1996a). Coassembly of KVLQT1 and minK (ISK) proteins to form cardiac IKs potassium channel. Nature. **384**:80-83.

Sanguinetti M, Curran M, Spector P, Keating M. (1996b). Spectrum of HERG K^+- channel dysfunction in an inherited cardiac arrhythmia. Proc. Natl. Acad. Sci. USA. **93**:2208-2212.

Schott J-J, Charpentier F, Peltier S, Foley P, Drouin E, Bouhour J-B, Donnelly P, Vergnaud G, Bachner L, Moisan J-P, Le Marec H, Pascal O. (1995). Mapping of a gene for long QT syndrome to chromosome 4q25-27. Am J Hum Genet. **57**:1114-1122.

Schulze-Bahr E, Wang Q, Wedekind H, Haverkamp W, Chen Q, Sun Y, Rubie C, Hordt M, Towbin J, Borggrefe M, Assmann G, Qu X, Somberg J, Breithardt G *et al.* (1997). KCNE1 mutations cause Jervell and Lange-Nielsen syndrome. Nat Genet. **17**:267-268.

Schwartz P, Moss A, Vincent G, Keating M. (1993). Diagnostic criteria for the long QT syndrome. An update. Circulation. **88**:782-784.

Schwartz K. (1994). On the pulse of genetic cardiology. Nat Genet. **8**:110-111.

Schwartz P, Stramba-Badiale M, Segantini A, Austoni P, Bosi G, Giorgetti R, Grancini F, Marni E, Perticone F, Rosti D, Salice P. (1998). Prolongation of the QT interval and the Sudden Infant Death Syndrome. New Engl J Med. **338**:1709-1714.

Scott D, Carmi R, Elbedour K, Yosefsberg S, Stone E, Sheffield V. (1996). An autosomal recessive nonsyndromic hearing loss locus identified by DNA pooling using two inbred Bedouin kindreds. Am J Hum Genet. **59**:385-391.

Scott D, Wang R, Kerman T, Sheffield V, Karniski L (1998a) The pendred syndrome gene product functions as an iodine chloride transporter Molecular Biology of Hearing and Deafness, Bethesda, MD. USA, pp 63

Scott D, Kraft M, Stone E, Sheffield V, Smith RJH. (1998b). Connexin mutations and hearing loss. Nature. **391**:32.

Sevior K, Hatamochi A, Stewart I, Bykhovskaya Y, Allen-Poweel D, Fischel-Ghodsian N, Maw MA. (1998). Mitochondrial A7445G mutation in two pedigrees with palmoplantar keratoderma and deafness. Am J Med Genet. **75**:179-185.

Shalaby F, Levesque P, Yang W-P, Little W, Conder M, Jenkins-West T, Blanar M. (1997). Dominant-negative KVLQT1 mutations underlie the LQT1 form of Long QT syndrome. Circulation. **96**:1733-1736.

Shapiro M, Senapathy P. (1987). RNA splice junctions of different classes of eukaryotes: sequence statistics and functional implications in gene expression. Nucl Acids Res. **15**:7155-7174.

Sheffield V, Nishimura D, Stone E. (1995). Novel approaches to linkage mapping. Curr Op Genet Develop. **5**:335-341.

Sheffield VC, Kraiem Z, Beck JC, Nishimura D, Stone EM, Salameh M, Sadeh O, Glaser M. (1996). Pendred syndrome maps to chromosome 7q21-34 and is caused by an intrinsic defect in thyroid iodine organification. Nat Genet. **12**:424-6.

Shimizu N, Antonarakis S, Van Broeckhoven C, Patterson D, Gardiner K, Nizetic D, Creau N, Delabar J-M, Korenberg J, Reeves R, Doering J, Chakravati A, Minoshima S, Ritter O *et al.* (1995). Report of the fifth international workshop on human chromosome 21 mapping 1994. Cytogenet Cell genet. **70**:148-165.

Skvorak A, Weng Z, Yee A, Robertson N, Morton CC. (1999). Human cochlear expressed sequence tags provide insight into cochlear gene expression and identify candidate genes for deafness. Hum Mol Genet. **8**:439-452.

Splawski I, Tristani-Firouzi M, Lehmann M, Sanguinetti M, Keating M. (1997a). Mutations in the hminK gene cause long QT syndrome and suppress IKs function. Nat. Genet. **17**:338-340.

Splawski I, Timothy K, Vincent G, Atkinson D, Keating M. (1997b). Molecular basis of the long QT syndrome associated with deafness. New Engl J Med. **336**:1562-1567.

Steel KP, Bock GR. (1983). Hereditary inner ear abnormalities in animals. Arch. Otolaryngol. **109**:22-29.

Steel KP. (1991). Similarities between mice and humans with hereditary deafness. Ann N Y Acad Sci. **630**:68-79.

Steel KP, Brown SDM. (1994). Genes and deafness. Trends Genet. **10**:428-435.

Steel KP. (1995). Inherited hearing defects in mice. Ann Rev Genet. **29**:675-701.

Steel KP, Brown SDM. (1996). Genetics of Deafness. Curr Op Neurobiol. **6**:520-525.

Steel KP, Palmer A (1996) Basic mechansims of hearing and hearing impairment. In: Martini A, Read A, Stephens D (Eds) Genetics of Hearing Impairment. Whurr Publishers. pp3-17.

Strautnieks SS, Thompson RJ, Hanukoglu A, Dillon MJ, Hanukoglu I, Kuhnle U, Seckl J, M GR, Chung E. (1996). Localisation of pseudohypoaldosteronism genes to chromosome 16p12.2-13.11 and 12p13.1-pter by homozygosity mapping. Hum Mol Genet. **5**:293-299.

Stryer L (1988) Biochemistry. W.H. Freeman and Co., New York, pp 43-70

Tai K-K, Goldstein S. (1998). The conduction pore of a cardiac potassium channel. Nature. **391**:605-608.

Takumi T, Ohkubo H, Nakanishi S. (1988). Cloning of a membrane-protein that induces a slow voltage-gated potassium current. Science. **242**:1042-1045.

Takumi T, Moriyoshi K, Aramori I, Ishii T, Oiki S, Okada Y, Ohkubo H, Nakanishi S. (1991). Alteration of potassium channel activities and gating by mutations of slow ISK potassium channel. J Biol Chem. **266**:22192-22198.

Tamagawa Y, Kitamura K, Ishida T, Ishikawa K, Tanaka H, Tsuji S, Nishizawa M. (1996). A gene for a dominant form of non-syndromic sensorineural deafness (DFNA11) maps within the region containing the DFNB2 recessive deafness gene. Hum Mol Genet. **5**:849-852.

Tesson F, Donger C, Denjoy I, Berthet M, Bennaceur M, Petit C, Coumel P, Schwartz K, Guicheney P. (1996). Exclusion of KCNE1 (IsK) as a candidate gene for Jervell and Lange-Nielsen syndrome. J Mol Cell Cardiol. **28**:2051-2055.

Tranebjaerg L, Schwartz C, Eriksen H, Andreasson S, Ponjavic V, Dahl A, Stevenson RE, May M, Arena F, Barker D, Elverland HH, Lubs H. (1995). A new X linked recessive deafness syndrome with blindness, dystonia, fractures, and mental deficiency is linked to Xq22. J Med Genet. **32**:257-263.

Vahava O, Morell R, Lynch E, Weiss S, Kagan M, Ahituv N, Morrow J, Lee M, Skvorak A, Morton C, Blumenfield A, Frydman M, Friedman T, King M-C *et al.* (1998). Mutations in transcription factor *POU4F3* associated with inherited progressive hearing loss in humans. Science. **279**:1950-1954.

Van Camp G, Coucke P, Balemans W, Van Velzen D, Van der Bilt C, Smith RJH, Fukushima K, Padberg G, Frants R, Van de Heyning O, Smith S, Huizing E, Willems PJ. (1995). Localisation of a locus for non-syndromic hearing loss (DFNA5) to chromosome 7p. Hum Mol Genet. **4**:2159-2163.

Van Camp G, Kunst H, Flothmann K, Wauters J, Bossuyt P, Verstreken M, Zlotogora J, Riess O, Marres H, Cremers C, Willems P (1997a) Linkage of a second family to the DFNA6 deafness locus on chromosome 4p16.3 and identification of a deaf patient with a chromosomal inversion through this region American Society of Human Genetics, USA, pp 1741

Van Camp G, Coucke PJ, Kunst H, Schatteman I, Van Velzen D, Marres H, van Ewijk M, Declau F, Van Hauwe P, Meyers J, Kenyon J, Smith SD, Smith RJ, Djelantik B, Cremers CW, Van de heyning PH, Willems PJ. (1997b). Linkage analysis of progressive hearing loss in five extended families maps the DFNA2 gene to a 1.25-Mb region on chromosome 1p. Genomics. 41:70-74.

Van Camp G, Smith RJH. (as of March 1999). Hereditary Hearing Loss Home Page. World Wide Web URL. **http:/dnalab-www.uia.ac.be/dnalab/hhh.html**

Van Hauwe P, Coucke PJ, Declau F, Kunst H, Ensink RJ, Marres HA, Cremers CWRJ, Djelantik B, Smith SD, Kelley P, Van de Heyning PH, Van Camp G. (1999). Deafness linked to DFNA2: one locus but how many genes? Nat Genet. **21**:263.

Van Lear L, Huizing E, Verstreken M, van Zuijlen D, Wauters J, Bossuyt P, Van de Heyning P, McGuirt W, Smith RJH, Willems PJ, Legan PK, Richardson GP, Van Camp G. (1998). Nonsyndromic hearing impairment is associated with a mutation in *DFNA5*. Nat Genet. **20**:194-197.

Verhoeven K, Van Camp G, Govaerts P, Balemans W, Schatteman I, Verstreken M, Van Laer L, Smith RJH, Brown M, van de Heyning P, Somers T, Offeciers F, Willems PJ. (1997). A gene for autosomal dominant non-syndromic hearing loss (DFNA12) maps to chromosome 11q22-24. Am J Hum Genet. **60**:1168-1174.

Verhoeven K, Van laer L, Kirschhofer K, Legan PK, Hughes D, Schatteman I, Verstreken M, Van Hauwe P, Coucke P, Chen A, Smith RJH, Somers T, Offeciers F, Van de Heyning P *et al.* (1998). Mutations in the alpha tectorin gene cause autosomal dominant non-syndromic hearing impairment. Nat Genet. **19**:60-62.

Veske A, Oehlmann R, Younus F, Mohyuddin A, Muller-Myhsok B, Qasim Mehdi S, Gal A. (1996). Autosomal recessive non-syndromic deafness locus (DFNB8) maps on chromosome 21q22 in a large consanguineous kindred from Pakistan. Hum Mol Genet. **5**:165-168.

Vetter DE, Mann JR, Wangemann P, Liu J, McLaughlin KJ, Lesage F, Marcus DC, Lazdunski M, Heinemann SF, Barhanin J. (1996). Inner ear defects induced by null mutation of the *isk* gene. Neuron. **17**:1251-1264.

Vincent GM, Timothy KW, Timothy BS, Leppert M, Keating, MT. (1992). The spectrum of symptoms and QT intervals in carriers of the gene for the Long QT syndrome. New Engl. J. Med. **327**:846-852.

Viskochil D, Cawthon R, O'Connell P, Xu G, Stevens J, Culver M, Carey J, White R. (1991). The gene encoding the oligodendrocyte-myelin glycoprotein is embedded within the neurofibromatosis type 1 gene. Mol Cell Biol. **11**:906-912.

Wallace M, Marchuk D, Andersen L, Letcher R, Odeh H, Saulino A, Fountain J, Brereton A, Nicholson J, Mitchell A, Brownstein B, Collins F. (1990). Type 1 Neurofibromatosis gene: identification of a large transcript disrupted in three NF1 patients. Science. **249**:181-186.

Wallis C, Ballo R, Wallis G, Beighton P, Goldblatt J. (1988). X-linked mixed deafness with stapes fixation in a Mauritian kindred: linkage to Xq probe pDP34. Genomics. **3**:299-308.

Wang Q, Shen J, Splawski I, Atkinson D, LI Z, Robinson JL, Moss AJ, Towbin JA, Keating MT. (1995). SCN5A mutations associated with an inherited cardiac arrhythmia, long QT syndrome. Cell. **80**:805-811.

Wang Q, Curran ME, Splawski I, Burn TC, Millholland JM, VanRaay TJ, Shen J, Timothy KW, Vincent GM, de Jager T, Schwartz PJ, Towbin JA, Moss AJ, Atkinson DL *et al.* (1996). Positional cloning of a novel potassium channel gene: KVLQT1 mutations cause cardiac arrhythmias. Nat Genet. **12**:17-23.

Wang K-W, Tai K-K, Goldstein S. (1996). MinK residues line a potassium channel pore. Neuron. **16**:571-577.

Wang Q, Bowles N, Towbin J. (1998). The molecular basis of long QT syndrome and prospects for therapy. Molec. Med. Today. pp 382-388.

Wang A, Liang Y, Fridell R, Probst F, Wilcox E, Touchman J, Morton C, Morell R, Noben-Trauth K, Camper S, Friedman T. (1998). Association of unconventional myosin MYO15 mutations with human nonsyndromic deafness DFNB3. Science. **280**:1447-1451.

Wangemann P, Liu J, Marcus D. (1995). Ion transport mechanisms responsible for K^+ secretion and the transepithelial voltage across marginal cells of stria vascularis *in vitro*. Hearing Res. **84**:19-29.

Ward O. (1964). A new familial cardiac syndrome in children. J Irish Med Assoc. **54**:103-106.

Wegner M, Drolet D, Rosenfeld M. (1993). POU-domain proteins: structure and function of developmental regulators. Curr Opin Cell Biol. **5**:488-498.

Weil D, Blanchard S, Kaplan J, Guilford P, Gibson F, Walsh J. (1995). Defective myosin VIIA gene responsible for Usher syndrome. Nature. **374**:60-61.

Weil D, Kussel P, Blanchard S, Levy G, Levi-Acobas F, Drira M, Ayadi H, Petit C. (1997). The autosomal recessive isolated deafness, DFNB2, and

the Usher 1B syndrome are allelic defects of the myosin-VIIA gene. Nat Genet. **16**:191-193.

White T, Deans M, Kelsell D, Paul D. (1998). Connexin mutations in deafness. Nature. **394**:630-631.

Winter R, Baraitser M (1998) Oxford Medical Database (Dysmorphology Database). Oxford University Press, Oxford

Wollnik B, Schroeder B, Kubisch C, Esperer H, Wieacker P, Jentsch T. (1997). Pathophysiological mechanisms of dominant and recessive KVLQT1 K^+ channel mutations found in inherited cardiac arrhythmias. Hum Mol Genet. **6**:1943-1949.

Xia J-H, Liu C-Y, Tang B-S, Pan Q, Huang L, Dai H-P, Zhang B-R, Xie W, Hu D-X, Zheng D, Shi X-L, wang D-A, Xia K, Yu K-P *et al.* (1998). Mutations in the gene encoding gap junction protein beta-3 associated with autosomal dominant hearing impairment. Nat Genet. **20**:370-373.

Xiang M, Zhou L, Peng Y-W, Eddy R, Shows T, Nathans J. (1993). *Brn-3b*: a POU domain gene expressed in a subset of retinal ganglion cells. Neuron. **11**:689-701.

Yang W-P, Levesque P, Little W, Conder M, Shalaby F, Blanar M. (1997). KvLQT1, a voltage-gated potassium channel responsible for human cardiac arrhythmias. Proc. Natl. Acad. Sci. USA. **94**:4017-4021.

Zelante L, Gasparini P, Estivill X, Melchionda S, D'Agruma L, Govea N, Mila M, Della-Monica M, Lufti J, Shohat M, Mansfield E, Delgrosso K, Rappaport E, Surrey S *et al.* (1997). Connexin26 mutations associated with the most common form of non-syndromic neurosensory autosomal recessive deafness (DFNB1) in Mediterraneans. Hum Mol Genet. **6**:1605-1609.

World wide web addresses:

GDB.
http://www.hgmp.mrc.ac.uk

Neural Network Splice prediction.
http://www-hgc.lbl.gov/projects/splice.html

Hereditary Hearing loss homepage.
http://dnalab-www.uia.ac.be/dnalab/hhh

Chromosome 11 sequencing at University of Texas Southwestern.
http://gestec.swmed.edu/sequence.htm

Morton fetal cochlear cDNA library.

http://www.bwh.partners.org/pathology

Human Gene Mutation Database.
http://www.uwcm.ac.uk/uwcm/mg/hgmd0.html

Human Molecular Genetics, 1996, Vol. 5, No. 12 2055–2060

Mapping of *DFN2* to Xq22

Jessica Tyson, Sue Bellman[1], Valerie Newton[2], Pat Simpson[3], Sue Malcoim, Marcus E. Pembrey and Maria Bitner-Glindzicz*

Units of Clinical and Molecular Genetics, Institute of Child Health, 30 Guilford Street, London, UK, [1]Department of Audiological Medicine, Great Ormond Street Hospital NHS Trust, London, UK, [2]CAEDSP, University of Manchester, Manchester, UK and [3]Childrens Hearing Services, Park Centre, Hindley, Wigan, UK

Received July 1, 1996; Revised and Accepted September 16, 1996

Non-syndromic X-linked deafness is a rare form of genetic deafness accounting for a small proportion of all hereditary hearing loss. It is both clinically and genetically heterogeneous and five loci have been described to date but only two of these have been mapped. *DFN2* represents a locus for congenital profound sensorineural hearing loss that has yet to be mapped. We describe a four generation family with this phenotype in which female carriers have a mild/moderate hearing loss affecting the high frequencies. The mutant gene has been mapped to Xq22 using polymorphic microsatellite markers. A maximum two point lod score of 2.91 at $\theta = 0$ was observed with a fully informative dinucleotide repeat at *COL4A5*, and flanking recombinations were observed at *DXS990* and *DXS1001*.

INTRODUCTION

Deafness is one of the most common human sensory defects affecting ~1 in 1000 live births and is thought to be inherited in more than half of cases (1). Of these, ~70% are considered to be non-syndromic, that is, not associated with other clinically recognisable features outside the auditory system. X-linked deafness accounts for only a few percent of all non-syndromic deafness but nevertheless is genetically heterogeneous.

McKusick has categorised X-linked deafness into four types according to age of onset and audiogram (2) but recent genetic work has shown this classification to be oversimplified. Genetically, the locus *DFN1* has been assigned to the phenotype of progressive sensorineural hearing loss, MIM 304700 (3), but recent restudy of the same family has revealed the additional clinical features of blindness, dystonia, spasticity and fractures, which define this clinical entity as a new syndrome, Mohr–Tranebjærg Syndrome (4). This syndrome has been mapped to Xq22 (4). The symbol *DFN2* has been assigned to profound congenital sensorineural deafness (MIM 304500) and is unmapped. The locus *DFN3*, to which the majority of families with non-syndromic X-linked deafness map, was assigned to a gene causing progressive mixed deafness with perilymphatic gusher at stapes surgery (MIM 304400) and mapped to Xq13–q21 (5,6,7). It is now known that both mixed and pure sensorineural deafness may be caused by mutations in the same gene, *POU3F4*, at this locus (8,9) and that they share the same radiological phenotype (10). However, not all cases of mixed or sensorineural deafness which map to Xq13–q21 are accounted for by mutations in *POU3F4* and there may be another gene in this region, mutation in which results in deafness (11,12). *DFN4* has been mapped to Xp21.2 in a region containing the Duchenne muscular dystrophy locus and mutation at this locus results in congenital, profound sensorineural deafness in males and mild to moderate high frequency sensorineural hearing loss of adult onset in females (15).

We describe the re-evaluation of a four generation British–American family with congenital profound sensorineural hearing loss in males, similar to that ascribed to the unmapped locus *DFN2*. We present evidence of linkage of the mutant gene in this family to markers in Xq22 and describe a smaller family which does not show linkage to any of the loci described previously.

RESULTS

Family 1

This family was typed using markers from Xq13–q21, to exclude the *DFN3* locus. *DXS995* and *DXS1002* are known to flank the *POU3F4* gene at *DFN3* (13). *DXS995* lies within 5 cM of *DFN3* (14) and physical data has shown that it actually lies within 20 kb of the *POU3F4* gene (8). Recombinations between individuals IV_7 and V_4, and individuals III_8 and IV_{11}, with *DXS995* and recombination between III_8 and IV_{11} with *DXS1002* effectively excludes *DFN3* as the causative locus. Lod scores are detailed in Table 1.

Both families were typed for microsatellite markers which span the *DMD* gene in Xp21.1 in order to exclude linkage to *DFN4*. Typing revealed different haplotypes in affected males across the entire *DMD* locus, excluding *DFN4* as the causative locus in family 1.

Re-examination of previous linkage data prompted a search for linkage on the long arm of the X chromosome. Typing with commercially available primer pairs detecting microsatellite polymorphisms revealed a region of linkage at Xq22.

The two-point lod scores between the disease gene and marker loci, generated by LIPED, are shown in Table 1. A maximum two-point LOD score of 2.91 at zero recombination was observed with dinucleotide repeats at *COL4A5* and at *DXS1106*. Likely recombinations occurred between individuals III_8 and IV_{11} between the markers *DXS990* and *DXS1106*, and between individual IV_{11} and her sons V_8 and V_9 between *DXS1220* and *DXS1001*.

*To whom correspondence should be addressed

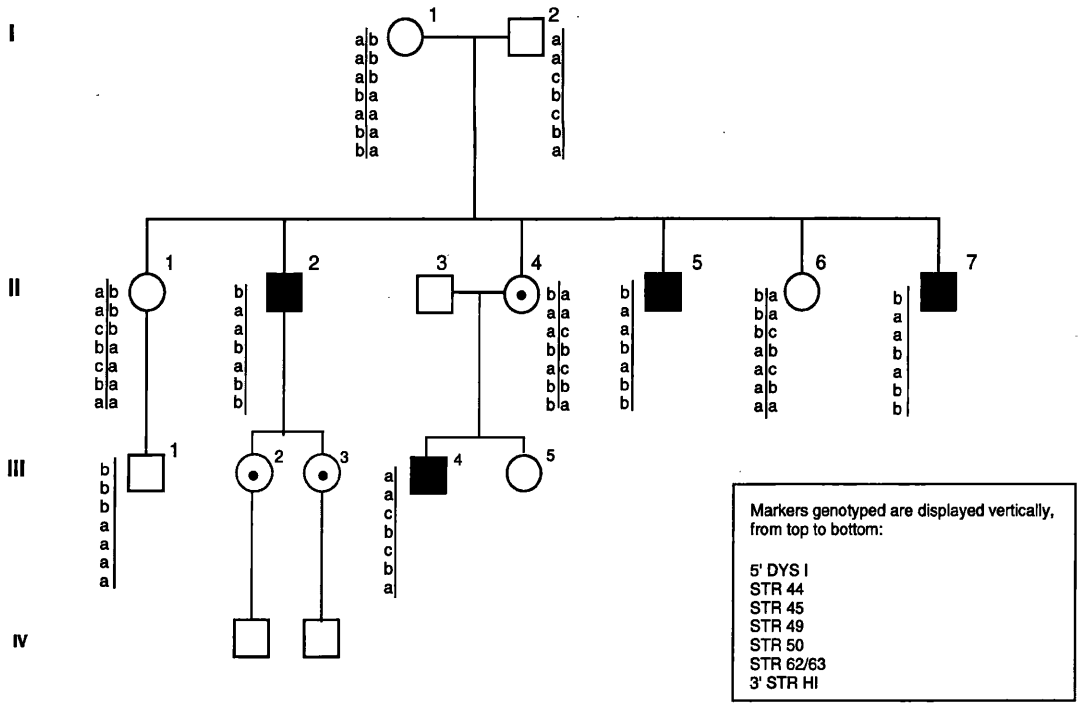

Figure 1. Family 2. Probable haplotypes across the *DFN4* locus at Xp21.1 assuming the least number of recombinations. *DFN4* is encompassed by the 5′ end of the *DMD* gene and a region between intron 50 (*STR50*) and the 3′ untranslated region (15).

Table 1. Pairwise LOD scores between the disease locus and Xq chromosome markers

Locus	LOD score at θ = 0	0.05	0.1	0.2	0.3	0.4	Z_{max}
DXS995	−99.99	−1.002	−0.509	−0.127	0.007	0.037	0.037
DXS1002	−99.99	0.057	0.293	0.429	0.390	0.243	0.429
DXS990	−99.99	0.057	0.293	0.429	0.390	0.243	0.429
DXS1106	2.913	2.671	2.42	1.894	1.327	0.706	2.913
PLP	1.408	1.297	1.182	0.934	0.661	0.353	1.408
DXS17	1.12	1.002	0.869	0.562	0.230	−0.016	1.12
DXS1230	0.505	0.461	0.416	0.322	0.222	0.116	0.505
COL4A5	2.913	2.671	2.42	1.894	1.327	0.706	2.913
DXS1210	1.408	1.297	1.182	0.934	0.661	0.353	1.408
DXS1220	1.138	1.046	0.951	0.749	0.527	0.280	1.138
DXS1001	−99.99	−0.148	0.284	0.504	0.412	0.166	0.504

Family 2

Analysis of this family with markers from Xq13–q21 showed multiple recombinations and excluded *POU3F4* (*DFN3*) as the disease gene, as indicated in Table 2. *DXS986* lies within 6 cM of *DFN3* (14) and so *DFN3* can be excluded as the disease gene if a lod score of −2 is taken as evidence against linkage (Haldane's mapping function).

The *DFN4* locus has previously been mapped between *DXS992*, a microsatellite marker which lies between intron 50 of the *DMD* gene and the 3′ untranslated region, and *DXS1068* which lies within 0.01 cM of the 5′ end of the gene (15). Family 2 was typed for the following microsatellite markers which span the *DMD* gene from the 5′ brain promoter to the 3′ untranslated region in Xp21.1 in order to exclude linkage to *DFN4*: 5′ *DYS I*, intron 44, intron 45, intron 49, intron 50, introns 62/63 and 3′ *STR-HI*. Typing revealed different haplotypes in affected males across the entire *DMD* locus, excluding *DFN4* as the causative locus in Family 2. The haplotypes are shown in Figure 1 and show that the affected males, II_2, II_5, II_7 and III_4 do not share a common haplotype in this region, effectively excluding linkage.

Subsequent to the observation of linkage of Family 1 to Xq22, Family 2 was typed for the marker at *COL4A5*. As shown in Figure 2, three of the affected males, II_5, II_7 and III_4, have different alleles, indicating that the COL4A5 gene is an unlikely candidate for this disorder in Family 2.

Figure 2. Microsatellite analysis of Family 2 with the dinucleotide repeat at *COL4A5*. The three affected males II_5, II_7 and III_4 have different alleles effectively excluding this as the disease gene. Individuals III_2, III_3, III_5, IV_1 and IV_2 were not typed for this marker since DNA was not available.

Table 2. Two point LOD scores between the disease gene and marker loci for Family 2

Locus	Lod score at θ =						
	0.0	0.001	0.05	0.1	0.2	0.3	0.4
COL4A5	–99.99	–4.673	–1.36	–0.843	–0.405	–0.200	–0.078
DXS986	–99.99	–7.371	–2.339	–1.505	–0.744	–0.365	–0.142
DXS1002	–99.99	–7.371	–2.339	–1.505	–0.744	–0.365	–0.142

DISCUSSION

Linkage of Family 1 to Xq22 provides a map location for *DFN2*. Several syndromic forms of deafness map to Xq22, including Alport syndrome, Mohr–Tranebjærg syndrome (MTS) and Pelizaeus–Merzbacher disease (PMD). At present it is not known whether our family represents an allelic form of one of these conditions although phenotypically this is very unlikely.

Normal ophthalmologic examination, normal urinalysis and lack of family history of renal disease, as well as the age of onset and pattern of hearing loss makes Alport syndrome unlikely. Nevertheless, screening of the *COL4A5* gene is being undertaken in Family 1 to exclude an unusual allelic variant; mutation in the *COL4A5* gene has been described in a family with characteristic renal disease but without hearing loss (16). The gene *COL4A6* which lies in a head to head configuration with *COL4A5*, remains a possible candidate, although deletions of the 5′ end of this gene and part of the neighbouring *COL4A5* gene are reported to cause diffuse leiomyomatosis (DL) and Alport's syndrome (17). However, no mutations in *COL4A6* alone have yet been described, so the phenotype associated with mutations in the gene is unknown. By itself, Family 2 is too small to establish or exclude linkage to a chromosomal region but recombinations with the intragenic marker in *COL4A5* exclude this as a candidate gene in this family.

The Mohr–Tranebjærg syndrome (MTS), which has been recently mapped to Xq22 (4), was originally described by Mohr in 1960 in a family with a non-syndromic form of progressive sensorineural deafness. However, recent re-evaluation has revealed additional clinical features which include progressive dystonia, spasticity, mental deterioration and visual symptoms leading to blindness. None of these features have been observed in Family 1, none having been present in the affected males of generation II or in individuals IV_1 and IV_{12} who are now in their thirties and forties. Furthermore, there is no evidence of progression of the deafness in this family. Whether or not MTS represents an allelic form of Pelizaeus–Merzbacher disease (PMD) is not yet known. This is a possibility since mutations in the proteolipid protein gene responsible for PMD have also been reported in families with complex X-linked spastic paraplegia (18).

It is therefore possible that the deafness in our Family 1 is caused by mutation in an unknown gene in Xq22. Expressed sequences in this region have been identified during work undertaken in the identification of the *btk* gene, mutations in which cause X-linked agammaglobulinaemia (19,20). Such ESTs will be considered as potential positional candidate genes during the course of future work.

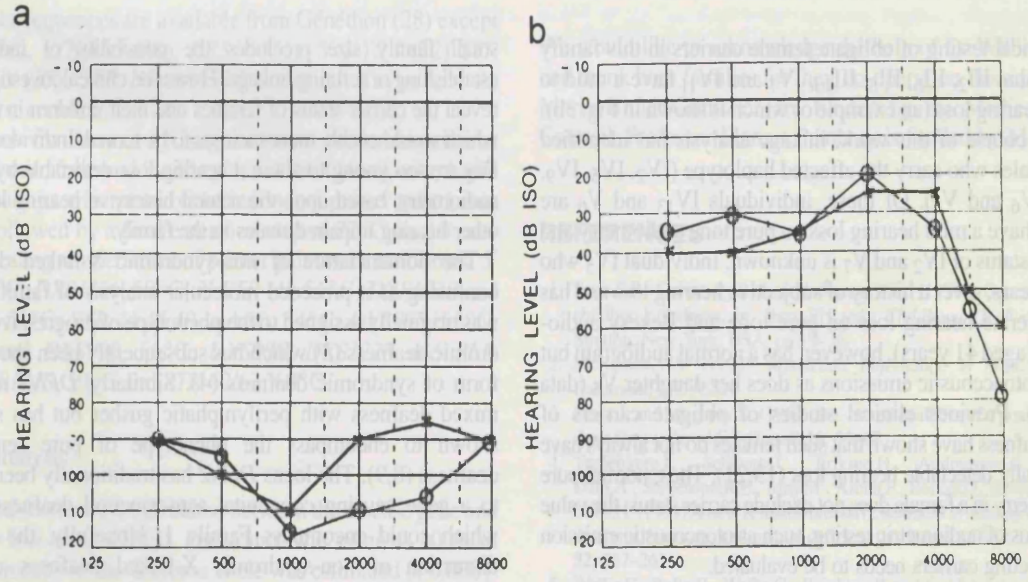

Figure 3. (**a**) Audiogram of affected male, Family 1, individual IV_1. (**b**) A typical audiogram of an obligate female carrier (IV_7) from Family 1.

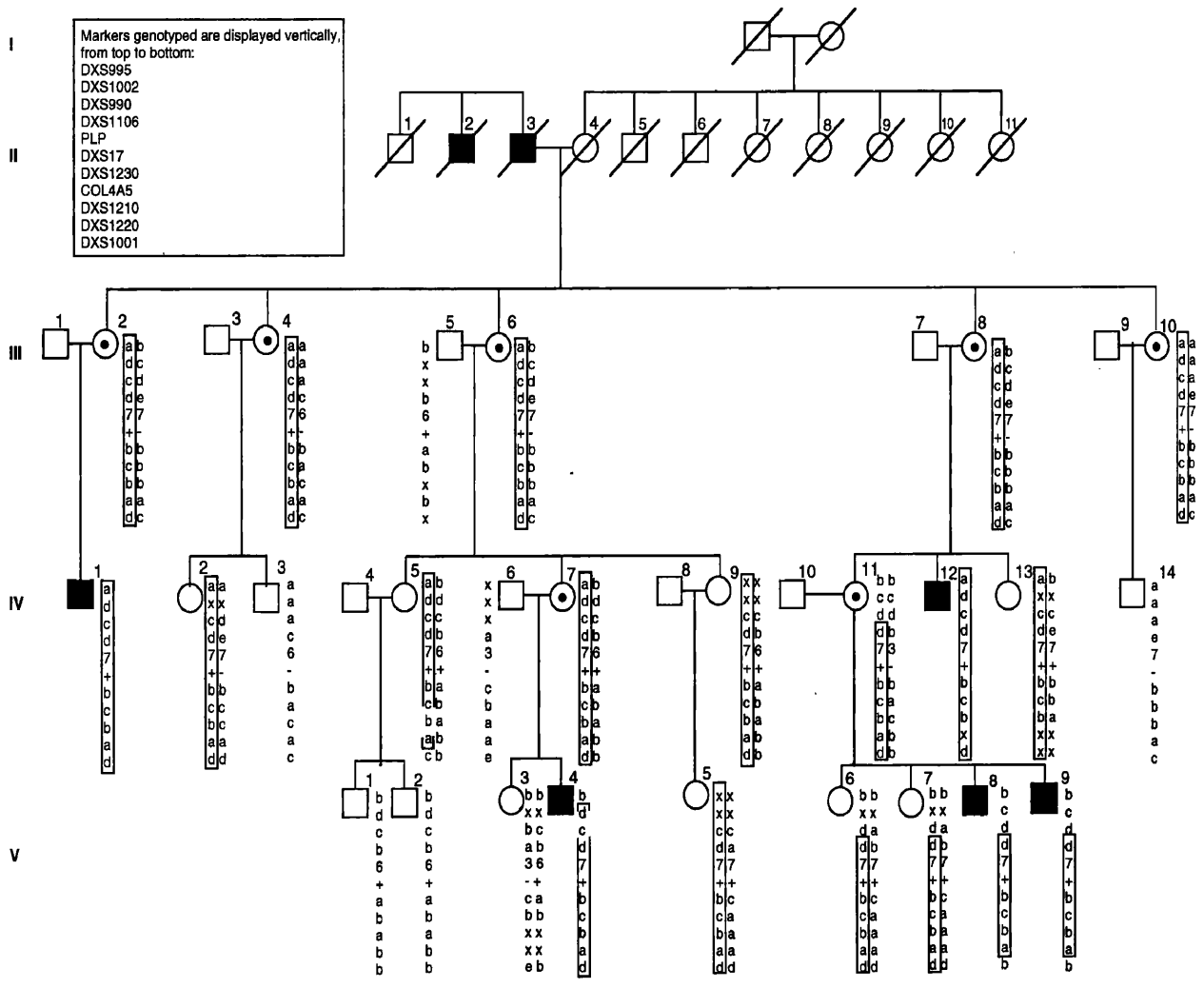

Figure 4. Family tree for Family 1, showing X-linked inheritance and probable haplotypes across Xq21–q24, assuming the least number of recombinations. Likely recombination has occurred between individuals III_8 and IV_{11} between the markers *DXS990* and *DXS1106*, and between individual IV_{11} and her sons V_8 and V_9 between *DXS1220* and *DXS1001*. An x symbol in the haplotype indicates that the individual was not typed for that marker.

Audiological testing of obligate female carriers in this family has shown that III_2, III_6, III_8, III_{10}, IV_7 and IV_{11} have a mild to moderate hearing loss (an example of which is shown in Fig. 3b). During the course of this work, linkage analysis has identified several females who carry the affected haplotype (IV_2, IV_5, IV_9, IV_{13}, V_5, V_6 and V_7). Of these, individuals IV_{13} and V_6 are reported to have a mild hearing loss on pure tone audiometry and the hearing status of IV_2 and V_7 is unknown. Individual IV_5 who is aged 37 years, gives a history of subjective hearing loss and has a mild/moderate hearing loss on pure tone and Bekesy audiometry; IV_9 (aged 41 years), however, has a normal audiogram but very small otoaccoustic emissions as does her daughter V_5 (data not shown). Previous clinical studies of obligate carriers of X-linked deafness have shown that such females do not always have audiometrically detectable hearing loss (13,21). Thus, normal pure tone audiometry in a female does not exclude carrier status; the value of other forms of audiometric testing, such as otoaccoustic emission data, in detecting carriers needs to be evaluated.

If new X-linked deafness genes are identified, Family 2 can be analysed for exclusion of a candidate gene. At the present time the small family size precludes the possibility of independently establishing or refuting linkage. However, clinical investigation may reveal the carrier status of females and their children in this family, which would enable more meioses to be scored. Individuals IV_1 and IV_2 are too young to show a hearing loss detectable by pure tone audiometry, based upon the natural history of hearing loss seen in other hearing impaired males in the family.

The nomenclature of non-syndromic X-linked deafness is confusing as it preceded molecular analysis of families. *DFN1* was originally assigned to the phenotype of progressive non-syndromic deafness (3) which has subsequently been shown to be a form of syndromic deafness (4). Similarly, *DFN3* represented mixed deafness with perilymphatic gusher but has since been shown to encompass the phenotype of pure sensorineural deafness (8,9). The locus *DFN2* has traditionally been allocated to a gene causing congenital sensorineural deafness (22–27), which could encompass Family 1. Hopefully, the molecular dissection of non-syndromic X-linked deafness will allow classification based upon genetic loci alone and elucidate a genotype–phenotype correlation.

MATERIALS AND METHODS

Family 1 (Fig. 4) has been described previously as family 7 (7). Re-evaluation of this family revealed that individual IV_{12} has congenital profound sensorineural hearing loss and also suffers from Down's Syndrome. In the past this individual was typed as unaffected because little was known about him. Individual II_4, previously shown to be affected with hearing loss but with no other family history, is shown as unaffected here since the sudden onset of her hearing loss was revealed to have dated from a severe head injury sustained in her teens. Affected males in this family suffer from a severe/profound pure sensorineural hearing loss which is prelingual in onset. The audiogram of an affected male (individual IV_1) is shown in Figure 3a. A CT scan of the petrous temporal bone in affected males showed no abnormality. All of the obligate female carriers have shown a mild/moderate hearing loss, more pronounced in the higher frequencies but none has complained of a subjective hearing loss. An example of this is shown in Figure 3b. There was no family history of renal disease and urinalysis was normal. Ophthalmic evaluation was also normal.

Family 2 has not been reported previously (Fig. 1). Affected males have a moderate to severe sensorineural hearing loss of childhood onset (age 3–9 years at diagnosis) and all have developed speech. Obligate female carriers have a mild hearing loss. CT scan of the petrous temporal bone of an affected male showed no abnormality.

PCR analysis

DNA was extracted from peripheral blood lymphocytes by standard techniques and was amplified in the polymerase chain reaction (PCR) by primers flanking dinucleotide repeat polymorphisms. Reaction mix consisted of 250 ng genomic DNA, 50 pmol of each primer, buffer consisting of 1.5 mM Tris pH 8.3, 1.5 mM KCl, 0.2 mM dGTP, dATP, dTTP and 0.02 mM dCTP, 1µl [^{32}P]dCTP (3000 Ci/mmol) per 1 ml of reaction mix, and 1 U *Taq* polymerase (Bioline) in a reaction mix of 50 µl. Products were separated on a 6% acrylamide–7 M urea denaturing gel at 60 W for 2–3 h. Dried gels were exposed to X-ray film (X-OMAT, Kodak) for 24 h.

All primer sequences are available from Généthon (28) except for *PLP* (29), *COL4A5* (30), *DXS17* (31), 5′ *DYS I* (32) *STR* 44/45/49/50 (33), *STR HI* and *STR* 62/63. (J. Taylor and A. Brinke, pers. comm.).

Conditions for thermal cycling consisted of denaturation at 94°C for 5 min, followed by 30 cycles of 94°C for 1 min, 1 min at the annealing temperature of the individual primer pair, 1 min at 72°C, followed by a final extension step of 72°C for 10 min.

The annealing temperatures of primer pairs were as follows: 5′ *DYS I*, 44°C; *DXS1106*, 50°C; 3′ *STR HI*, 51°C; *DXS1230* and *DXS1001*, 53°C; *STR* 44,45,49 and 50, 54°C; *DXS995*, 55°C; *COL4A5* and *DXS990*, 56°C; *DXS986*, *DXS1220* and *PLP*, 58°C; *DXS1210*, 59°C and *STR* 62/63, 60°C.

Linkage analysis

Pairwise lod scores were calculated between the disease gene and the marker loci using LIPED. Penetrance was taken as 100% in males. Frequency of the deafness allele was estimated at 0.0001.

Locus order and interloci distances were determined from the most recently available data (13)(Fig. 5).

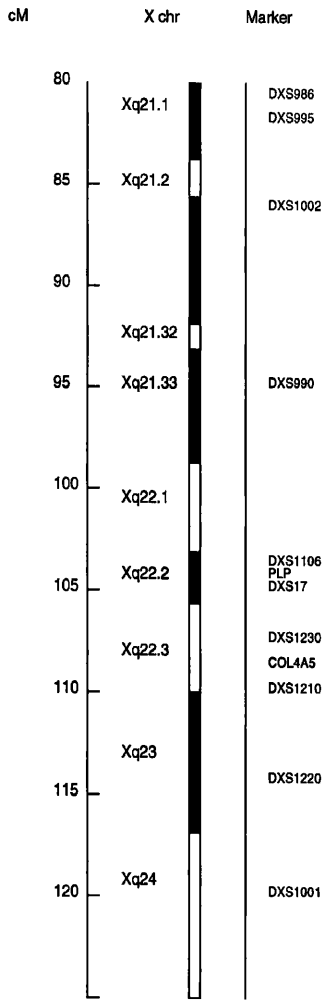

Figure 5. Postulated order of X chromosome markers used in this study (13).

ACKNOWLEDGEMENTS

We would like to acknowledge the help of Dr William Reardon and thank both families for their co-operation. Jessica Tyson and Maria Bitner-Glindzicz are funded by the Medical Research Council. Professor Marcus Pembrey is funded by Mothercare.

REFERENCES

1. Rose,S.P., Conneally,P.M. and Nance,W.E. (1977). Genetic analysis of childhood deafness. In: Bess FH (ed.) *Childhood Deafness*. Grune and Stratton, New York, USA. pp 19–36.
2. McKusick,V.A. (1992). *Mendelian Inheritance in Man*. 10th edition. Baltimore, MD, USA.
3. Mohr,J. and Magerøy,K. (1960) Sex-linked deafness of a possibly new type. *Acta Genet. Stat. Med.* (Basel) **10**, 54–62.
4. Tranebjœrg,L., Schwartz,C., Eriksen,H., Andreasson,S., Ponjavic,V., Dahl,A., Stevenson,R.E., May,M., Arena,F., Barker,D., Elverland,H.H. and Lubs,H. (1995) A new X linked recessive deafness syndrome with blindness, dystonia, fractures, and mental deficiency is linked to Xq22. *J. Med. Genet.* **32**, 257–263.
5. Wallis,C., Ballo,R., Wallis,G., Beighton,P. and Goldblatt,J. (1988) X-linked mixed deafness with stapes fixation in a Mauritian kindred: linkage to Xq probe pDP34. *Genomics* **3**, 299–308.

6. Brunner,H.G., van Bennekom,C.A., Lambermon,E.M.M., Oei,T.L., Cremers,C.W.R.J., Wieringa,B. and Ropers,H-H. (1988). The gene for X-linked progressive mixed deafness with perilymphatic gusher during stapes surgery (DFN3) is linked to PGK. *Hum. Genet.* **80**, 337–340.
7. Reardon,W., Middleton-Price,H.R., Sandkuijl,L., Phelps,P., Bellman,S., Luxon,L., Pembrey,M.E. and Malcolm,S. (1991). A multipedigree linkage study of X-linked deafness: linkage to Xq13-q21 and evidence for genetic heterogeneity. *Genomics* **11**, 885–894.
8. de Kok,Y.J.M., van der Maarel,S.M., Bitner-Glindzicz,M., Huber,I., Monaco,A.P., Malcolm,S., Pembrey,M.E., Ropers,H-H. and Cremers,F.P.M. (1995). Association between X-linked mixed deafness and mutations in the POU domain gene *POU3F4*. *Science* **267**, 685–688.
9. Bitner-Glindzicz,M., Turnpenny,P., Höglund,P., Kääriänen,H., Sankila,E-M., van der Maarel,S.M., de Kok,Y.J.M., Ropers,H-H., Cremers,F.P.M., Pembrey,M.E. and Malcolm,S. (1995). Further mutations in *Brain 4 (POU3F4)* clarify the phenotype in the X-linked deafness, DFN3. *Hum. Mol. Genet.* **4**, 1467–1469.
10. Phelps,P.D., Reardon,W., Pembrey,M.E., Bellman,S. and Luxon,L. (1991). X-linked deafness, stapes gushers and a distinct defect of the inner ear. *Neuroradiology* **33**, 326–330.
11. Dahl,N., Laporte,J., Hu,L.J., Biancalana,V., Le Paslier,D., Cohen,D., Piussan,C. and Mandel,J.L. (1995). Deletion mapping of X-linked mixed deafness (DFN3) identifies a 265–525-kb region centromeric of DXS26. *Am. J. Hum. Genet.* **56**, 999–1002.
12. de Kok,Y.J.M., Vossenaar,E.R., Cremers,C.W.R.J., Dahl,N., Laporte,J., Hu,L.J., Lacombe,D., Fischel-Ghodsian,N., Friedman,R.A., Parnes,L.S., Thorpe,P., Bitner-Glindzicz,M., Pander,H-J., Heilbronner,H., Graveline,J., den Dunnen,J.T., Brunner,H.G., Ropers,H-H. and Cremers,F.P.M. (1996). Novel microdeletions in 6 patients with X-linked deafness type 3 (DFN3) are located 900 kb proximal to the DFN3 gene, *POU3F4*. *Hum. Mol. Genet.* **5**, 1229–1235.
13. Nelson,D., Ballabio,A., Cremers,F., Monaco,A. and Schlessinger,D. (1995). Report of the sixth international workshop on X chromosome mapping 1995. *Cytogenet. Cell. Genet.* **71**, 308–336.
14. Bitner-Glindzicz,M., de Kok,Y.J.M., Summers,D., Huber,I., Cremers,F.P.M., Ropers,H-H., Reardon,W., Pembrey,M.E. and Malcolm,S. (1994). Close linkage of a gene for X-linked deafness to 3 microsatellite repeats at Xq21 in radiologically normal and abnormal families. *J. Med. Genet.* **31**, 916–921.
15. Lalwani,A.K., Brister,J.R., Fex,J., Grundfast,K.M., Pikus,A.T., Ploplis,B., San Agustin,T., Sharka,H. and Wilcox,E.R. (1994). A new non-syndromic X-linked sensorineural hearing impairment linked to Xp21.2. *Am. J. Hum. Genet.* **55**, 685–694.
16. Kawai,S., Nomura,S., Harano,T., Harano,K., Fukushima,T., Osawa,G. and the Japanese Alport Network (1996). The COL4A5 gene in Japanese Alport syndrome patients: spectrum of mutations of all exons. *Kidney Int.* **49**, 814–822.
17. Heidet,L., Dahan,K., Zhou,J., Xu,Z., Cochat,P., Gould,J.D.M., Leppig,K.A., Proesmans,W., Guyot,C., Guillot,M., Roussel,B., Tryggvason,K., Grünfeld,J-P., Gubler,M-C. and Antignac,C. (1995). Deletions of both α5(IV) and α6(IV) collagen genes in Alport syndrome and in Alport syndrome associated with smooth muscle tumours. *Hum. Mol. Genet.* **4**, 99–108.
18. Saugier-Veber,P., Munnich,A., Bonneau,D., Rozet,J-M., Le Merrer,M., Gil,R. and Bœspflugtanguy,O. (1994). X-linked spastic paraplegia and Pelizaeus-Merzbacher disease are allelic disorders at the proteolipid protein locus. *Nature Genet.* **6**, 257–262.
19. Vetrie,D., Vorechovsky,I., Sideras,P., Holland,J., Davies,A., Flinter,F., Hammarström,L., Kinnon,C., Levinsky,R., Bobrow,M., Smith,C.I.E. and Bentley,D.R. (1993). The gene involved in X-linked agammaglobulinaemia is a member of the *src* family of protein-tyrosine kinases. *Nature* **361**, 226–233.
20. Vorechovsky,I., Vetrie,D., Holland,J., Bentley,D.R., Thomas,K., Zhou,J.N., Notaragelo,L.D., Plebani,A., Fontan,G., Ochs,H.D., Hammarström,L., Sideras,P. and Smith,C.I.E. (1994). Isolation of cosmid and cDNA clones in the region surrounding the *BTK* gene at Xq21.3-q22. *Genomics* **21**, 517–524.
21. Reardon,W., Bellman,S., Phelps,P., Pembrey,M.E. and Luxon,L. (1993). Neuro-otologic function in X-linked hearing loss:A multipedigree assessment and correlation with other clinical parameters. *Acta Oto-Laryngologica* **113**, 706–714.
22. Deraemaeker,R. (1958). Sex-linked congenital deafness. *Acta Genet. Statist. Med.* **8**, 228–231.
23. Fraser,G.R. (1965). Sex-linked recessive congenital deafness and the excess of males in profound childhood deafness. *Ann. Hum. Genet.* **29**, 171–196.
24. McRae,K., Uchida,I., Lewis,M. and Denniston,C. (1969). Sex-linked congenital deafness. *Am. J. Hum. Genet.* **21**, 415–422.
25. Parker,N. (1958). Congenital deafness due to a sex-linked recessive gene. *Am. J. Hum. Genet.* **10**, 196–200.
26. Richards,B. (1963). Sex-linked deaf-mutism. *Ann. Hum. Genet.* **26**, 195–199.
27. Sataloff,J., Pastore,P.H. and Bloom,E. (1955). Sex-linked hereditary deafness. *Am. J. Hum. Genet.* **7**, 201–203.
28. Gyapay,G., Morisette,J., Vignal,A., Dib,C., Fizames,C. and Millasseau,P. (1994). The 1993–1994 Généthon human genetic-linkage map. *Nature Genet.* **7**, 246–339.
29. Mimault,C., Cailloux,F., Giraud,G., Dastugue,B. and Bœspflugtanguy,O. (1995). Dinucleotide repeat polymorphism in the proteolipid (PLP) gene. *Hum. Genet.* **96**, 236.
30. Barker,D., Clecerly,J. and Fain,P. (1992). Two CA-dinucleotide polymorphisms at the COL4A5 (Alport syndrome) gene in Xq22. *Nucleic Acids Res.* **20**, 929.
31. Arveiler,B., Oberlé,I. and Mandel,J.L. (1987). Genetic mapping of nine DNA markers in the q11-q22 region of human X chromosome. *Genomics* **1**, 60–66.
32. Feener,C.A., Boyce,F.M. and Kunkel,L.M. (1991). Rapid detection of CA polymorphisms in cloned DNA: Application to the 5′ region of the dystrophin gene. *Am. J. Hum. Genet.* **48**, 621–627.
33. Clemens,P., Fenwick,R., Chamberlin,J., Gibbs,R., Deandrade,M., Chakraborty,R. and Caskey,C. (1991). Carrier detection and prenatal diagnosis in Duchenne and Becker muscular dystrophy families, using dinucleotide repeat polymorphisms. *Am. J. Hum. Genet.* **49**, 951–960.

NOTE ADDED IN PROOF

It is now known that Mohr-Tranebjaerg syndrome, originally mapped to Xq22, is caused by a mutation in a novel X-linked gene, *DDP*. [Jin, H., May, M., Tranebjaerg, L., Kendall, E., Fontan, G., Jackson, J., Subramony, S.H., Arena, F., Lubs, H., Smith, S., Stevenson, R., Schwartz, C. and Vetrie, D. (1996) A novel X-linked gene, *DDP*, shows mutations in families with deafness (DFN-1), dystonia, mental deficiency and blindness. *Nature Genet.* **14**, 177–180.]

two other levothyroxine-treated patients with thyroid cancer whose serum thyrotropin concentrations had been deliberately suppressed (Patients 10 and 11), the values rose into the normal range during sertraline therapy. The value for the serum free thyroxine index decreased in all patients in whom it was measured (Table 1). No patient had symptoms of hypothyroidism at this time. The patients ranged in age from 37 to 70 years (mean, 49), and all but one were women. The causes of hypothyroidism had included chronic autoimmune thyroiditis (in six patients), radioiodine therapy (three patients), and thyroidectomy (two patients). The duration of hypothyroidism ranged from 1 to 23 years (mean, 6).

Since this phenomenon had not been specifically sought, it was noticed only at the time of scheduled follow-up visits six weeks to six months after the start of sertraline therapy. All the patients had been taking the same dose of levothyroxine for at least six months, and all were thought to be taking it as recommended. The elevation in serum thyrotropin was confirmed one to three weeks later in six patients who were retested. The dose of levothyroxine was increased for all the patients. Two months after the increase, the serum thyrotropin concentration had returned to base line in seven patients, whereas in the remaining four a further dose increase was necessary.

The mechanism by which sertraline lowers serum thyroxine concentrations (and raises those of serum thyrotropin) is uncertain. We doubt that the absorption of levothyroxine is altered, because there was an appropriate increase in the serum thyroxine concentration,[1] from 6.6 to 8.5 μg per deciliter (85 to 109 nmol per liter) in one patient three hours after an oral dose of 0.35 mg of levothyroxine. Serum concentrations of thyroxine-binding globulin, measured in six patients, did not change during sertraline therapy. Although some patients were taking medications that can alter the serum thyroxine concentration (ethinyl estradiol, conjugated estrogen, and phenytoin), these medications antedated the therapy with sertraline, and we doubt that they were responsible for the observed effects. One reported case in which sertraline caused a low serum total thyroxine concentration but normal concentrations of thyrotropin and free thyroxine in an adolescent patient[2] indicates that sertraline may increase the clearance of thyroxine. We know of three other levothyroxine-treated patients whose serum thyrotropin concentrations remained stable after the initiation of sertraline therapy, but we have not yet determined the frequency with which patients treated with sertraline have altered requirements for thyroxine.

KAREN C. MCCOWEN, M.B., M.R.C.P.I.
JEFFREY R. GARBER, M.D.
Harvard Pilgrim Health Care

RICHARD SPARK, M.D.
Beth Israel Deaconess Medical Center
Boston, MA 02215

1. Ain KB, Pucino F, Shiver TM, Banks SM. Thyroid hormone levels affected by time of blood sampling in thyroxine-treated patients. Thyroid 1993;3:81-5.
2. Harel Z, Biro FM, Tedford WL. Effect of long term treatment with sertraline (Zoloft) simulating hypothyroidism in an adolescent. J Adolesc Health 1995;16:232-4.

Spokespersons for Pfizer reply:

To the Editor: The letter from McCowen and colleagues describing small decreases in serum thyroxine concentrations and small increases in serum thyrotropin concentrations after the initiation of sertraline treatment in thyroxine-treated patients with hypothyroidism is consistent with previous reports of similar changes in patients treated with other antidepressant drugs. Post-treatment declines in serum thyroxine (sometimes with resultant increases in serum thyrotropin) have been described in euthyroid patients receiving other treatments for affective illness, including tricyclic antidepressant drugs, selective serotonin-reuptake inhibitors, lithium, and carbamazepine.[1]

We reviewed Pfizer's early-alert safety data base for sertraline through July 31, 1997, and identified 14 cases of hypothyroidism for which there was no other obvious cause and for which a possible relation to sertraline could not be excluded. Seven of the patients were taking thyroxine. In one case, the patient had a history of hypothyroidism during previous fluoxetine therapy; in another, hypothyroidism was diagnosed after the patient discontinued sertraline and initiated fluoxetine. Hypothyroidism is listed in the new product labeling for sertraline as an adverse event observed during post-marketing evaluation.[2]

In view of the literature indicating potential changes in thyroid function with many antidepressant drugs and the complex interrelation between the hypothalamic–pituitary–thyroid axis and affective illness, optimal management of patients with thyroid disease who are receiving any type of treatment for depression should include periodic reassessment of thyroid function.

CATHRYN M. CLARY, M.D.
WILMA M. HARRISON, M.D.
Pfizer
New York, NY 10017

1. Shelton RC, Winn S, Ekhatore N, Loosen PT. The effects of antidepressants on the thyroid axis in depression. Biol Psychiatry 1993;33:120-6.
2. Sertraline. New York: Pfizer, 1997 (package insert).

Molecular Basis of the Long-QT Syndrome

To the Editor: Splawski et al. (May 29 issue)[1] and others[2] have shown at the molecular level that the Jervell and Lange–Nielsen syndrome (prolonged QT interval on the electrocardiogram, associated with profound congenital deafness) may be caused by a homozygous mutation in the *KVLQT1* gene, confirming that the Jervell and Lange–Nielsen syndrome and the Romano–Ward syndrome are allelic. Genetic heterogeneity has previously been demonstrated in the Romano–Ward syndrome, in that a heterozygous mutation in any of three genes, *KVLQT1* (at the LQT1 locus), *HERG* (at the LQT2 locus), and *SCN5A* (at the LQT3 locus), and another as yet unidentified gene (at the LQT4 locus) can cause isolated long-QT syndrome.[3]

Genetic heterogeneity has now been suggested in the Jervell and Lange–Nielsen syndrome[1,2] because of the results of linkage analysis in a sibship that was described previously.[4] The affected siblings in this family were found to have inherited different paternal alleles for a marker closely

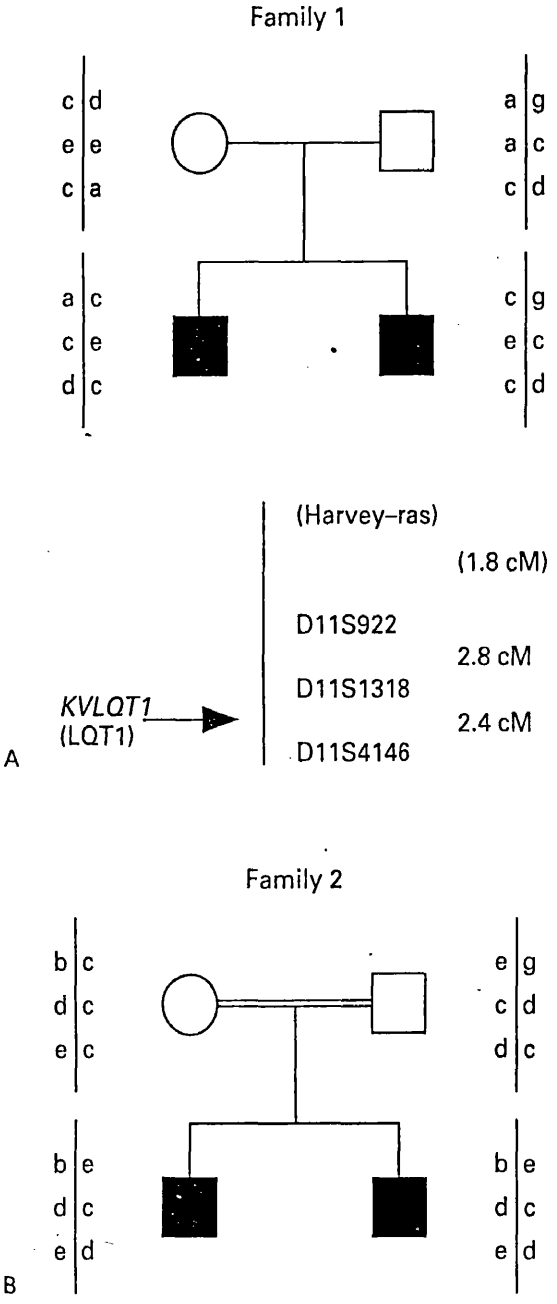

Figure 1. Results of Haplotyping for Three Markers, D11S922, D11S1318, and D11S4146, on Chromosome 11 around the LQT1 Locus in Two British Families.

The position of the Harvey–ras locus and its distance from D11S922 are indicated in parentheses. Previous analysis of Family 1 with a probe at the Harvey–ras locus showed that the brothers had inherited different alleles from their father, implying that the Jervell and Lange–Nielsen syndrome is not linked to the LQT1 locus in this family.[4] However, reanalysis shows that a recombination has occurred on the paternal chromosome and that both sons have inherited the same parental alleles flanking the LQT1 locus (Panel A). Haplotyping in a second, previously undescribed family (Panel B) shows that although the two boys in this family have inherited the same alleles flanking this locus, they are not homozygous for any of the markers. Circles indicate female family members, squares male family members, and solid symbols affected members. The double line between the parents indicates consanguinity.

linked to the LQT1 locus (Harvey–ras). The Harvey–ras marker had not previously shown any recombinations with the disease locus in families with the Romano–Ward syndrome.

Refined mapping of the LQT1 locus, placing it distal to the marker D11S1318,[2,5] together with the availability of polymorphic markers closer to the *KVLQT1* gene, prompted reanalysis of this family. Haplotyping showed that recombination has occurred distal to the Harvey–ras marker on the paternal chromosome and that both boys have inherited the same parental alleles flanking the disease gene (Fig. 1A). Therefore, the data in this family are now consistent with mutation at the LQT1 locus and should no longer be cited as evidence of the existence of genetic heterogeneity in the Jervell and Lange–Nielsen syndrome.

Haplotyping of another British family, however, does provide strong evidence of genetic heterogeneity in the Jervell and Lange–Nielsen syndrome. The parents of the affected boys are consanguineous (first cousins once removed). In the context of a rare recessive disorder, the boys should be homozygous for a single mutation inherited from a common ancestor and homozygous for genetic markers around the mutant gene.[5] Haplotyping shows that although the boys have inherited the same parental alleles, they are not homozygous at any of the surrounding marker loci (Fig. 1B). Furthermore, haplotyping for markers around LQT2, LQT3, and LQT4 shows no evidence of homozygosity in these regions, which suggests that mutation of a different gene must cause the Jervell and Lange–Nielsen syndrome in this family.

MARIA BITNER-GLINDZICZ, M.R.C.P., PH.D.
JESSICA TYSON, B.SC.
Institute of Child Health
London WC1N 1EH, United Kingdom

RUTH JAMIESON, PH.D.
St. George's Hospital Medical School
London SW17 0RE, United Kingdom

1. Splawski I, Timothy KW, Vincent GM, Atkinson DL, Keating MT. Molecular basis of the long-QT syndrome associated with deafness. N Engl J Med 1997;336:1562-7.
2. Neyroud N, Tesson F, Denjoy I, et al. A novel mutation in the potassium channel gene KVLQT1 causes the Jervell and Lange-Nielsen cardioauditory syndrome. Nat Genet 1997;15:186-9.
3. Third and long (QT). Nat Genet 1996;12:1-2.
4. Jeffery S, Jamieson R, Patton MA, Till J. Long QT and Harvey-ras. Lancet 1992;339:255.
5. Dausse E, Denjoy I, Kahlem P, et al. Readjusting the localization of long QT syndrome gene on chromosome 11p15. C R Acad Sci III 1995; 318:879-85.

Dr. Keating replies:

To the Editor: In our article, we proposed that mutations in the *minK* (*IsK*) gene might also be responsible for the Jervell and Lange–Nielsen syndrome.[1] This hypothesis was based on data showing that minK joins with KVLQT protein to form cardiac I_{Ks} channels[2,3] and that *KVLQT1* mutations cause this disorder.[1,4] The data presented by Bitner-Glindzicz et al. support, but do not prove, the hypothesis that mutations in a second gene can cause the Jervell and Lange–Nielsen syndrome. Mutational analysis of DNA from

this and other consanguineous families may prove that homozygous mutations of the *minK* gene also cause the Jervell and Lange–Nielsen syndrome.

MARK T. KEATING, M.D.
Howard Hughes Medical Institute
Salt Lake City, UT 84112

1. Splawski I, Timothy KW, Vincent GM, Atkinson DL, Keating MT. Molecular basis of the long-QT syndrome associated with deafness. N Engl J Med 1997;336:1562-7.
2. Sanguinetti MC, Curran ME, Zou A, et al. Coassembly of K(V)LQT1 and minK (IsK) proteins to form cardiac I(Ks) potassium channel. Nature 1996;384:80-3.
3. Barhanin J, Lesage F, Guillemare E, Fink M, Lazdunski M, Romey G. K(V)LQT1 and IsK (minK) proteins associate to form the I(Ks) cardiac potassium current. Nature 1996;384:78-80.
4. Neyroud N, Tesson F, Denjoy I, et al. A novel mutation in the potassium channel gene KVLQT1 causes the Jervell and Lange-Nielsen cardioauditory syndrome. Nat Genet 1997;15:186-9.

Perforated Duodenal Ulcer

To the Editor: Molmenti (May 22 issue)[1] presented an Image in Clinical Medicine showing a perforated duodenal ulcer. The surgeon closed the ulcer with several stitches but subsequently performed a vagotomy. Vagotomy was once the standard surgical treatment as prophylaxis against recurrence of the ulcer. We now know that infection with *Helicobacter pylori* is the main cause of duodenal ulcers.[2] If this infection is cured, ulcers and their complications rarely recur.[3] A very small percentage of duodenal ulcers are caused by aspirin or nonsteroidal antiinflammatory drugs, and these can be managed safely by stopping treatment with these drugs or, if this is impossible, adding misoprostol or acid-reducing drugs. Because antibiotics can cure duodenal ulcer disease, a surgeon operating on an ulcer complication should ligate the bleeding or patch the perforation but should not perform a prophylactic vagotomy.[4,5]

In my teaching hospital, the professor of medicine always threatened to cut off a finger of every resident who had not performed a digital rectal examination. Although I have no recollection of any of my colleagues going through life with fewer than 10 fingers, his oft-repeated threat taught us never to forget this part of the physical examination. It is time to threaten our surgical colleagues that we will cut off one of their fingers if they dare to put a knife in the precious vagus nerve. Apparently, they must be taught that ulcer disease is managed medically and that vagotomy is no longer appropriate.

WINK A. DE BOER, M.D.
Sint Anna Hospital
NL-5340 BE Oss, the Netherlands

1. Molmenti EP. Perforated duodenal ulcer. N Engl J Med 1997;336:1499.
2. Walsh JH, Peterson WL. The treatment of *Helicobacter pylori* infection in the management of peptic ulcer disease. N Engl J Med 1995;333:984-91.
3. Hopkins RJ, Girardi LS, Turney EA. Relationship between *Helicobacter pylori* eradication and reduced duodenal and gastric ulcer recurrence: a review. Gastroenterology 1996;110:1244-52.
4. Sebastian M, Chandran VP, Elashall YI, Sim AJ. *Helicobacter pylori* infection in perforated peptic ulcer disease. Br J Surg 1995;82:360-2.
5. Witte CL. Is vagotomy and gastrectomy still justified for gastroduodenal ulcer? J Clin Gastroenterol 1995;20:2-3.

The author replies:

To the Editor: Dr. de Boer states that "antibiotics can cure duodenal ulcer disease" and threatens any surgeon who "dare[s] to put a knife in the precious vagus nerve." Not everybody, however, is quite so dogmatic.

In a recent review in the *Journal,* Walsh and Peterson point out that "despite the fact that *H. pylori* is necessary for the development of peptic ulcers in most patients, it is far from sufficient."[1] Others have observed that *H. pylori* had a limited role in causing disease in surgical patients, and suggested that an "adequate acid reduction procedure will still be the main objective of surgical treatment and prevention of . . . ulcer recurrence."[2] Still others corroborate our observations that omental-patch closure combined with parietal-cell vagotomy is an excellent approach to the treatment of patients with perforated pyloroduodenal ulcers.[3] It not only allows the resolution of an emergency but simultaneously provides protection for patients who would have required additional surgical interventions for continued ulcer disease. The most recent textbooks of medicine and surgery assert that vagotomy is an acceptable treatment for perforated duodenal ulcers.[4,5]

ERNESTO P. MOLMENTI, M.D.
University of Pittsburgh
Pittsburgh, PA 15213

1. Walsh JH, Peterson WL. The treatment of *Helicobacter pylori* infection in the management of peptic ulcer disease. N Engl J Med 1995;333:984-91.
2. Lee WJ, Wu MS, Chen CN, Yuan RH, Lin JT, Chang KJ. Seroprevalence of *Helicobacter pylori* in patients with surgical peptic ulcer. Arch Surg 1997;132:430-3.
3. Jordan PH Jr, Thornby J. Perforated pyloroduodenal ulcers: long-term results with omental patch closure and parietal cell vagotomy. Ann Surg 1995;221:479-86.
4. Kelley WN, ed. Textbook of internal medicine. 3rd ed. Philadelphia: Lippincott–Raven, 1997:700.
5. Sabiston DC Jr, ed. Textbook of surgery: the biological basis of modern surgical practice. 15th ed. Philadelphia: W.B. Saunders, 1997:860.

Use of Veterans Affairs Medical Care by Enrollees in Medicare HMOs

To the Editor: Older people in the United States who use the medical services of the Veterans Health Administration are frequently also entitled to health care through Medicare. Although most do not use both these federally funded systems at the same time, substantial use of both the Veterans Health Administration and Medicare fee-for-service care has been documented.[1-5] Less is known about the use of Veterans Health Administration services by enrollees in Medicare health maintenance organizations (HMOs). We studied the dual use of these two federal programs with respect to inpatient and outpatient services.

We merged inpatient and outpatient data from the Miami Veterans Affairs Medical Center (VAMC) for 1992 and 1993 with data on Medicare enrollment in Florida in those years, to determine eligibility for Medicare. We obtained information on HMO enrollment, age, and race from the Medicare files of the Health Care Financing Administration. Our analyses were limited to men 65 years of age or older.

Of 5074 inpatient admissions to the Miami VAMC of Medicare beneficiaries over the age of 65, 27.5 percent in-

Human Molecular Genetics, 1997, Vol. 6, No. 12 2179–2185

IsK and KvLQT1: mutation in either of the two subunits of the slow component of the delayed rectifier potassium channel can cause Jervell and Lange-Nielsen syndrome

Jessica Tyson[1], Lisbeth Tranebjærg[2], Sue Bellman[3], Christopher Wren[4], James F.N. Taylor[4], Jørn Bathen[5], Bjørn Aslaksen[6], Svein Jan Sørland[7], Ole Lund[8], Sue Malcolm[1], Marcus Pembrey[1], Shomi Bhattacharya[9] and Maria Bitner-Glindzicz[1,*]

[1]Units of Clinical and Molecular Genetics, Institute of Child Health and Great Ormond Street Hospital for Children NHS Trust, UCL Medical School, 30 Guilford Street, London WC1N 1EH, UK, [2]Department of Medical Genetics, University Hospital of Tromsø, N-9038 Tromsø, Norway, [3]Department of Audiological Medicine, Great Ormond Street Hospital NHS Trust, UCL Medical School, London WC1N 3JH, UK, [4]Department of Cardiology, Great Ormond Street Hospital NHS Trust, UCL Medical School, London WC1N 3JH, UK, [5]Department of Cardiology, Regional Hospital, Trondheim, Norway, [6]Department of Internal Medicine, Central Hospital, Arendal, Norway, [7]Department of Paediatric Cardiology, University Hospital, Oslo, Norway, [8]Department of Otorhinolaryngology, Namdal Hospital, Namdal, Norway and [9]Department of Molecular Genetics, Institute of Ophthalmology, UCL, 11–43 Bath Street, London EC1V 9EL,UK

Received June 13, 1997; Revised and Accepted August 26, 1997

The Jervell and Lange-Nielsen syndrome (JLNS) comprises profound congenital sensorineural deafness associated with syncopal episodes. These are caused by ventricular arrhythmias secondary to abnormal repolarisation, manifested by a prolonged QT interval on the electrocardiogram. Recently, in families with JLNS, Neyroud *et al.* reported homozygosity for a single mutation in *KVLQT1*, a gene which has previously been shown to be mutated in families with dominantly inherited isolated long QT syndrome [Neyroud *et al.* (1997) *Nature Genet.*, 15, 186–189]. We have analysed a group of families with JLNS and shown that the majority are consistent with mutation at this locus: five families of differing ethnic backgrounds were homozygous by descent for markers close to the *KVLQT1* gene and a further three families from the same geographical region were shown to be homozygous for a common haplotype and to have the same homozygous mutation of the *KVLQT1* gene. However, analysis of a single small consanguineous family excluded linkage to the *KVLQT1* gene, establishing genetic heterogeneity in JLNS. The affected children in this family were homozygous by descent for markers on chromosome 21, in a region containing the gene *IsK*. This codes for a transmembrane protein known to associate with *KVLQT1* to form the slow component of the delayed rectifier potassium channel. Sequencing of the affected boys showed a homozygous mutation, demonstrating that mutation in the *IsK* gene may be a rare cause of JLNS and that an indistinguishable phenotype can arise from mutations in either of the two interacting molecules.

INTRODUCTION

The cardioauditory syndrome of Jervell and Lange-Nielsen (JLNS) was first described in 1957 in a Norwegian family (1). Four of six children born to unrelated parents suffered from profound congenital deafness associated with syncope and prolongation of the QT interval on electrocardiograms. Syncope arises as a consequence of abnormal ventricular repolarisation, which triggers potentially life-threatening ventricular arrhythmias. Untreated, the syndrome has a very high mortality. Although the condition is very rare, with an estimated prevalence of up to 10 per million, a number of other cases have been reported since the original description and autosomal recessive inheritance has been confirmed (2). A hypothesis, many years ago, suggested that the connection between the auditory and the

*To whom correspondence should be addressed. Tel: +44 171 242 9789; Fax: +44 171 404 6191; Email:mbitnerg@hgmp.mrc.ac.uk

Figure 1. Family UK1S with haplotype data for chromosome 21 markers. The *IsK* gene is situated between markers D21S1254 and D21S1895 (36).

cardiac defect in JLNS may be due to transmembrane electrolyte imbalance (2).

The cardiac action potential consists of a depolarisation phase, due mainly to a large influx of sodium ions, a plateau phase dependent mainly on calcium influx and repolarisation, associated with an increase in potassium permeability. This repolarising potassium current, the delayed rectifier current, has a rapidly activating component and a slowly activating component I_{Ks}.

In the ear, endolymphatic fluid produced by the stria vascularis surrounds the sensory hair cells of the cochlea. This fluid has a high concentration of potassium and a low concentration of sodium, resulting in a resting potential of about +100 mV with respect to other parts of the cochlea (3). Developmental abnormalities of the stria vascularis in mice and in humans may result in reduction of the normal osmotic pressure in the endolymphatic duct, resulting in collapse of Reissner's membrane and features similar to those seen in post-mortem studies of humans with JLNS (4–6).

Phenotypically, JLNS has similarities to the Romano–Ward syndrome, in which there is an isolated long QT interval without deafness, transmitted as an autosomal dominant condition. It has been hypothesised that the two conditions could be allelic (2). Three genes are known to underlie dominantly inherited isolated long QT syndrome (Romano–Ward syndrome), *HERG*, *SCN5A* and *KVLQT1*, and a fourth as yet unknown gene has been mapped to chromosome 4 (7–10). The three known genes all encode ion channels: *HERG* encodes a potassium channel gene, related to the *Drosophila ether-a-go-go* gene, which underlies I_{Kr}, the rapidly activating component of the delayed rectifier current responsible for cardiac repolarisation; *SCN5A* encodes an α subunit of a cardiac sodium channel; *KVLQT1* encodes a potassium channel. KvLQT1, the product of the *KVLQT1* gene, has been shown to associate with IsK, a small membrane-spanning glycoprotein. Together these two molecules reproduce the properties of I_{Ks}, the slowly activating component of the delayed rectifier current (11,12). Recently it has been shown at the molecular level that JLNS and Romano–Ward syndrome can be caused by mutations in the same gene, *KVLQT1*, JLNS being the homozygous form of Romano–Ward syndrome (13,14).

We analysed a single small family with JLNS and excluded the *KVLQT1* gene as the disease locus, proving that genetic heterogeneity exists in JLNS as it does in Romano–Ward syndrome. Using this family, a genome search, combined with exclusion of other candidate loci, identified a region of homozygosity on chromosome 21, in a region harbouring the candidate gene *IsK*. We demonstrate a homozygous mutation in *IsK* in this family. Haplotyping of a group of families with JLNS shows that the majority of families are consistent with mutation in *KVLQT1*, but that mutation in *IsK*, whose protein product associates with that of the *KVLQT1* gene to form the delayed rectifier potassium channel, may be a rare cause of JLNS, phenotypically indistinguishable from that caused by mutation in *KVLQT1*.

RESULTS

Chromosome 21-linked family

Haplotype analysis in family UK1S excluded linkage to the *KVLQT1* locus on chromosome 11, as the affected brothers were not homozygous by descent for any markers in this region of chromosome 11 (data not shown). In addition, all the other known long QT loci, as well as all loci for non-syndromic recessive and dominant deafness described to date, were not linked to the disease (15). Non-syndromic loci were tested on the basis of observations that syndromic and non-syndromic forms of deafness may map to the same loci and therefore could be allelic (16,17). A genome-wide search in family UK1S demonstrated a region of homozygosity by descent on chromosome 21 with D21S261 after 50 markers had been genotyped. Other markers which showed homozygosity are D21S1895 and D21S1252, but not D21S268 (D21S1254 was uninformative). Markers are in the order cen, D21S261, D21S1254, D21S1895, D21S1252, D21S268, tel. Marker haplotypes in this region are shown in

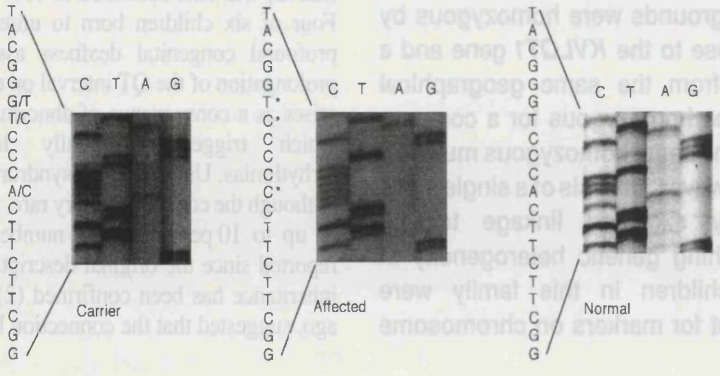

Figure 2. Sequence analysis of the mutation in an affected individual is shown together with that of a normal and a carrier parent. Substituted bases are marked * in the affected individual. The carrier parent is clearly heterozygous for the mutation.

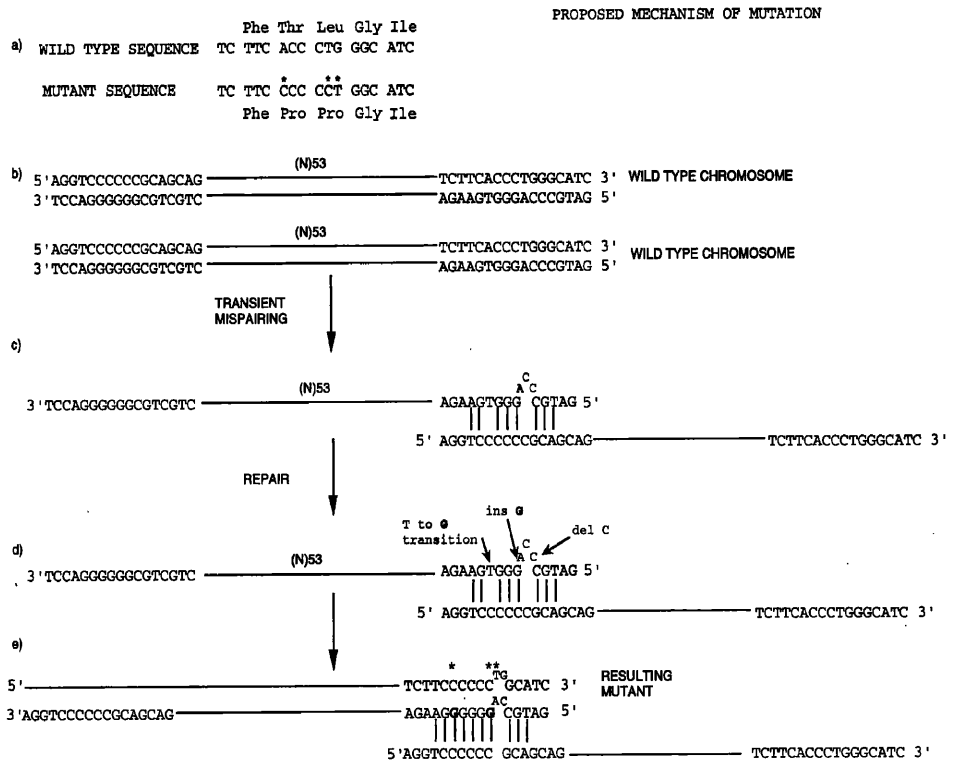

Figure 3. (**a**) The wild type and mutant sequences. There are three nucleotide substitutions which are indicated by * in the mutant sequence. (**b–d**) A proposed mechanism for the complex mutation. There are two regions of sequence similarity ~60 bases apart in the gene. Transient mispairing between these two regions is shown in (c). Attempted correction of the 3′-sequence based on the template of the 5′-sequence is shown in (d). Partial correction results in the changes observed in the mutant sequence.

Figure 1. The maximum lod scores for this small family at zero recombination were 1.47 for D21S1252 and 1.69 for D21S1895.

A candidate gene, the potassium channel *IsK* (minK) mapping to the homozygous region, was screened for mutations in family UK1S using SSCP (18). Previously described intragenic polymorphisms were detected (19,20) and shifted bands were observed in both parents in family UK1S in double-stranded DNA (possibly heteroduplexes), which were not seen in over 60 control individuals (120 chromosomes) or in any other individuals with JLNS from 11 families. Sequencing of the PCR products of the *IsK* gene showed the changes illustrated in Figures 2 and 3a, in which three separate nucleotides have been altered. The changes cause Thr59 and Leu60 each to be replaced by Pro in the transmembrane region of the predicted protein.

Chromosome 11-linked families

Haplotype data from eight families are shown in Figure 4. The offspring of families N8A and UK2T are the product of first cousin marriages. In families N1H, N3S, N5B and N10D, consanguinity or a founder effect is suspected (represented by a dashed line), as the parents originate from the same county in Norway. Parents of families N6K and N7J are not known to be related.

Homozygosity by descent was seen for all the markers typed, D11S4046, D11S1318, D11S4088 and D11S4146, in families UK2T and N3S. In family N8A and family N5B, markers distal to D11S1318 were homozygous, whereas in family N1H, homozygosity was observed for D11S1318 itself and the marker proximal to it, D11S4046. In family N10D, homozygosity was observed for the following markers, D11S4046, D11S1318 and D11S4088, as shown in Figure 4.

SSCP screening of the *KVLQT1* gene corresponding to the S2–S3 domains of the protein (PCR primers 1F and1R) (9) showed an aberrant conformer which is homozygous in the affected individuals in families N1H, N5B and N10D and present in the heterozygous state in their parents (not shown). Sequencing of the PCR product showed a homozygous 5 bp deletion of nt 187–191 (according to the numbering in 9) in affected individuals, which abolishes a *Hha*I restriction enzyme site (Fig. 5). This was not seen in 40 normal controls (80 chromosomes).

DISCUSSION

We provide evidence that mutation in the gene *IsK* can cause JLNS, which appears to be clinically indistinguishable from cases caused by mutation in *KVLQT1*. The biological interaction of the two molecules supports this observation. The product of the *KVLQT1* gene has been shown to associate with the product of the *IsK* gene to form a channel with properties of the slow component of the delayed rectifier current in the heart (11,12). In the ear, IsK appears to have a role in the transport of high concentrations of K^+ into the extracellular endolymph surrounding the hair cells (21). Mice homozygous for a complete targeted disruption of the *IsK* gene show shaker/waltzer behaviour characteristic of inner ear dysfunction and inner ear pathology closely resembling that seen in human subjects who have died from JLNS (21). Combined with the mapping data in family UK1S, this rendered

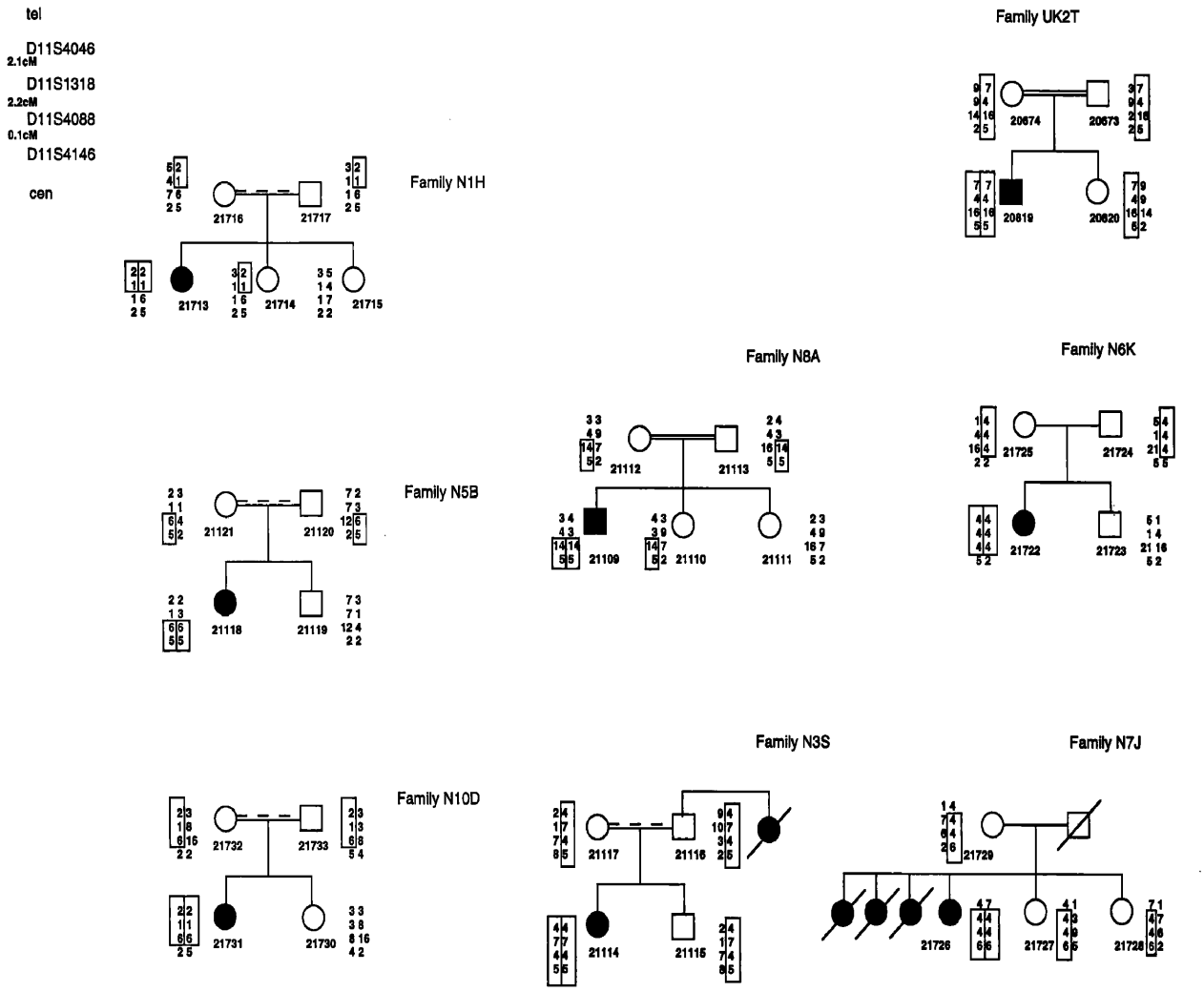

Figure 4. Haplotype analysis of eight families. Dashed line indicates suspected consanguinity (see text). Families UK2T and N3S are homozygous by descent for all the markers typed, D11S4046, D11S1318, D11S4088 and D11S4146. In families N8A and N5B markers distal to D11S1318 are homozygous, whereas in family N1H homozygosity is seen for D11S1318 itself and the marker proximal to it, D11S4046. Order of markers is as indicated in the key.

IsK an excellent candidate gene for JLNS in a family in whom the *KVLQT1* gene had been excluded.

The minK protein (product of the *IsK* gene) has an unusually simple structure for an ion channel, consisting of only 130 amino acids. The molecule has an extracellular portion, a transmembrane α-helical region and an intracellular region (22). Sequencing of the PCR products of the *IsK* gene in the affected boys in family UK1S showed the changes illustrated in Figures 2 and 3a in which three separate nucleotides have been altered. The changes cause Thr59 and Leu60 each to be replaced by Pro in the transmembrane region of the predicted protein.

The cyclical structure of proline is expected to influence the resulting protein structure, since it causes bending of folded protein chains (23). Indeed, observations of the relative occurrence of amino acid residues in α-helices show that proline is the least likely of all the amino acids to be found in this secondary structure (23). Site-directed mutagenesis of the *IsK* gene has also contributed insight into the functional domains of this small protein. Amino acid substitutions at a number of positions within and outside the transmembrane region were found to have varying effects on the functional activity of the channel. Mutation of Thr59 to a structurally related amino acid, valine, was shown to cause a reduction in channel activity as judged by electrophysiological measurements in oocyte systems (22). The mutation in family UK1S alters both this amino acid, Thr59 and the one adjacent to it, Leu60, and is therefore very likely to be of functional significance and disease causing. *In vitro* studies in oocyte systems should confirm the functional significance of this mutation.

A recent survey of published databases has indicated that complex changes such as the one described here are very rare (24). It is interesting to speculate how such a mutation may have arisen and a proposed mechanism is outlined in Figure 3. Approximately 60 bases upstream of the mutation is a small region of sequence similarity sufficient to allow transient mispairing of the two regions in the germline of an ancestor (Fig. 3c). This would be followed by attempted correction of the 3′-sequence, based on the template of the upstream 5′-sequence. Certainly the base changes that have arisen as a result of the mutation create greater homology between these two regions. These changes are present in carriers and in both affected individuals.

In family UK1S, the following are evidence that mutation in the *IsK* gene causes JLNS: mutation at *KVLQT1* has been excluded in this family due to the absence of homozygosity by descent for markers in this region, but homozygosity for markers flanking the *IsK* gene is demonstrated. The chromosome 21 markers typed are highly polymorphic, with D21S1895 having 10 alleles and

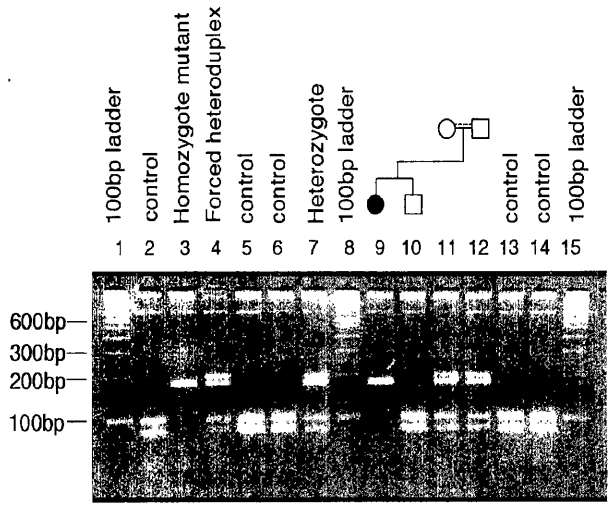

Figure 5. PCR amplification products from the S2–S3 domains of the *KVLQT1* gene (9) after digestion with the enzyme *Hha*I. In normal controls, digestion yields fragments of 98 and ~80 bp (lanes 2, 5, 6, 13 and 14). In the homozygous mutant, the 5 bp deletion abolishes the cut site for the enzyme, resulting in a single fragment of ~180 bp (lanes 3 and 9). In heterozygotes after *Hha*I digestion there are fragments of ~180, 98 and ~80 bp and an additional fainter band at 200 bp (lanes 7, 11 and 12). This faint band at 200 bp probably represents heteroduplexes, partially resistant to *Hha*I digestion. This band, which is not present in normals or homozygous mutants, can be created by mixing PCR products from a normal and a homozygous mutant and then digesting with *Hha*I (lane 4).

heterozygosity of 82%. The sequence changes in *IsK* in the affected boys of family UK1S are not seen on SSCP analysis of 120 normal chromosomes. This mutation results in substitution of two proline residues, predicted to cause severe disruption to the helical structure of the transmembrane region of the molecule. Functional studies on one of the mutated residues has previously shown this to be important for channel activity. Interaction of the *IsK* gene product with that of the *KVLQT1* gene, already known to cause JLNS, provides a plausible biological mechanism for the disease pathology. The rarity of mutations in the *IsK* gene in JLNS is accounted for by demonstrating that the majority of cases of this rare condition are very likely to be caused by mutation in *KVLQT1*. The identification of *IsK* as a gene underlying JLNS in humans is strongly supported by observations in *Isk* knockout mice.

Although 11 unrelated individuals/families with JLNS were screened for mutations in the *IsK* gene, none were found. This is not surprising, as haplotyping of eight of the families, presented here, together with the mutation described in *KVLQT1*, provide good evidence that the majority of families map to the *KVLQT1* locus. Of the remaining three families, all are non-consanguineous and provide very little mapping information (pedigrees not shown). However, two of these three non-consanguineous families are heterozygous for the 5 bp deletion characterised here and the third shows a heterozygous SSCP shift in the *KVLQT1* gene, indicating that they may also be accounted for by mutation at the major locus, *KVLQT1* (data not shown). Thus all individuals with JLNS available to us for study are accounted for.

Since families N1H, N5B and N10D originate from the same part of Norway, a founder effect is likely to account for the mutation in these families and, indeed, a common haplotype is seen in these three families, suggestive of linkage disequilibrium. The 5 bp deletion in the *KVLQT1* gene encoding the S2–S3 membrane-spanning segment of the predicted channel will cause a frameshift and is highly likely to be disease causing.

The results shown in Figure 4 refine previous combined mapping data on the location of the *KVLQT1* gene, probably because a large number of ancestral meioses have been sampled. Previous analysis of recombinants in families with JLNS had indicated that the *KVLQT1* gene mapped between D11S922 and D11S4146 (13), with the presumed order being D11S922, D11S4046, D11S1318, (D11S4088), D11S4146. The mapping of 12 recombinants in eight French families with dominant long QT syndrome placed the gene distal to D11S1318 (25). Our data indicate that the mutant gene is located between the markers D11S1318 and D11S4088, but given that the *KVLQT1* gene covers a large genomic region (at least 300 kb), it is possible that some of these markers may lie within the gene itself (26).

Not all families of Norwegian origin share the common haplotype or demonstrate the SSCP shift seen in families N1H, N5B and N10D. Families N6K and N7J share a haplotype which differs from that seen in families N1H, N5B and N10D, suggesting that more than one mutation in the *KVLQT1* gene must be present in the Norwegian population. However, this group of eight families shown in Figure 4 originates from several different ethnic backgrounds, including Turkey, Pakistan and Norway. This indicates that the majority of cases of JLNS can be accounted for by mutation in the *KVLQT1* gene.

Now that it has been shown that homozygous mutations in either *KVLQT1* or *IsK* can cause JLNS in humans, it remains to be seen whether JLNS can result from compound heterozygosity for mutations in both genes, so-called digenic inheritance (27), or whether the resulting phenotype may differ. Certainly, families have been reported in which there is both deafness and a long QT interval but in whom the pattern of inheritance is not completely consistent with an autosomal recessive mode of transmission (28,29).

MATERIALS AND METHODS

Family data

Individuals were considered to have JLNS if they had profound sensorineural deafness and a prolonged QT_c interval. Most individuals were ascertained following syncopal episodes (although families N5B and N8A were ascertained following ECG screening of deaf children). QT_c intervals were calculated using Bazett's formula and a QT_c interval of >440 ms is generally considered to be prolonged (30). Some gene carriers fulfil the criteria for a prolonged QT interval.

Family UK1S is a British family. II_1 and II_2 have congenital profound sensorineural hearing loss with absent vestibular function. II_2 had three episodes of syncope on exertion prior to diagnosis and treatment, one of which required resuscitation. II_2 has a QT_c interval of 488 ms and II_1 a QT_c interval of 478 ms. QT_c intervals are 414 ms in the father and 418 ms in the mother (30). II_2 has retinal pigmentation of unknown origin but both boys have normal electroretinograms, excluding a diagnosis of Usher syndrome.

Family UK2T comes from Turkey but is resident in the UK. Parents are first cousins. The proband has prelingual deafness and

suffered from syncope. His QT_c is 480 ms and that of his sister is 374 ms.

Family N1H originates from Norway and has been reported previously (case 1, 31). The mother has a QT_c of 430 ms and the father's is 400 ms.

Family N3S originates from Norway. The proband is congenitally deaf and suffered from syncopal episodes elicited by stress. Her QT interval is 600 ms, but no other information is available.

Family N5B originates from Norway and has not been reported previously. The proband is congenitally deaf and the diagnosis was made on ECG examination (customary practice for all deaf children in Norway). The affected girl's QT_c is 540 ms, her father's is 410 ms, her brother's is 370 ms and that of her mother is 470 ms at rest, increasing to 540 ms on exercise.

The proband in Family N6K is congenitally deaf and comes from the same geographical region in Norway as family N7J. No QT_c intervals are available.

Family N7J has been reported previously (1) and formed the basis of the original description of this condition by Jervell and Lange-Nielsen.

Family N8A comes from Pakistan but is resident in Norway. The parents are first cousins. The diagnosis was made neonatally based on the family history and finding of a QT_c of 650 ms in the proband. He is congenitally deaf. The QT_c of the mother is 450 ms, that of the father is 410 ms, that of the proband's older sibling (21727) is 430 ms and that of the younger sister (21728) is 400 ms.

Family N10D originates from Norway. The proband is congenitally deaf and has suffered from episodes of syncope. The proband has a QT_c of 500 ms, that of her father is 470 ms, her mother's is 430 ms and her sister's is 360 ms.

PCR analysis

DNA was prepared from blood using standard protocols or from buccal swabs (32). Information on $(CA)_n$ microsatellite markers were provided by Généthon human genetic linkage maps (33), the Hereditary Hearing Loss Homepage (15) and published references (7–10,25). All genotyping was performed in 96-well Omniplates (Hybaid) under oil. PCR was performed with 40 ng genomic DNA in a 10 µl volume containing 10 pmol 3′-primer, 1× Bioline buffer (Bioline), 1.5 mM Mg^{2+}, 0.2 mM dGTP, dATP, dTTP and dCTP and 0.2 U Taq polymerase (Bioline) under standard conditions. Prior to amplification, 10 pmol 5′-primer per 10 µl reaction were end-labelled with 0.5 µl [γ-^{32}P]dATP(3000 Ci/mmol) with 0.5 U polynucleotide kinase (Promega) for 30 min. Alleles were separated as described previously (34) and sizes were determined by comparing migration relative to an M13 sequencing ladder.

Linkage analysis was performed using the MLINK programme of LINKAGE. Marker allele frequencies were obtained from Généthon (33). Penetrance was assumed to be 100% and gene frequency 0.00001.

SSCP analysis

SSCP analysis of the *KVLQT1* gene was performed using published primer sequences (10). The coding sequence of the *IsK* gene was amplified by PCR using primer pairs at 56°C according to Tesson *et al.* (20). Non-radioactive PCR products were analysed on 1× Mutation Detection Enhancement gel (FMC Bioproducts) at 4°C or room temperature, with or without 10% glycerol, at 45 W, 0.5× TBE, for 4 h. This allowed visualisation of both single and double-stranded DNA. The gels were stained with 0.012 M silver nitrate as described previously (35).

Sequence analysis of *IsK*

Biotinylated PCR products were purified using Dynabeads (Dynal, UK) and single-stranded products sequenced using the USB Sequenase v.2.0 kit, according to the manufacturer's instructions.

Sequence analysis of *KVLQT1*

PCR products demonstrating SSCP variants were sequenced directly on both strands using the fluorescent dideoxy terminator method and analysed using an ABI 377 DNA sequencer.

ACKNOWLEDGEMENTS

We would like to thank the families for their help and cooperation and Professor Bryan Winchester and Professor David Cooper for helpful discussions. We would like to thank Miss Isabelle Russell-Eggitt and Dr Tony Kriss for ophthalmological evaluations. Our thanks are due to Neil Ebeneezer, Charlotte Rose and Paul Rutland for technical advice and Miss Aideen MacInerney and Dr Magdi el Habbel for help with the families. L.T. would like to thank the Research Foundation for Studies of Deafness in Denmark (Forskningsfondet til studier vedroerende tunghoerhed og doevhed). M.B.-G. and J.T. are funded by the Medical Research Council. M.E.P. is funded by Mothercare. We would also like to thank Defeating Deafness for additional financial support and the Warriner Youth Choir for fundraising.

REFERENCES

1. Jervell,A. and Lange-Nielsen,F. (1957) Congenital deaf-mutism, functional heart disease with prolongation of the QT interval, and sudden death. *Am. Heart J.*, **54**, 59–68.
2. Fraser,G. (1976) Deafness with abnormal EKG (Jervell and Lange-Nielsen Syndrome). In *The Causes of Profound Deafness in Childhood.* Johns Hopkins University Press, London, UK.
3. Steel,K.P. and Brown,S.D.M. (1994) Genes and deafness. *Trends Genet.*, **10**, 428–435.
4. Steel,K.P. and Bock,G.R. (1983) Hereditary inner ear abnormalities in animals. *Arch. Otolaryngol.*, **109**, 22–29.
5. Friedmann,I., Fraser,G.R. and Froggatt,P. (1966) Pathology of the ear in the cardioauditory syndrome of Jervell and Lange-Nielsen (recessive deafness with electrocardiographic abnormalities). *J. Laryngol. Otol.*, **80**, 451–470.
6. Friedmann,I., Fraser,G.R. and Froggatt,P. (1968) Pathology of the ear in the cardio-auditory syndrome of Jervell and Lange-Nielsen syndrome. *J. Laryngol. Otol.*, **82**, 883–896.
7. Curran,M.E., Splawski,I., Timothy,K.W., Vincent,G.M., Green,E.D. and Keating,M.T. (1995) A molecular basis for cardiac arrhythmia: HERG mutations cause long QT syndrome. *Cell*, **80**, 795–803.
8. Wang,Q., Shen,J., Splawski,I., Atkinson,D., Li,Z., Robinson,J.L., Moss,A.J., Towbin,J.A. and Keating,M.T. (1995) SCN5A mutations associated with an inherited cardiac arrhythmia, long QT syndrome. *Cell*, **80**, 805–811.
9. Wang,Q., Curran,M.E., Splawski,I., Burn,T.C., Millholland,J.M., VanRaay,T.J., Shen,J., Timothy,K.W., Vincent,G.M., de Jager,T., Schwartz,P.J., Towbin,J.A., Moss,A.J., Atkinson,D.L., Landes,G.M., Connors,T.D. and Keating,M.T. (1996) Positional cloning of a novel potassium channel gene: KVLQT1 mutations cause cardiac arrhythmias. *Nature Genet.*, **12**, 17–23.
10. Schott,J.-J., Charpentier,F., Peltier,S., Foley,P., Drouin,E., Bouhour,J.-B., Donnelly,P., Vergnaud,G., Bachner,L., Moisan,J.-P., Le Marec,H. and Pascal,O. (1995) Mapping of a gene for long QT syndrome to chromosome 4q25–27. *Am. J. Hum. Genet.*, **57**, 1114–1122.

11. Barhanin,J., Lesage,F., Guillemare,E., Fink,M., Lazdunski,M. and Romey,G. (1996) K_VLQT1 and IsK (minK) proteins associate to form the I_{KS} cardiac potassium current. *Nature*, **384**, 78–80.
12. Sanguinetti,M., Curran,M.E., Zou,A., Shen,J., Spector,P.S., Atkinson,D.L. and Keating,M.T. (1996) Coassembly of K_VLQT1 and minK (IsK) proteins to form cardiac I_{KS} potassium channel. *Nature*, **384**, 80–83.
13. Neyroud,N., Tesson,F., Denjoy,I., Leibovici,M., Donger,C., Barhanin,J., Faur,S., Gary,F., Coumel,P., Petit,C., Schwartz,K. and Guicheney,P. (1997) A novel mutation in the potassium channel gene KVLQT1 causes the Jervell and Lange-Nielsen cardioauditory syndrome. *Nature Genet.*, **15**, 186–189.
14. Splawski,I., Timothy,K.W., Vincent,G.M., Atkinson,D.L. and Keating,M.T. (1997) Molecular basis of the long-QT syndrome associated with deafness. *New Engl. J. Med.*, **336**, 1562–1567.
15. Van Camp,G. and Smith,R.J.H. (1997) Hereditary hearing loss home page, World Wide Web URL, http:/dnalab-www.uia.ac.be/dnalab/hhh.html.
16. Coyle,B., Coffey,R., Armour,J.A., Gausden,E., Hochberg,Z., Grossman,A., Britton,K., Pembrey,M., Reardon,W. and Trembath,R. (1996) Pendred syndrome (goitre and sensorineural hearing loss) maps to chromosome 7 in the region containing the nonsyndromic deafness gene DFNB4. *Nature Genet.*, **12**, 421–423.
17. Sheffield,V.C., Kraiem,Z., Beck,J.C., Nishimura,D., Stone,E.M., Salameh,M., Sadeh,O. and Glaser,M. (1996) Pendred syndrome maps to chromosome 7q21–34 and is caused by an intrinsic defect in thyroid iodine organification. *Nature Genet.*, **12**, 424–426.
18. Shimizu,N., Antonarakis,S., Van Broeckhoven,C., Patterson,D., Gardiner,K., Nizetic,D., Creau,N., Delabar,J.-M., Korenberg,J., Reeves,R., Doering,J., Chakravati,A., Minoshima,S., Ritter,O. and Cuticchia,J. (1995) Report of the fifth international workshop on human chromosome 21 mapping. *Cytogenet. Cell Genet.*, **70**, 148–165.
19. Lai,L.-P., Deng,C.-L., Moss,A.J., Kass,R.S. and Liang,C.-S. (1994) Polymorphism of the gene encoding a human minimal potassium ion channel (minK). *Gene*, **151**, 339–340.
20. Tesson,F., Donger,C., Denjoy,I., Berthet,M., Bennaceur,M., Petit,C., Coumel,P., Schwartz,K. and Guicheney,P. (1996) Exclusion of KCNE1 (IsK) as a candidate gene for Jervell and Lange-Nielsen syndrome. *J. Mol. Cell. Cardiol.*, **28**, 2051–2055.
21. Vetter,D.E., Mann,J.R., Wangemann,P., Liu,J., McLaughlin,K.J., Lesage,F., Marcus,D.C., Lazdunski,M., Heinemann,S.F. and Barhanin,J. (1996) Inner ear defects induced by null mutation of the isk gene. *Neuron*, **17**, 1251–1264.
22. Takumi,T., Moriyoshi,K., Aramori,I., Ishii,T., Oiki,S., Okada,Y., Ohkubo,H. and Nakanishi,S. (1991) Alteration of potassium channel activities and gating by mutations of slow ISK potassium channel. *J. Biol. Chem.*, **266**, 22192–22198.
23. Stryer,L. (1988) *Biochemistry*. W.H.Freeman and Co., New York, NY.
24. Oldridge,M., Lunt,P.W., Zacki,E.H., McDonald-McGinn,D.M., Muenke,M., Moloney,D.M., Twigg,S., Heath,J.K., Howard,T.D., Hoganson,G., Gagnon,D.M., Wang Jabbs,E. and Wilkie,A.O.M. (1997) Genotype–phenotype correlation for nucleotide substitutions in the IgII–IgIII linker of FGFR2. *Hum. Mol. Genet.*, **6**, 137–143.
25. Dausse,E., Denjoy,I., Kahlem,P., Bennaceur,M., Faure,S., Weissenbach,J., Coumel,P., Schwartz,K. and Guicheney,P. (1995) Readjusting the localization of long QT syndrome gene on chromosome 11p15. *C.R. Acad. Sci. Paris*, **318**, 879–885.
26. Lee,M.P., Hu,R.-J., Johnson,L.A. and Feinberg,A.P. (1997) Human KVLQT1 gene shows tissue-specific imprinting and encompasses Beckwith–Wiedeman syndrome chromosomal rearrangements. *Nature Genet.*, **15**, 181–185.
27. Kajiwara,K., Berson,E.L. and Dryja,T.P. (1994) Digenic retinitis pigmentosa due to mutations at the unlinked peripherin/RDS and ROM1 loci. *Science*, **264**, 1604–1608.
28. Drescher,D.G., Green,G.E. and Lehman,M.H. (1997) Hearing impairment in patients with long QT syndrome. *Hered. Deafness Newsl.*, **13**, 24.
29. Reardon,W., Lewis,N. and Hughes,H. (1993) Consanguinity, cardiac arrest, hearing impairment, and ECG abnormalities: counselling pitfalls in the Romano–Ward syndrome. *J. Med. Genet.*, **30**, 325–327.
30. Schwartz,P.J., Moss,A.J., Vincent,G.M. and Keating,M. (1993) Diagnostic criteria for the long QT syndrome. An update. *Circulation*, **88**, 782–784.
31. Jervell,A., Thingstad,R. and Endsjö,T.Ö. (1966) The surdo-cardiac syndrome. *Am. Heart J.*, **72**, 582–593.
32. Muelenbelt,I., Droog,S., Trommelen,G.J.M., Boomsa,D.I. and Slagboom,E.P. (1995) High-yield non-invasive human genomic DNA isolation method for genetic studies in geographically dispersed families and populations. *Am. J. Hum. Genet.*, **57**, 1254–1255.
33. Dib,C., Faure,S., Fizames,C., Samson,D., Drouot,N., Vignal,A., Millasseau,P., Marc,S., Hazan,J., Seboun,E., Lathrop,M., Gyapay,G., Morisette,J. and Weissenbach,J. (1996) A comprehensive genetic map of the human genome based on 5,264 microsatellites. *Nature*, **380**, 152–154.
34. Tyson,J., Bellman,S., Newton,V., Simpson,P., Malcolm,S., Pembrey,M. and Bitner-Glindzicz,M. (1996) Mapping of DFN2 to Xq22. *Hum. Mol. Genet.*, **5**, 2055–2060.
35. Tyson,J., Ellis,D., Fairbrother,U., King,R.H.M., Muntoni,F., Jacobs,J., Malcolm,S., Harding,A.E. and Thomas,P.K. (1997) Hereditary demyelinating neuropathy of infancy. A genetically complex syndrome. *Brain*, **120**, 47–63.
36. Collins,A., Frezal,J., Teague,J. and Morton,N.E. (1996) A metric map of humans: 235000 loci in 850 bands. *Proc. Natl. Acad. Sci. USA*, **93**, 14771–14775

Splice Mutations in *KVLQT1*?

To The Editor:

Li et al[1] propose that 2 new mutations in *KVLQT1* in Romano-Ward syndrome (RWS) disrupt splicing, leading to frameshift and premature protein truncation, acting through a loss-of-function mechanism. This is surprising because missense mutations in KVLQT1, acting in a dominant-negative manner, predominate in RWS. In Table 2 of the article by Li et al, 24 of the 26 mutations are missense (the 2 remaining being discussed here). We suggest alternative interpretations.

The SP/A249/g-a mutation is a substitution G to A at the third position of codon 249, in which GCG is altered to GCA, occurring at the donor splice junction of exon 6. Mutation of splice sites can cause skipping of the affected exon, activation of cryptic splice sites, or retention of the intron.[2] Exon skipping is common. If this occurs in SP/A249/g-a, the predicted protein will lack part of the pore and S6 transmembrane domain but may still multimerise, because if exon 6 is skipped, the resulting mRNA would still read "in frame." In-frame but deleted transcripts may be stable and translated into protein, as shown for the dystrophin gene.[3] The effect of the mutation should be confirmed in RNA, because frameshift and premature truncation of the KVLQT1 protein, as suggested by Li et al, would be a truly novel type of *KVLQT1* mutation in RWS.

The second mutation is the 3-bp deletion across an exon/intron boundary (denoted SP/V212/ΔGGT), disrupting the 5′ donor site of exon 5. A donor consensus splice site consists of CAG.gtaagt.[4] In the patient in the study by Li et al, the wild-type exonic sequence GGG.GTG.gtaagt is mutated to GGG.GTaagt by deletion of 3 nucleotides, Ggt. The authors propose that the mutation SP/V212/ΔGGT alters splicing, leading to a 1-bp deletion in the coding region, causing frameshift and premature truncation of the predicted protein (see Figure).

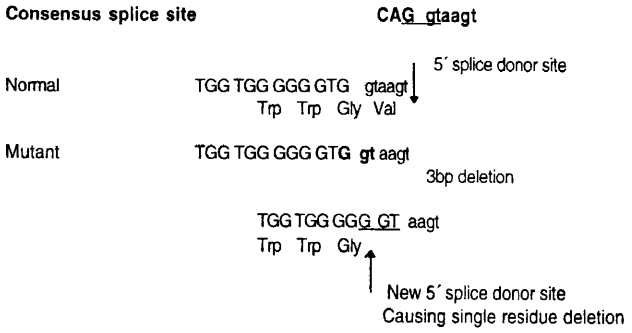

However, a potential splice sequence, GGG.gtaagt, remains.[4] Splicing here would delete a single valine,[5] causing a mutant protein capable of dominant-negative action.

Missense mutations in KVLQT1 predominate in RWS, whereas nonsense mutations predominate in Jervell and Lange-Nielsen syndrome (Tyson, 1998, unpublished data). Carriers of nonsense mutations rarely manifest RWS clinically. The gene product of the null allele should not interfere with the wild-type allele in a dominant-negative manner.

Jessica Tyson, BSc
Sue Malcolm, PhD
Maria Bitner-Glindzicz, MRCP, PhD
Molecular Genetics Unit
Institute of Child Health
London, UK

1. Li H, Chen Q, Moss AJ, Robinson J, Goytia V, Perry JC, Vincent GM, Priori SG, Lehmann MH, Denfield SW, Duff D, Kaine S, Shimizu W, Schwartz PJ, Wang Q, Towbin JA. New mutations in the *KVLQT1* potassium channel that cause long-QT syndrome. *Circulation.* 1998;97: 1264–1269.
2. Maquat LE. Defects in RNA splicing and the consequence of shortened translational reading frames. *Am J Hum Genet.* 1996;59:279–286.
3. Dunckley MG, Manoharan M, Villiet P, Eperon IC, Dickson G. Modification of splicing in the dystrophin gene in cultured *Mdx* muscle cells by antisense oligoribonucleotides. *Hum Mol Genet.* 1998;7:1083–1090.
4. Shapiro M, Senapathy P. RNA splice junctions of different classes of eukaryotes: sequence statistics and functional implications in gene expression. *Nucleic Acids Res.* 1987;15:7155–7174.
5. Chouabe C, Neyroud N, Guicheney P, Lazdunski M, Romey G, Barhanin J. Properties of KvLQT1 K+ channel mutations in Romano-Ward and Jervell and Lange-Nielsen inherited cardiac arrhythmias. *EMBO J.* 1997; 16:5472–5479.